U.S. Geological Survey.
Reports-Open file series

SITE SELECTION AND INVESTIGATION FOR SUBSURFACE DISPOSAL OF RADIOACTIVE WASTES IN HYDRAULICALLY INDUCED FRACTURES

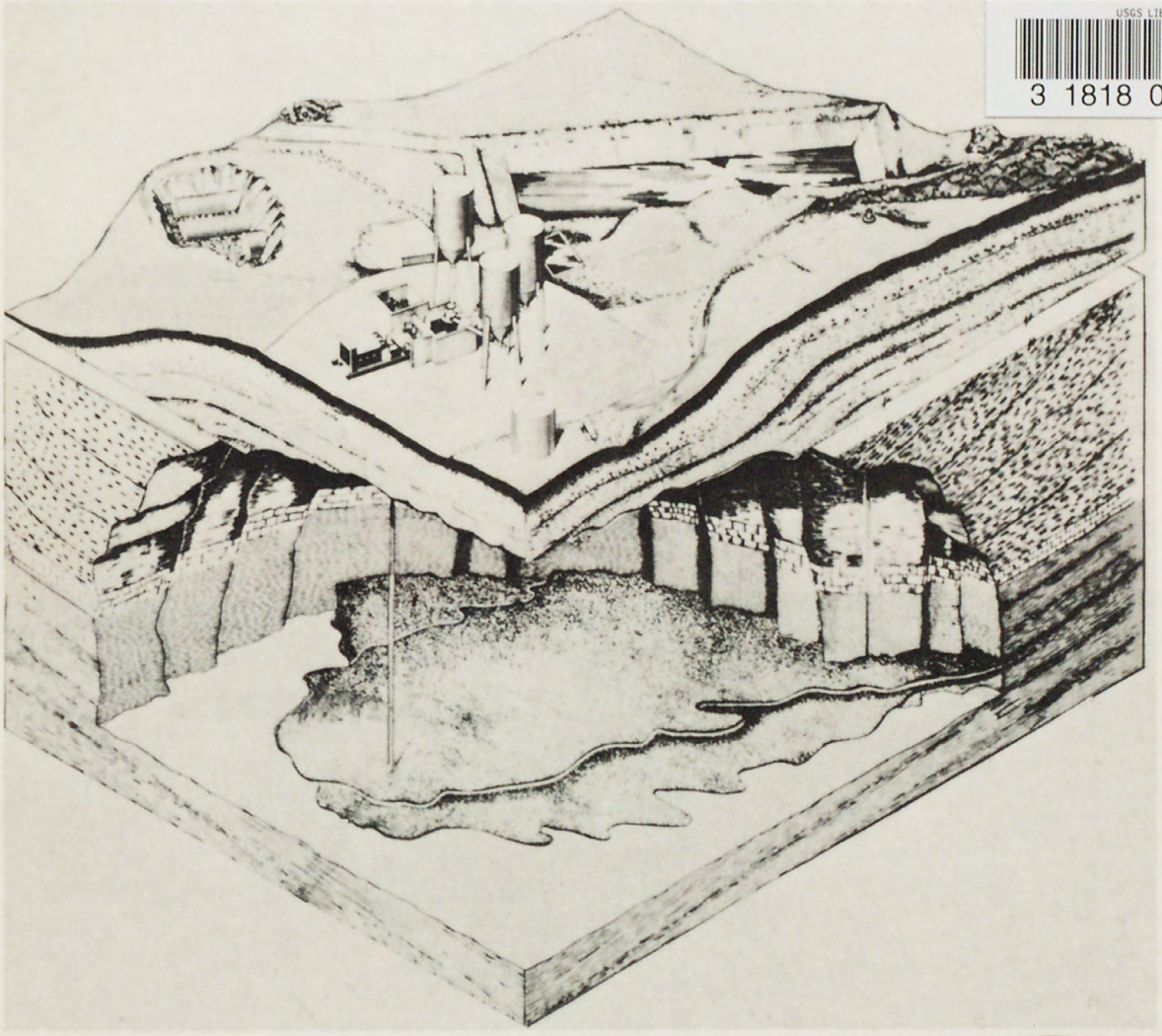

U.S. GEOLOGICAL SURVEY
Open-File Report 80—450

SITE SELECTION AND INVESTIGATION FOR SUBSURFACE DISPOSAL OF RADIOACTIVE WASTES IN HYDRAULICALLY INDUCED FRACTURES

By Ren Jen Sun

U.S. GEOLOGICAL SURVEY
Open-File Report 80—450

1980

UNITED STATES DEPARTMENT OF THE INTERIOR
CECIL D. ANDRUS, Secretary

GEOLOGICAL SURVEY
H. William Menard, Director

Prepared in cooperation with the U.S. Department of Energy for the International Atomic Energy Agency

---

For additional information write to:

Chief Hydrologist
433 National Center
U.S. Geological Survey, WRD
Reston, Virginia 22092

CONTENTS

Contents (cont.) Page

Contents (cont.) Page

Contents (cont.) Page

Illustrations

Illustrations (cont.) Page

Illustrations (cont.) Page

Illustrations (cont.) Page

Illustrations (cont.) Page

Illustrations (Cont.) Page

Illustrations (cont.) Page

Illustrations (cont.) Page

TABLES

Tables (cont.) Page

Tables (cont.) Page

Conversion Table

Multiply metric (SI) unit	by	to obtain inch-pound unit
Millimeter (mm)	3.9370×10^{-2}	inch (in)
Centimeter (cm)	3.9370×10^{-1}	inch (in)
Meters (m)	3.2808×10^{0}	foot (ft)
Kilometers (km)	6.2137×10^{-1}	miles (mi)
Square kilometers (km^2)	3.8610×10^{-1}	square miles (mi^2)
Cubic meters (m^3)	3.5315×10^{1}	cubic feet (ft^3)
Cubic meters (m^3)	2.6417×10^{2}	gallons (gal)
Milliliters (ml)	2.6417×10^{-4}	gallons (gal)
Milliliters (ml)	3.5315×10^{-5}	cubic feet (ft^3)
Meters per second (m/s)	3.2808×10^{0}	feet per second (ft/s)
Kilograms per second (kg/s)	2.2046×10^{0}	pounds per second (lb/s)
Cubic meters per second (m^3/s)	3.5315×10^{1}	cubic feet per second (ft^3/s)
Cubic meters per second (m^3/s)	1.5850×10^{4}	gallons per minute (gal/min)
Kilogram per cubic meters (kg/m^3)	6.2427×10^{-2}	pounds per cubic feet (lb/ft^3)
Kilogram per cubic meters (kg/m^3)	8.3454×10^{-3}	pounds per gallons (lb/gal)
Pascal (Pa)	1.4504×10^{-4}	pounds per square inch (lb/in^2)
Megapascal (MPa)	1.4504×10^{2}	pounds per square inch (lb/in^2)
Curies per liter (Ci/l)	2.8317×10^{1}	curies per cubic feet (Ci/ft^3)
Curies per liter (Ci/l)	3.7854×10^{0}	curies per gallon (Ci/gal)

ABSTRACT

Injection into a thick shale formation of intermediate-level radioactive wastes (specific activity of less than 6×10^3 μCi/mℓ consisting mainly of radionuclides such as strontium and cesium with half-lives of less than 50 years)mixed with cement is a promising and feasible disposal method. Hydraulic fracturing provides openings in the shale to accommodate the wastes. Ion exchange and radionuclide adsorption materials can be added to the grout during mixing to further increase the radionuclide retaining capacity of the grout. After solidification of the grout, the injected wastes become an integral part of the shale formation and thus the wastes will remain at depth and in place as long as the injection zone is not subjected to erosion or dissolution.

Problems concerning safety of the disposal method are: (1) potential of inducing vertical fractures; (2) phase separation during and after injections; (3) reliability of methods for determining orientation of induced fractures; (4) possibility of triggering earthquakes; and (5) radionuclides leaching and transporting by ground water.

In bedded shale, a difference in tensile strength between the direction normal and parallel to bedding planes favors the formation of fractures along bedding planes which are nearly horizontal. Even in areas where vertical stress is slightly higher than the horizontal stresses, nearly horizontal bedding-plane fractures can be hydraulically induced in shale at depths less than about 1,000 m. Test injections should be made during site evaluation to determine if horizontal bedding-plane fractures can be induced.

Orientation of induced fractures can be indirectly monitored by observing injection pressure during injection time, and by pressure decay of water injections and uplift of ground surface after injections; however, it can be

directly determined by gamma-ray logs made in observation wells before and after each injection if the injected fluid or wastes contain enough gamma-emitting radionuclides.

If waste grout is properly mixed, phase separation should be less than one percent of the total injection volume. The mobility of waste in the separated liquid is further reduced by low permeability (less than 10^{-6} darcy), high ion-exchange and adsorption capacity of shale, thus reducing the contamination potential.

Grout injections do not cause extensive increases in pore pressure within the shale mass, and a disposal site should be located in a geologically stable and tectonically relaxed area, that is, without local active faults; thus the disposal method can avoid the two necessary and essential conditions (increase of pore pressure and rock already stressed near its breaking strength) for triggering earthquakes by fluid injections.

Waste injections are made in multiple-layer injection stages in an injection well. After the first series of injections are made at the greatest depth, the well is plugged by cement at the injection depth. The depth of the second series of injections is located at a suitable distance above the first injection depth. The repeated use of the injection well distributes the cost of construction of injection and monitoring wells over many injections, thereby making hydraulic fracturing and grout injection economically attractive as a method for disposal of radioactive wastes.

Theoretical considerations of inducing nearly horizontal bedding-plane fractures in shale and field procedures for site selection, safety, monitoring and operation of radioactive waste disposal are discussed. Case histories are used as examples to demonstrate the theoretical applications and field operations.

1. INTRODUCTION

Radioactive waste is the inevitable byproduct of the generation of electricity by nuclear reactors as well as other nuclear applications. An effective solution to the problem of disposal of the long-lived and highly toxic radioactive waste is essential to the expanded use of nuclear energy. Numerous methods for the disposal of radioactive waste have been proposed or studied in the last two decades. To name a few, disposal on or in suitable goelogical formations, disposal in the ocean bottoms including subduction zones, disposal by shooting the wastes into space, disposal in polar ice and disposal by transmutation (Winograd, 1974; Interagency Review Group on Nuclear Waste Management, 1979). Judged by existing technology, disposal of waste in geologic formations is probably the most feasible and practical method among the proposed alternatives.

One of the geologic-disposal methods is to inject intermediate-level radioactive wastes (specific activity of less than 6×10^3 μCi/mℓ consisting mainly of radionuclides with half-lives ranging less than 50 years such as stronium and cesium) mixed with cement and additives through a deep well into hydraulically induced fractures formed in nearly impervious formations (permeability less than 10^{-6} darcy). The injected grout is allowed to solidify under pressure to form grout sheets which will become an integral part of the rock (fig. 1), thereby immobilizing the wastes in a desired horizon of the low permeability medium. Fractures created by hydraulic pressure during the injection provide openings in the rock to accept the wastes.

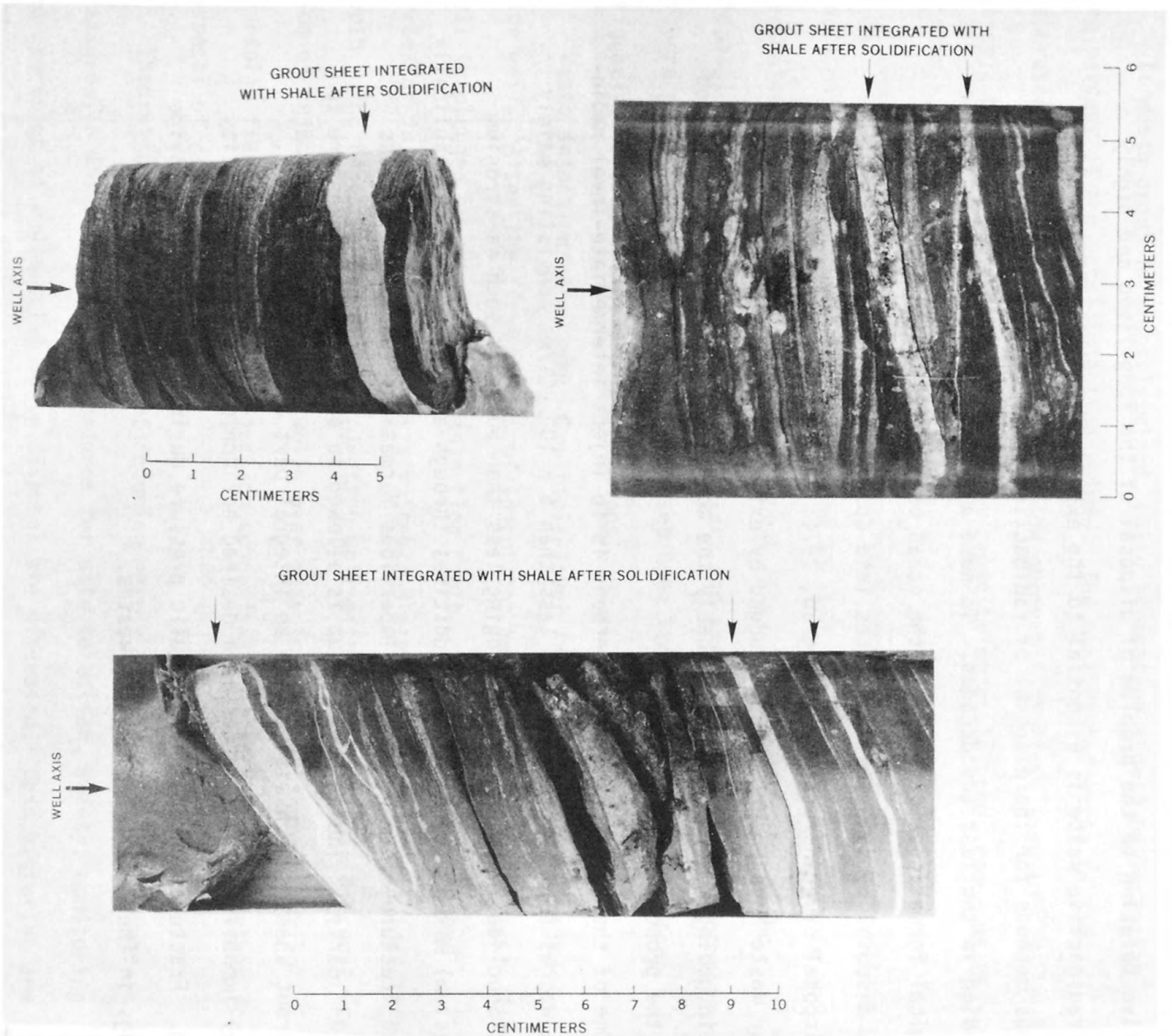

Figure 1.--Core showing grout sheets integrated with shale after solidification. Arrowheads indicate grout sheets. Cores shown here were obtained from different injections. (Courtesy of Oak Ridge National Laboratory)

The techniques of hydraulic fracturing have been widely used in the petroleum industry for recovery of oil since 1947 (Clark, 1949; Howard and Fast, 1970). However, disposal of wastes by grout injection using hydraulic fracturing as a means had not been tested until 1959. In 1958, D. A. Shock of the Continental Oil Company suggested to the U.S. Atomic Energy Commission (AEC, presently U.S. Department of Energy) that hydraulic fracturing with grout injection into impermeable rocks might be used in the disposal of highly toxic radioactive waste (deLaguna, et al, 1968). The US AEC accepted the suggestion and the Oak Ridge National Laboratory (ORNL) was chosen as an experimental site.

Requirements for radioactive waste disposal by this technique include the following items: (1) the induced fractures should be horizontal or nearly horizontal, and (2) the wastes should be contained in a known and well defined horizon for a sufficient length of time until the wastes decay to innocuous radiation-emission levels.

From 1959 through 1960, three experimental injections by hydraulic fracturing without wastes were made into the Conasauga shale at two different locations at ORNL. The grout was tagged with radioactive isotope Cs^{137}. The first injection was at a shallow depth, 88 m below land surface. After the injection, 22 coreholes were drilled in the vicinity of the injection area. The core data showed that the solidified grout sheet was formed nearly parallel with bedding planes (fig. 1). The second and third experiments were made at a new well which was drilled 1,830 m east of the first injection well. Similar grout was used in these two injections, which were made at depths of 285 m and 212 m, respectively. After the injections, 24 coreholes were drilled in the vicinity of the second experimental site. The corehole data confirmed again that the

grout sheets were formed parallel with bedding planes and became an integral part of the shale (fig. 1). The grout sheets are confined in an area with a maximum radius of 100 m and the observed thickness of grout sheets is between 3 to 12 mm (figs. 2 and 3). A third well with 14-cm casing was drilled in the Conasauga shale to a depth of 329 m, 0.8 km west of the second experimental site. From 1964 through 1965, seven experimental injections with liquid radioactive wastes produced at ORNL were injected. The injections were made progressively in shallower depths, from 288 m to 265 m. From 1966 through 1978, regular waste-disposal operations were carried out through the well from depths of 265 m to 245 m. A total volume of 11,000 m^3 of grout containing 7,000 m^3 of radioactive wastes produced at ORNL was injected. These wastes contained 640,000 curies of radionuclides. Core drilling and gamma-ray logs made in observation wells constructed in the vicinity of the injection well also indicated that the grout sheets were formed parallel with bedding planes (deLaguna, et al., 1968, 1971; Weeren, 1974, 1976).

The demonstration at ORNL shows that disposal of intermediate-level radioactive wastes in bedded shale by hydraulic fracturing is feasible. However, most of the experience of hydraulic fracturing in oil wells indicates that hydraulically induced fractures are generally vertical (Hubbert, 1971). Because of this experience, earth scientst advised the US AEC, through the U.S. National Academy of Sciences, not to extrapolate the results obtained at ORNL site to other locations (Belter, 1972).

In view of this advice, the US AEC sponsored an experimental program carried out jointly by ORNL and the U.S. Geological Survey (USGS), with the permission

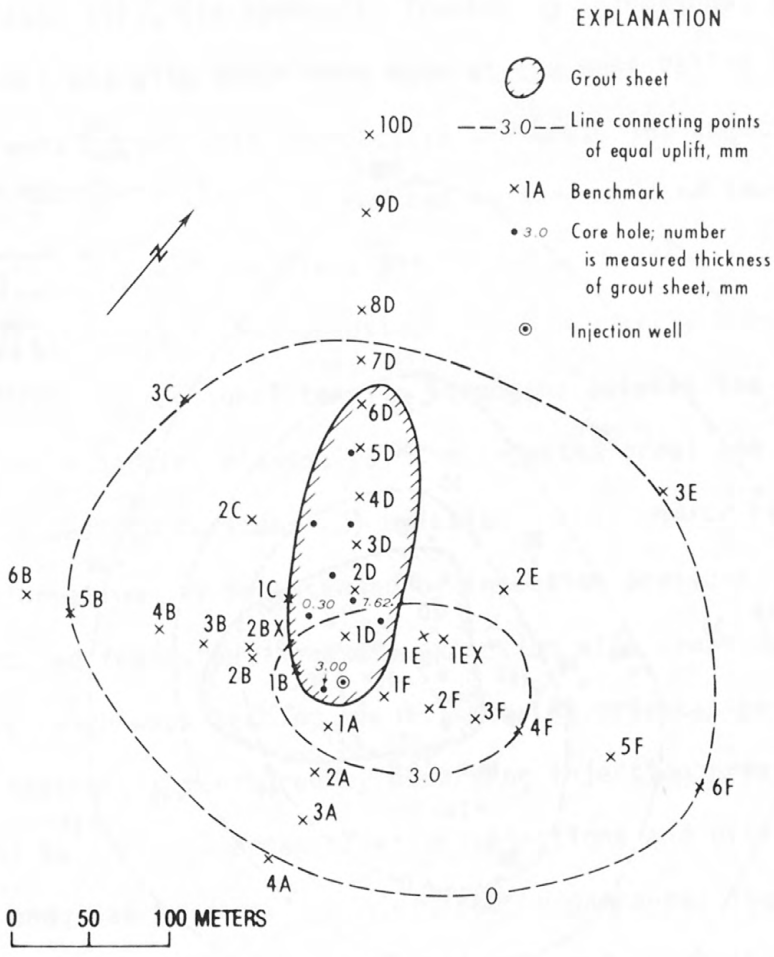

Figure 2.--Observed surface uplift, extent, and thickness of grout sheet resulting from the injection, September 3, 1960, second experiment site, Oak Ridge National Laboratory, Tennessee (from DeLaguna and others, 1968).

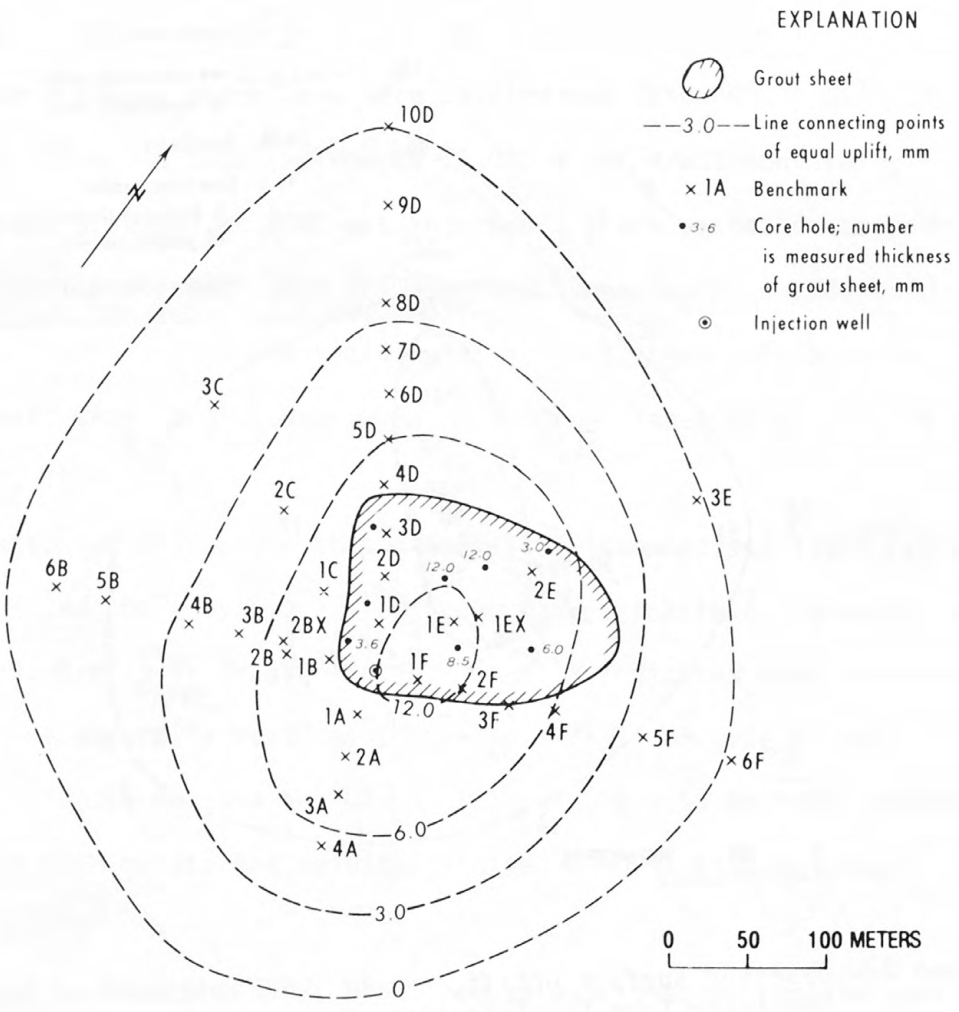

Figure 3.--Observed surface uplift, extent, and thickness of grout sheet resulting from the injection, September 10, 1960, second experiment site, Oak Ridge National Laboratory, Tennessee (from deLaguna and others, 1968).

of the State of New York, to test the concept of disposal of radioactive wastes into shale by hydraulic fracturing further at the Western New York Nuclear Fuel Service Center near West Valley in Cattaraugus County, New York. The objectives of this program were: (1) to demonstrate the applicability of disposal of radioactive wastes in nearly horizontally bedded shale through hydraulic fracturing at another location; (2) to develop an economic yet practical method for estimating and monitoring the orientation of hydraulically induced fractures; and (3) to develop site evaluation procedures (Belter, 1972).

From 1969 through 1971, six hydraulic fracturing injections, all with water except the last one with grout were made at the West Valley site. Most of the injections were tagged with radioactive tracers. The injection depths ranged from 152 to 442 m. Conclusions reached on the basis of the test results are: (1) at certain shallow depth (less than 1,000 m) bedding-plane fractures can be induced hydraulically in an approximately horizontally bedded shale characterized by strong directional tensile strengths between the direction normal and parallel to bedding planes; (2) the injected grout can be kept within a narrow range of a desired horizon; (3) existing joints and/or high-angle fractures of the formation may be extended by injection pressure if they are intercepted by induced fractures, however, extension will cease when the extended vertical fractures reach weak bedding planes; and (4) orientation of induced fractures can be indirectly monitored by observing injection pressures during injection time and by pressure-decay of water injections and uplift of ground surface after injections and, can be directly determined by gamma-ray logs made in observation wells which were constructed within the extent of the grout, if the grout contains gamma-emitting radionuclides (Sun, 1973; Sun and Mongan, 1974).

The present existing hydraulic fracturing disposal facility at ORNL was designed for experimental injections. Because of the experiment success, the

facility was modified in 1966 for the routine disposal of radioactive wastes with a specific activity of less than 530 μCi/mℓ. The facility can neither be used for disposal of sludge of which 1,500 m^3 has accumulated at ORNL, nor for wastes with a specific activity higher than 530 μCi/mℓ without extensive equipment modifications. Also, the disposal capacity of the shale underlying the present facility will be exhausted within 5 to 10 years of operation if the present waste generation rate at ORNL is maintained (U.S. Energy Research and Development Administration (ERDA), 1977).

The ORNL proposed to establish a new hydraulic fracturing disposal facility with the capacity to dispose sludges as well as wastes with a specific activity up to 6 x 10^3 μCi/mℓ. The proposed new site is 245 m south of the present site. A site feasibility study was made jointly by ORNL and USGS in 1974 by applying the methods developed during the experiments conducted at ORNL and West Valley.

Since enactment of the National Environmental Policy Act in 1969, all major government projects require environmental impact statements which should evaluate all possible environmental impacts of a proposed action as well as the feasible alternatives to the proposed action. The environmental impact statement for the proposed new waste disposal facility at ORNL concluded that the hydraulic fracturing disposal of radioactive wastes at ORNL is the safest method with the least cost among the alternatives, such as tank storage and fixation in glass (US ERDA, 1977).

1.1 Purpose and scope of the report

The feasibility of subsurface disposal of certain types of radioactive wastes in hydraulically induced fractures in shale by grout injection has been studied and well demonstrated in the USA. The purpose of this report is to

provide guidelines for the authorities, who are responsible for planning, approving, and executing radioactive waste management programs, to evaluate whether disposal of intermediate-level radioactive wastes (specific activity of less than 6×10^3 μCi/mℓ containing mainly of radionuclides with half-lives ranging less than 50 years such as strontium and cesium) by hydraulic fracturing is an acceptable alternative. The information herein is also intended to be used for the selection and evaluation of suitable sites. Safety assessment of the disposal method is also included. The safety assessment is important and necessary for the waste management authorities who use the information to evaluate the hydraulic fracturing disposal technique among other alternatives so that the disposed waste can be isolated in the formation safely at least for the desired length of time. However, comparison of the risk analyses with those for other disposal means is beyond the scope of the report.

The report contains sufficient theoretical discussions and case histories (in Appendices) to allow the reader who will evaluate whether the conclusions presented in the report are justified.

1.2 Acknowledgment

This report was sponsored by the Division of Waste Management of the U.S. Department of Energy for the International Atomic Energy Agency.

The author wishes to thank Messrs. R. A. Robinson and H. O. Weeren, ORNL, for providing information on hydraulic-fracturing disposal at ORNL. The author also is indebted to R. A. Farrow, U.S. Geological Survey, for determination of tensile strength of shale from core during a site evaluation study at ORNL.

2. THEORY OF FRACTURE MECHANICS

Rock deformation can be classified into three main categories: (1) folds; (2) shear fractures; and (3) extension fractures. Ideally, folds are produced by rock deformations under stresses without failure (in a macroscopic sense). Shear fractures result from movements parallel to the plane of the fracture. Faults are special cases of shear fracturing. Extension fractures are separations of rocks across a surface normal to the direction of the least principal stress without offset of movement parallel to the fracture surface. Extension fractures involve loss of cohesion, separation into two parts and release of stored elastic strain energy (Badgley, 1965). Joints and hydraulically induced fractures are extension fractures.

Three well established theories that can be applied to rock fracturing are: (1) the Coulumb-Navier theory; (2) the Mohr theory; and (3) the Griffith theory (Jaeger and Cook, 1969). The first two theories are applicable to rock failure under maximum shear stress. The last theory discusses rock failures under tension and can be used to explain extension fractures. Therefore, only the Griffith theory is used to discuss hydraulic fracturing mechanics.

Two stages are involved in the formation of fractures, namely fracture initiation and fracture propagation. Fracture initiation is defined as the failure process by which one or more pre-existing fractures in rocks start to extend. Fracture propagation is a stage subsequent to fracture initiation in which a fracture is extending. Two kinds of fracture propagation may be defined, stable propagation and unstable propagation (Bieniawski, 1967).

Stable fracture propagation is the process of rupture by which the extension of a fracture has a definite relationship between the applied stress and the length of the fracture, and the fracture extension can be controlled accordingly,

This kind of fracture propagation can be examined under static condition. If the fracture extension is governed by factors other than stresses, for example, the velocity of propagation, it becomes uncontrollable. The fracture expands rapidly to complete rupture of the material with the applied load maintained constant, for example, a fracture in glass. This kind of propagation is called unstable propagation and has dynamic characteristics.

The extension of hydraulically induced fractures is dependent on the applied hydraulic pressure; a fracture will cease extending when applied pressure falls below a critical level. Therefore, it can be concluded that the extension of a hydraulically induced fracture is a stable propagation.

When sediments are deposited, individual grains are discrete and the sediments are without cohesion. As sediments are buried beneath younger deposits, they become compacted and cemented. Compaction and cementation result in cohesion of grains, so that the rock takes on cohesive/or tensile strength. The greater the cementation and compaction the greater is the cohesion.

In the propagation of extension fractures, work must be done against the stress normal to the fracture plane and the cohesive force of the grains at the fracture tip. As the hydraulic pressure increases the pre-existing fracture in the rock does not extend when the pressure is small. Upon reaching a certain pressure which overcomes the sum of the normal stress and the maximum cohesive force at the fracture tip, the fracture begins to extend.

The cohesive force under tensile stresses/in perfect crystals is a function of the intermolecular distance b (Cottrell, 1964; Kunz, 1971) as shown in figure 4. Consider two

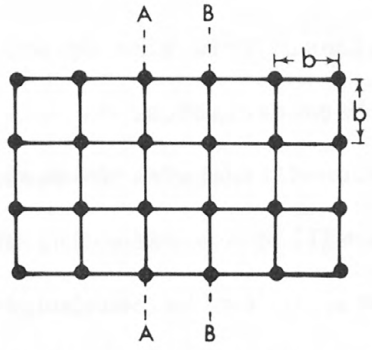

(a) Crystal grain in equilibrium condition

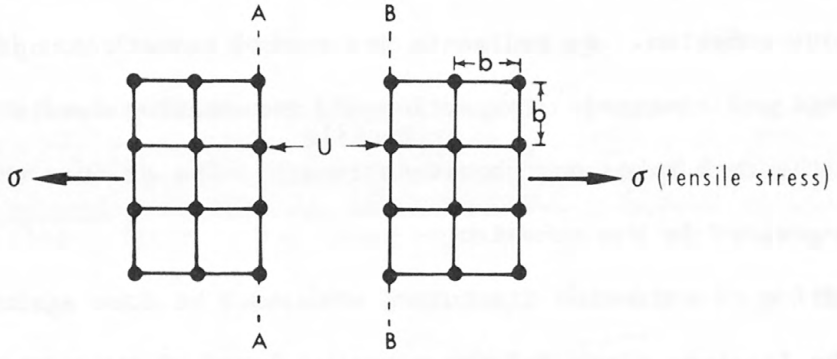

(b) Two molecular planes being pulled apart

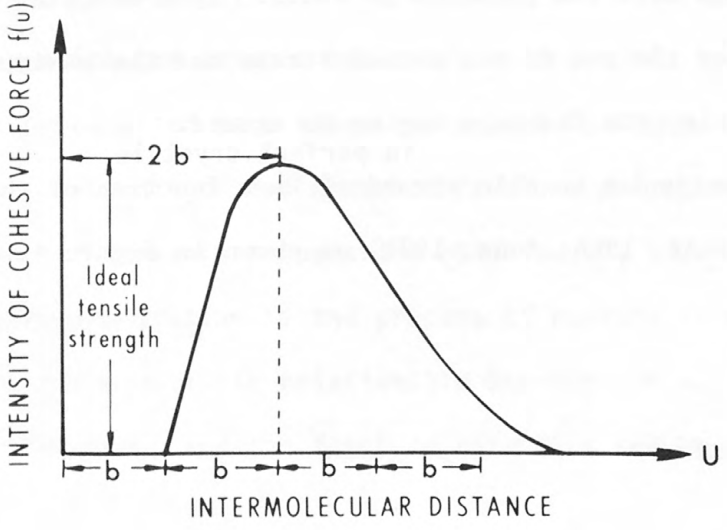

(c) Theoretical cohesive force under tensile stress

Figure 4.--Fracturing of a perfect crystal under tensile stresses (from Cottrell, 1964).

atomic planes under tensile stresses; the molecular cohesive force is zero before the tensile stresses are applied, then it rises in proportion to the amount of separation between the separated molecules, and reaches the maximum value when the separation has reached approximately one intermolecular distance from the equilibrium condition. Further increase of separation will reduce the cohesive force which diminishes nearly to zero when the separation between the molecules is greater than three intermolecular distances from the equilibrium condition. The maximum molecular cohesive force defines the ideal tensile strength of the material under consideration, that is, the tensile strength of a material if it were a perfect crystal. The actual tensile strength of a material is usually several orders of magnitude lower than the ideal tensile strength because of: (1) defects of crystal structure; (2) variation of mineralogy of constituent detrital grains and extent of cementation in a granular medium; and (3) variation in type of cement.

Figure 5 shows a schematic, idealized structure of molecules around a fracture tip. Consider the fracture extending from the left towards the right; the first pair of molecules at the fracture tip begins to separate as the tensile stresses increase. An increase in the applied stresses will increase the separation between the pair. The intermolecular distance increases from the equilibrium condition, b, to 2b, then to 4b; at this stage the fracturing process is completed and the fracture extends one molecular distance b, and the applied stresses fall. The second pair of molecules now becomes the new fracture tip. The applied stresses again rise and fall. The fracturing process goes on from one pair of molecules to another pair.

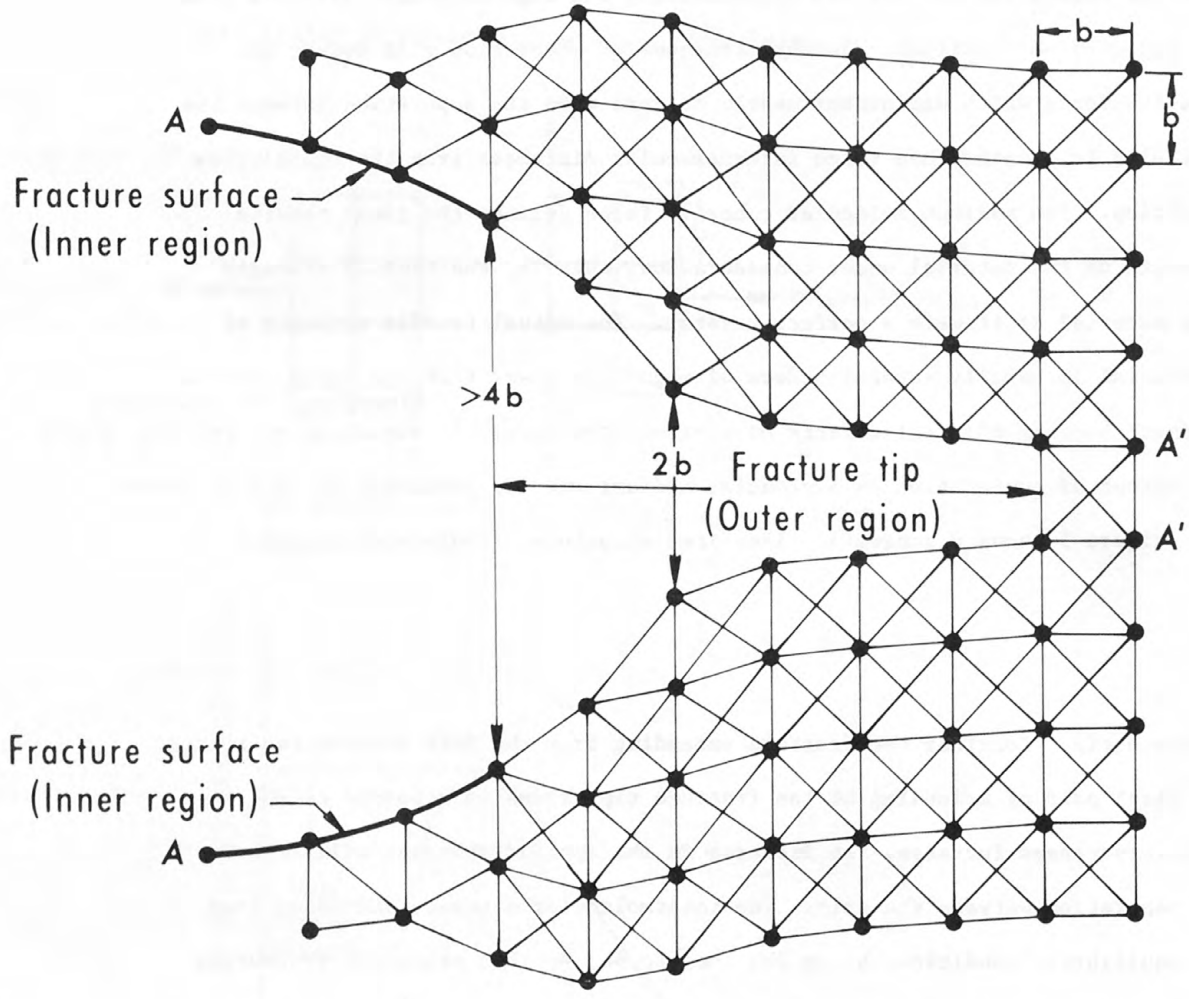

Figure 5.--Schematic diagram showing molecular structures around a fracture tip.

To avoid solving complex non-linear integral equations of the fracture problem, Barenblatt (1962) divided the fracture area into two regions (fig. 6).

In the inner region the opposite fracture walls are relatively far apart, hence, there is no molecular cohesive force, and the fracture walls can be considered as free from such stress. The linear theory of elasticity is fully adequate to describe this region. In the edge region, the opposite fracture walls are sufficiently close to each other so that there is strong molecular cohesive force between them. Plastic yielding occurs in this region. To avoid the complex non-linear theory of elasticity and to work within the framework of the linear theory, Barenblatt made two assumptions to solve the fracture problem: (1) the size of edge region of the fracture is small compared with the size of the whole fracture; and (2) when the fracture extends, the shape of the section normal to the fracture surface in the edge region (and consequently the local distribution of the cohesive force over the fracture surface) does not depend on the pressure in the fracture and is always the same for a given conditions of temperature and composition. These assumptions are considered to be realistic by the author.

Based on these assumptions, the average cohesive force at a fracture tip is defined as fT, where T is the average tensile strength of the rock and f is a constant which depends on physical properties of the rock. The value of f is $0 \leq f \leq 1$ (Barenblatt, 1962; Kenny and Campbell, 1967; Perkins and Krech, 1968; Goodier, 1968; and Rice, 1965).

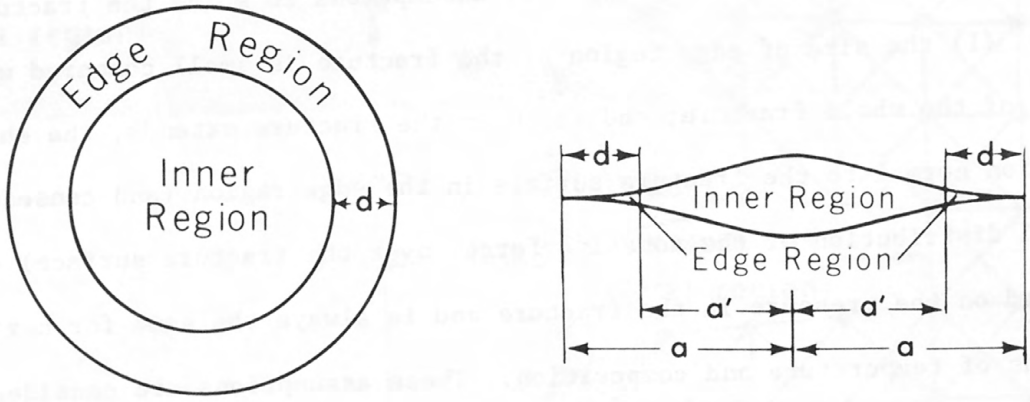

Figure 6.--Two regions of a brittle fracture (from Barenblatt, 1962).

3. FACTORS CONTROLLING INJECTION OF RADIOACTIVE WASTES IN HYDRAULICALLY INDUCED FRACTURES

The technique of disposal of radioactive wastes in a geologic formation by hydraulic fracturing is that the waste is mixed with cement and additives, then injected through a well under pressure. The injection well fully penetrates the host rock and is fully cased and pressure cemented between casing and formation. A horizontal slot (360 degrees) which cuts casing and cement wall, and penetrates the host rock is made by hydraulic-sand jet before injection. The applied hydraulic pressure separates the rock to form openings into which the injected waste is placed. Fracture at the tip of the pre-cut slot usually is initiated by water injection. After a fracture has been initiated it is followed by waste grout injection. The injected grout will solidify under pressure. After solidification the injected grout becomes an integral part of the host rocks, thereby immobilizing waste in a finite area. Waste injection can be made through the same slot for two or three consecutive injections, thereafter the well is plugged by cement to the next injection depth, and again a horizontal slot is made. Waste injections are made in a sequence from bottom upward until the disposal capacity of the injection formation is exhausted.

The major concern of the hydraulic fracturing waste disposal technique is whether horizontal fractures can be induced in the host rocks, so that the injected waste can be immobilized in a desired horizon. The overwhelming experience of hydraulic fracturing in oil wells indicates that hydraulically induced fractures are generally vertical (Hubbert, 1971) which is unfavorable for disposal of radioactive wastes. The possibility of inducing horizontal fractures by hydraulic fractures is discussed below.

The discussions are based on the assumption that the formation is isotropic and homogeneous. Admittedly this is not the case. Geologic formations generally are heterogeneous and anisotropic, especially shale formation; however, the simplified assumption appears to be valid in general as indicated by the experiments made at ORNL and West Valley, New York (Sun, 1969; 1973; 1976; Sun and Mongan, 1974). These experiments are presented in the Appendices.

3.1 Earth Stresses

In the propagation of a fracture in depth, the applied pressure in the fracture must overcome the stress normal to the fracture plane and the cohesive force at the fracture tip. Therefore, during hydraulic fracturing the amount of earth stress normal to the fracture plane must be considered.

The amount of stress at a given point in depth generally results from three types of stress components. They are: (1) gravitational stress; (2) tectonic stress; and (3) fluid pressure within the rock.

Gravitational stress results fundamentally from the weight of overlying strata. Two aspects of this stress need to be differentiated; (a) stress effects that result from the present topographic conditions and (b) stress effects that result from past topographic conditions. Tectonic stresses are induced by mobility of the earth's crust resulting from various influences, such as temperature and geochemical effects, and fluid pressure is caused by fluid in pores, such as oil, gas, and water.

3.1.1 Vertical earth stress

Consider a small element of rock at a depth z in a Cartesian coordinate system with its z-axis in the vertical direction (fig. 7). The equation of

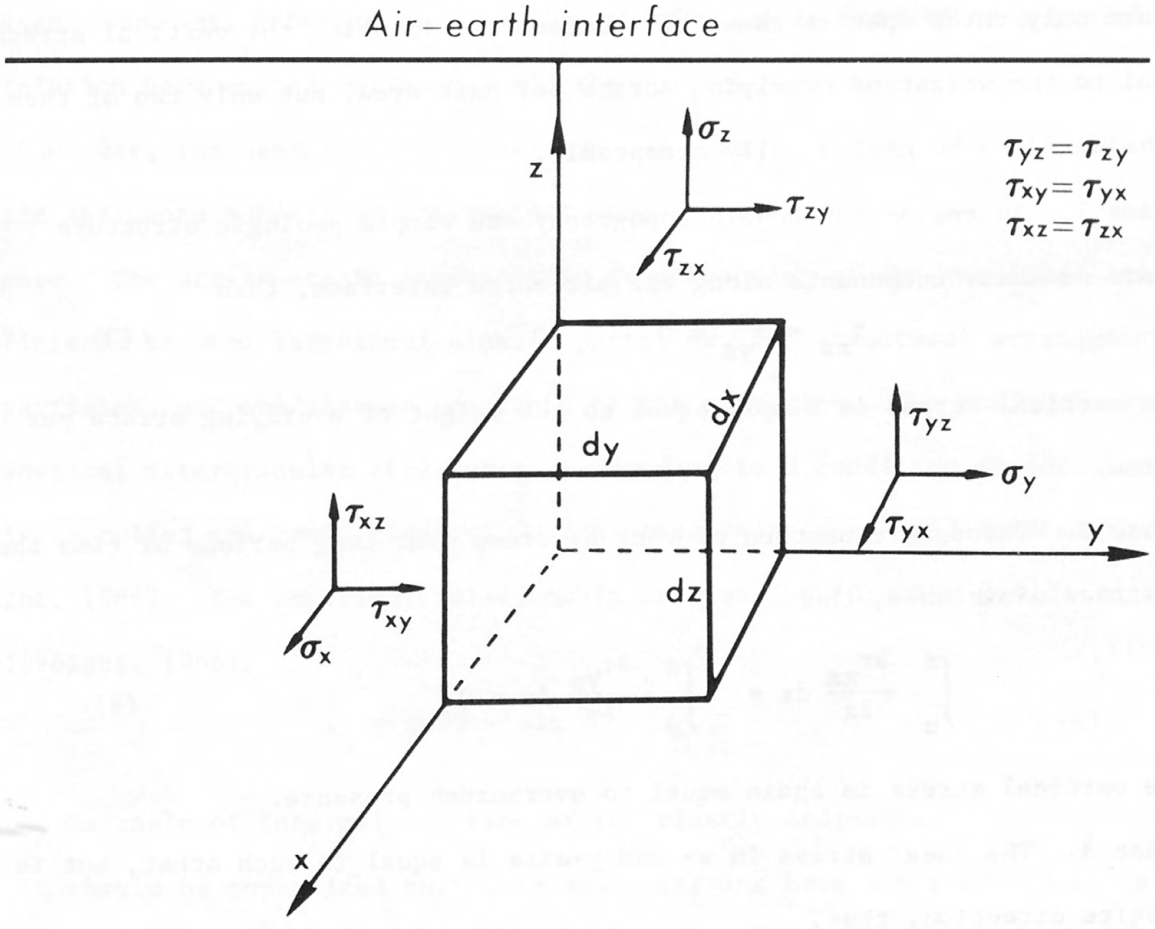

Figure 7.--Stresses on a small rectangular parallelepiped element located at depth z.

equilibrium in terms of vertical stress (Jaeger and Cook, 1969) is given by:

$$\frac{\partial \sigma_z}{\partial z} + \frac{\partial \tau_{yz}}{\partial y} + \frac{\partial \tau_{xz}}{\partial x} - \rho g = 0 \qquad (1)$$

where σ_z is the vertical stress, τ_{yz} and τ_{xz} are shear stresses, and ρ and g are density of the rock and acceleration of gravity, respectively.

Integrating equation (1) with respect to z:

$$\sigma_z = \gamma z - \int_o^z \frac{\partial \tau_{yz}}{\partial y}\, dz - \int_o^z \frac{\partial \tau_{xz}}{\partial x}\, dz \qquad (2)$$

where γ is the weight density (ρg) of overlying strata. Howard (1966) states that there are only three special cases of equation (2) in which the vertical stress is equal to the weight of overlying strata per unit area, but only two of them are considered to be geologically acceptable.

Case 1. In regions of gentle topography and simple geologic structure there are no shear components along the air-earth interface, then

$$\tau_{xz} = \tau_{yz} = 0 \qquad (3)$$

and the vertical stress is simply equal to the weight of overlying strata per unit area.

Case 2. Through relaxation of rock by creep over long periods of time the shear stress diminishes, then

$$\int_o^z \frac{\partial \tau_{xz}}{\partial x}\, dz = \int_o^z \frac{\partial \tau_{yz}}{\partial y}\, dz = 0 \qquad (4)$$

and the vertical stress is again equal to overburden pressure.

Case 3. The shear stress in x- and y-axis is equal to each other, but in an opposite direction, thus,

$$\int_o^z \frac{\partial \tau_{xz}}{\partial x}\, dz = - \int_o^z \frac{\partial \tau_{yz}}{\partial y}\, dz \qquad (5)$$

This case is geologically improbable and the condition is very restrictive, especially when compounded by choice of geographic direction for x and y axes.

Therefore, it can be concluded that in a relatively flat area with simple geologic structure, the vertical stress can be calculated as the weight of overlying strata per unit area. However, in a topographically irregular area or in a region having complex geologic structures, the vertical stress may or may not be the overburden pressure alone.

3.1.2 Horizontal earth stress

No adequate analytical models are available to estimate horizontal stresses. However, experiences in soil mechanics can be used to help explain the relation between the horizontal and the vertical stresses.

Consider, for example, the simple case of sedimentary accumulation of clastic sediments subject to a principal stress solely derived from overburden pressure. The stress-strain relationship is a function of the mobilized friction coefficients between individual clastic particles, the structural arrangement of the particles, and the elastic constants of the particles. The ratio of horizontal and vertical intergranular stresses corresponding to a condition of zero lateral strain is called the coefficient of "earth pressure at rest" and denoted by K_o (Voight, 1966). The empirical relationship is given by (Brooker and Ireland, 1965; Voight, 1966):

$$K_o = 0.95 - \sin \phi \qquad (6)$$

where ϕ is angle of internal friction of the clastic sediments.

It should be emphasized that very small strains have a marked effect on the value of horizontal stress. It was found that strains on the order of 10^{-3} are

sufficient to fully mobilize the shear strength--that is, to reduce the ratio of horizontal-to-vertical stress to the coefficient of "active earth pressure" K_a (Voight, 1966), where

$$K_a = (1 - \sin \phi)/(1 + \sin \phi) \quad (7)$$

Very little is known about the precise nature of lateral restraint to be found on the geological scale. Voight (1966) believes that horizontal strains may, in fact, vanish for certain types of sedimentary basins. The horizontal stress coefficient K which is defined as σ_h/σ_v must lie between the limiting values of the "active earth pressure" and "earth pressure at rest", and is given by:

$$(1 - \sin \phi)/(1 + \sin \phi) \leq \sigma_h/\sigma_v \leq (0.95 - \sin \phi) \quad (8)$$

In general, the angle of internal friction, ϕ, is $27\text{-}30^{\circ}$ for unjointed hard sedimentary rocks such as sandstone and limestone, and $0\text{-}20^{\circ}$ for soft sedimentary rocks such as shale and clay (Fenner, 1938; Harrison and others, 1954; Perkins, 1967; Jaeger and Cook, 1969). Then, the ratio of horizontal to vertical stresses, σ_h/σ_v, can be considered to be between 0.33 and 0.55 for hard sedimentary rocks, and between 0.49 and 0.95 for soft rocks. The average measured σ_h/σ_v in sedimentary basins in the United States containing sandstone and shale is 0.6 (McGarr and Gay, 1978).

Laboratory experiments show that a hysteresis effect exists during loading and unloading of rocks (Brooker and Ireland, 1965; Voight, 1966) thus horizontal stress is higher during unloading than loading (fig. 8). If this hysteresis effect exists in areas which have experinece significant denudation or ice sheeting unloading in the Quaternary Period, then horizontal stress probably would be higher than that calculated on the basis of the present overburden pressure.

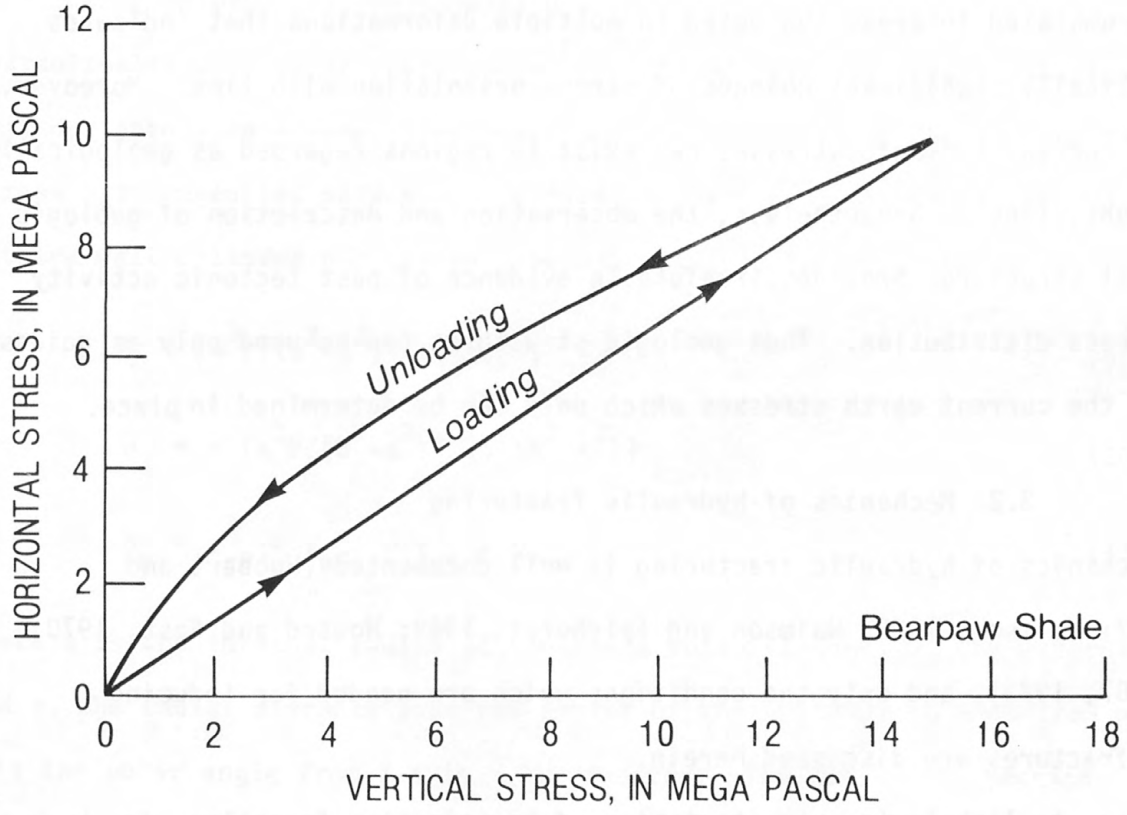

Figure 8.--Hysteresis during loading and unloading in uniaxial compression tests of Bearpaw Shale (from Brooker and Ireland, 1965).

3.1.3 Tectonic stress

The earth stresses discussed above are a result from gravitational stresses only. In addition to these stresses, rocks are also subjected to tectonic stresses. Unfortunately no analytical theory is available to estimate tectonic stresses. It also should be noted that regions subjected to current tectonic stresses are not limited to seismically active regions. Nor are such regions necessarily characterized by tectonic structures which reflect the past stress distribution. There is no requirement for current stresses to bear a geometrical relation with structures produced in prior deformational phases. There is much geologic evidence accumulated in areas subjected to multiple deformations that indicates characteristically significant changes of stress orientation with time. Moreover, significant current tectonic stresses can exist in regions regarded as geologically stable (Voight, 1966). Nevertheless, the observation and description of geologic deformational structures provides irrefutable evidence of past tectonic activity and past stress distribution. Thus geologic structures can be used only as guides in studying the current earth stresses which only can be determined in place.

3.2 Mechanics of hydraulic fracturing

The mechanics of hydraulic fracturing is well documented (Hubbert and Willis, 1957; Haimson, 1968; Haimson and Fairhurst, 1969; Howard and Fast, 1970; Daneshy, 1967, 1973), and only the conditions which are needed for inducing horizontal fractures are discussed herein.

According to lithologic characteristics of an injection formation, fracture walls can be classified in two categories: (1) both walls are relatively impermeable as fractures formed in thick shale; and (2) one or both walls are permeable, as fractures formed along the interface of shale and sandstone or within sandstone.

For disposal of radioactive wastes, one of the required conditions is to minimize the possibility of grout leaching by ground water and to reduce the potential for grout dilution by ground water during injection, therefore, it is mandatory to select low permeability (less than 10^{-6} darcy) formations as injection host rocks. Also the injection well should be cased and pressure cemented in full length. Therefore, only the case of fractures with relatively impervious walls induced by non-penetrating fluid is considered.

3.2.1 Stresses around uncased boreholes

During injections, the injection well is enclosed at the well head, and hydraulically induced stresses around the well can be determined by thick wall cylinder stress equations (Timoshenko and Goodier, 1951). The induced radial stress σ_r; tangential stress σ_t; vertical stress σ_z; and shear stress τ, of a thick wall cylinder subject to internal pressure P, are given by:

$$\sigma_r = [a^2P/(b^2-a^2)]\ [(b^2/r^2) - 1] \tag{9}$$

$$\sigma_t = -\ [a^2P/(b^2-a^2)]\ [1+(b^2/r^2)] \tag{10}$$

$$\sigma_z = \tau_{r\theta} = \tau_{z\theta} = \tau_{rz} = 0 \tag{11}$$

where a is the internal radius of the thick wall cylinder, b, the external radius, and r, the radial distance from the center of the cylinder to a desired point, and θ is the polar angle from X-axis. The negative sign represents tension.

Because the injection well is constructed in a thick impervious formation which extends radially to a great distance, the value of b can be considered to be very large as compared with the value of well radius a. Equations (9), (10), and (11) can be rewritten as:

$$\sigma_r = P(a^2/r^2) \tag{12}$$

$$\sigma_t = -P(a^2/r^2) \tag{13}$$

$$\sigma_z = \tau_{r\theta} = \tau_{z\theta} = \tau_{rz} = 0 \tag{14}$$

The induced radial and tangential stresses will reach maximum, the value of P, at the well face and diminish quickly away from the well.

The effects of a well on a pre-existing stress field can be calculated by analogy to an infinitely large plate, subjected to uniaxial stress and containing a circular hole with its axis perpendicular to the plate, which was solved by Kirsch in 1898 (Timoshenko and Goodier, 1951). The stresses in the vicinity of a well, subjected to two horizontal stresses σ_x and σ_y, can be obtained by the Kirsch solution and the law of superposition (fig. 9). The

results are given by:

$$\sigma_r = [(\sigma_x + \sigma_y)/2]\ (1 - a^2/r^2) + [(\sigma_x - \sigma_y)/2]\ (1 + 3a^4/r^4 - 4a^2/r^2)\ \cos 2\theta \tag{15}$$

$$\sigma_t = [(\sigma_x + \sigma_y)/2][(1 + a^2/r^2) - [(\sigma_x - \sigma_y)/2]\ (1 + 3a^4/r^4)\ \cos 2\theta \tag{16}$$

$$\sigma_{r\theta} = [(\sigma_x - \sigma_y)/2](1 - 3a^4/r^4 + 2a^2/r^2)\ \sin 2\theta \tag{17}$$

where a, is the radius of the well, r, the radial distance from the center of the well, and θ, the polar angle from the x-axis moving counterclockwise (fig. 9).

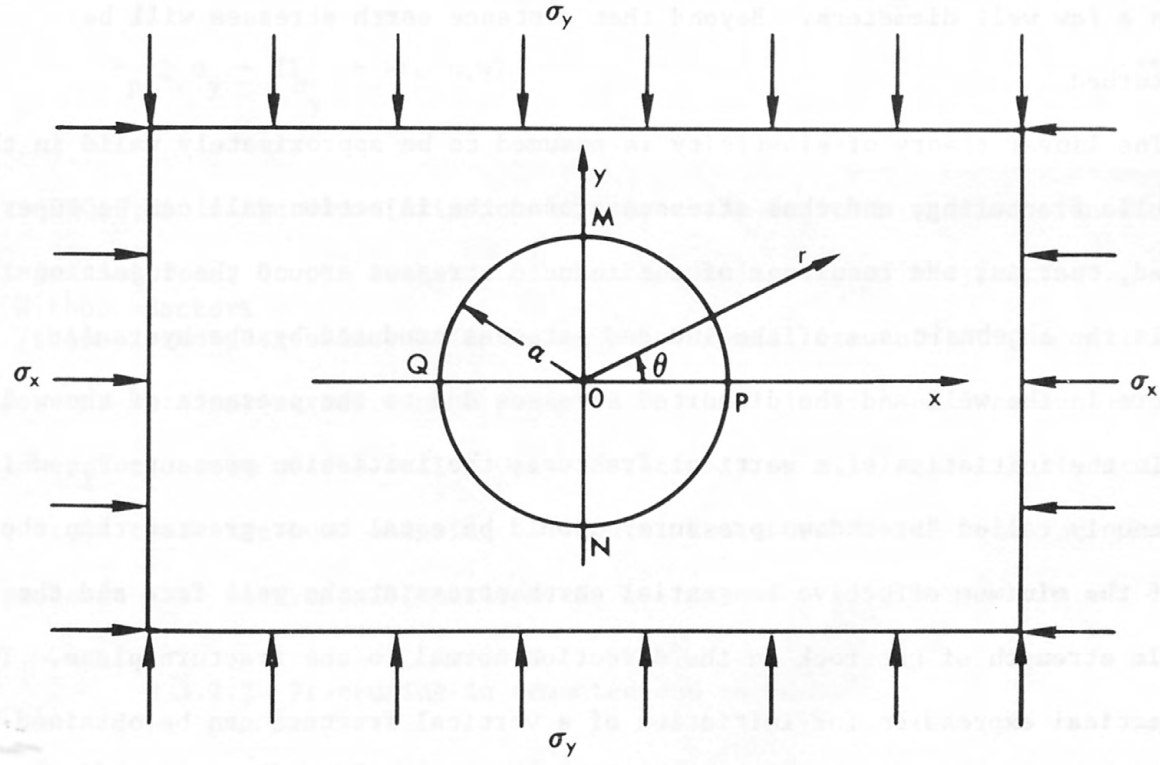

Figure 9.--Stresses on an infinitely large plate with a circular hole.

From eqs. (15) and (17), it can be seen that the radial and shear stresses are zero at the well face and increase rapidly toward the undisturbed stress field within a few well diameters. Equation (16) shows that, at the well face (r=a), the tangential stress reaches a minimum value at $\theta=0°$ and $\theta=180°$, with a magnitude of $(3\sigma_y - \sigma_x)$, if $\sigma_x > \sigma_y$. This minimum stress can be either compressional or tensional depending on the ratio of σ_x/σ_y. When σ_x is greater than $3\sigma_y$ the stress is in tension. The maximum stress on the well face is at $\theta=90°$ and $\theta=270°$, with a magnitude of $(3\sigma_x - \sigma_y)$ and is always in compression. In the case where both horizontal stresses are equal, $\sigma_x=\sigma_y$, then the tangential stress around the well face is the same everywhere, with a magnitude of $2\sigma_h$.

In conclusion, the effect of a well on horizontal stresses is localized within a few well diameters. Beyond that distance earth stresses will be undisturbed.

The linear theory of elasticity is assumed to be approximately valid in the hydraulic fracturing, and thus stresses around the injection well can be superimposed, that is, the resultant of the induced stresses around the injection well is the algebraic sum of the induced stresses produced by the hydraulic pressure in the well and the distorted stresses due to the presence of the well.

In the initiation of a vertical fracture, the initiation pressure P_i, which is commonly called "breakdown pressure" should be equal to or greater than the sum of the minimum effective tangential earth stress at the well face and the tensile strength of the rock in the direction normal to the fracture plane. The mathematical expression for initiation of a vertical fracture can be obtained from eqs. (13) and (16), and when r=a, $\theta=0°$ and 180°, the result is:

$$P_i - p_o \geq 3(\sigma_y - p_o) - (\sigma_x - p_o) - T_{\sigma_y}; \text{ if } \sigma_x > \sigma_y \qquad (18)$$

or

$$P_i \geq 3\sigma_y - \sigma_x - p_o - T_{\sigma_y} \qquad (19)$$

where T_{σ_y} is the tensile strength of the rock in the direction of σ_y and is considered to be negative, and p_o is the pore pressure at a depth where the hydraulic fracturing is being made.

Because the presence of a well distorts the existing stresses only in an area within a distance of a few well diameters from the well, the required "propagation pressure" P_p to extend the initiated vertical fracture is the sum of the minimum effective earth stress, the cohesive force at the fracture tip and the fluid frictional loss in the fracture. The mathematical expression is given by:

$$P_p - p_o \geq \sigma_y - p_o - fT_{\sigma_y} + F(Q,L,W); \text{ if } \sigma_x > \sigma_y \tag{20}$$

or

$$P_p \geq \sigma_y - fT_{\sigma_y} + F(Q,L,W) \tag{21}$$

Where F(Q,L,W) is the fluid frictional loss in the fracture and is a function of injection rate, Q, the length, L, and the opening, W, of the fracture.

Without packers /there is no possibility of inducing a horizontal fracture at the well face, because no vertical stress can be produced in the injection well except at the well head or bottom of the well. Only if there is an artifical horizontal cut, or if there are some existing horizontal fractures at the well face is it probable that horizontal fractures can be induced.

3.2.2 Fracturing in cemented and cased holes

In this case, the injection well is cased and pressure cemented in full length. Before injection, a horizontal cut (360 degrees) is made by hydraulic-sand jetting. The cut, which extends about 30 cm into the host rock serves as

a weak plane. During an injection, the well head is enclosed, the injection fluid enters the cut and creates vertical stresses.

Due to additional tensile strength (at least several tens of mega pascals) provided by casing and cement and a weak horizontal plane (the pre-cut) at the well face, the induced fracture undoubtedly is initially in the horizontal direction, at least to a moderate depth of several thousands of meters, in spite of the horizontal direction of the least principal stress. However, at a greater depth, the additional tensile strengh provided by the casing and cementing may be overcome by the great overburden pressure and thus a vertical fracture could be induced at cemented and cased wells.

In areas where the least stress (sum of the earth stress and the cohesive force at the fracture tip) is in one of the horizontal directions, even if the fracture initiated at the well face is horizontal, the induced fracture should turn vertical when the fracture propagates away from the injection well, so that the plane of the fracture will be normal to the least stress, and the required work to rupture the rock is minimum.

The breakdown pressure to form a horizontal fracture is equal to or greater than the sum of the vertical stress (σ_z) and the tensile strength of the rocks in the vertical direction. The mathematical expression is given by:

$$P_i \geq \sigma_z - T_{\sigma_z} \tag{22}$$

The propagation pressure is:

$$P_p \geq \sigma_z - fT_{\sigma_z} + F(Q,r,W) \tag{23}$$

where T_{σ_z} is the tensile strength of the rock in the vertical direction, and $F(Q,r,W)$ is the fluid frictional loss in the fracture and is a function of injection rate, Q, the radial distance, r, and the opening, W, of the fracture.

3.2.3 Fracturing in bedded rocks

Experimental results and geological observations show that bedded rocks have directional tensile strength. Because of low cohesion between bedding planes and the lineation of clay mineral and microfractures parallel to bedding planes, bedded rocks frequently have the smallest tensile strength in a direction normal to bedding planes and have the greatest tensile strength in the direction parallel to bedding planes. Laboratory data indicate that the value of tensile strength of bedded rocks, such as shale, in the direction normal to bedding planes ranges from about 20 to 80 percent of the values in a direction parallel to bedding planes, but in most cases, the value is on the order of 30 percent (Hobbs, 1964; Chenevert and Gatlin, 1965; Youash, 1965; and Obert and Duvall, 1967).

Let σ_1, σ_2, and σ_3 be three principal stresses of different magnitudes. The order of magnitude is represented by subscript numbers, respectively, σ_3 being the least stress. If the stress condition that is the most favorable for producing vertical fractures is assumed, then the maximum principal stress, σ_1, should be in the vertical direction and the least stress, σ_3, lies in one of the horizontal directions. Also assume the bedding planes of the host rock making an angle of ω with the well axis (fig. 10), then the stresses along the

bedding planes, σ_a, and normal to bedding planes, σ_n, can be calculated by Mohr's stress circle; and are given by,

$$\sigma_a = (\sigma_1 + \sigma_3)/2 + [(\sigma_1 - \sigma_3)/2] \cos 2\omega \qquad (24)$$

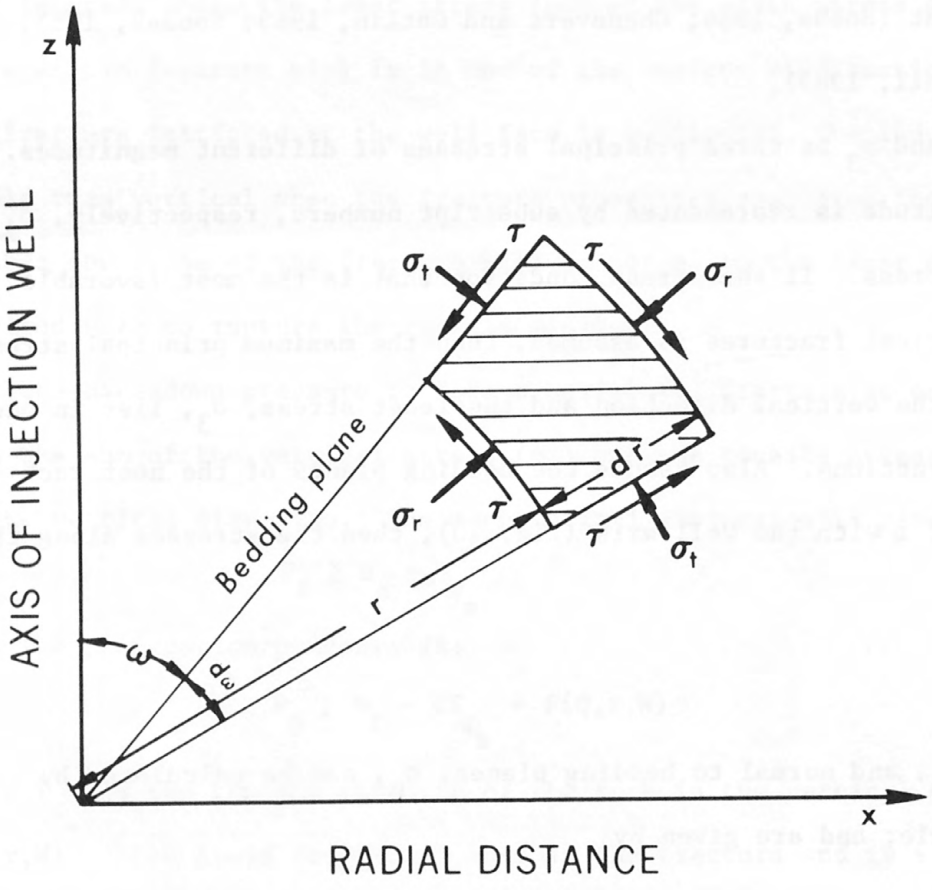

Figure 10.--Stresses on a bedding plane of rock with respect to axis of injection well.

$$\sigma_n = (\sigma_1 + \sigma_3)/2 - [(\sigma_1 - \sigma_3)/2] \cos 2\omega \quad (25)$$

$$\tau_{an} = [(\sigma_1 - \sigma_3)/2] \sin 2\omega \quad (26)$$

Pressure required to initiate a fracture along or normal to bedding planes should be equal or greater than the sum of the stress given by eq. 24 or eq. 25 and the tensile strength of the rock in the direction parallel (T_a) or normal to the bedding planes (T_n). The mathematical expressions are given by:

$$P_i \geq (\sigma_1 + \sigma_3)/2 + [(\sigma_1 - \sigma_3)/2] \cos 2\omega - T_a \quad (27)$$

for a fracture initiated in the direction normal to the bedding planes; and

$$P_i \geq (\sigma_1 + \sigma_3)/2 - [(\sigma_1 - \sigma_3)/2] \cos 2\omega - T_n \quad (28)$$

for a fracture initiated in the direction parallel to bedding planes.

Pressure required to propagate a fracture along or normal to bedding planes should be equal or greater than the sum of the stress given by eq. 24 or eq. 25; the cohesive force at the fracture tip; and fluid frictional loss in the fracture. The mathematical expressions are:

$$P_p \geq (\sigma_1 + \sigma_3)/2 + [(\sigma_1 - \sigma_3)/2] \cos 2\omega - fTa + F(Q,r,W) \quad (29)$$

for a fracture extending in the direction normal to bedding planes, and

$$P_p \geq (\sigma_1 + \sigma_3)/2 - [(\sigma_1 - \sigma_3)/2] \cos 2\omega - fT_n + F(Q,r,W) \quad (30)$$

for a fracture extending in the direction parallel to bedding planes. The condition for extending a bedding-plane fracture is as follows:

$$(\sigma_1+\sigma_3)/2 - [(\sigma_1-\sigma_3)/2] \cos 2\omega - fT_n \leq (\sigma_1+\sigma_3)/2 + [(\sigma_1-\sigma_3)/2] \cos 2\omega - fT_a \quad (31)$$

When ω is equal or less than 45 degrees, a bedding-plane is always to be extended. However, when ω is greater than 45 degrees, then the condition for extending a bedding-plane fracture is:

$$(\sigma_3 - \sigma_1)\cos 2\omega \leq f\,(T_n - T_a) \quad (32)$$

3.2.4 Fracturing in fractured and jointed bedded rocks

Virtually all rocks including glacial tills have fractures or joints. Some investigators believed that hydraulic pressure in the injection well causes joints or existing fractures to extend (Bugbee, 1953; Heck, 1955, 1960), and therefore, the orientation of hydraulically induced fractures is controlled by joints or by existing natural fractures; hence, it can be predicted by studying the surface joint patterns (Overby and Rough, 1968). However, laboratory studies by Lamont and Jessen (1963) showed that the orientation of hydraulically induced fractures would be determined primarily by the orientation of the least principal stress; hence hydraulic fractures can extend across pre-existing joints or fractures. The location of an existing plane of weakness, such as joints and fractures, does not alter the orientation of induced fractures appreciably. Are the latter statements true, if so, under what conditions?

Again it is assumed that: (1) the dominant principal stress σ_1, is in the vertical direction and the least principal stress σ_3 lies in one of the horizontal directions; and (2) the existing fracture or joint plane makes an angle β, and the bedding planes make an angle ω with the well axis (fig. 11). Under such conditions the pressure required to propagate an existing vertical fracture is given by:

$$P_p \geq (\sigma_1+\sigma_3)/2 - [(\sigma_1-\sigma_3)/2] \cos 2\beta - fT_n \cos(\omega-\beta) - fTa \sin(\omega-\beta) + F(Q,r,W) \quad (33)$$

The pressure required to extend a bedding-plane fracture is given by:

$$P_p \geq (\sigma_1+\sigma_3)/2 - [(\sigma_1-\sigma_3)/2] \cos 2\omega - fT_n + F(Q,r,W) \quad (34)$$

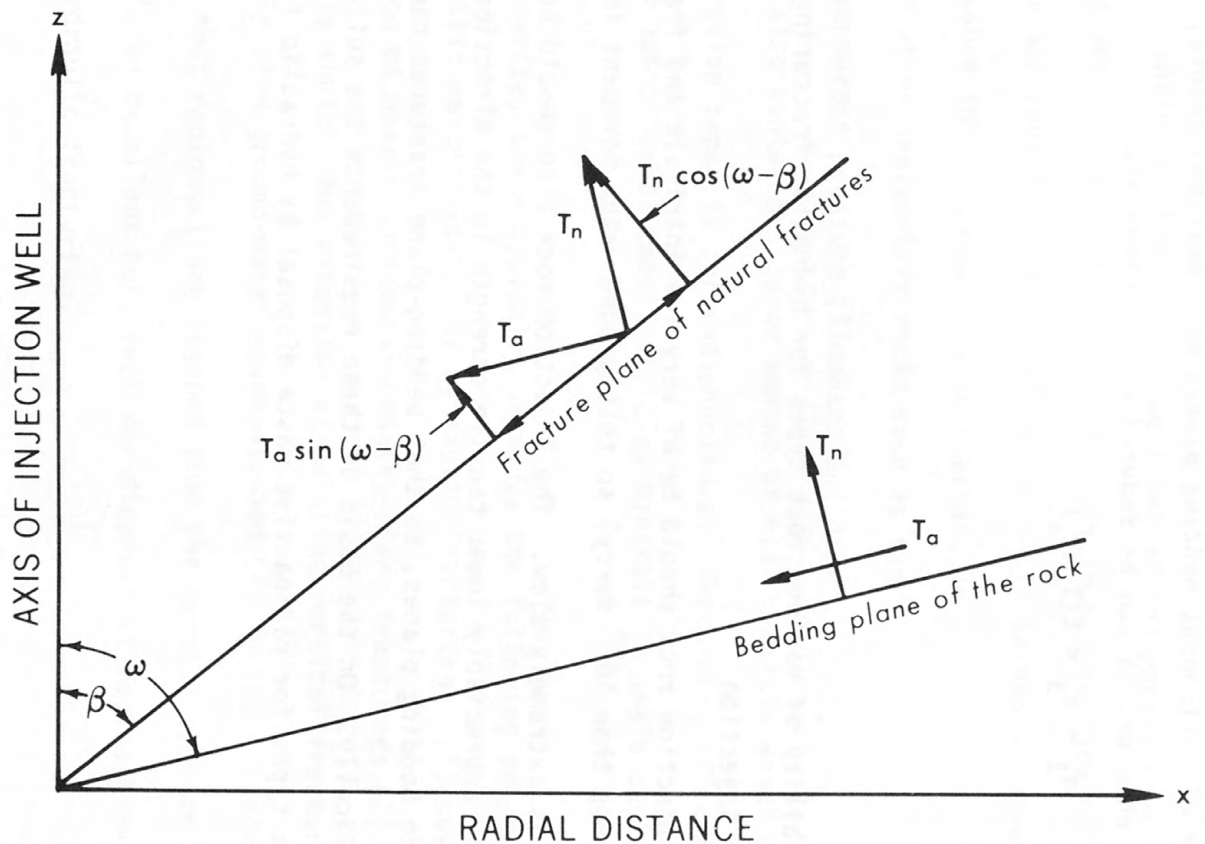

Figure 11.--Tensile stresses on a fracture plane of a natural fracture and bedding plane of rock with respect to axis of injection well.

The condition for propagating a bedding-plane fracture without extending an existing fracture is that the value of P_p calculated by eq. 34 should be less than that calculated by eq. 33. The result is given by:

$$[(\sigma_3-\sigma_1)/2] \cos 2\omega - fT_n \leq [(\sigma_3-\sigma_1)/2] \cos 2\beta - fT_n \cos(\omega-\beta) - fT_a \sin(\omega-\beta) \quad (35)$$

In the case of vertical joints, that is, $\beta=0°$, eq. 35 can be written as:

$$[(\sigma_3-\sigma_1)/2] \cos 2\omega - fT_n \leq (\sigma_3-\sigma_1)/2 - fT_n \cos\omega - fT_a \sin\omega \quad (36)$$

In the case of horizontal bedding planes with vertical joints, that is, $\omega=90°$ and $\beta=0°$, then eq. 35 can be reduced and is given by,

$$\sigma_1 - \sigma_3 < f(T_n-T_a) \quad (37)$$

3.3 Suitability of various rock types for hydraulic fracturing and waste injection

The host injection rock should be of very low intrinsic and fracture permeability (less than 10^{-6} darcy) so that ground water movement in the injection zone is extremely slow. The injection rock also should be characterized by appreciably lower tensile strength in the direction normal than parallel to bedding planes, so that bedding-plane fractures can be induced hydraulically. On the basis of these requirements the suitability of various rock types for radioactive waste disposal by hydraulic fracturing is discussed.

3.3.1 Shale

Permeability of shale without closely spaced fractures or joints is low, generally ranging from 10^{-6} to 10^{-9} darcy (Magara, 1978; Davis, 1969; Young, et al, 1964).

Layered sedimentary rocks usually have directional tensile strengths (Hobbs, 1964), however, the difference in tensile strength between the direction normal and parallel to bedding planes is more dominant in bedded shale than that in other sedimentary rocks. Field evidence indicates that joints or fractures in shale usually stop at well bedded and poorly cemented zones.

Direct measurements of in-situ stresses in sedimentary rocks suggests that the minimum horizontal principal stress in shale is nearly equal to the overburden pressure in geologically stable areas, however, the horizontal stresses measured in other sedimentary rocks such as sandstone are generally much less than the overburden pressure (Simonson and others, 1978).

Shale also contains a large amount of clay minerals which usually have large adsorption capacity for radionuclides. Therefore, if some radionuclides are leached out of grout sheet, the clay minerals in shale can further retard their movement.

To summarize, shale typically provides the following properties favorable for radioactive waste disposal by hydraulic fracturing: (1) susceptibility to the induction of nearly horizontal bedding-plane fractures; (2) bedding planes that probably inhibit the extension of existing vertical fractures and joints; (3) extremely slow ground-water movement; and (4) further retardation by clay minerals of most radionuclides leached from the grout. Thus it is concluded that shale is an excellent host rock for disposal of radioactive wastes by grout and hydraulic fracturing.

3.3.2 Sandstone and limestone

The permeability of sandstone and limestone generally ranges between 10^{-1} and 10^{-4} darcy (Davis, 1969), which is about five orders of magnitude greater than the shale permeability. Further, the difference between the tensile strength in the direction normal and parallel to bedding planes is small, therefore, except under particular circumstances, sandstone and limestone are not recommended as host rocks for disposal of radioactive wastes by hydraulic fracturing.

3.3.3 Crystalline igneous and metamorphic rocks

Permeability of most crystalline igneous and metamorphic rocks probably is in the same order of magnitude or even lower than the shale permeability; however, the difference in directional tensile strength as related to bedding planes diminishes. On the other hand, most crystalline rocks have considerable vertical fractures. Nearly horizontal fractures probably can be induced hydraulically only in the areas with the least principal earth stress in the vertical direction, that is, in areas with residual stresses evidence by earth movements, or in areas undergoing greatly induced isostatic rebound. Unless field evidence or in-situ stress measurements indicate that the least principal earth stress is in the veritcal direction and without closely spaced vertical fractures, crystalline igneous and metamorphic rocks should not be considered as radioactive waste disposal host rocks by hydraulic fracturing.

4. SITE EVALUATION

The geohydrologic investigation during site evaluation should cover an area of at least several square kilometers beyond a site under consideration and should include the following items.

4.1 Geology

Well-bedded shale with nearly horizontal and loosely cemented bedding planes, without known fault(s) or closely spaced joints or natural fractures, appears to be the best injection formation. Shale is frequently interbedded with other sedimentary rocks, such as sandstone or limestone. Thickly interbedded shale, if possible, should not be selected as host rock.

To assure inducing nearly horizontal bedding-plane fractures and to reduce the complexity of interpreting investigation results, areas with simple geologic structures and flat topography are preferred. Areas with high topographic relief and complex geologic conditions, if possible, should be avoided. The host rock should be at depth shallower than 1,000 m, thus reducing the potential for inducing vertical fractures.

The possibility of chemical and physical changes of rock characteristics by waste injection needs to be evaluated. Normally, characteristics of shale will not be changed or altered by wastes as long as radioactive decay will not raise temperature above 100^{o}C. However, at elevated temperatures in shale, montmorillonite-illite undergoes a phase transition involving increase in illite and liberation of free water. This water plus preexisting pore water will probably be in the form of steam or at least become hot water. Oxygen, carbon dioxide, hydrogen sulfide, and other gases may also be released. Interaction among preexisting minerals, volatile components, and waste will be promoted by high temperatures. Experience indicates that hot moving fluids may alter

existing minerals and form new ones, thus causing significant changes in permeability (Bredehoeft and others, 1978) and adsorbability. Limited by present knowledge, radioactive waste whose cumulative decay temperature plus existing ground water temperature are above 100°C at the disposal depth is not recommended for disposal in shale or other rocks by grout injection and hydraulic fracturing without further studies.

4.2 Hydrology

The major concern about hydrology related to disposal of radioactive wastes by hydraulic fracturing is ground-water movement. It is perferable to know the regional and local ground water flow in the host rock. Based on this information the average travel time of ground water flow to points of discharge can be estimated. Ground-water investigation methods have been well documented (Hantush, 1964; Walton, 1970; Bear, 1972; Prickett and Lonnquist, 1971; Freeze and Cherry, 1979) and will not be discussed in this report.

Information on total sediment load carried by streams in the area of the proposed disposal site is also valuable. This information can be used to estimate long term erosion rates at the proposed site.

Surface runoff is not only one of the major forces for erosion, but also can be a source or sink of local ground water flow. Therefore, it is important to understand the interaction between streamflow and ground water flow and the depth of interaction. Interaction ideally should be limited to approximately the upper few tens of meters below ground surface, whereas the injection rock should be at a depth of at least several hundreds of meters.

4.3 Geologic stability

The chance of successfully immobilizing the radioactive wastes in the injected rocks depends on the geologic stability of the disposal site for many

thousands of years so that radionuclides can decay to a point at which their concentrations no longer constitute a health hazard. Tectonism, diapirism, volcanism, glaciation, climatic change, seismicity and erosion are the major activities causing geologic instability. Presently no reliable methods can be used to predict these activities for millions of years to come. However, if injected wastes are diluted to lower concentrations (below the specific activity of 6×10^3 μCi/mℓ as experienced at ORNL) and limited to radionuclides having half-lives of less than 50 years, such as Sr^{90} and Cs^{137}, then the time period for which geologic stability has to be predicted can be reduced to about one thousand years. The degree of reliability of predictions for this time period is increased considerably (Interagency Review Group on Nuclear Waste Management, 1979). However, it is still impossible to predict precisely about the behavior of the grout and the ability of rocks to sorb the radionuclides of the waste. However, the degree of uncertainty of prediction is reduced greatly.

Past geologic events such as faulting, glaciation, and seismicity have not been random, therefore, past records might be used for estimation. Regional on site stress measurements are used not only to estimate or determine whether nearly horizontal bedding-plane fracture can be induced but also to evaluate the geologic stablity. Any evidence of tectonic instability, local or nearby, seismicity in the disposal area should be certain cause for elimination from the candidate list.

4.4 Interference with resources exploitation

Resources beneath the injection zones can be developed after the disposal of wastes as long as precautions are taken during and construction of mining shafts or drill holes. Because the solidified grout sheet becomes an integral part of the host rock, penetration of radiation to mining shafts can be avoided or reduced to acceptable levels by sealing off the injection zone using strong casing and thick cement walls. If doubts remain on the acceptability of mining shafts through the injection zone, the future value of potential resources must be weighed against the benefits of disposal of the radioactive wastes.

5. SITE INVESTIGATIONS

After a site is selected, the site must be investigated specifically to see whether nearly horizontal bedding-plane fractures can, in fact, be induced without possibility of inducing vertical fractures, and whether permeability of the host rock is sufficiently low. The site investigation should follow the procedures discussed below.

5.1 Test drilling

At least one corehole is needed to obtain geophysical logs and on site subsurface geology including lithology, frequency and condition of joints or fractures, elastic constant and directional tensile strength of the host rock. If possible, the corehole should be drilled by air. The corehole should be tested by injected water in determining formation permeability. If a significant amount of water is transmitted by interconnected joints or fractures then the selected site should be abandoned. The corehole should be drilled to the full depth of the total injection thickness. If all evidence indicates that the selected site is suitable for waste disposal then the corehole can be constructed either as a future injection well or as one of the observation wells. An injection well is cased with fairly heavy casing and pressure cemented in full depth. Observation wells should also be cased with strong tubing or casing and also pressure cemented to full depth. The size of observation wells should be large enough for free movement of a logging probe along the well and for free movement of drilling tools if the well is to be serviced after completion.

If the corehole is converted to an injection well, then at least four observation wells should be constructed at a radial distance of about 50 m from the injection well in the same manner as the injection well, except for a smaller diameter. These observation wells will be used in locating the position of

induced fractures after each fracturing, if the injection fluid is tagged with gamma-emitting radionuclides.

5.1.1 Geophysical logging

In addition to geophysical logs--such as electric log, caliper log, and fracture televiewer log for lithologic identification, determination of borehole conditions, and altitude presence/of joints and fractures--gamma-ray logs and borehole deviation logs must be run in all wells. Deviation logs will be used to obtain true position and vertical distance/of the well at any desired depth. The following formulas (Gatlin, 1960) are suggested to be used in calculating the true positions.

$$Z = MD \cos \alpha \tag{38}$$

$$H = MD \sin \alpha \tag{39}$$

$$y = H \cos \beta \tag{40}$$

$$x = H \sin \beta \tag{41}$$

where

Z = true vertical distance between well survey points 1 and 2;

MD = measured distance along the well axis between points 1 and 2;

H = horizontal displacement of well at any desired depth/ from the well center at surface;

y = horizontal departure/ at any desired depth, distance north or south / from the East-West axis;

x = horizontal departure/ at any desired depth, distance east or west / from the North-South axis

(the origin of the East-West and the North-South axis is located at surface of the well);

α = vertical deviation angle determined by deviation log;

β = bearing (compass direction) determined magnetically during logging.

A whole well-length gamma-ray log should be carefully run in all wells before and after each injection. The logs should be recorded on paper, rather than by visual inspection during logging. A full-length gamma-ray log

not only gives opportunities for careful office studies but also serves as a public documentation of the site investigation.

The initial gamma-ray logs during well construction are not only used to identify rock units but also serve as baseline information of natural gamma radiation of the rock. The baseline information will be compared with the logs made after an injection to determine the location and depth of the induced fractures in the vicinity of the observation wells.

To reduce complexity of comparing the pre- and past-injection gamma-ray logs, logs should be run at the same speed and instrumental settings. Variation of instrumental/settings during logging not only increases the complexity of data interpretation but also increases chances of missing evidence for determination of induced fractures.

5.1.2 Core analyses

Cores obtained at a potential injection zone should be used for determining directional tensile strengths and elastic constants. Permeability (vertical and horizontal) and radionuclide adsorption properties of the rock should also be evaluated in a laboratory by using cores. These data will be useful for the study of the safety of radioactive waste disposal at the site.

5.1.3 Strikes and dips of host rocks

The average strike and dip of the selected host rock should be measured or estimated. These data will be used in the prediction and confirmation of induced bedding-plane fractures near observation wells. This prediction and confirmation increases the reliability of site-investigation results and the confidence in the disposal method.

Strike and dip of rock units can be calculated from gamma-ray logs and the three-point method described by Lahee (1952, p. 711-714) and from surface mapping data. The results discussed in Appendice (section A2.8) indicate that the method was reliable when used in the ORNL site evaluation.

5.2 Hydraulic fracturing tests

The selected site should be tested by actual injections. At least one water injection and one grout injection with a total volume of about 400 m^3 per injection should be made to determine whether bedding-plane fractures can be induced. Each of the injection tests should be made with a short-lived gamma-emitting radioactive isotope as a tracer, such as Zr^{95} or Nb^{95}. The probable altitude and orientation of induced fractures should be projected before injection by using the calculated strike and dip of the rock unit. After injection, the predicted altitudes and orientation of the induced fractures should be checked using the gamma-ray logs made in observation wells after the injection.

A water injection should be made first. The purpose of a water injection is to ascertain whether the injected shale has very low permeability and no interconnecting fractures, and to determine the vertical earth stress which may or may not be the weight of overburden at the site. For example, Moye (1958) pointed out that the field measured vertical earth stress is about 1.3 to 2.1 times greater than the calculated overburden pressure at Tumut Valley, Snowy Mountains, Australia. The well head of the injection well should be closed under pressure upon termination of the water injection, so that pressure decay in the well can be observed thereafter. If the pressure decay is very slow (maintain wellhead pressure for weeks or months), it indicates that the injection rock is sufficiently impermeable for ground-water movement. If nearly horizontal bedding-plane fractures have been induced as indicated by gamma-ray logs made in

observation wells after the injection, the vertical earth stress can be calculated from the pressure decay-time data (see section 5.3). The information on vertical earth stress at the site is useful for safety monitoring during waste injections. If injection pressure falls below the calculated vertical earth stress during a waste injection, the injection should be terminated immediately to ascertain whether induced fractures have intercepted a well interconnected joint system or have become vertically orientated.

Some investigators may question the wisdom of having a water injection during a site investigation, because they believe that several hundred cubic meters of water may be left in the host rock. The water could mix with injection grout during future waste injections and adversely affect the retention of radionuclides. The host rock probably is already saturated with water. The rock, , despite the low permeability of the host/ injected water eventually leaks out of the induced fractures/ into the rock mass during the period of construction of disposal equipment, if the site is finally selected. The volume of water injected would be small compared to the total volume of water held by the host rock in the injection zone. Therefore, the injected water left in the host rock by a water injection should not disturb the injection formation, and thus no adverse effect would be anticipated during waste injections.

The importance of a grout injection during a site investigation is that it not only will simulate actual waste injections, but also can confirm the results obtained from the water injection. This confirmation is important for increasing the confidence in the suitability of the site for waste disposal.

5.3 Interpretation of hydraulic fracturing test data

Injection pressure, pressure decay, and uplift produced by injections will give indirect evidence of the orientation of the induced fractures. Gamma-ray logs made in observation wells after and before each injection will give the

actual orientation of the induced fractures within the area between the injection well and the observation well, if the injection fluid is tagged with gamma-emitting radionuclides.

5.3.1 Interpretation of pressure data

Injection pressure, pressure decay, rate of injection and volume of injection should be observed at the well head of an injection well. Pressure decay of a water injection is a complicated phenomena. At the present time, no analytical solution has been established. An empirical relation between pressure decay and time has been found during field experiments at West Valley, New York (Sun and Mongan, 1974); the relationship is given by:

$$P - p_o = Ct^{-k} \qquad (42)$$

where P is the observed pressure decay at a particular time t, and p_o is the formation fluid pressure at the injection depth. C and k are constants. Plotting $(P - p_o)$ against t on log-log graph paper should result in a straight line, if k remains unchanged. However, if the geometry of the induced fractures changes, then the value of k will change.

As the well is shut-in, the fluid pressure in the induced fracture is much higher than the fluid pressure in the formation surrounding the fracture, thus, water starts to flow from the induced fracture into the formation, despite the low permeability of the host rock. Fluid pressure in the induced fractures declines, thus affecting the fluid pressure in the injection well; and the plot of the observed $(P - p_o)$ against t on log-log graph paper will fall on a single line. As soon as the fluid pressure in the induced fracture is reduced to a value which is less than the effective earth stress normal to the fracture plane, the fracture is reduced in size. Thus the pressure decay in the induced fracture is not only

affected by water leaking out of the fracture, but also by the reduction of the fracture volume, therefore, the slope of the line of $(P - p_o)$ versus t will change. The pressure at the discontinuity point of the $(P - p_o)$ and t curve can be interpreted as the effective earth stress normal to the fracture plane. If the evidence obtained from gamma-ray logs made in observation wells after the injection indicates that nearly horizontal bedding-plane fractures have been induced then the vertical earth stress, σ_z , can be estimated as the pressure at the discontinuity point shown by the $(P - p_o)$ and t curve.

Injection pressure is composed of three elements: (1) breakdown pressure; (2) propagation pressure; and (3) instantaneous shut-in pressure. Breakdown pressure and propagation pressure have been defined previously (section 3.2.1). Instantaneous shut-in pressure is the pressure at the instant the injection pump is stopped. At this time, no fluid is entering the injection well, therefore, the flow resistance in the induced fracture is zero, thus the instantaneous shut-in pressure is equal to the sum of earth stress normal to the fracture plane and cohesive force at the fracture tip. From equation 23, it can be shown that the propagation pressure is equal to the instantaneous pressure after the injection pump has stopped.

If flow through induced fractures is assumed to be laminar and it obeys Darcy's law, then the injection pressure at the well should be linearly proportional to the injection rate. This assumption has been proven to be correct by using polynomial regression of the injection data observed at West Valley, New York site which showed that only the linear term of injection rate, Q, has significance statistically by F-tests (Sun and Mongan, 1974).

During the stage of fracture initiation, the injection pressure must be built up to overcome the tensile strength of the rock. After the rock is broken,

the injection pressure gradually decreases to the required propagation pressure. During this transitional stage, the injection pressures are not linearly proportional to the injection rates. Excluding these pressures, a linear regression equation can be established, and is given by

$$P_p = A + BQ \tag{43}$$

Where P_p is the bottom-hole injection pressure; Q is the injection rate; A and B are regression constants. If a nearly horizontal bedding-plane fracture has been induced, then A is the sum of the vertical earth stress and the cohesive force, fT, at the tip of the induced fracture. The reliability of the regression constant, A, can also be checked by observed instantaneous shut-in pressure, that is, when Q is equal to zero

$$P_p = A \tag{44}$$

Where A is the instantaneous shut-in pressure.

If a nearly horizontal bedding-plane fracture has been induced, the tensile strength of the rock can be estimated from equation 22 and is given by,

$$T_{\sigma_z} = \sigma_z - P_i \tag{45}$$

Where T_{σ_z} is the tensile strength in the direction normal to bedding planes; σ_z the vertical earth stress; and P_i the breakdown pressure.

After the tensile strength in the direction normal to bedding plane and the vertical earth stress have been determined, the cohesive force at the tip of the nearly horizontal bedding-plane fracture also can be calculated by equations 23 and 44; and is given by,

$$\sigma_z - f\, T_{\sigma_z} = A \tag{46}$$

After tensile strength in the direction normal to nearly horizontal bedding planes of the rock, the vertical earth stress at the site, the cohesive force at fracture tip and the pressure required to overcome flow resistance has been determined or estimated, then the breakdown and propagation pressures can be forecast. The predicted values will be used in safety monitoring during waste injection. The above discussions have been illustrated by the case histories presented in Appendices.

5.3.2 Interpretation of uplift data

A large amount of foreign material is injected into a host rock which must yield space to accommodate the injected material. Because only nearly horizontal bedding-plane fractures are expected to be induced at a waste disposal site, the dominant force applied to the host rock during injection should be in a nearly vertical direction. No significant amount of injection fluid is expected to leak out of the induced fractures during injection, and the fractures will not be closed completely by the vertical earth stress after solidification of the grout. Uplift of ground surface is expected to result from injections. Field experiments in ORNL and West Valley, New York, sites indicate that ground surface had been uplifted by injections (deLaguna and others, 1968; Sun, 1969; Sun and Mongan, 1974; Weeren, 1974).

Sun (1969) demonstrated an example of the rational approach to the study of the uplift problem. He first assumed the host rock to be an impervious, homogeneous, isotopic, and elastic medium. Then he developed a mathematical model for calculating the amount of uplift of ground surface, the separation of horizontally induced fracture, and radius of extension of fracture. From the analysis of field data, a reasonable agreement between predicted and observed data is obtained (Sun, 1969; Sun and Mongan, 1974). Several examples of predicted and observed uplift data are shown in case histories in Appendices. The uplift, $\bar{W}$, and the horizontal displacement, U, of ground surface, the maximum fracture separation, B, and the radius of the induced fracture, a', can be estimated by the following equations (Sun, 1969):

$$\bar{W} = B\,(\sqrt{k}\,\sin\,(\theta/2)) - [(h/a\sqrt{k})\,\cos\,(\theta/2)] \tag{47}$$

$$U = \frac{Brh}{a}\,\{(a+a\sqrt{k}\,\sin\,(\theta/2)/[(h+a\sqrt{k}\,\cos(\theta/2))^2+(a+a\sqrt{k}\,\sin(\theta/2))^2]$$

$$-\,[h\sqrt{k}\,\cos(\theta/2) - a\sqrt{k}\,\sin(\theta/2) + ak\,\cos\,\theta)]/[(h\sqrt{k}\,\cos(\theta/2) - a\sqrt{k}\,\sin(\theta/2)$$

$$+\,ak\,\cos\,\theta)^2 + (a\sqrt{k}\,\cos(\theta/2) + h\sqrt{k}\,\sin(\theta/2) + ak\,\sin\,\theta)^2]\} \tag{48}$$

$$B = 8\,(1 - \nu^2)\,(P_p - \sigma_z)\alpha^2\,\, a/\pi E \tag{49}$$

$$(1 - \alpha^2)^{1/2} = (P_p - \sigma_z)/P_p \tag{50}$$

$$a = a'/\alpha = \{3EQ/[16(1 - \nu^2)\alpha^5\,(P_p - \sigma_z)]\}^{1/3} \tag{51}$$

Where $k = [(r^2/a^2 + h^2/a^2 - 1)^2 + (2h/a)^2]^{1/2}$

θ = arccot $[(r^2 + h^2 - a^2)/2ah]$

h = depth of induced fracture

r = radial distance from injection well

a' = radius of induced fracture from injection well

a = maximum radius of stress-altered fracture region shown in figure 6

α = a'/a

ν = Poisson ratio

E = Young's modulus

P_p = injection pressure at injection depth

σ_z = vertical stress or overburden pressure

Comparison of the predicted value and corehole data observed at ONRL site indicated that the fracture area sometimes is in elongated shape instead of circular (fig. 2). However, no grout sheet was observed beyond the area twice the calculated radius (Sun, 1969). Therefore, for safety monitoring purposes, some observation wells should be constructed in a perimeter four to five times the calculated radius of induced fractures. None of the injected grout sheets should extend to those wells as detected by gamma-ray logs.

5.3.3 Interpretation of gamma-ray logs

If bedding-plane fractures are induced then the altitude of the induced fracture in the vicinity of an observation well can be estimated by the following equation.

$$\text{Fracture altitude} = \text{Altitude of the injection level} \pm C \tan \theta \qquad (52)$$

where C is the horizontal distance measured perpendicular to the average strike of the shale beds between the injection altitude and the altitude of induced fracture at the observation well; and θ is the average dip angle. The plus or minus sign should be used according to the direction of dip. For observation wells located at updip from the injection well, it should be a positive sign, otherwise it is a minus sign. The estimated altitude should be compared with the observed altitude of the induced fracture determined from gamma-ray logs made in the observation wells after injection. Because of well deviations, the comparison of estimated and observed fractures should be made at the time after the true horizontal position and true depth are calculated from well deviation records. The intensity of gamma activity which indicates induced fractures reaching the observation well should be several orders of magnitude higher than the background value of the host rock, so that the evidence is clearly indicated by gamma-ray logs made in observation wells before and after an injection, if the amplifier range of the logging unit is kept constant.

6. SAFETY CONSIDERATIONS

The potential for waste migration during and after waste injections, and other adverse effects resulting from waste disposal such as triggering earthquakes must be evaluated when the method of disposal of radioactive waste by grout injection and hydraulic fracturing is considered among other alternatives.

Ideally, after solidification of the grout, the injected wastes should become an integral part of the host rock and remain there as long as the host rock is not subject to severe erosion and dissolution. However, a number of questions concerning the safety of the method have been raised. They are: (1) the possibility that liquid waste might separate from the grout during and after injection migrate through existing fractures or joints; (2) whether waste can be leached out of grout sheet by ground water; (3) reliability of methods of determining with certainty that orientation of the induced fractures is horizontal, or nearly so; (4) whether grout injection and hydraulic fracturing has potential for triggering earthquakes; and (5) safe isolation time required for the disposed wastes. These concerns are discussed below.

6.1 Waste migration due to separation of liquid from grout

One of the major concerns of waste migration of this disposal technique is radionuclide-loss from the injected grout while it was still in the liquid phase and radionuclide-loss from the fraction remaining in the liquid phase through phase separation during solidification. These two losses can be eliminated or reduced through correct solid/waste mixing ratio and with carefully selected solids through laboratory experiments with simulated or actual wastes. The criteria of mixing are: (1) slurry consistency must remain stable and pumpable for several hours during injection, but must permit setting soon

(24 hours or less)
after completion of injection/ (2) free liquid separated from grout during solidification should be as low a quantity as possible and should contain no, or only very small quantities of radionuclides; (3) leach rate of radionuclides from solidified grout should be low and decrease rapidly with time; and (4) within tolerable compressive strength of grout, weight of cement added to waste should be kept low, thus reducing cost and increasing volume of waste to be disposed. These criteria can be achieved by a proper selection of cement and additives and by correct mixing ratios determined in a laboratory.

Experiments at ORNL indicate that both radiocesium and radiostrotium reacted rapidly with solids in mixing. Very little Sr^{90} (less than 2 percent) was found in the liquid phase after contact with solids.

The rapid reaction of Sr^{90} with small particles might be explained on the basis of the composition of Portland cement. Portland cement is composed mainly of calcium silicates, which react with water to form hydrated calcium silicates. Since strontium and calcium have similar chemical behavior, Sr^{90} rapidly entered into these reactions that are common in calcium (deLaguna and others, 1968).

Retention of radiocesium by cement solids has proven to be unsatisfactory (about 70 percent). Bentonite was used as an additive at ORNL to provide the capacity for retention/radiocesium/and for reducing fluid loss; however, under high molarity of salt solutions--in excess of 5 M, bentonite fluctuates and is ineffective as a suspending agent. Attapulgite, known to be more effective than bentonite as a suspending agent in such solutions, was therefore substituted for bentonite. To further improve radiocesium retention, illite clay was added to the ORNL wastes.

Pozzolanic material such as fly ash is also found to be effective and can improve radiostrontium retention and reduce required amounts of cement, thus reducing the cost of mix.

Length of pumping time can be controlled by adding different amounts of delta gluconolactone (DGL). Phase separation was found to be highly sensitive to composition of waste and of solids. Both DGL and attapulgite were found to affect phase separation. The higher the content of attapulgite, the lower the phase separation, but also the more viscous the slurry. Higher amounts of DGL can reduce the slurry viscosity, however, at the expense of increase phase separation. The ultimate blend of solids can only be achieved through laboratory experiments. The following mixing procedure recommended by ORNL for wastes similar to those produced in ORNL is listed for reference (deLaguna and others, 1969; written commun., H. O. Weeren, ORNL, 1980).

1. Sample and analyze waste to be injected
2. Prepare solids blend containing the following materials:

	Percent by weight
Portland cement type I, gypsum retarded or equivalent	38.45
Pozzolan	38.45
Attapulgite gelling clay	15.38
Illite	7.69
Delta gluconolactone	0.03

3. Prepare slurry using 550 cc of waste in 1-liter blender. Add solids, using 15 sec to pour into blender and 15 sec of additional stirring. Record the amount of solids. Blender is calibrated to rotate at 2000 rpm at no load.
4. Pour slurry into 250-ml graduate to estimate phase separation.
5. After 2 to 4 hours, determine phase separation. Increase or decrease proportion of solids, depending on phase separation. If no phase separation occurs, decrease the amount of solids to obtain minimum solids content

necessary to prevent phase separation. Generally 5 to 10 percent of change in solids is sufficient to obtain slurry with no phase separation.

6. Increase addition of solids by 10 percent over that amount which yielded no phase separation, and mix as in step 3. (The increase over the minimum anount is suggested to allow $\pm$ 10 percent in the control of solids/liquid proportioning.) Determine pumpable time (thickening time) of the slurry by measuring viscosity.

7. Increase or decrease delta gluconolactone (DGL) content to obtain desired pumpable time; redetermine phase separation if DGL content is changed. Desired pumpable time depends on the volume of waste to be disposed of and the rate of injection.

No matter how well or carefully the slurry is mixed, phase separation is unavoidable, however, the quantity of the unbound water in the injection zone can be reduced by back bleeding after the grout solidifies. Experience at ORNL indicates that concentration of radionuclides in bleedback water is low (table 16). With low permeability, as that of shale, unbound water probably would be trapped in the grout sheets, this has been indicated during drilling at ORNL site. If some of the unbound water does move away from grout sheet then the small quantity of radionuclides in the unbound water / probably would be further reduced by adsorption or decay and dispersion if the flow path from disposal site to discharge area is long. Nevertheless, the disposal site should be monitored by a series of observation wells constructed along perimeter of the disposal site as well as in the overlying formation above the injection zone.

6.2 Leaching of grout by ground water

In order to reduce radionuclides leaching from the grout by ground water to the lowest rate, possible studies with different minerals as additives over a wide range of particle sizes and size distribution are important. The overall

results of ORNL grout mixture tested by a modified IAEA (1971) testing method (Moore and others, 1975; Moore, 1976) indicated that the grout could give leach rates comparable to those obtained for waste incorporated in borosilicate glasses. The leach rates of the radionuclides contained in the ORNL waste are in the following orders: Cs > Sr > Cm > Pu. The maximum amount of radionuclides leached out from grout sheet seems independent of the type of water such as tap water, ground water or sea water (Moore and others, 1975). The cumulative fraction of cesium and strontium leached from grout depended on the time and manner of curing. The amount of leached radionuclides decreased with an increase in curing time. Short-term (140 days) leach studies at ORNL indicated that increasing the overall waste concentration had little effect on the leachability of strontium or cesium (Moore, 1976).

Core grout (cured for about 10 months underground) was also used in leaching studies at ORNL. Because the thin grout sheets in the core were not of uniform geometry, the grout was ground and sieved, and only those particles passing a mesh screen with 250-μ diameter hole were used in the studies. Leaching was carried out in plastic bottles containing 1 g of solids per 100 ml of distilled water. The results from use of grout containing illite show that less than a few hundredths of a percent of the injected amount of radionuclides was leached out of the grout during a 504-hr test (Tamura, 1971). Conditions of these leaching studies deviate greatly from those in the ground. Cores of the grout sheets obtained at ORNL indicate that the solidified grout sheets are strongly integrated with shale (see fig. 1), therefore, ground water probably has less chance to move through the solidified grout sheet than implied by fine particles of the ground grout in contact with distilled water. On the other hand, the laboratory studies were made over extremely short periods, and the results may be different from long-term leaching by ground water flow. However, the low permeability, high ion-exchange and adsorption capacity of shale, size of shale body (several hundreds of meters in thickness), and low concentration of radionuclides in liquid during phase separation and leaching--all suggest that the possibility of

contamination of the biosphere by injected radioactive wastes is likely to be remote. If a very low concentration of radionuclides did reach a water source then the concentration of radionuclides would be further diluted by that water body.

6.3 Creation of vertically oriented fractures

Careful monitoring of injection pressure during injection time will give indirect indication of orientation of induced fractures. Any sudden drop in injection pressure, especially when the pressure is near or below the estimated vertical stress, will be a positive signal to stop the injection for evaluation of the cause. Gamma-ray logs made in observation wells will give positive evidence of the fracture orientation, and the more observation wells used the better the resolution of orientation. The possibility of inducing vertical fractures should be fully evaluated during site investigations, and carefully monitored during each injection.

6.4 Triggering earthquakes by hydraulic fracturing

In 1965, Evans (1966) showed a correlation between pressure of fluid injection, the volume of liquid wastes injected into a 3660-m disposal well at the Rocky Mountain Arsenal, Denver, Colorado, and the number of earthquakes reported in the Denver area. He concluded that the waste injection at the arsenal well had caused the Denver area earthquakes. In December 1965, the U.S. Geological Survey, in cooperation with the Colorado School of Mines, Regis College, and the University of Colorado, undertook a series of studies to determine the relationship, if any, between the disposal of wastes in the arsenal well and the location and frequency of earthquakes. The results of these studies supported Evans' conclusion (Healy and others, 1966).

In February 1966 the disposal well was shut down. Despite the cessation of injection, earthquakes continued to plague the Denver area through August 1967. Two earthquakes (magnitude 5.0 of Richter scale, April 10, 1967, at a depth of 5 km), the largest in Denver area since 1882, were strongly felt throughout the Denver metropolitan area. Because these seismic events occurred 14 to 18 months after termination of the well injection, Major and Simon (1968) concluded that the correlation between fluid injection and earthquake occurrence upon which Evans based his view had been reduced. The overall number of earthquakes in the Denver area, however, has declined exponentially since 1967. This reduction of earthquake occurrence suggests that tremors in the Denver area were caused by release of tectonic stresses and that deep-well injection was simply the triggering force (Sun, 1977).

In 1969, U.S. Geological Survey in cooperation with Chevron Oil Company studied the relationship between fluid injection for water flooding of the Rangely Oil Field, Rio Blanco County, Colorado, and the number of earthquakes in the area, and installed 16 seismographs around the oil field and concluded that: (1) there is an apparent relation between the number of earthquakes and the annual volume of injected fluid; (2) changes in the quantity of injection of fluid are related to changes in the number of earthquakes recorded; and (3) parts of the field without natural faults do not produce earthquakes even when the pore pressures in the rock are quite high (Gibbs and others, 1972). In November 1970, four injection wells straddling a fault zone were backflowed to reduce the pore pressure in the hypocentral region. The wells were backflowed and pumped for a period of 6 months. Within a very short time following the initiation of backflowing, earthquake occurrence within an area of about a 900-m radius of the backflowing wells decreased markedly in frequency and ultimately almost ceased (Raleigh, 1972).

From the foregoing discussion it can be concluded that injection of fluid does have the potential to trigger earthquakes under certain conditions. It is important to know if disposal of radioactive wastes through grout injection and hydraulic fracturing also has the potential to trigger earthquakes. The following discussion is to evaluate this potential.

6.4.1 Historical manmade earthquakes

Manmade earthquakes associated with dam construction have long been acknowledged and well documented. Carter (1945, 1970) associated earthquakes near Hoover Dam, Boulder City, Nevada, with the filling of Lake Mead. He suggested that the earthquakes around Lake Mead were directly or indirectly a result of fluctuation in surficial crustal loading. Anderson and Laney (1975), however, offered a different explanation. They suggested that a hydraulic connection between the lake water and the deep aquifer system, which includes buried faults, is needed to cause the release of seismic energy in the Lake Mead area. Where hydraulic connection between the lake and the aquifer is prevented by strata of very low permeability (evaporites), as in the eastern basin, seismicity does not occur despite the large volume of impounded water in the area.

The Palisades Reservoir in southeast Idaho, also triggers earthquakes. Epicenters are concentrated near the reservoir, and the number of earthquakes is related to water fluctuations in the reservoir. Schleicher (1975) suggested that the area around the Palisades Reservoir would almost certainly be subject to earthquakes even if the reservoir were not there. The effect of construction of the reservoir was to trigger faulting when tectonic stresses were on the verge of causing it anyway.

Earthquakes attributed to fluctuation of water levels and filling of reservoirs are also reported and documented in other parts of the world. For example, Marathon and Kremasta Lakes in Greece, Vajont Dam in Italy, Lake Eucumbene of Snowy Mountains in Australia, Kariba Dam in Rhodesia and Koyna Dam in India all reported small to moderate earthquakes that began a few months after river closure (Carter, 1970). All these reservoirs are located in areas that were generally considered aseismic, however, potentially active or active faults are found in all these reservoir sites (Carter, 1970).

Even river flooding has been related to the occurrence of earthquakes. McGinnis (1963) observed that an abnormally high number of earthquake epicenters have been detected within 320 km of New Madrid, Missouri. The area is composed of extensive alluvial valleys, is extensively fractured, and shows evidence of major and minor faults. McGinnis concluded that the correlation of the mean monthly river stage and the earthquake frequency in the alluvial valleys indicates that an increase in the rate of change of water-load variation tends to increase earthquake activity.

6.4.2 Mechanism of triggering earthquakes

The mechanism by which earthquakes are triggered by man's activity is not clearly known. However, most investigators (Healy and others, 1966; Carter, 1970; Gibbs and others, 1972; Schleicher, 1975) generally agree that the following conditions are associated with manmade earthquakes: (1) rock at the site must be under high stress and near its breaking strength or on the brink of sliding on preexisting fault plane(s); (2) rock is possibly associated with potentially active fault(s); and (3) change of pore pressure in the rock is probably the triggering force.

If rock pores are saturated with water, then the rock is also subject to a hydraulic pressure, p, throughout the interconnected pores. The three principal earth stresses, σ_1, σ_2, σ_3 will be reduced to $\sigma_1 - p$, $\sigma_2 - p$, and $\sigma_3 - p$ and the normal and shear stresses acting across a plane perpendicular to σ_1, σ_3-plane and making an arbitrary angle α with the direction of the least principal stress σ_3 are given by (Hubbert and Rubey, 1959):

$$\sigma = \frac{\sigma_1 + \sigma_3}{2} + \frac{\sigma_1 - \sigma_3}{2} \cos 2\alpha - p \qquad (53)$$

and

$$\tau = \frac{\sigma_1 - \sigma_3}{2} \sin 2\alpha \qquad (54)$$

The relation of pore pressure to rock failure is shown in figure 12. At first, the rock is assumed to be dry and under three principal stresses of differing magnitude, and is not subject to fracture. Now, without changing the magnitude of the principal stresses, let the rock be saturated with water and the pore pressure in the rock increase from 0 to p. From equation 53, it is seen that the diameter of the Mohr circle remains constant but the center of the Mohr circle is moved towards the left along the normal stress axis by a distance equal to the pore pressure, p, as shown in figure 12. If the pore pressure is continuously increased from p to p + Δp, the diameter of the Mohr circle still remains constant but the center of the circle is translated further left by a distance equal to the increment of the pore pressure Δp. Obviously, if the pore pressure in the rock increases sufficiently, the Mohr circle will be continuously moved

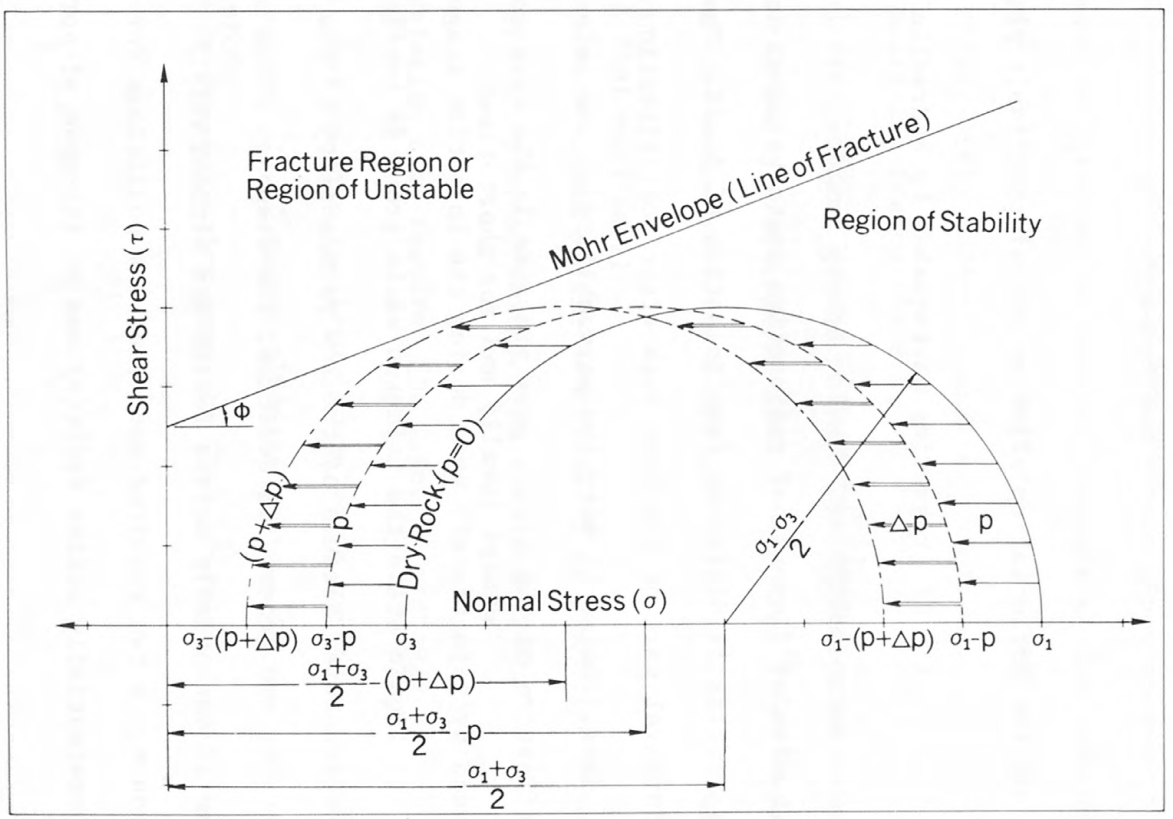

Figure 12.--Coulomb-Navier fracture criteria showing how rock failure can be affected by increase of pore pressure (principal stresses are kept constant).

to the left until it touches the Mohr envelope (line of fracture) and then the rock starts to fracture (Hubbert and Rubey, 1960; Jaeger, 1962).

Injection of fluid and seepage from reservoirs certainly will increase pore pressure in the rock. If rock in the area of potentially active fault(s) has already been stressed to the verge of breaking, then the increasing pore pressure would positively contribute to fracturing or slippage of the rock. Fracturing and/or slippage of rock would release elastic energy which had already been stored in the rock thus triggering earthquakes. Therefore, fluid injection and reservoir seepage would simply modify earthquake timing, intensity, and location when the rock is already stressed to the verge of breaking by tectonic stresses or has the potential to slide on preexisting fault plane(s).

6.4.3 Possibility of triggering earthquakes by hydraulic fracturing and grout injection

The mechanism of disposal of radioactive waste by grout injection and hydraulic fracturing is different from injection of fluid. The injected grout becomes an integral part of the host rock after solidification which occurs within one or two days. Owing to very low permeability (less than 10^{-6} darcy) of the selected host rock and quick solidification of the grout, pore pressure in the host rock is unlikely to be increased by injections except locally and for short times. Even during the injection stage when the waste grout is in its liquid state the injected waste grout is confined in the induced bedding-plane fractures because of the low permeability of the host rock and high viscosity of the grout. In addition, the disposal sites are to be located in areas free of potentially active faults and without very closely spaced fractures and joints. Because the two required and necessary conditions for triggering earthquakes--potentially active fault(s) and an increase of pore pressures--are

not associated with the waste grout injection technique, therefore, it is concluded that the possibility of triggering earthquakes by grout injection and hydraulic fracturing does not occur.

In an attempt to obtain seismic signals during grout injection and hydraulic fracturing at ORNL, an array of six micro-seismometers was installed in an area of approximately 450 m in diameter with the injection well in the center at the first two of the four injections in 1972. During the last two injections, the diameter of the seismometer array was increased to 600 m and a downhole seismometer was installed during the fourth injection to reduce surface noise and to improve sensitivity. All the four injections were made at a depth of 254 m. No meaningful seismic signals were obtained from any of the four injections (Weeren, 1974). This indicates that seismic signals generated by grout injection and hydraulic fracturing are, if at all, so small that they can not be differentiated from ambient ground noise. The inconclusive seismic result is expected, because the energy required to induce fractures along weakly bedded shale to overcome the tiny cohesive force along the shale bedding planes is small (Sun and Mongan, 1974).

In conclusion, no earthquake should be triggered by hydraulic fracturing and grout injection either during or after injection.

6.5 Isolation time required for injected wastes

The length of isolation time required for injected waste is primarily dependent on the decay periods of radionuclides contained in the disposed waste and can be estimated by the following equation (U.S. Bureau of Radiological Health, 1970).

$$C = C_o \, e^{-0.693n} \tag{55}$$

where C_o is the activity of a particular radionuclide contained in the waste at the disposal time; C activity remaining after a time interval, t; n number of half-lives, $n = t/T_{1/2}$; $T_{1/2}$, half-life of the radionuclide.

If the safe activity of radionuclides is assumed to be one millionth (10^{-6}) of its initial activity, then the required containment time can be calculated as 20 half-lives of a particular radionuclide (eq. 55). For example, for waste containing 99 percent of Sr^{90} and Cs^{137}, only 600 years of isolation is required. For the radionuclides having half-lives of only 28 and 30 years, respectively, the projection of geologic and hydrologic factors controlling processes such as erosion and leaching for the isolation period probably can be estimated with confidence on the basis of geologic and hydrologic knowledge and conceptual models. However, if I^{129} is the major concern among the radionuclides, then even its one half life (17×10^6 years) is too long for any reliable prediction of the isolation time.

7. CONCLUSION

In a shale formation characterized by directional tensile strength, the pressure needed to induce a vertical fracture across horizontally orientated bedding planes is much higher than the pressure needed to form bedding-plane fractures. Existing joints and/or high-angle natural fractures may be extended by pressure if they are intercepted by induced bedding-plane fractures, however, vertical extension will cease where these natural fractures or joints intercept weak bedding planes. It is therefore concluded that horizontal bedding-plane fractures can be induced hydraulically in a nearly horizontally bedded shale at depths shallower than 1,000 m. Deeper than that depth the advantage of directional tensile strength may be overcome by the large overburden pressure. The injection experience at Oak Ridge, Tennessee, and West Valley, New York, supports the conclusion that induced fractures may migrate up and down as much as 20 meters from injection altitude at a distance several hundreds of meters from an injection well (see case histories in Appendices).

The orientation of the induced fractures can be indirectly monitored by observing injection pressures during injection time, and by pressure decay of water injections and uplift of ground surface after injections. The orientation, however, can be confirmed by gamma-ray logs made in observation wells before and after each injection if the injected fluid or grout contains gamma-emitting radionuclides.

At least one water injection test and one grout injection test should be made during a site evaluation. Pressure-decay data obtained from a water injection can be used, not only to evaluate the orientation of induced fractures and the permeability of the injection shale, but also to determine the effective stress normal to the fracture plane. The vertical stress may or may not be equal to the calculated overburden pressure. At Oak Ridge, Tennessee, the vertical earth stress is about twice that of the calculated overburden pressure indicated by the pressure decay data of water injections (see case histories of Oak Ridge in Appendices). A grout injection

not only confirms the conclusions made after a water injection, but also simulates conditions encountered during waste injections.

Intermediate-level radioactive wastes (specific activity of less than 6×10^3 μCi/mℓ consisting mainly of radionuclides with half-lives ranging less than 50 years such as strontium and cesium) mixed with cement and ion-exchange and adsorption materials can be injected into shale by hydraulic fracturing and grout injections. After solidification of grout the wastes will be immobilized and become an integral part of the shale, and remain at depth as long as the shale is not subjected to severe erosion and dissolution. The injected wastes thus will be kept within a known horizon. It can be concluded that grout disposal of radioactive wastes in shale using hydraulic fracturing as a means is safe and feasible, if the shale formation is carefully selected, tested and evaluated, and the grout is properly mixed and the injection is cautiously conducted. However, risk analyses against other alternatives should be carefully evaluated before the grout injection method is selected.

At least four observation wells with strong tubing and pressure cemented should be constructed at a radial distance of 50 m in four directions from the injection well for determining the orientation of induced fractures after injections. Four or more additional observation wells should be constructed at radial distances far enough away from the injection well greater than that expected to be reached by any grout sheet. The distance beyond which the grout is not expected to extend can be estimated by equation (51). If the injected wastes contain gamma-emitting radionuclides these observation wells are used in monitoring. More observation wells will increase the confidence of isolation of the injected wastes in a known horizon.

Because a waste disposal site must be in a geologically stable area without potentially active faults, and because there is no general and extensive increase in pore pressure of the rock mass due to waste grout injections, it is concluded that there is no danger that grout injection would trigger earthquakes during or after the injections.

Waste disposal is conducted in multiple-layer injection stages. The first series of injections starts at the greatest depth, then the injection zone is plugged off by cement. The next series of injections are started at a suitable distance above the first injection zone. The repeated use of the injection well distributes the cost of construction of injection and monitoring wells over many injections, thereby making hydraulic fracturing and grout injection economically attractive as a method for disposal of the intermediate-level radioactive wastes.

8. APPENDICES

A. CASE HISTORIES

The technique of hydraulic fracturing has been widely applied in water flooding of oil fields since 1947 (Howard and Fast, 1970), it was first proposed as a means to dispose of radioactive waste in shale by grout injection in 1958, and used in experimental studies at the Oak Ridge National Laboratory from 1959 through 1965. A total of 10 experimental injections were made at three different injection wells. Since 1966 the hydraulic fracturing and grout injection disposal techniques have become operational and 17 operational injections were made up to 1978. A total volume of 6,400 m^3 of radioactive waste with 641,300 curies of radionuclides has been injected for disposal.

To further study the feasibility of this disposal method at another location and to develop economic and reliable methods for determining the orientation of the hydraulically induced fractures to insure that the disposed wastes are isolated in a desired horizon, experimental studies were made jointly by the Oak Ridge National Laboratory and the U.S. Geological Survey from 1969 through 1971 at West Valley, New York. Five water injections, and one grout injection tagged with gamma-emitting radioisotopes as tracers, were made in another shale formation. No actual waste was disposed during these experimental studies.

Because the methods developed during the West Valley studies can be applied to ORNL disposal site, the West Valley case histories which have been fully discussed by Sun and Mongan (1974), are discussed first.

A1. HYDRAULIC FRACTURING AT WEST VALLEY, NEW YORK

West Valley is located approximately 56 km south-southeast of Buffalo, New York, and is in the north portion of Cattaraugus County with an elevation of about 457 m. The hydraulic fracturing study site is located on the property of Western New York Nuclear Service Center near the town of West Valley (fig. 13). The area is drained by Buttermilk Creek which flows north-south and enters Cattaraugus Creek, then drains into Lake Erie.

The injection depths ranged from 152 m through 442 m. Injections were made in the injection well in a sequence from the bottom upward. For a given test the well was plugged by cement to the desired injection depth and a horizontal slot (360 degrees) was made near the bottom of the unplugged part of the well (as described in detail in Section A2.5).

A1.1 Site geology

Because the purpose of the study was to evaluate the feasibility of the disposal method without intention of selecting a site, the regional geology and hydrology were not investigated for the study. Only the site geology which might affect the orientation of the hydraulically induced fractures was briefly examined.

The test site is underlain by sedimentary rocks of Cambrian through Devonian age and is within the Appalachian Plateau Province. The area has been only slightly affected by tectonic events. No faults or folds have been mapped at the site. The nearest mapped fault is the Clarendon-Linden fault, approximately 45 km east of the site.

The rocks involved in the tests mostly are Devonian shales with some interbedded siltstone. The area is covered by glacial deposits as much as 60 m in thickness. The rocks involved in fracturing injections probably belong to the Canadaway Group of New State usage of the Devonian shale. The shale involved in the first two injections (442 m)

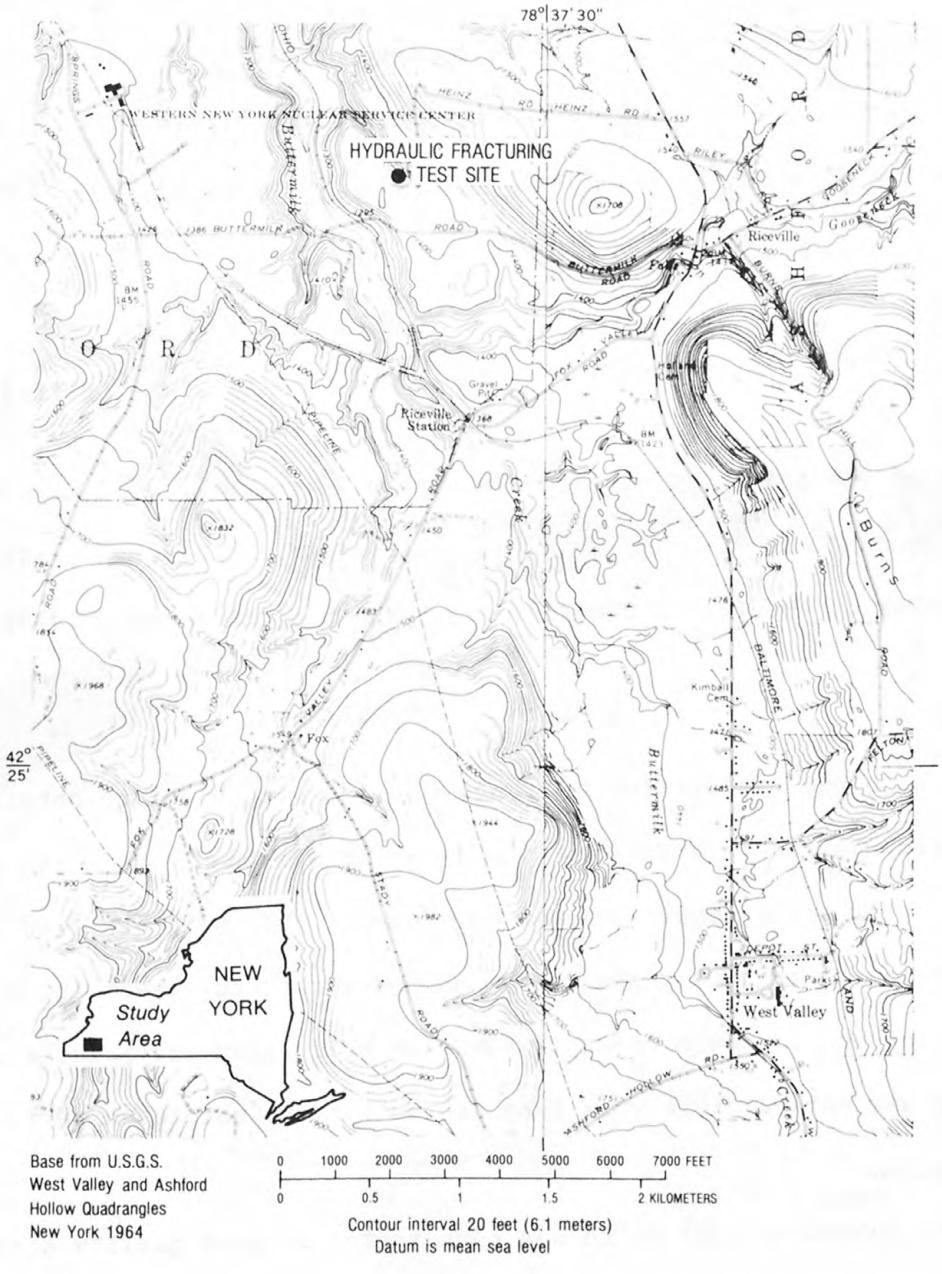

Figure 13.--Map showing location of hydraulic fracturing test site, West Valley, New York.

may belong to the older Rhinestreet Shale Member of the West Falls Formation (Sun and Mongan, 1974). A layer of 30 m of siltstone was found in a corehole at a depth of 290 to 320 m. The siltstone contains thin layers of silty shale. The bedding planes of the shale were found to be nearly horizontal, probably dipping southward with the regional dip by one to two degrees.

Three sets of principal joints have been identified by G. H. Chase of the U.S. Geological Survey at the outcrop area near the test site. Their trends are N68°E, N45°W, and N13°W, in the descending order according to the frequency of occurrence (fig. 14). All joints are vertical or nearly so. The average joint spacing is about 60 cm and the average wall separation is 3 mm. The vertical length of the joints ranges from less than 30 cm to 2 m. Most of them are 30 cm or less. From core and geophysical logs it was estimated by Chase that 20 percent of the joints probably are open (Sun and Mongan, 1974).

filled with sediments

surface studies,

A1.2 Well construction

A corehole was drilled to a depth of 463 m in order to obtain lithologic and petrophysical information. The corehole was then cased with rather weak steel tubing and pressure cemented in place. This well was used as one of the four observation wells during the study and named the East-observation well. Before converting the corehole to an observation well, gamma-ray, electric, 3-D sonic, density and caliper logs were made in the hole to obtain subsurface geological information.

The injection well which was constructed of good quality steel casing and pressure cemented to a full depth of 463 m, and was located 46 m from the

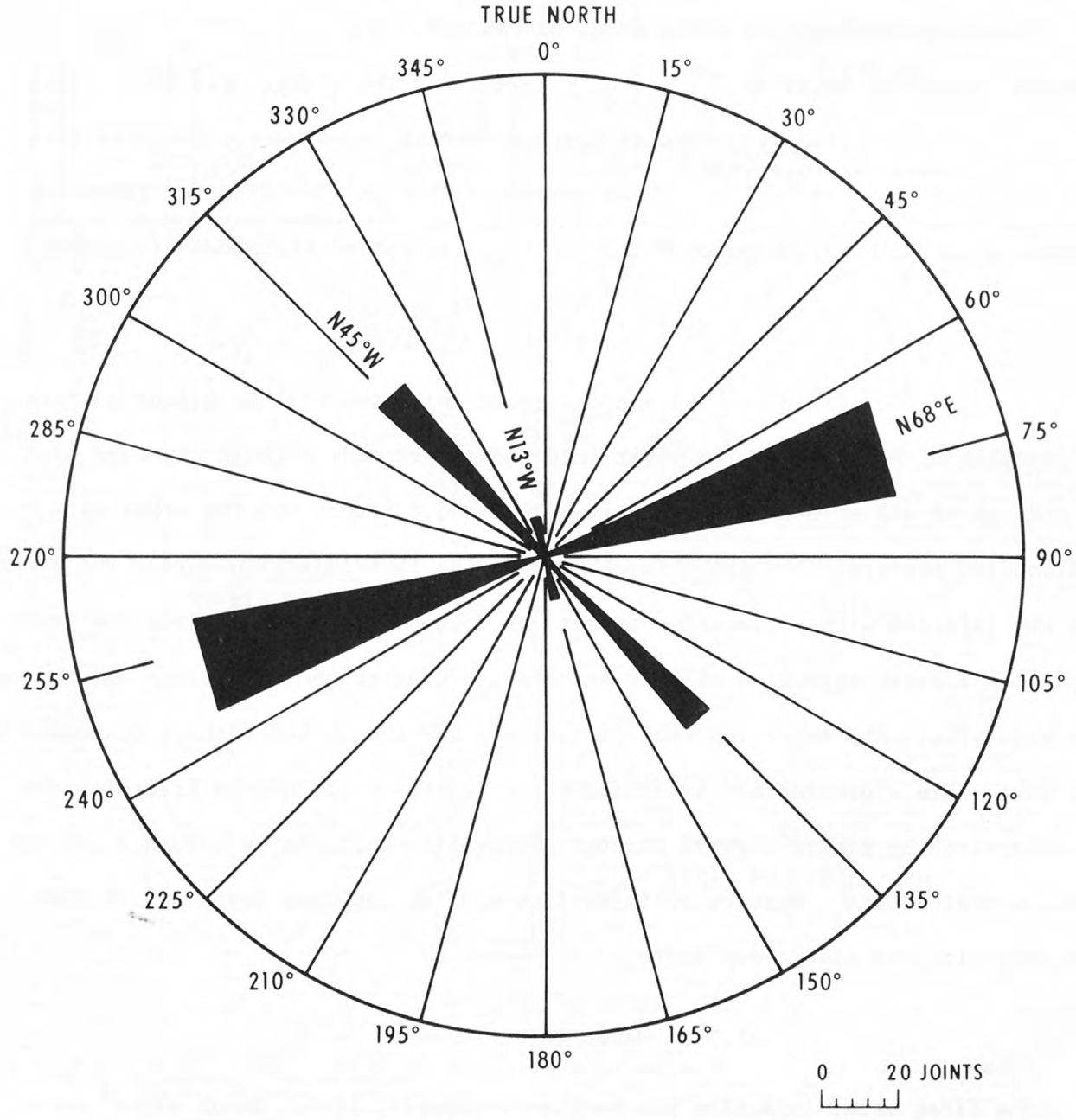

Figure 14.--Diagram showing observed trend of three principal joint sets, West Valley, New York (written commun., G. H. Chase, U.S. Geol. Survey, 1969).

gamma-ray
corehole (figs. 15 and 16). Density, caliper, and hole-deviation surveys were made in the injection well before the well was cased and pressure cemented.

Three more observation wells were constructed, each 46 m distant from the injection well, to the south, the west and the north (fig. 16). These observation wells were also cased with strong tubing and pressure cemented to a full depth of 463 m. Gamma-ray logs were also made in all wells. All these observation wells were used for gamma-ray logging after each injection to determine the orientation of induced fractures.

A1.3 Injections

Only three water injections and one grout injection will be discussed here as examples of the study. Two water injections were made through the same slot at a depth of 442 m; one injection was made without tracer and the other with radioactive tracers. The grout injection was the last injection during the study and was injected with radioactive tracer at a depth of 152 m. Before the grout injection a water injection without tracers was made at the same depth and through the same slot. All injection results indicate the theory and methods discussed in the text are approximately valid and the orientation of induced fractures can be determined by direct surveys through observation wells or by evidence deduced from injection data. Results of injections made at the same depth and through the same slot are almost duplicate.

A1.3.1 Water injections

The first water injection was made on October 9, 1969. About 433 m^3 of water without tracer was injected through a pre-cut slot at a depth of 442 m.

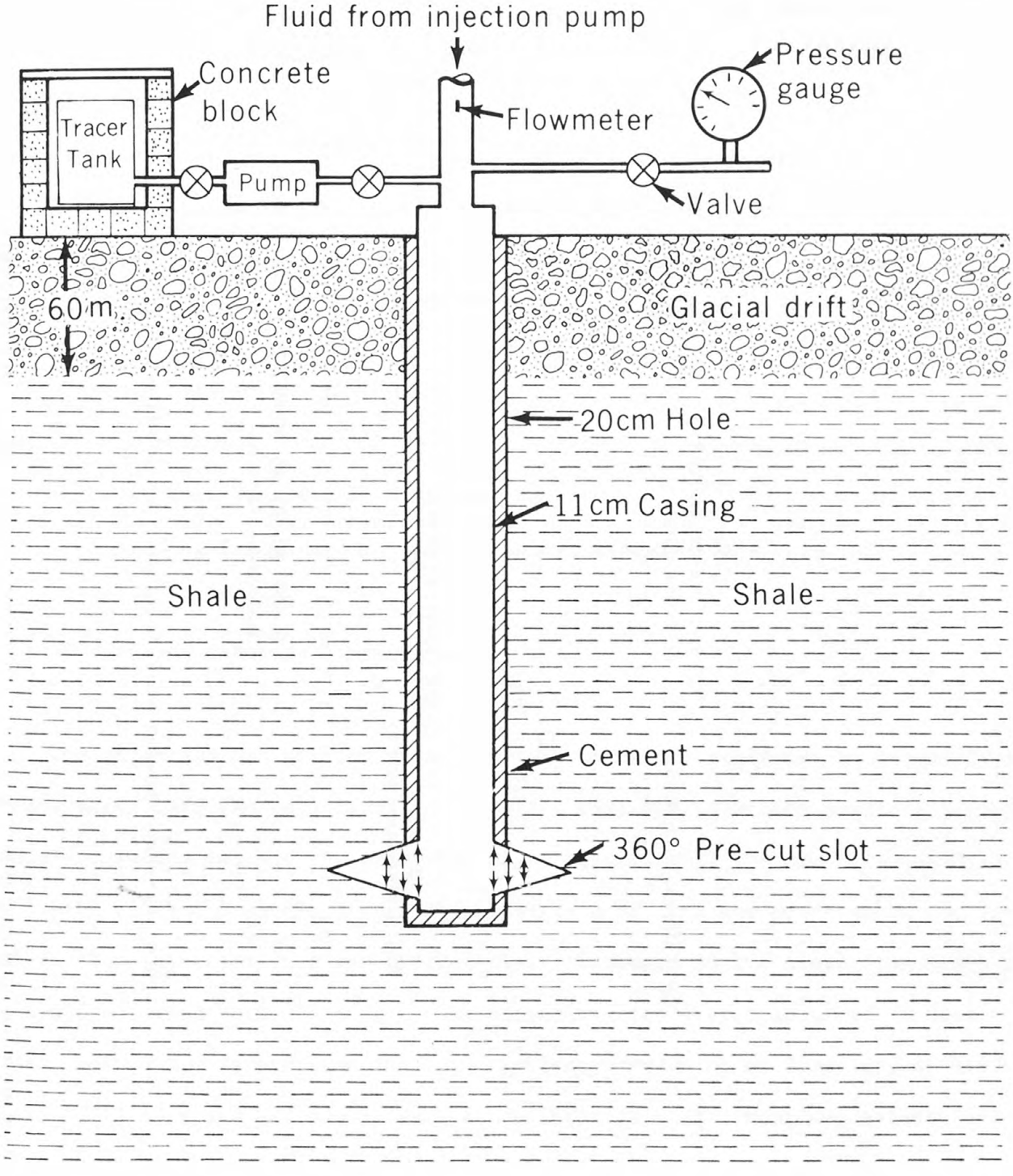

Figure 15.--Schematic diagram showing injection well, West Valley, New York.

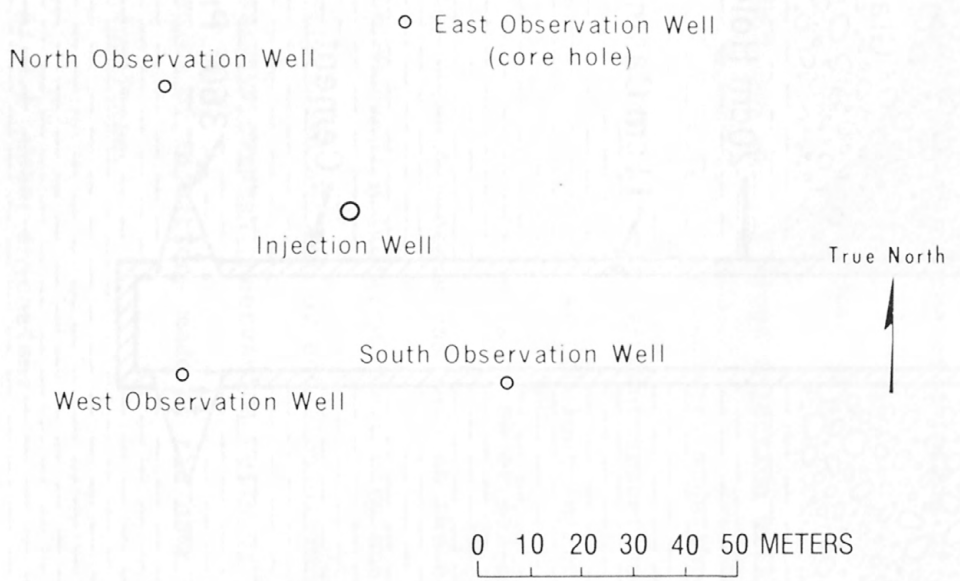

Figure 16.--Map showing well location, West Valley, New York.

The rock at this depth is well bedded petroliferous shale. From 439 to 442 m, a zone of vertical joints had been observed by G. H. Chase, U.S. Geological Survey, from geophysical log.

Pressures discussed in the theory are pressures at injection depth, commonly called "bottom-hole pressures", however, pressures observed during test injections were surface pressures measured at the well head of an injection well (fig. 15). Bottom-hole pressures used in interpretation of water injections were computed from observed pressures by adding/static pressure in well casing and the calculated by subtracting pressure loss due to friction in injection pipe. For water injections, the frictional pressure-loss in injection pipe was calculated by Darcy-Weisbach equation (Davis and Sorensen, 1969) which is given as follows:

$$\Delta p = 500\ f\ L\ V^2/D \qquad (56)$$

where

Δp = pressure loss due to friction, Pa

f = Fanning frictional factor of casing, dimensionless

L = length of pipe, m

D = inside diameter of pipe, m

V = flow velocity, m/s

The injection was started at a very low rate which could not be detected on a flow meter near the well head. At this low rate the injection pressure increased rapidly. Twenty-two minutes after the injection started, the pressure near the well head reached 9.65 MPa (table 1) and a trace of flow was detected on the flow meter. The injection rate was progressively increased in two steps from 0.001 m^3/s to 0.002 m^3/s and to 0.003 m^3/s. Each injection step lasted about 10 minutes. After the 0.003 m^3/s step, an injection pattern consisting of flow rate of 0.006 m^3/s, 0.013 m^3/s and 0.025 m^3/s each at an interval of 1/2 hour was established.

This pattern was repeated over and over until the end of the injection (fig. 17).

Six hours from the start, after a total of 223 m^3 of water had been injected, the injection was stopped to allow for instrument adjustment. The injection was resumed 45 minutes later with the regular injection pattern, but this time starting at the rate of 0.025 m^3/s. The observed pressures, injection rates, as well as the calculated bottom-hole pressures are shown in table 1.

If flow through an induced fracture is assumed to be laminar and to obey Darcy's law. then the injection pressure at the well should be linearly proportional to the injection rate. This assumption has been proven to be at least approximately correct by using polynomial regression of the injection data, which showed that only the linear term of Q (injection rate) has significance by F-tests (Ostle, 1954).

During the stage of fracture initiation, injection pressure must be built up to overcome the tensile strength of the rock. After rock is broken, injection pressure gradually decreases to the required propagation pressure. During this transitional stage, injection pressures are not linearly proportional to the injection rates. Excluding these pressures a linear regression equation before the injection pause with a correlation coefficient of 0.88 has been found (fig. 18) and the result is:

$$P = 11.96 + 24.05\ Q \qquad (57)$$

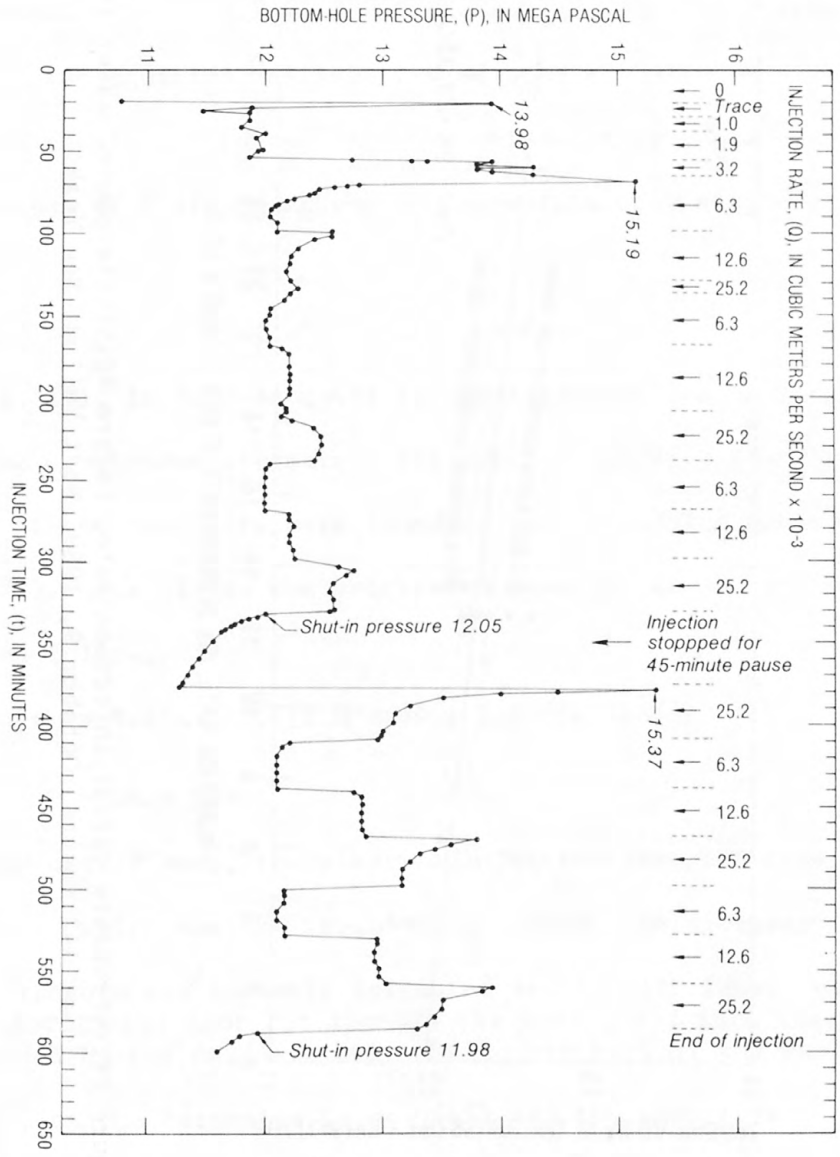

Figure 17.--Pressure versus time, water injection at 442 meters, October 9, 1969, West Valley, New York.

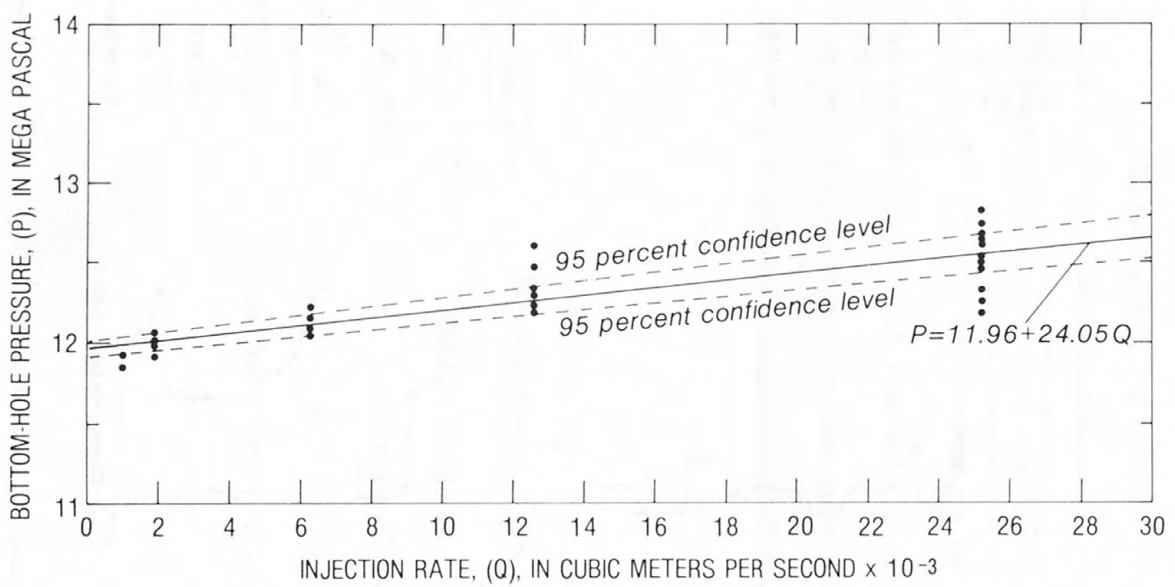

Figure 18.--Pressure versus injection rate, before 45-minute pause, water injection at 442 meters, October 9, 1969, West Valley, New York.

where P is bottom hole pressure, in MPa and Q injection rate in cubic meters per second.

Because the regression coefficient of Q was determined from a small sample size of P and Q taken from the true population, it is possible that the values of P and Q may be independent in the true population and the regression equation has no meaning statistically. Therefore, it is essential to test whether the regression coefficient determined from the sample size is significant in a statistical sense. The significance of the regression coefficient of 24.05 of Q in the regression equation has been tested statistically by assuming a probability of Type I error equal to 5 percent (95 percent level of confidence). The conclusion is that the values of P are dependent on the values of Q statistically (Sun and Mongan, 1964).

Because of simple geological structure and relatively flat topography at the test site (fig. 13), it is reasonable to consider that the vertical earth stress is equal to the overburden pressure. The average specific gravity of shale and glacial drift at the test site were found to be 2.6 and 2.0 respectively (deLaguna, 1972). Therefore, the overburden pressure at the injection depth can be estimated as follows:

$$\sigma_z = 9.8 \times 10^{-3} [2.0 \times 60 + 2.6 (442-60)]$$

$$= 10.9 \text{ MPa}$$

When Q was nearly zero, the observed injection pressure rose to 14 MPa (figs. 17) which was the breakdown pressure. As discussed previously, a horizontal fracture was probably initiated at the well face, due to high tensile strength provided by the casing and the horizontal slot cut through the casing and into the shale. The tensile strength of the shale in the vertical direction, T_{σ_z}, can be estimated by eq. (45) and the result is:

$$T_{\sigma_z} = 10.9 - 14 = -3.1 \text{ MPa}$$

After 3 m^3 of water had been injected, the injection pressures increased rapidly beyond the propagation pressures predicted by the regression equation (eq. 57). These high pressures might suggest the formation of additional fractures.

From eq. (57), the normal propagation pressure at the rate of 0.006 m^3/s is 12.1 MPa, however, the observed highest pressure at 0.006 m^3/s was 15.2 MPa (figs. 17 and 18). This pressure could be the breakdown pressure at the stage of formation of additional fractures. The tensile strength of the shale calculated on the basis of this breakdown pressure is 4.2 MPa which is about 1.1 MPa higher than the value estimated based on the first breakdown pressure.

When the injection is stopped, Q will be zero. The instantaneous shut-in pressure can be obtained from eq. (57), resulting in 12 MPa. The observed instantaneous shut-in pressure during the 45-minute pause was 12.1 MPa (fig. 17), virtually the same as the value predicted by eq. (57).

The average cohesive force at the fracture tip can be estimated by eq. (46) if Q is equal to zero, and the result is:

$$fT_{\sigma_z} = 10.9 - 12 = -1.1 \text{ MPa}$$

and

$$f = 0.35$$

After the 45-minute pause the injection was resumed at a rate of 0.025 m^3/s. The calculated propagation pressure for this rate should be 12.6 MPa (eq. 57) however, the observed pressure was 15.4 MPa which probably was the breakdown pressure at reinjection stage. The estimated tensile strength of the shale based on this breakdown pressure is 3.9 MPa, which is 0.8 MPa higher than the first calculated value, 3.1 MPa, but is close to the value calculated on the basis of breakdown pressure observed at 0.006 m^3/s.

After the fracture was reinitiated, the injection pressure diminished to the normal propagation pressure. The regression equation (fig. 19) with a correlation coefficient of 0.89 for the injection period after the pause is:

$$P = 11.96 + 60.01\ Q \qquad (58)$$

Again the regression coefficient has been found to be significant on the 95 percent confidence level.

After completion of the injection, the well was shut-in at the well head. The observed instantaneous shut-in pressure was 12 MPa closely matching the estimated shut-in pressure obtained by eqs. (57) and (58). Pressure decay was observed for about 8 days, the results are shown in table 2 and figure 20.

The observed injection pressure at the end of the first part of the injection before 45-minute pause, with an injection rate of 0.025 m^3/s, was 12.6 MPa and the observed shut-in pressure was 12.05 MPa (table 1); the difference between the two pressures was 0.55 MPa. Therefore, the pressure needed to overcome friction loss of one unit of injection rate was 22(MPa)/(m^3/s), which is close to the regression coefficient of Q determined statistically, that is 24(MPa)/(m^3/s) (eq. 57). The observed injection pressure at the end of the injection with an injection rate of 0.025 m^3/s was 13.4 MPa and the observed shut-in pressure was 12 MPa (table 1); the difference between the two pressures is 1.4 MPa. The pressure required to overcome frictional loss of one unit of injection rate was 56(MPa)/(m^3/s) which is close to the regression coefficient of 60(MPa)/(m^3/s)

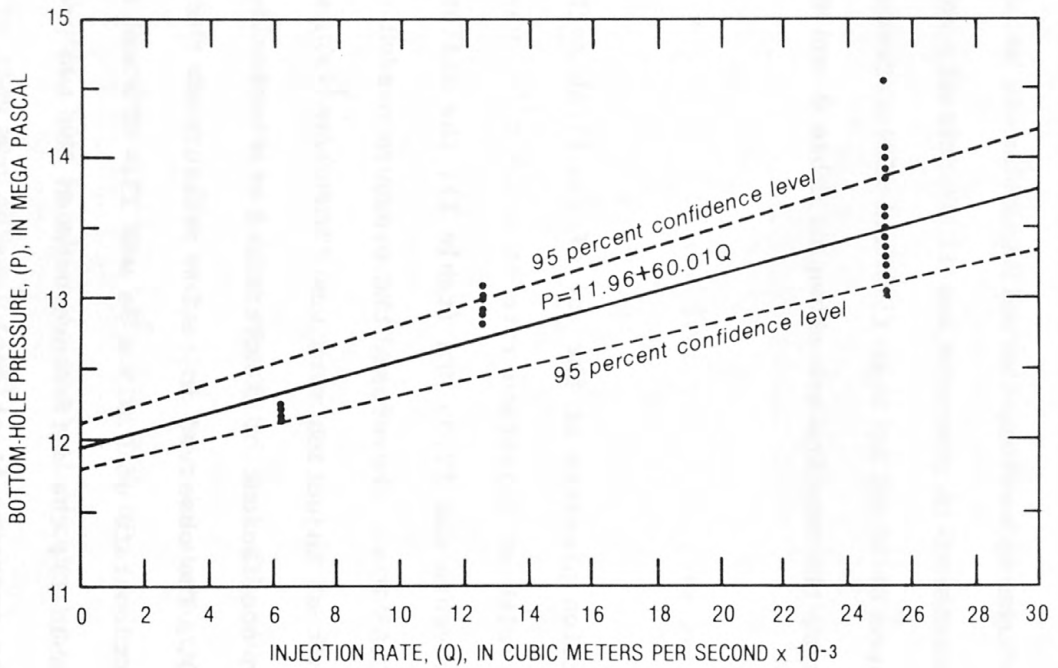

Figure 19.--Pressure versus injection rate, after 45-minute pause, water injection at 442 meters, October 9, 1969, West Valley, New York.

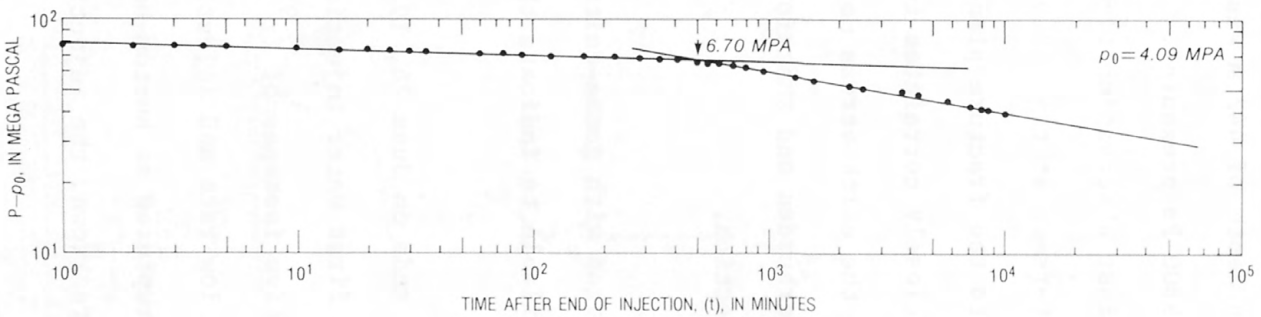

Figure 20.--Pressure decay versus time, water injection at 442 meters, October 9, 1969, West Valley, New York.

(eq. 58). From these correlations, it probably can be concluded that the determined regression equations (eqs. 57 and 58) are meaningful.

Water level was measured in the corehole by G. H. Chase (U.S. Geological Survey, written commun., 1970) on May 22, 1969, and was found to be 18 m below land surface. Adjusted by altitude difference between corehole and the injection well, the depth to water was 24 m in the injection well. The hydraulic pressure p_o in the formation at the injection depth of 442 m was, therefore, calculated as 4.1 MPa (a meter of water produces 9800 Pa pressure).

The log-log plot of $(P-p_o)$ against observation time t (fig. 20) appears to fall on two straight lines which intersect at t = 500 minutes and $(P-p_o)$ = 6.7 MPa. Therefore, the earth stress normal to the fracture plane is estimated to be 10.79 MPa (4.09 + 6.7 = 10.79 MPa) which closely correlates to the calculated overburden that is 10.9 MPa.
pressure/ It can be concluded that the earth stress normal to the fracture planes is simply equal to the weight of overburden and therefore the induced fracture is probably in a nearly horizontal direction.

The injection water was not tagged with gamma-emitting radioactive isotopes, therefore, no field evidence is available to indicate the orientation of the induced fractures.

The second water injection was made on June 26, 1970, at the same depth and through the same slot where the first water injection was made. A total of 425 m^3 of water tagged with radioactive isotopes of Zr^{95} and Nb^{95} was injected. The injection was started at a very low rate and injection pressure built up steadily. The rock apparently was ruptured at bottom-hole pressure of 16.1 MPa (fig. 21 and table 3). After the breakdown, the injection rate was increased to

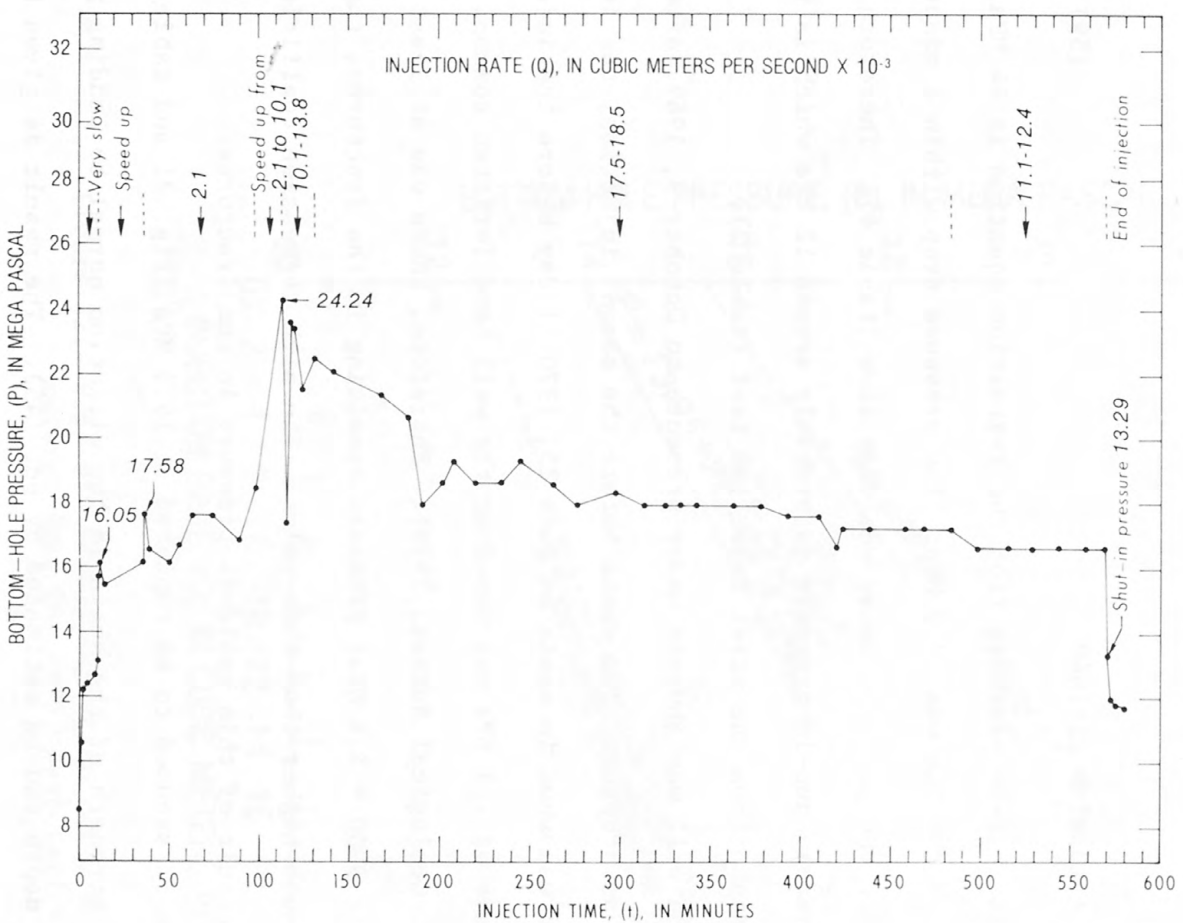

Figure 21.--Pressure versus time, water injection at 442 meters, June 26, 1970, West Valley, New York.

0.002 m^3/s. This rate was maintained for 70 minutes. When the injection rate was increased again, the pressure rose quickly until it reached a peak of 24.2 MPa; at this time the injection rate was 0.01 m^3/s. This second peak may indicate the formation of additional fractures. Thereafter the pressure dropped to normal propagation pressure (fig. 21). The regression equation of P and Q with a correlation coefficient of 0.73, is found (fig. 22) to be:

$$P = 13.95 + 224.06Q \tag{59}$$

Instantaneous shut-in pressure from the regression equation is 14 MPa, however, the observed value was 13.3 MPa. The pressure drop within 1 minute was 1.2 MPa, thereafter the pressure decay was very slow (table 4). Therefore, the correct instantaneous shut-in pressure is probably around 12 MPa which is the same as that obtained from the first injection test (table 2).

The injection well was shut-in under pressure on October 9, 1969, after the first injection was stopped. Two weeks before the second injection, the injection well was bled and was shut in again on June 25, 1970, 1 day before the injection. A residual pressure of 1.1 MPa was noted at the well head (written commun., G. H. Chase, U.S. Geological Survey, 1970). Therefore, there was at least 5.4 MPa ($1.1 \times 10^6 + 442 \times 9800 = 5.4$ MPa) pressure remaining in the fractures, though probably it was much higher than this value. The high regression coefficient of Q likely is the result of this residual pressure in the fractures.

If the shale is assumed to be ruptured at 16.1 MPa (fig. 21 and table 3), then the tensile strength of the shale in the direction normal to bedding planes at the injection depth can be estimated by eq. (45). The result is given by:

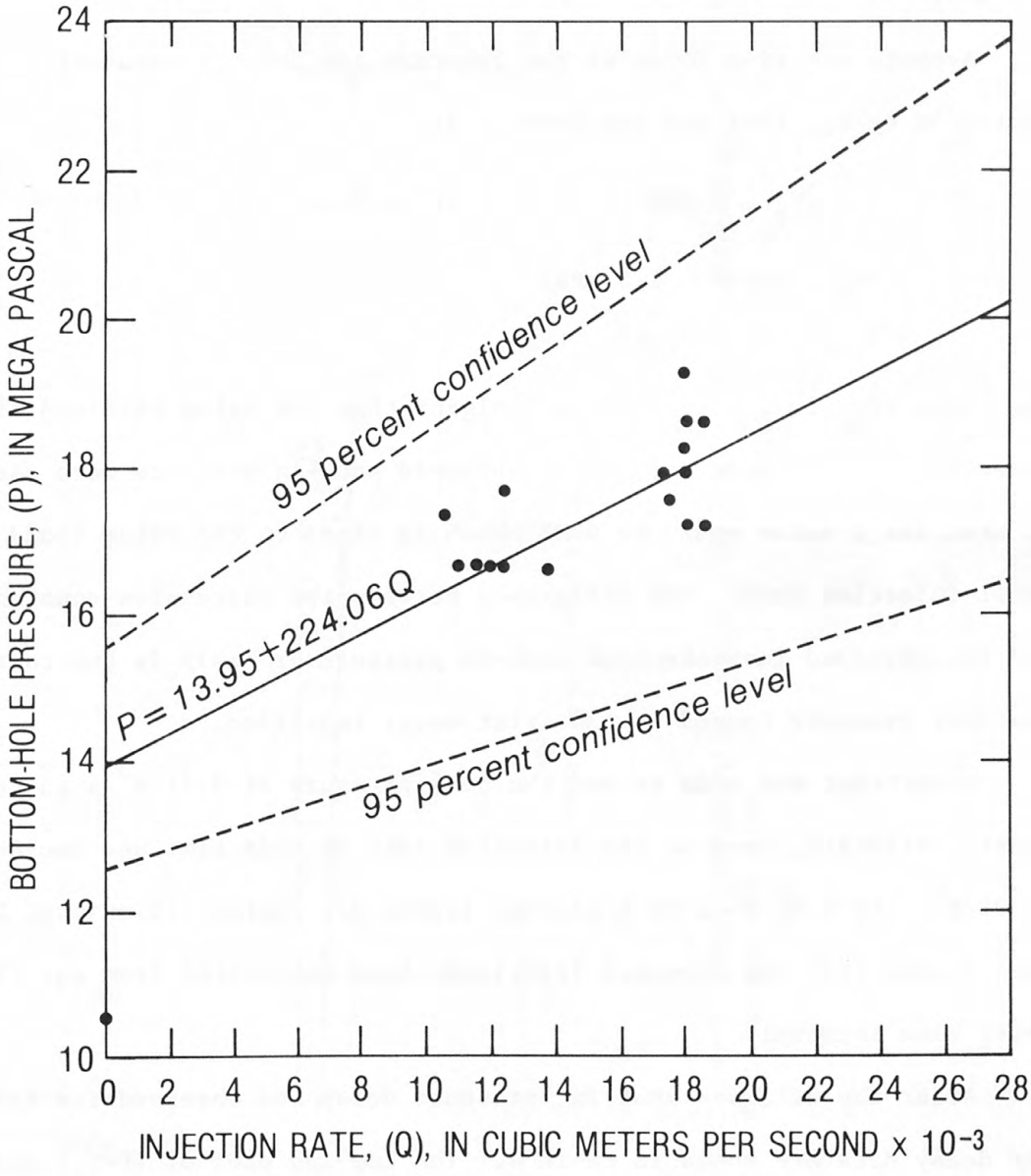

Figure 22.--Pressure versus injection rate, water injection at 442 meters, June 26, 1970, West Valley, New York.

$$T_{\sigma_z} = (10.9 - 4.1) - (16.1 - 5.4)$$

$$= - 3.9 \text{ MPa}$$

which is close to the tensile strengths calculated from the first water injection on October 9, 1969, at the same injection depth, they are in the range of 3.1 to 4.2 MPa.

Average cohesive force at the fracture tip and the value of f can be estimated by eq. (46) and the results are:

$$fT_{\sigma_z} = (10.9 - 4.1) - (14 - 5.4)$$

$$= - 1.8 \text{ MPa}$$

$$f = 0.46$$

The value of f is 35 percent higher than the value obtained from the first water injection. However, if the observed shut-in pressure were used, that is 12 MPa, the f value would be 0.28 which is close to the value found by the first water injection data. The difference between the regression constant at Q=0 and the observed instantaneous shut-in pressure probably is due to the observed residual pressure caused by the first water injection.

No attempt was made to use the peak pressure at 0.01 m^3/s to estimate the tensile strength, because the injection rate at this time was increased from 0.002 m^3/s to 0.01 m^3/s in 5 minutes (table 3). Actual frictional loss would be much higher than the expected frictional loss calculated from eq. (59) during this short time interval.

After the well was shut-in, pressure decay was observed for nearly 13 days. The decay data are shown in table 4. The log-log plot of $(P-p_o)$ against time t is shown in figure 23. All data apparently fall on two straight lines.

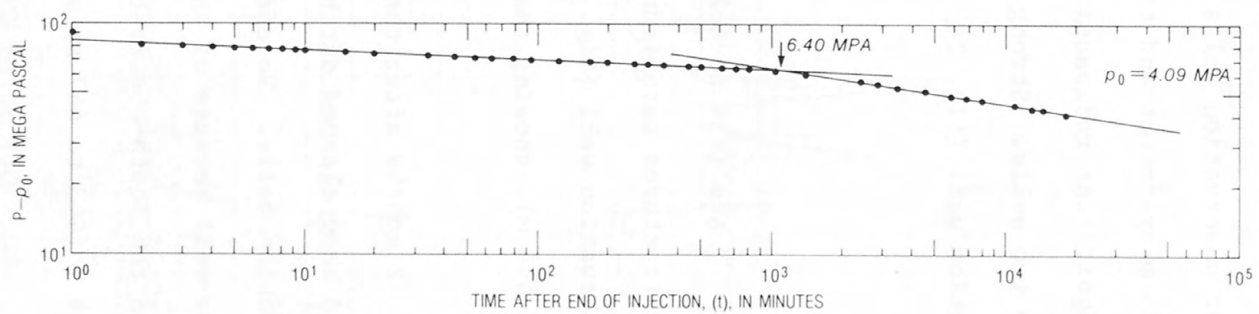

Figure 23.--Pressure decay versus time, water injection at 442 meters, June 26, 1970, West Valley, New York.

$(P-p_o)$ at the point of intersection of the two lines is 6.4 MPa, therefore, the estimated earth stress normal to the fracture plane is 10.5 MPa (6.4 + 4.09 = 10.49 MPa) which is close to the estimated overburden pressure, 10.9 MPa. Therefore, it can be concluded that the induced fractures are probably nearly horizontal.

Ten days after the end of the water injection, July 6, 1970, gamma-ray logs were made in all four observation wells. The East-observation well was found to be plugged at 424 m by cement and the South-observation well was also blocked at 442 m. No significant radioactivity above the background level was recorded in either of the two wells. Strong gamma-activity was, however, recorded in the North-observation well (fig. 24). The radioactivity was observed over a vertical distance of 6 m (436 to 442 m) indicating that at least three layers of bedding-plane fractures were induced. Strong gamma-activity was also recorded in the West-observation well (fig. 24) and observed over a vertical distance of 2 m (443 to 444 m), showing that only one layer of bedding-plane fracture was induced.

On August 24, 1970, 2 months after the water injection and after the South-observation well had been cleaned out by a rig, gamma-ray logs were run again in the three observation wells. No efforts were made to clearn out cement in the East-observation well because of the small diameter well tubing. Strong gamma-activity was recorded in the South-observation well at this time and a vertical spread of less than 4 m (443 to 447 m) was observed (fig. 25), and two

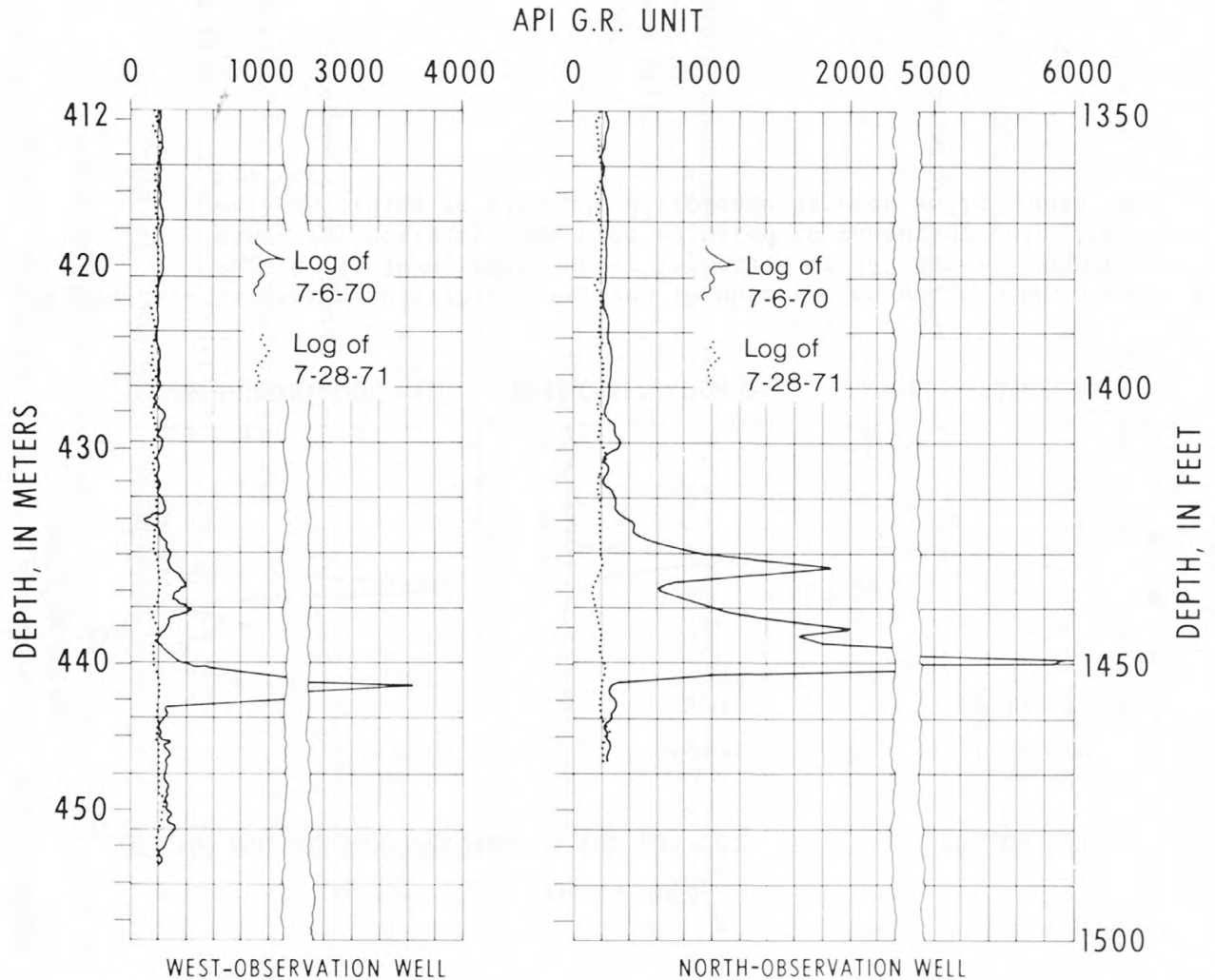

Figure 24.--Gamma-ray activities surveyed in observation wells along casing axis, July 6, 1970, after water injection at 442 meters; depths to gamma-ray activity have been adjusted to measuring point at injection well according to altitude difference between wells, West Valley, New York.

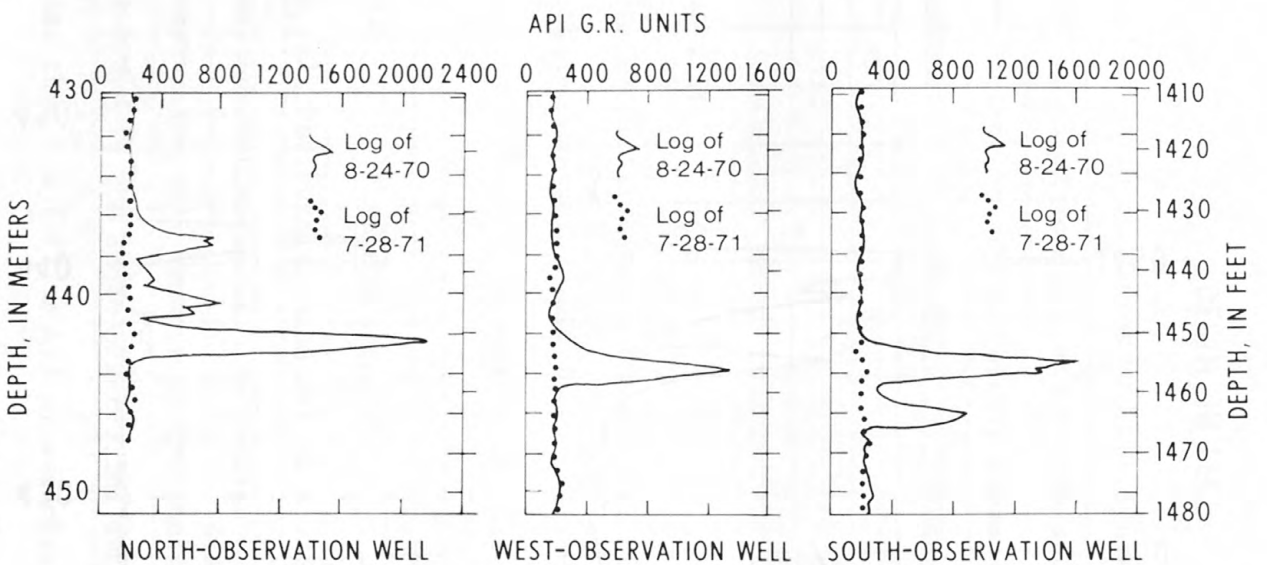

Figure 25.--Gamma-ray activities surveyed in observation wells along casing axis, August 24, 1970, after water injection at 442 meters; depths to gamma-ray activity have been adjusted to measuring point at injection well according to altitude difference between wells, West Valley, New York.

layers of bedding-plane fractures were induced. The gamma-activity observed at the other two observation wells, North- and West-observation wells, was approximately at the same depth as recorded before, however, the intensity was reduced to less than half of the values recorded on July 6, 1970, because of radioactive decay (figs. 24 and 25).

A1.3.2 Grout injection

Only one grout injection was made at a depth of 152 m at the West Valley site during the study. Before the grout injection a total of 195 m^3 of water without radioactive tracer was injected. The observed injection pressures associated with injection rates are shown in table 5 and figure 26. The regression equation of P and Q with a correlation coefficient of 0.91 was found (fig. 27) and is given by:

$$P = 3.88 + 10.93\ Q \qquad (60)$$

Observed shut-in pressure was 3.8 MPa (table 6) which is close to the value indicated by the regression equation. Pumping rate was kept at 0.002 m^3/s during the first hour of the injection. Then it was increased to 0.028 m^3/s over a 1-1/2 hour interval. The rock was ruptured at 4.3 MPa (fig. 26).

The overburden pressure estimated from the density of rock at a depth of 152 m is 3.5 MPa. The difference between the overburden pressure and the rupture pressure is the value of the tensile strength of shale in the direction normal to the fracture plane. If nearly horizontal bedding-plane fractures

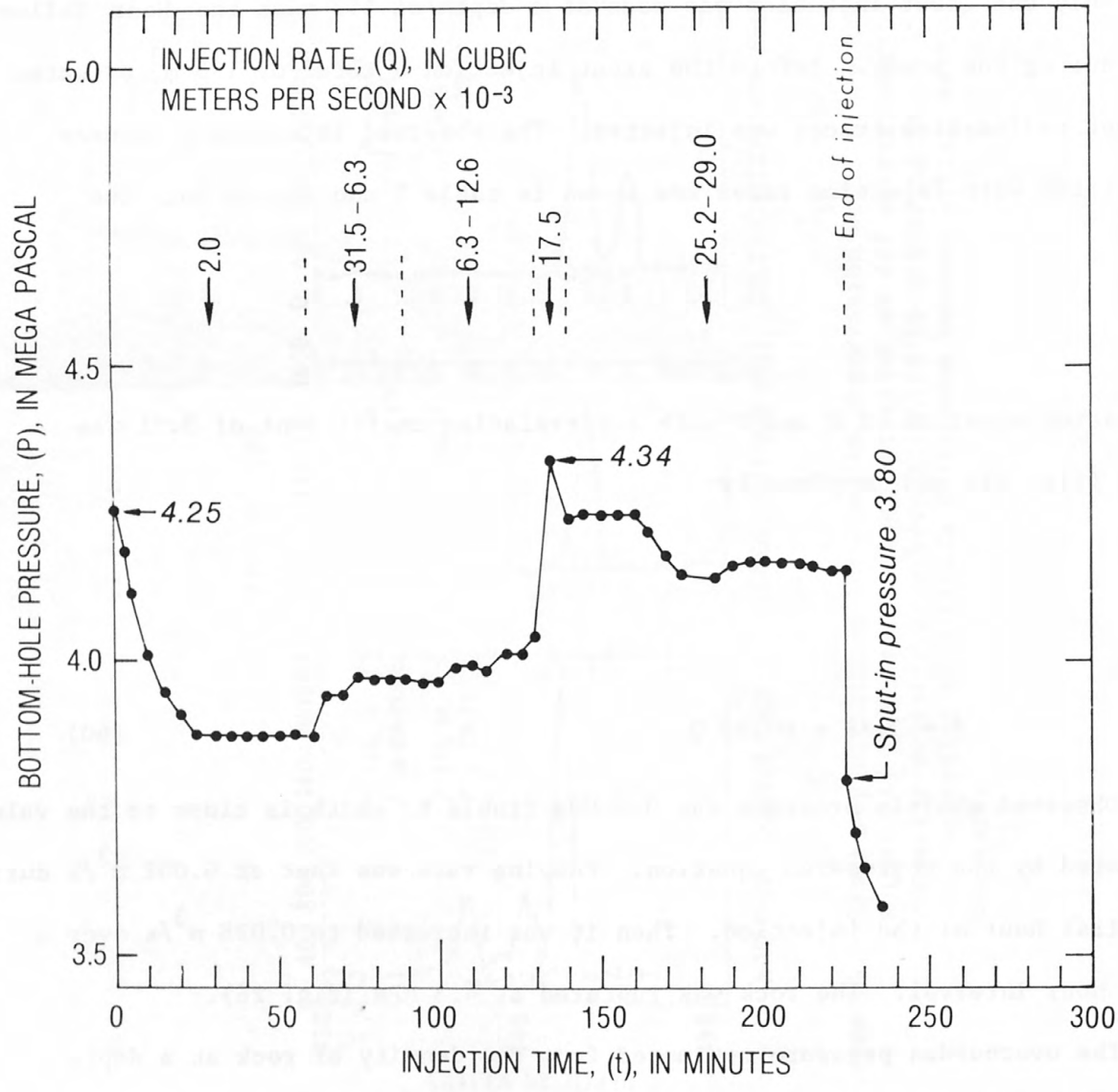

Figure 26.--Pressure versus time, water injection at 152 meters, May 29, 1971, West Valley, New York.

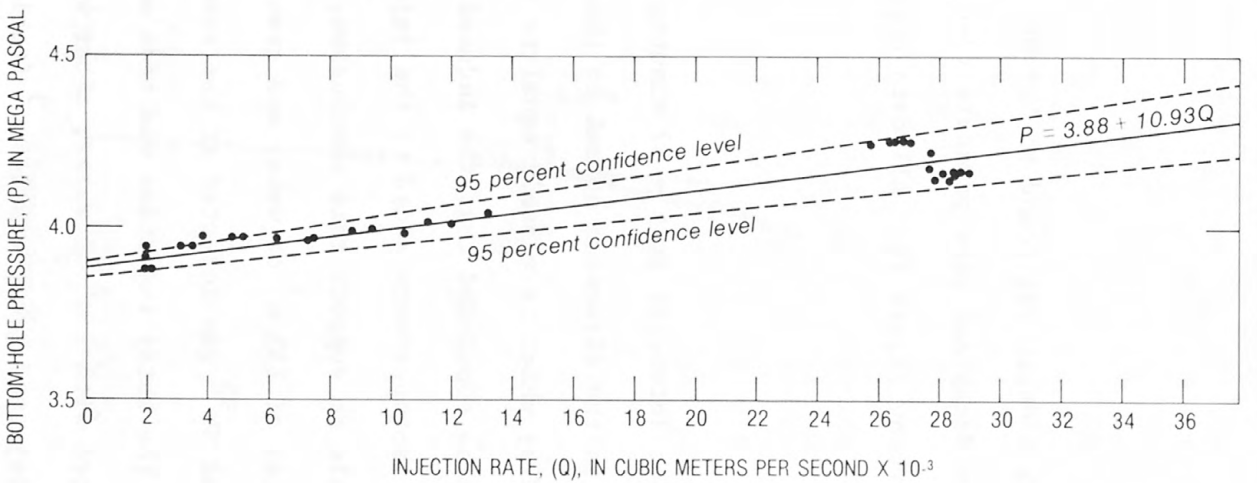

Figure 27.--Pressure versus injection rate, water injection at 152 meters, May 29, 1971, West Valley, New York.

are assumed to be induced, then the tensile strength of shale in the direction normal to bedding planes at the injection depth was found to be 0.8 MPa, which is one-fourth of the value found by the water injections made at 442 m. By inspecting cores the shale at 152 m depth was found to be more easily ruptured along bedding planes than the shale at 442 m depth.

Average cohesive force at fracture tip is calculated as:

$$fT_{\sigma_z} = 3.5 - 3.9 = -0.4 \text{ MPa}$$

and $$f = 0.50$$

The pore pressure at 152 m depth was found to 1.3 MPa. The differences between the observed pressure decay and pore pressure ($P-p_o$) against time t are plotted on log-log graph paper shown by figure 28. All data appear to fall on two straight lines. The two lines intersect at t = 37 minutes and ($P-p_o$) = 2.1 MPa. Therefore, the earth stress in the direction normal to the fracture plane is 3.4 MPa (2.1 + 1.25 = 3.35 MPa) which is closely equal to the calculated overburden pressure. Therefore, it can be concluded that the induced fractures probably are horizontal. No radioactive isotopes were added to the injection water, therefore, no field evidence is available to support this conclusion.

On July 23, 1971, a total of 155 m^3 of water and grout tagged with gamma-emitting isotopes of Zr^{95} and Nb^{95} was injected at the same depth, 152 m, and through the same slot where the water injection was made on May 21, 1971.

The injection was started with 9 m^3 of water, after which cement and bentonite were added. The volume of injected grout was 146 m^3 (table 7).

Because grout has high viscosity, the friction loss in casing was calculated by using a non-Newtonian flow equation (Slagle, 1962; Melton and Saunders, 1957) which is expressed as follows:

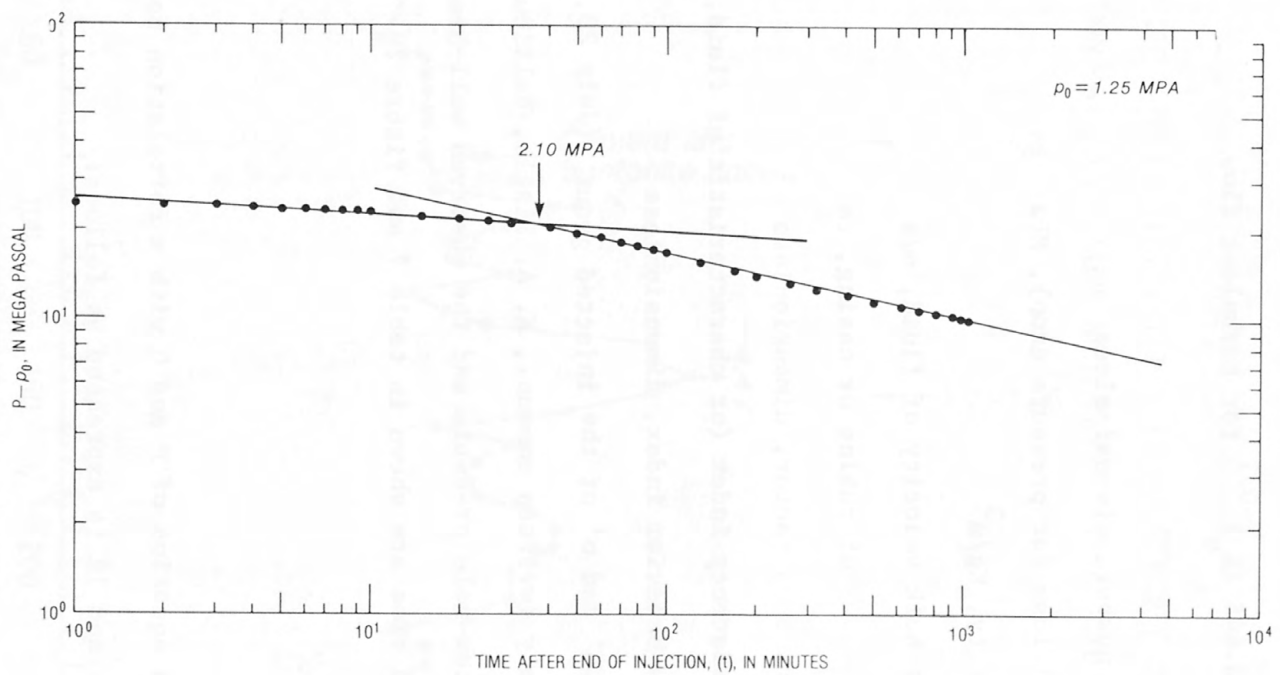

Figure 28.--Pressure decay versus time, water injection at 152 meters, May 29, 1971, West Valley, New York.

$$R_e = (0.816\ v^{2-n'}\rho)/[K'(800/D)^{n'}] \quad (61)$$

$$\Delta P = 2.0 \times 10^{-4}\ \frac{L\ \rho v^2\ f}{D} \quad (62)$$

$f = 16/R_e$ for laminar flow when $R_e \leq 2100$

$f = 0.0045 + 0.645\ (R_e)^{-0.7}$ for turbulent flow

where

R_e = Reynold's number, dimensionless

ΔP = frictional loss (or pressure drop), MPa

ρ = fluid density, Kg/m^3

v = average or bulk velocity of fluid, m/s

D = inside diameter of tubing or casing, cm

f = Fanning friction factor, dimensionless

K' = fluid consistency index (or characteristic of fluid, Newton $- sec^{n'}/m^2$

n' = fluid flow behavior index, dimensionless

The values of K' and n' of the injected grout (July 23, 1971) were 32.52 and 0.09 respectively (written commun., K. A. Slagle, Halliburton Co., 1971). The calculated bottom-hole pressure and the observed well-head pressure with injection rates and time are shown in table 7 and figure 29.

The regression equation of P and Q with a correlation coefficient of 0.65 was found (fig. 30) and it is expressed as follows:

$$P = 4.0 + 13.12Q \quad (63)$$

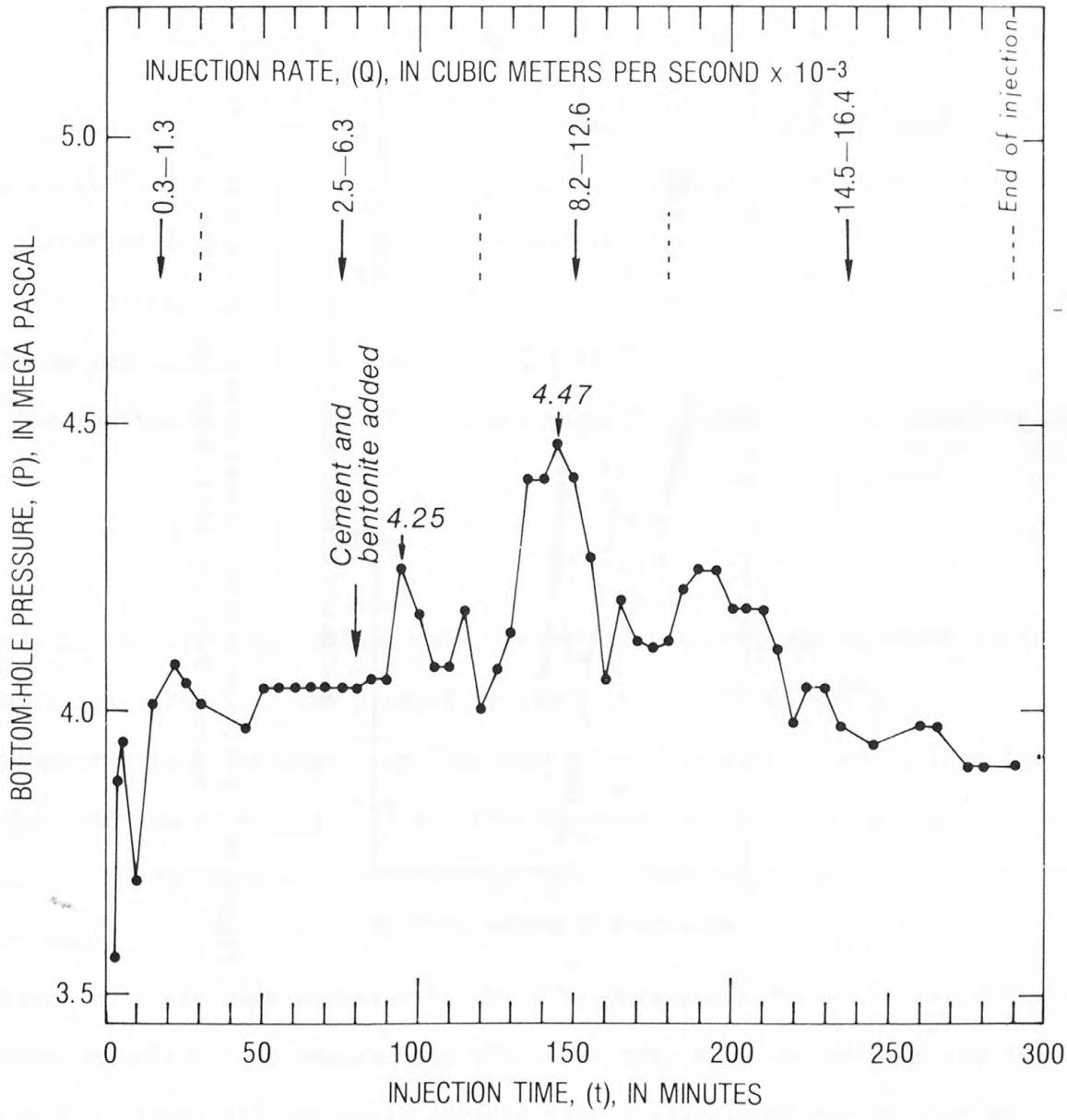

Figure 29.--Pressure versus time, grout injection at 152 meters, July 23, 1971, West Valley, New York.

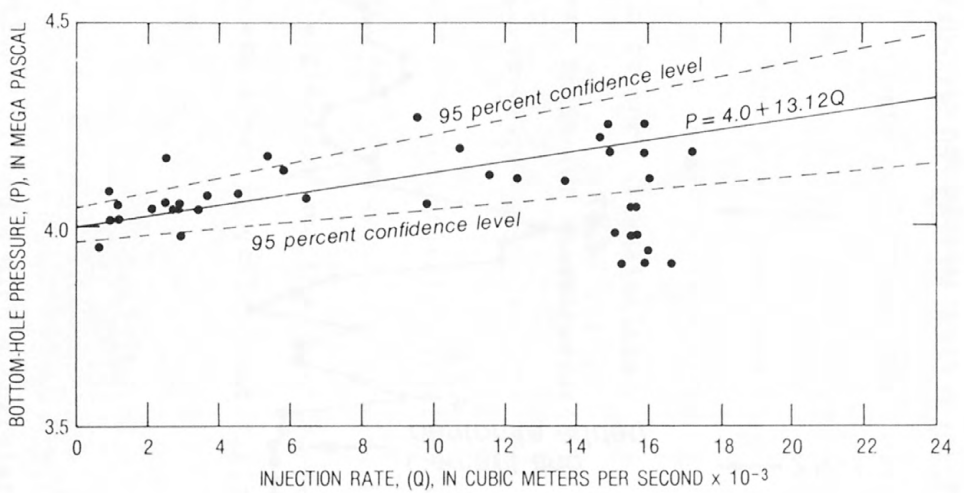

Figure 30.--Pressure versus injection rate, grout injection at 152 meters, July 23, 1971, West Valley, New York.

No breakdown pressure was observed. However, several high pressures indicating the formation of new fractures were noted during the injection. The tensile strength of the rock at the injection depth probably could be estimated from these high pressures. The injection pressure at 0.003 m^3/s was 4.3 MPa, from which the tensile strength of shale at the injection depth of 152 m in the direction normal to fracture plane was estimated as:

$$T_{\sigma_z} = 3.5 + 13.12 \times 0.0003 - 4.3$$

$$= - 0.8 \text{ MPa}$$

From other high pressures the estimated tensile strength of the shale is also in the range of 0.8 MPa. The estimated values of the tensile strength from this grout injection is similar to that estimated from the previous water injection at the same depth.

Gamma-ray logs were made on July 28, 1971, five days after the injection, in three observation wells. The results are shown in figure 31. No gamma-ray survey was made in the East-observation well, because its casing was ruptured during the injection. The well was plugged by grout at a depth of 151 m.

Gamma-ray logs obtained from the other three observation wells together with the evidence of plugging of the East-observation well strongly suggest that bedding-plane fractures were induced, at least within a radius of 46 m from the injection well.

Precise levels were surveyed by the U.S. Geological Survey before and after the grout injection. To insure that the level rods would be held on the highest point at all times, all benchmark tablets were straightened and leveled by a

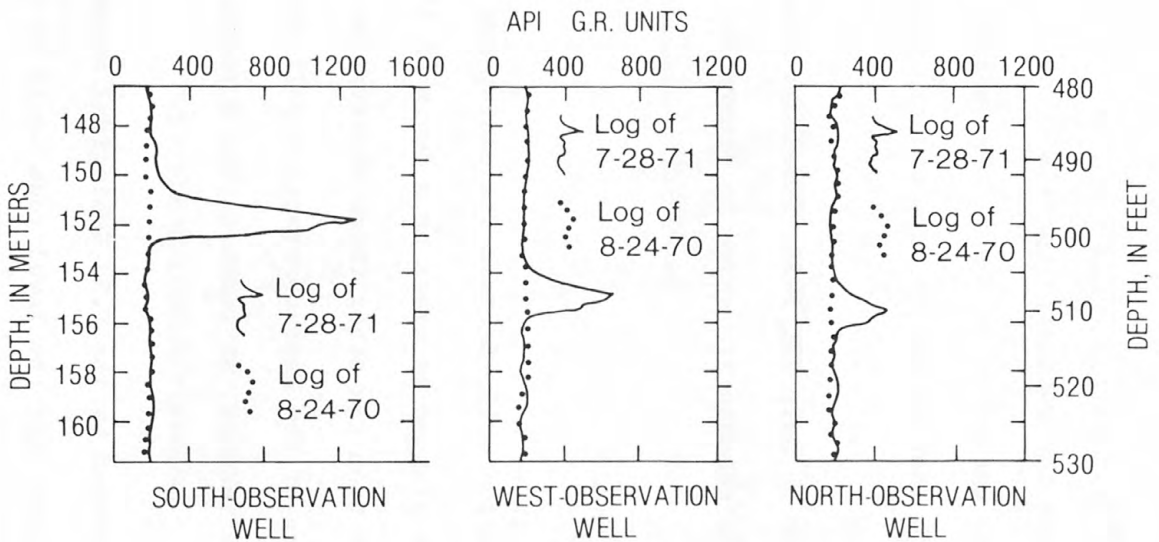

Figure 31.--Gamma-ray activities surveyed in observation wells along casing axis, July 28, 1971, after grout injection at 152 meters; depths to gamma-ray activity have been adjusted to measuring point at injection well according to altitude difference between wells, West Valley, New York.

hand-level before the precise levelings were made. The leveling results are shown in table 8 and figure 32.

The correlation between the observed uplift and the uplift calculated by equation (47) is shown in figure 33. The calculated radius of the induced fracture is 110 m and the calculated maximum separation of the fracture during injection time is 6.5 mm.

A1.4 Summary

Table 9 summarizes the results of all six injections made at West Valley, New York (Sun and Mongan, 1974). Results from injections made at the same depth at different times are consistent. No actual data on tensile strength of the shale, are available, therefore, there is no way to check whether the calculated tensile strengths are approximately right.

Bedding-plane fractures had been induced, as indicated by gamma-ray logs, within 10 m of the injection depth. Orientation of the induced fractures can be monitored indirectly by injection pressure during injection time and by pressure decay of water injection and uplift of ground surface. Constructing observation wells with strong tubing and good cement helps prevent damage of the well by induced fractures, and the size of observation well needs to be large enough to accommodate drilling tools if the well needs to be serviced after completion. The unsuitability of the East-observation well during the study indicates the importance of proper well construction.

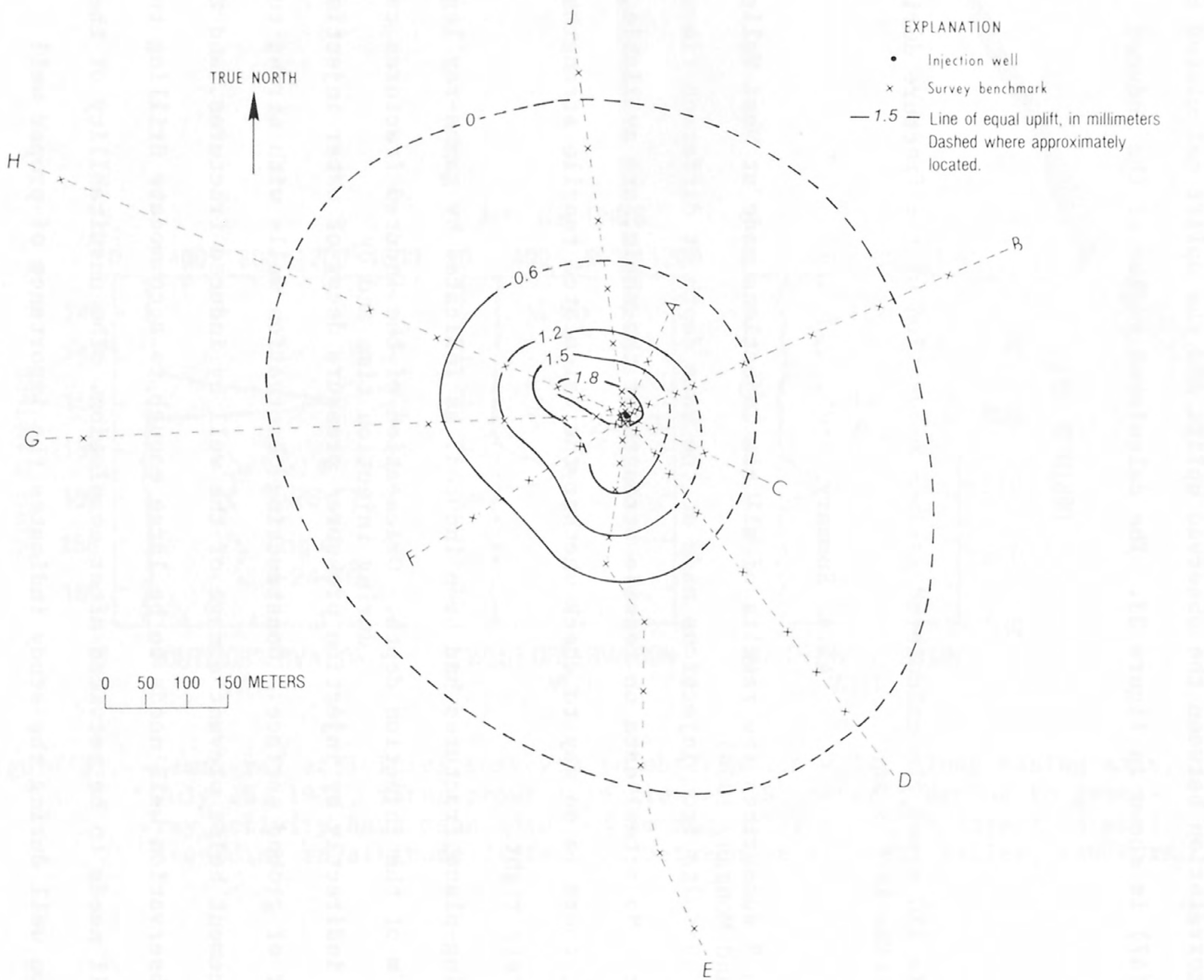

Figure 32.--Map showing uplift produced by grout injection at 152 meters, West Valley, New York.

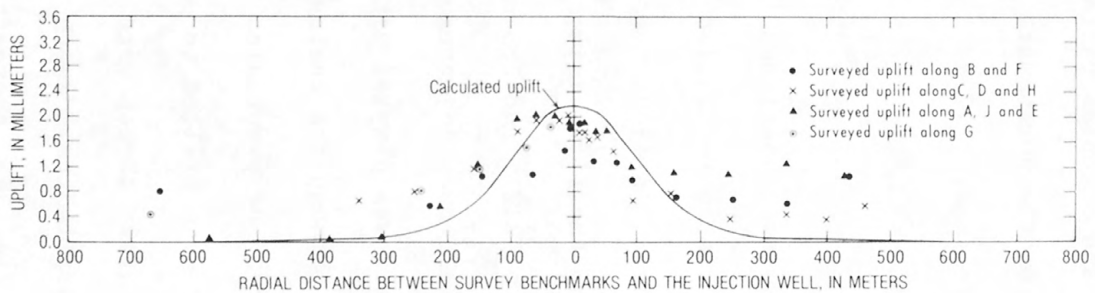

Figure 33.--Calculated and surveyed uplift produced by grout injection at 152 meters, West Valley, New York.

A2. RADIOACTIVE WASTE DISPOSAL AT OAK RIDGE NATIONAL LABORATORY, TENNESSEE

The Oak Ridge National Laboratory waste disposal site is located in Melton Valley, Oak Ridge, Tennessee (fig. 34), within the reservation of the U.S. Department of Energy (DOE). The reservation is in the Tennessee Section of the Appalachian Valley and Ridge province and occupies parts of Anderson and Roane Counties. The reservation is bounded on the northeast, southeast, and southwest by the Clinch River. The area is approximately 22 km long, 10 km in width, and comprises an area of about 220 km^2.

The first grout injection was made in 1959 at a shallow depth of 90 m. A total volume of 102 m^3 of grout with water, cement and bentonite tagged with Cs^{137} was injected. Twenty-two core holes were drilled and indicated that bedding-plane fractures had been induced. In 1960, a second experimental well was constructed roughly 1.83 km east of the first injection site. Two injections were made through this well at depths of 212 m and 285 m, respectively. A total volume of 345 m^3 of grout containing Cs^{137} was injected at a depth of 285 m. After this injection, the injection well was plugged with cement to a depth of 213 m. A new horizontal slot was cut through the casing and cement wall at a depth of 212 m. A total volume of 502 m^3 of grout also tagged with Cs^{137} was injected again. Twenty-four coreholes were drilled to determine the positions of the two grout sheets. Both of the grout sheets were found to be conformable to bedding planes. A third well was drilled to a depth of 329 m, 0.8 km west of the second experimental site (fig. 34), thereafter named as the present injection well. From 1964 through 1965, eight experimental injections with actual radioactive wastes produced at ORNL were injected through this well. The

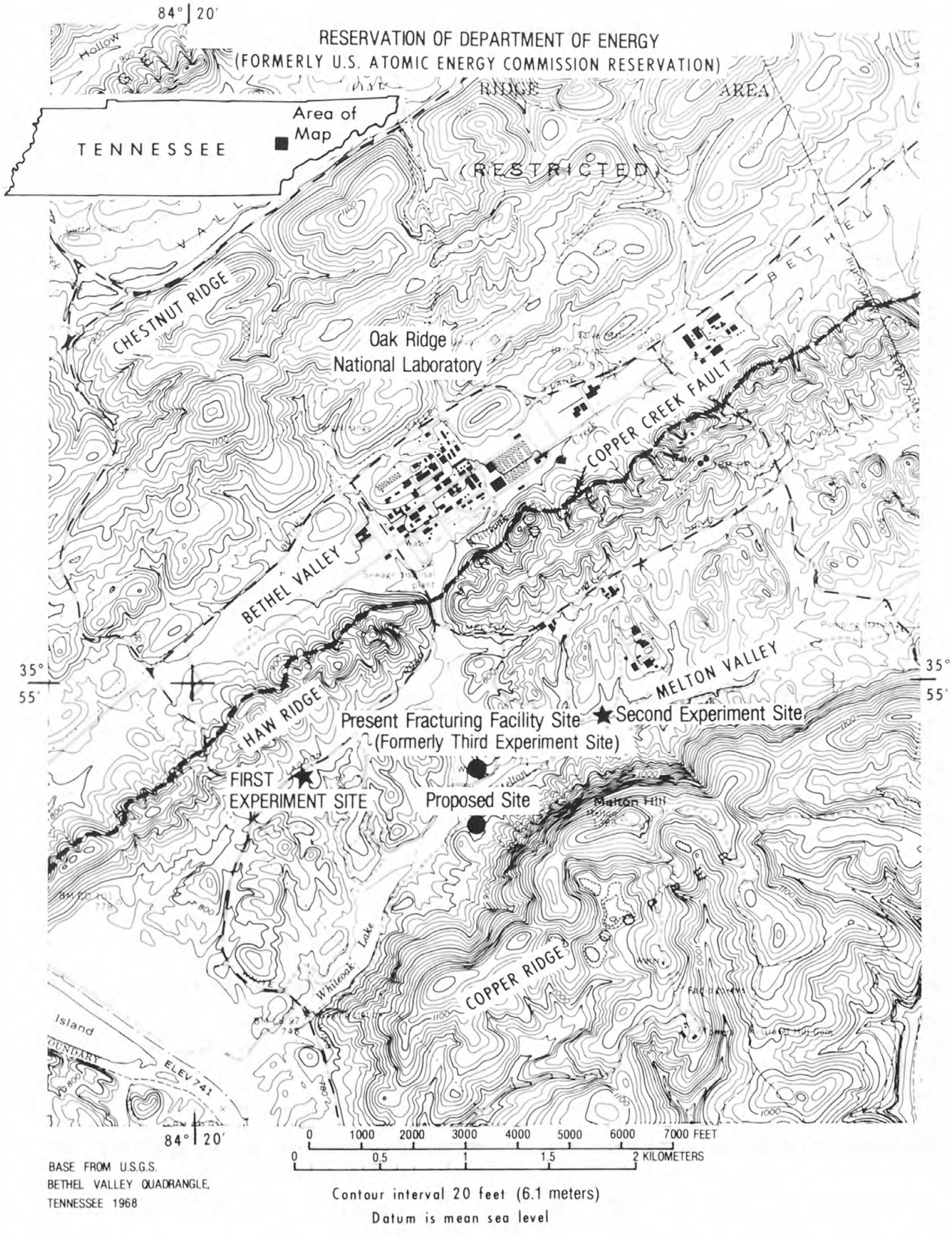

Figure 34.--Map showing location of hydraulic fracturing experiment sites, present fracturing site and proposed site, Oak Ridge National Laboratory, Tennessee.

results strongly indicated that the disposal of wastes in shale by grout injection is safe and economical. Operational injections then began in 1966. The disposal site will reach full capacity within 5 to 10 years from 1978. A new disposal site was selected at a distance of 245 m south of the present injection well (fig. 34), and a site evaluation study was conducted. The results indicate that the proposed site is acceptable. The following discussions summarize the experimental and operational injections, and the site evaluation.

A2.1 Geology and hydrology

The Appalachian Valley and Ridge Province in the Oak Ridge area is about 80 km wide and is marked by a series of major subparallel thrust faults that trend northeast and dip southeast. In each of the faults, layers of rock units roughly 3 km thick have moved as much as several tens of kilometers to the northwest. The old formation has been thrust over younger formations. Deformation of the rock strata of the Oak Ridge area resulted from compressional forces originating to the southeast of the Valley and Ridge Province at the end of Paleozoic time during the Appalachian revolution. The strata reacted to the pressure by developing faults and folds (Eardley, 1951; McMaster, 1963; deLaguna and others, 1968). At least 3,000 m of rock has been eroded after the thrust faults were formed (deLaguna and others, 1968).

The thrust fault of immediate interest to the waste disposal at ORNL is the Cooper Creek thrust fault which affects of four formations at the site (fig. 35),

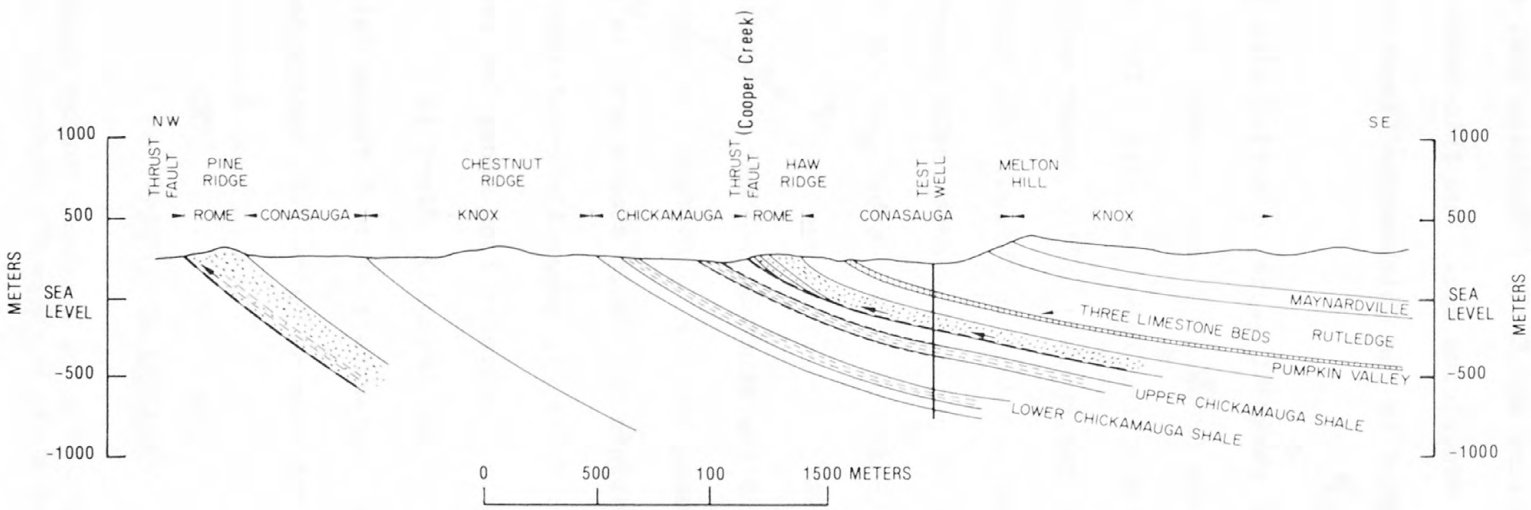

Figure 35.--Subsurface geology at hydraulic fracturing sites, Oak Ridge National Laboratory, Tennessee (from deLaguna and others, 1968).

They are, the Rome Formation (interbedded sandstone, siltstone, shale and locally, dolomite) of Early Cambrian age, the Conasauga Group (calcareous shale interlayered with limestone and siltstone) of Middle and Late Cambrian age, the Knox Group (dolomite) of Late Cambrian and Early Ordovician age, and the Chickamauga Limestone of Middle and Late Ordovician age. Two thin-bedded red calcareous shales each 60 m thick were found in the Chickamauga Limestone at ORNL during drilling a test well (fig. 35).

The formation exposed at the ORNL waste injection site is the Conasauga Group, all formations above the Group have been eroded. The thickness of the Conasauga Group is 400 m at the injection site. The injection rock is the bottom 90 m of the Conasauga, the Pumpkin Valley member which is a dense argillaceous shale that is very thin bedded and dominantly red. The Pumpkin Valley is overlain by the Rutledge, 300 m thick, of gray calcareous shale interbedded with generally thin beds or lenses of limestone. The contact between the Pumpkin Valley and the Rutledge is marked by three layers of limestone.

The formations all dip to the southeast. Near the outcrop area, the Rome formation dips 45 degrees, however, away from the outcrop dips flatten out to 10 to 20°. The beds within the fault sheets are, in general, relatively little deformed. The Pumpkin Valley is generally undeformed but locally it is marked by drag folds varying in amplitudes from about few centimeters up to a couple of meters. The measured geothermal gradient is 1.34 degree Celsius per 100 m with an average air temperature of 14.5 degree Celsius as shown in figures 36 and 37, respectively /(deLaguna and others, 1968; U.S. Energy Research and Development

Administration, 1977).

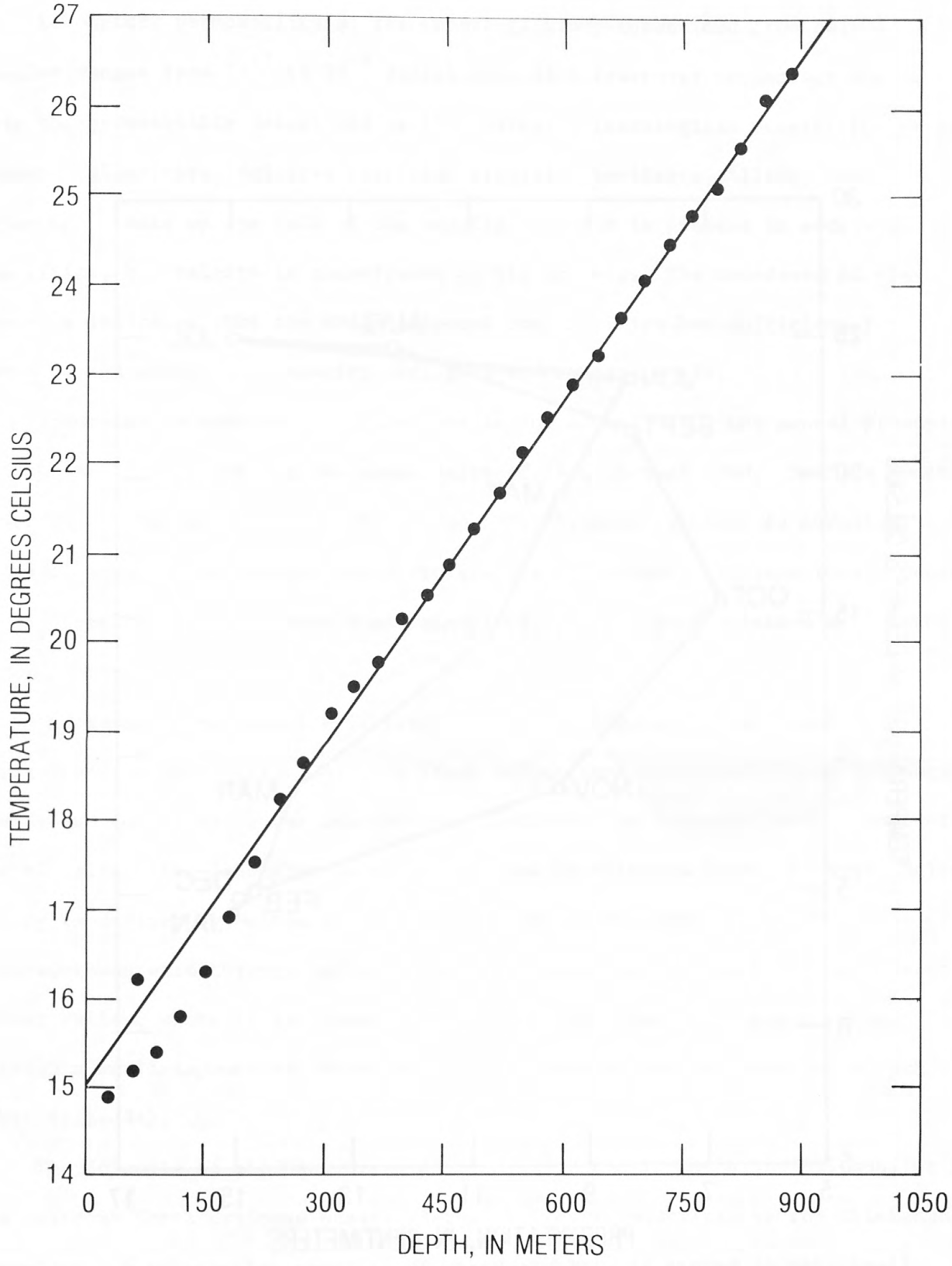

Figure 36.--Temperature versus depth at present fracturing site, Oak Ridge National Laboratory, Tennessee (from deLaguna and others, 1968).

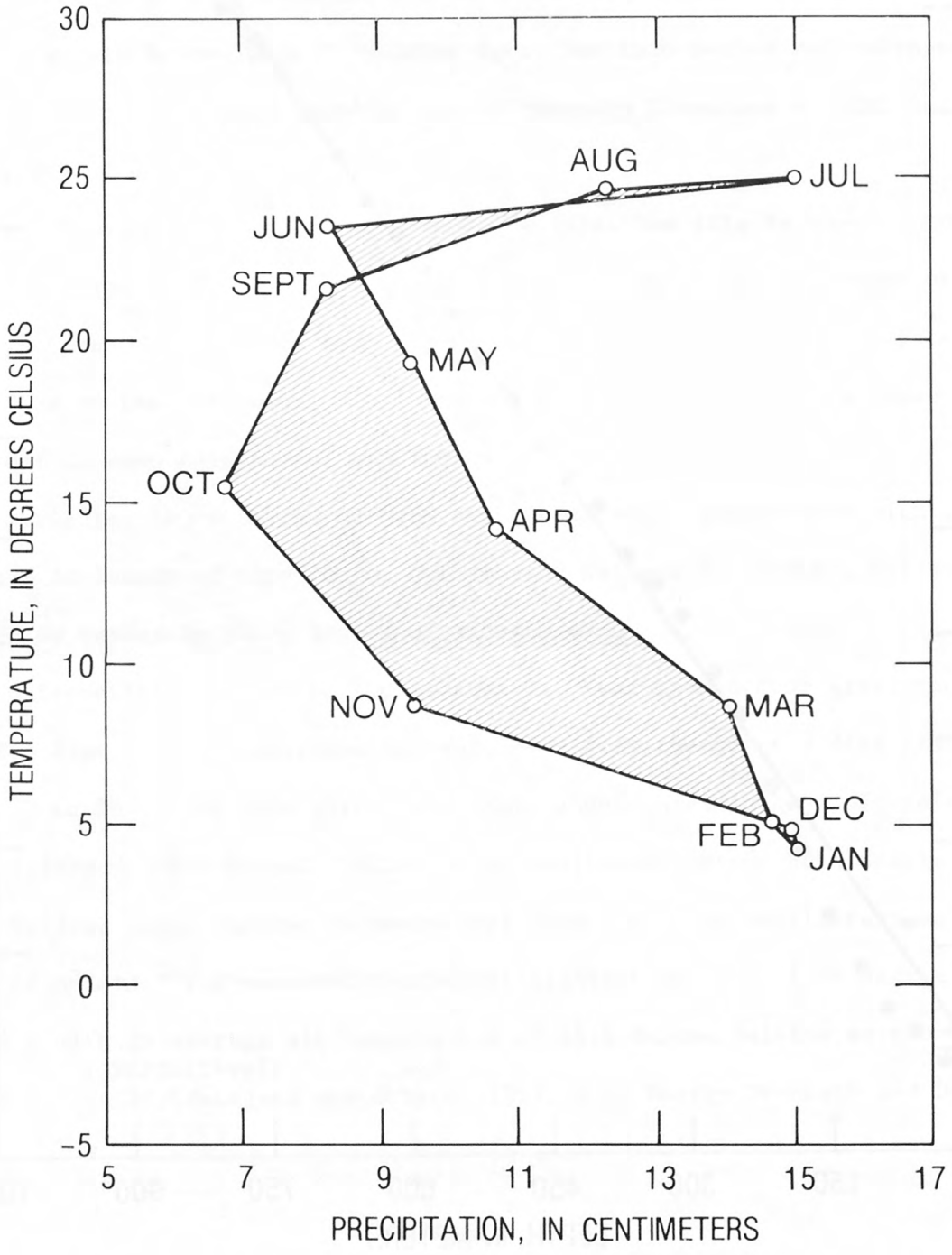

Figure 37.--Average monthly temperature and precipitation, Oak Ridge, Tennessee (from U.S. Energy Research and Development Administration, 1977).

Laboratory permeability of the Conasauga Group determined from core samples ranges from 10^{-7} to 10^{-8} darcy; even with fractures present in the core the permeability determined is 10^{-5} darcy. Mineralogical examination of the Pumpkin Valley core indicates that clay minerals, kaolinite, illite, and chlorite make up the bulk of the samples. Quartz is present in moderate quantities, but calcite is conspicuous by its absence. The abundance of clay minerals indicates that the shale selected for injection has sufficient ion exchange and adsorption capacity (deLaguna and others, 1968).

According to records of 11 stations in and around ORNL, the annual precipitation is 130 cm for the water years of 1936 through 1960. Maximum monthly runoff is likely to be in December through March, when rainfall is normally high and soil moisture and ground water storage are at maximum. Minimum runoff occurs in September through November when rainfall is low and soil moisture and ground water storage are at minimum (McMaster, 1967).

The waste injection site is located in Melton Valley, a part of the Whiteoak Creek drainage basin (fig. 34). Chestnut Ridge forms the northwestern drainage divide and Cooper Ridge the southeastern divide of the drainage basin. Most of Bethel Valley (the laboratory area) is drained by Whiteoak Creek, however, Melton Valley is drained by Melton Branch, a tributary to Whiteoak Creek. Whiteoak Creek flows southwestward through Bethel Valley to a water gap in Haw Ridge and enters Melton Valley, where it is joined by Melton Branch, then flows southwestward through a small impoundment known as Whiteoak Lake before entering the Clinch River (fig. 34).

The dolomite of the Knox Group of Chestnut Ridge is the principal aquifer in the Whiteoak Creek drainage basin. Bethel Valley is underlain by the Chickamauga Limestone. A substantial quantity of water probably is stored in many small openings in the weathered zone of the limestone within 30 m of land surface.

Low-flow measurements (flow equaled or exceeded 90 percent of time is 0.085 m^3/s) show that 90 percent of Whiteoak Creek low flow originates as ground-water discharge from the dolomite of the Knox Group of Chestnut Ridge and the Chickamauga Limestone of Bethel Valley, and from ORNL plant effluents (McMaster, 1967).

The Rome Formation of Haw Ridge forms the northwestern water divide of Melton Branch. This formation has very little capacity for receiving, storing, and transmitting water. In the weathered rock, the occurrence of ground water is largely limited to small openings that occur along joints and bedding planes. Melton Valley is underlain by the Conasauga Group. Ground water in the Conasauga occurs principally in the weathered zone where openings along joints and bedding planes have been slightly enlarged by weathering and circulating water. Because these enlarged openings occur only at shallow depths 0 to 10 m below land surface, the total capacity of the Conasauga shale for receiving, storing, and transmitting water is small (McMaster and Waller, 1965). In the late fall, periods of no flow have frequently occurred in Melton Branch (McMaster, 1963).

There is no known movement of ground water below a depth of 100 m. The isolation of the Pumpkin Valley member of the Conasauga Group is further demonstrated by the fact that the Pumpkin Valley member contains small amounts of disseminated sodium chloride and methane gas (U.S. Energy Research and Development Administration, 1977). Core taken 30 m below land surface showed no signs of iron stains, weathering and solution cavity. A geothermal measurement (fig. 36) also indicates that there is no significant movement of ground water deeper than 200 m.

A2.2 Seismicity

Available information from 1699 through 1973 indicates that no earthquakes have been reported within 16 km of Oak Ridge; however, earthquakes have been reported in the area predominantly to the south and east (fig. 38). The

largest earthquake (intensity Modified Mercali VII) was recorded near Luttrell, Tennessee, March 28, 1913 (McClain and Meyers, 1970; U.S. National Oceanic and Atmospheric Administration and U.S. Geological Survey, 1975). However, no field evidence of literature on active or potentially active faults in the vicinity of the ORNL site has been found.

A2.3 Nature of radioactive wastes produced at Oak Ridge National Laboratory

Radioactive wastes disposed of by grout injection and hydraulic fracturing are produced by a number of different research, development, and production programs conducted at ORNL, including basic radiochemistry studies, development of reactor fuel reprocessing methods, production of radioisotopes for medical, industrial and research uses, production of transuranium isotopes for research and operation of research reactors. The wastes are neutralized with sodium hydroxide to reduce corrosiveness and stored in underground stainless steel tanks which are periodically pumped to underground concrete collection tanks. The addition of sodium hydroxide causes some of the dissolved materials to precipitate from the waste solution. The precipitates settle as sludge at the bottom of the storage tanks. The liquid above the sludge is fed to an evaporator which concentrates the liquid waste by a factor of 20 to 30. The concentrated waste is stored in one of the underground concrete collection tanks for temporary storage, then is disposed in shale by grout injection periodically. Roughly 300 m^3 of concentrated liquid waste is produced at ORNL each year (U.S. Energy Research and Development Administration, 1977). The approximate chemical composition and radionuclide content of the ORNL waste are shown in table 10 (deLaguna and

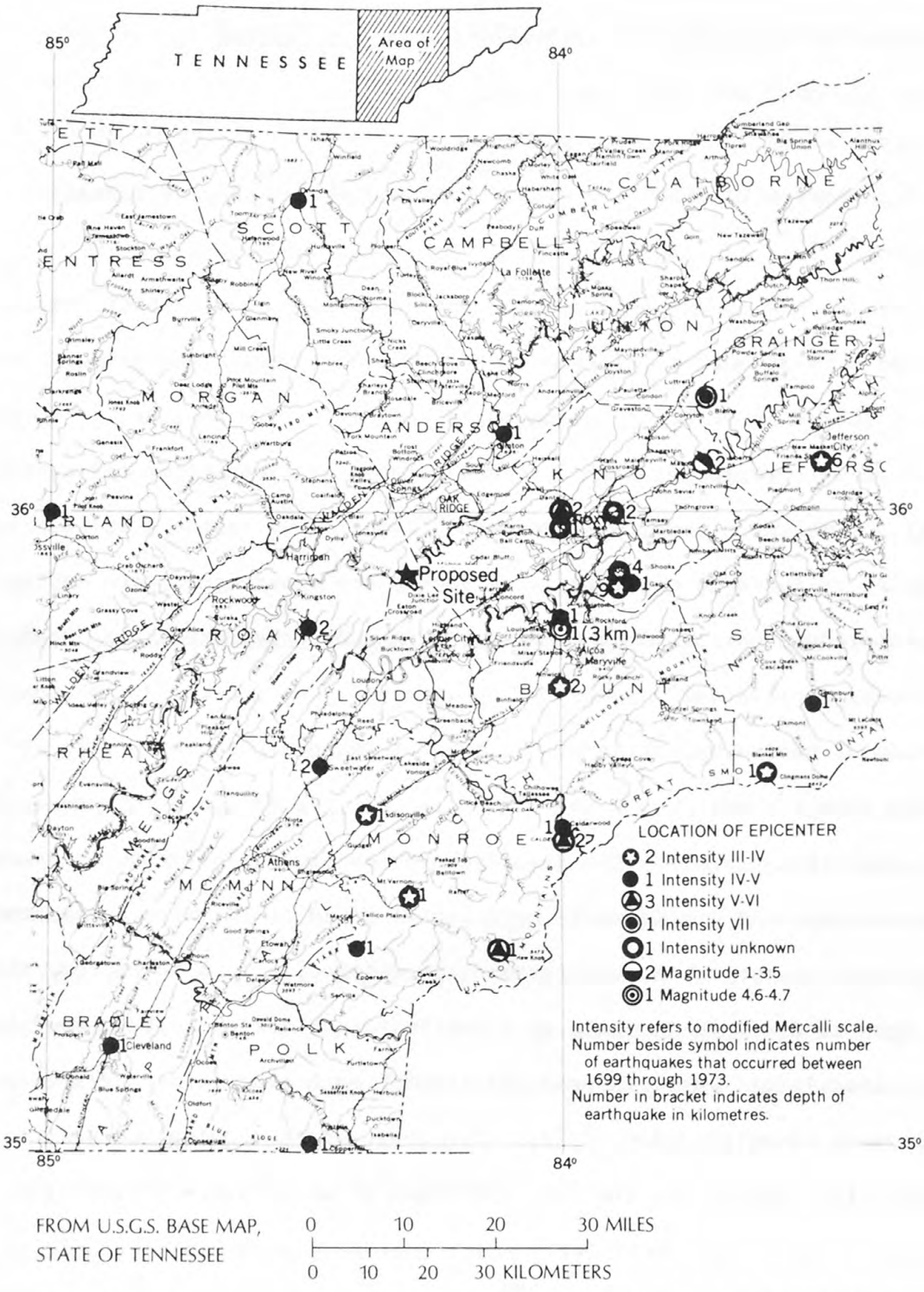

Figure 38.--Map showing location of epicenters in the vicinity of Oak Ridge, Tennessee, on the basis of available information (McClain and Meyers, 1970; U.S. National Oceanic and Atmospheric Administration and U.S. Geological Survey, 1975) from 1699 through 1973.

others, 1971; Weeren, 1976; U.S. Energy Research and Development Administration, 1977).

A2.4 Summary of disposed radioactive wastes

During 1964 and 1965, seven experimental injections had been made through the present disposal well. The first two experimental injections were made with synthetic wastes and the last 5 injections were made with actual wastes. Experimental results have indicated that grout injection by hydraulic fracturing is suitable and economical for disposal of the radioactive wastes at ORNL, therefore, since 1966 operational injections have been made periodically. At the end of 1978, a total of 17 operational injections were made.

From 1964 through 1978, a total volume of 6,400 m^3 (excluding synthetic waste) of intermediate-level radioactive waste (5.6×10^{-3} $\mu Ci/m\ell \leq$ specific activity $\leq$ 5.3×10^{2} $\mu Ci/m\ell$ containing mainly of Sr^{90} and Cs^{137}) was disposed of through the present injection well at depths ranging from 244 to 288 m (table 11). The waste contained a total activity of 641,300 curies among which were 590,400 curies of Cs^{137}, 40,100 curies of Sr^{90}, 80 g of Pu^{239}, 3 g of Cm^{244} and 10,500 curies of other radionuclides including Co^{69}, Ru^{106} and Ce^{144}.

A2.5 Injection processes and disposal plant

The injection processes and disposal plant at ORNL have been discussed by many investigators (deLaguna and others, 1968 and 1971; Weeren, 1974 and 1976). The following is a summation of these reports.

The major equipment used in injection consists of a waste pump, a jet mixer, a surge tank and an injection pump (fig. 39). An artist's sketch of the disposal

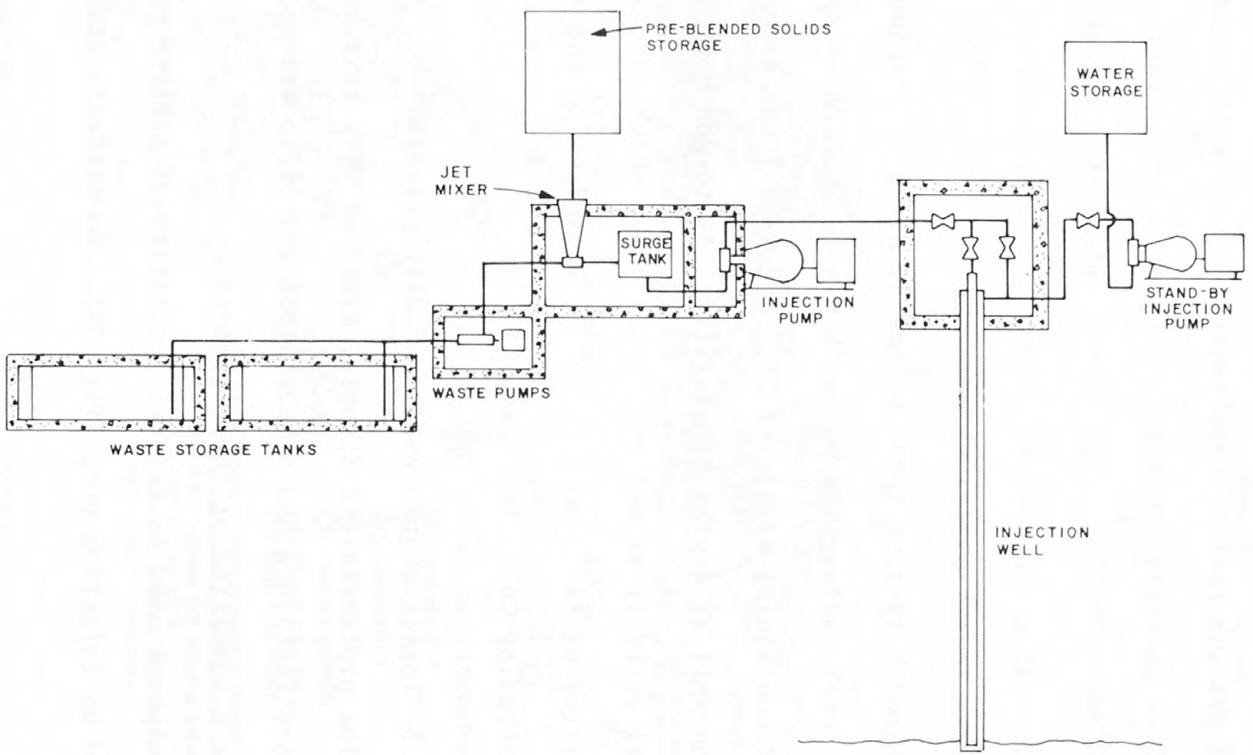

Figure 39.--Schematic diagram of hydraulic fracturing and waste grout injection facility, Oak Ridge National Laboratory, Tennessee (Courtesy of Oak Ridge National Laboratory).

plant is shown in figure 40. The injection capacity of the waste injection pump is 40 MPa at 3 m^3/s and 7 MPa at 20 m^3/s. A standby injection pump (fig. 39) with a similar injection capacity is equipped to flush the injection well free of grout with water in the unlikely event of failure of the injection pump. Five underground waste storage tanks (figs. 39 and 40) with a total capacity of 340 m^3 were constructed at the disposal site to receive wastes delivered from storage tanks at the laboratory site before injections.

Solids which consist of cement, fly ash, attapulgite clay, illite or its equivalent, and a retarder such as delta gluconolactone are preblended before injection according to the desired proportion designed by laboratory tests. The solids are mixed by blowing them back and forth between two pressure tanks, then stored in four bulk storage bins for injection use (fig. 41). During each injection the preblended solids are aerated and flow through a metering hopper into a mixer. A mass flowmeter was installed below the metering hopper to continuously weigh the solids. Concentrated liquid waste is pumped into the mixer under pressure (0.7 MPa). Preblended solids then drop into the mixer by gravity through a chute and are mixed thoroughly with the waste by jet stream (figs. 42 and 43) thus forming the grout which is continuously

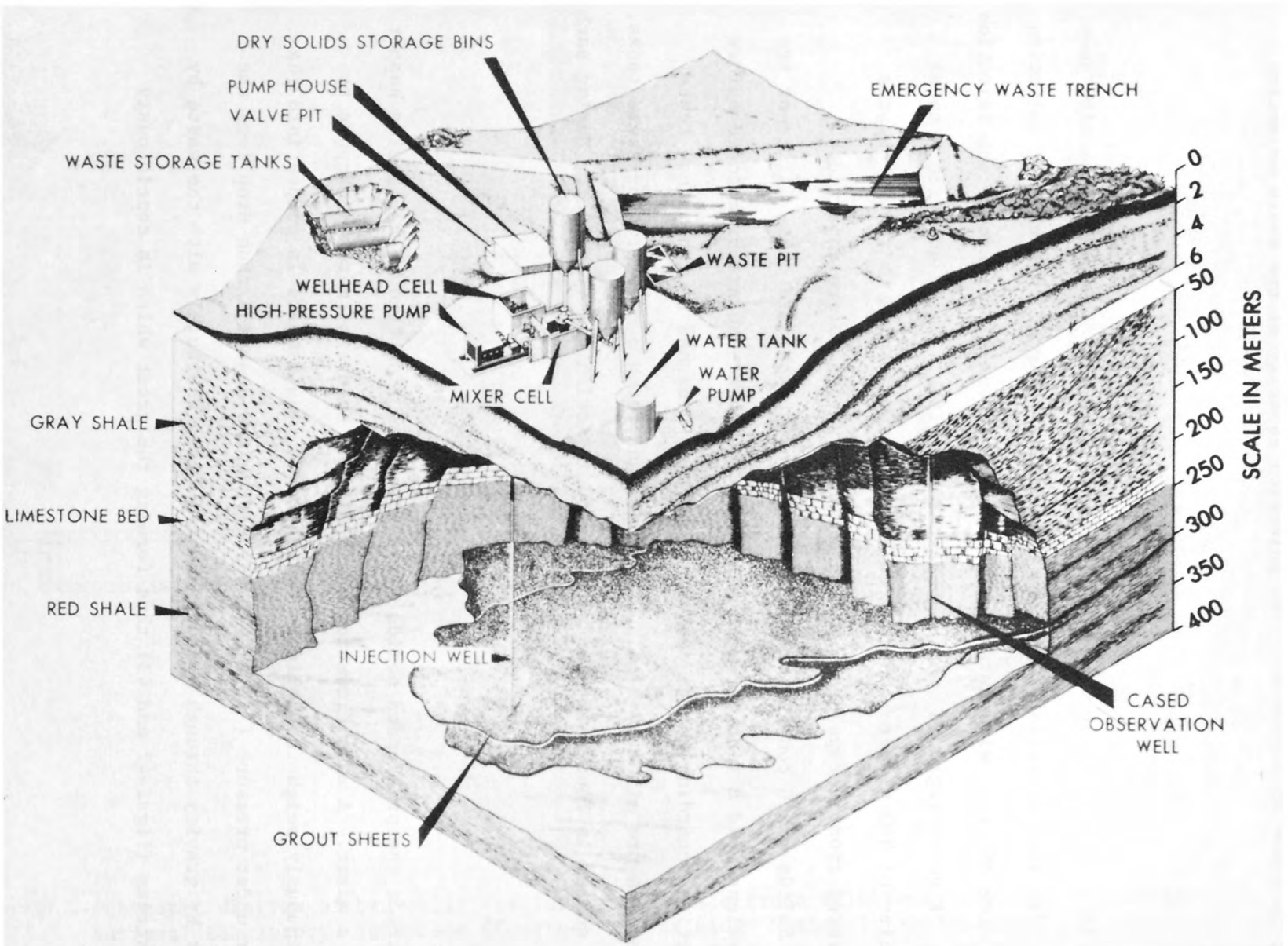

Figure 40.--Artist's sketch of hydraulic fracturing and waste grout injection, Oak Ridge National Laboratory, Tennessee (Courtesy of Oak Ridge National Laboratory).

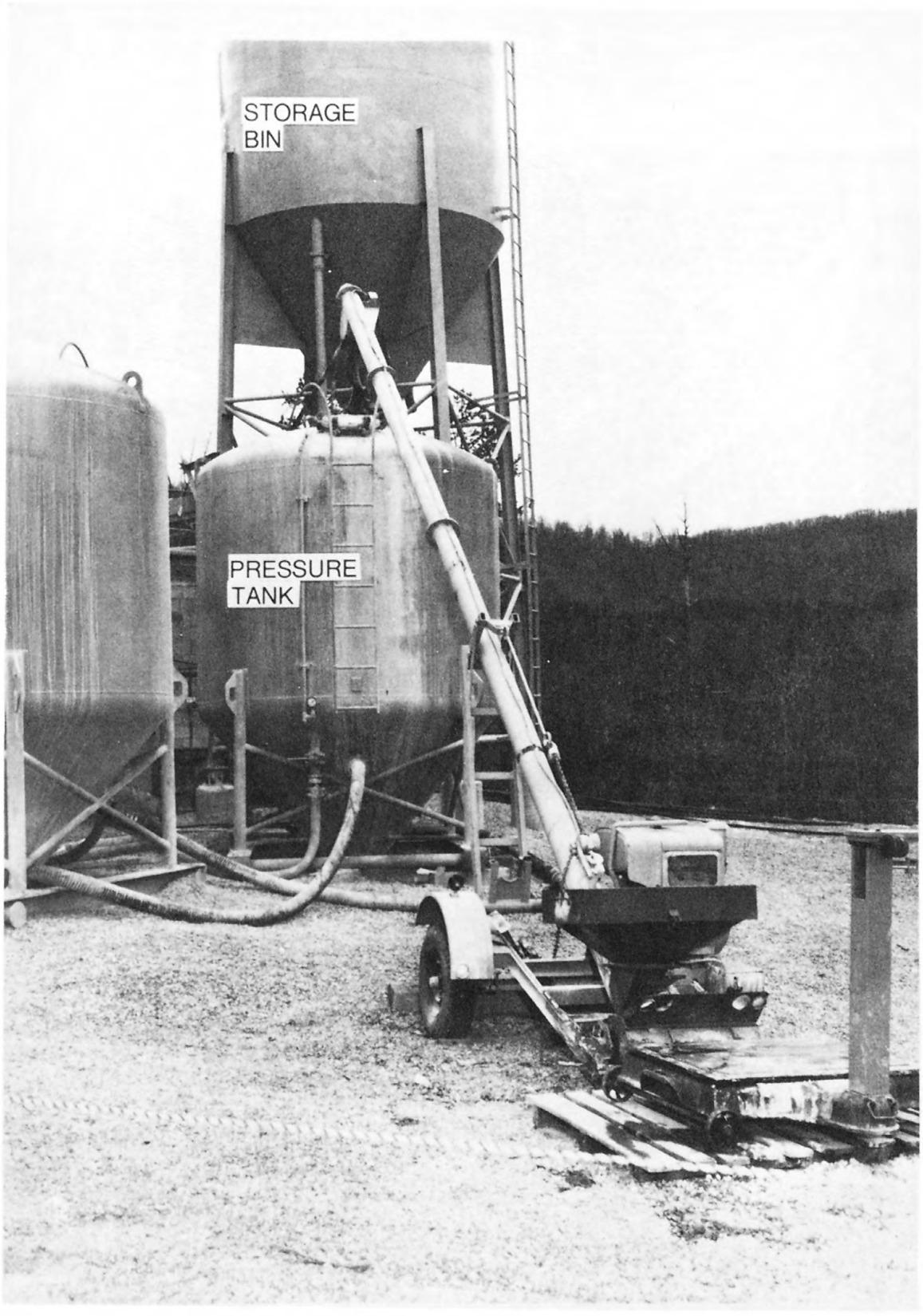

Figure 41.--Equipment for proportioning and blending dry solids for waste grout injection, Oak Ridge National Laboratory, Tennessee (Courtesy of Oak Ridge National Laboratory).

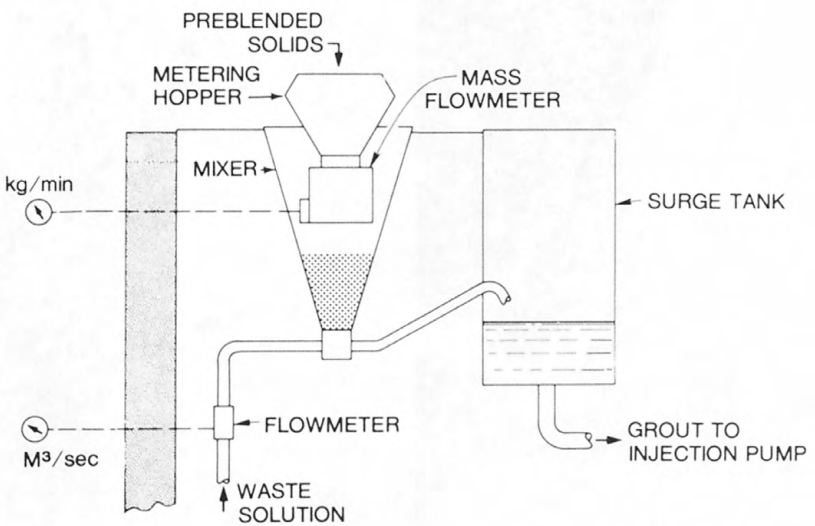

Figure 42.--Arrangement of mass flow meter in mixer cell for waste grout injection, Oak Ridge National Laboratory, Tennessee (from deLaguna and others, 1968).

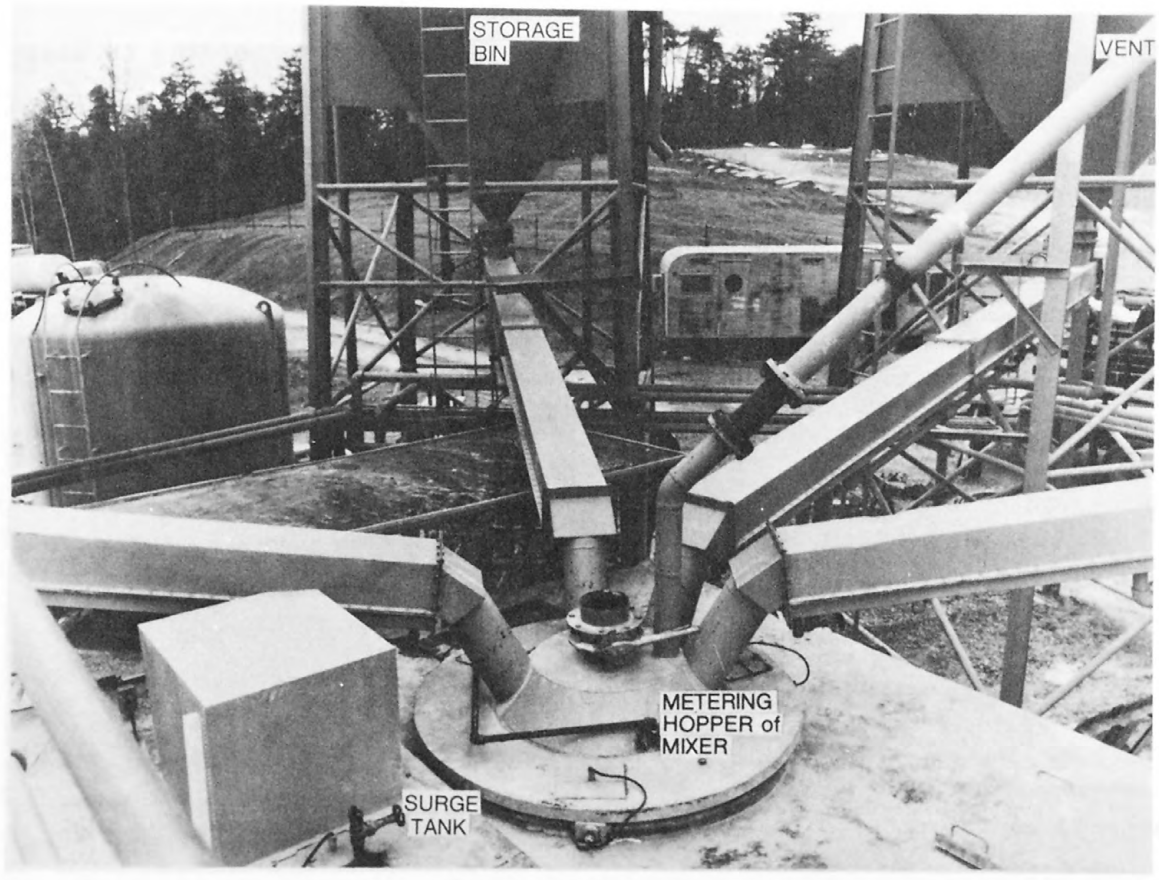

Figure 43.--Conveyors for moving preblended solids from storage bins to mixer for waste grout injection, Oak Ridge National Laboratory, Tennessee (Courtesy of Oak Ridge National Laboratory).

discharged to a surge tank and injected into shale by injection pump (fig. 42). The control of the proportion of waste to preblended solids is critical. The variation should be within 5 percent of the designed proportion but not exceeding 10 percent. The mix ratio is controlled manually according to mass-flow meter and waste-flow meter readings.

A considerable volume of water is required for casing slotting and equipment washing. The water is contaminated and must be injected with waste. To achieve a maximum disposal efficiency the contaminated water must be reused, and for this purpose a concrete lined waste pit was constructed to temporarily store the contaminated water (fig. 40).

An emergency waste trench was also dug as a precaution against the possibility of a well-head rupture (fig. 40). During such an incident the pressurized grout could flow back from the injection well and discharge to the trench, and then the trench would be covered with earth fill.

The mixer, surge tank, injection pump, waste pump and injection well head are all enclosed in concrete cells with 30-cm walls and roofed with sheet metal to avoid radiation exposure of operators and to limit areas that could be contaminated if piping or equipment ruptures or develops leaks (figs. 44 and 45)

A safety glass window was installed on a wall of each cell for inspection during injections.

The injection well consists of a surface casing of 46 m in length and 25 cm in diameter. The surface casing was cemented by pressure over the entire length. A small casing, 14 cm in diameter and 320 m in length was placed inside the

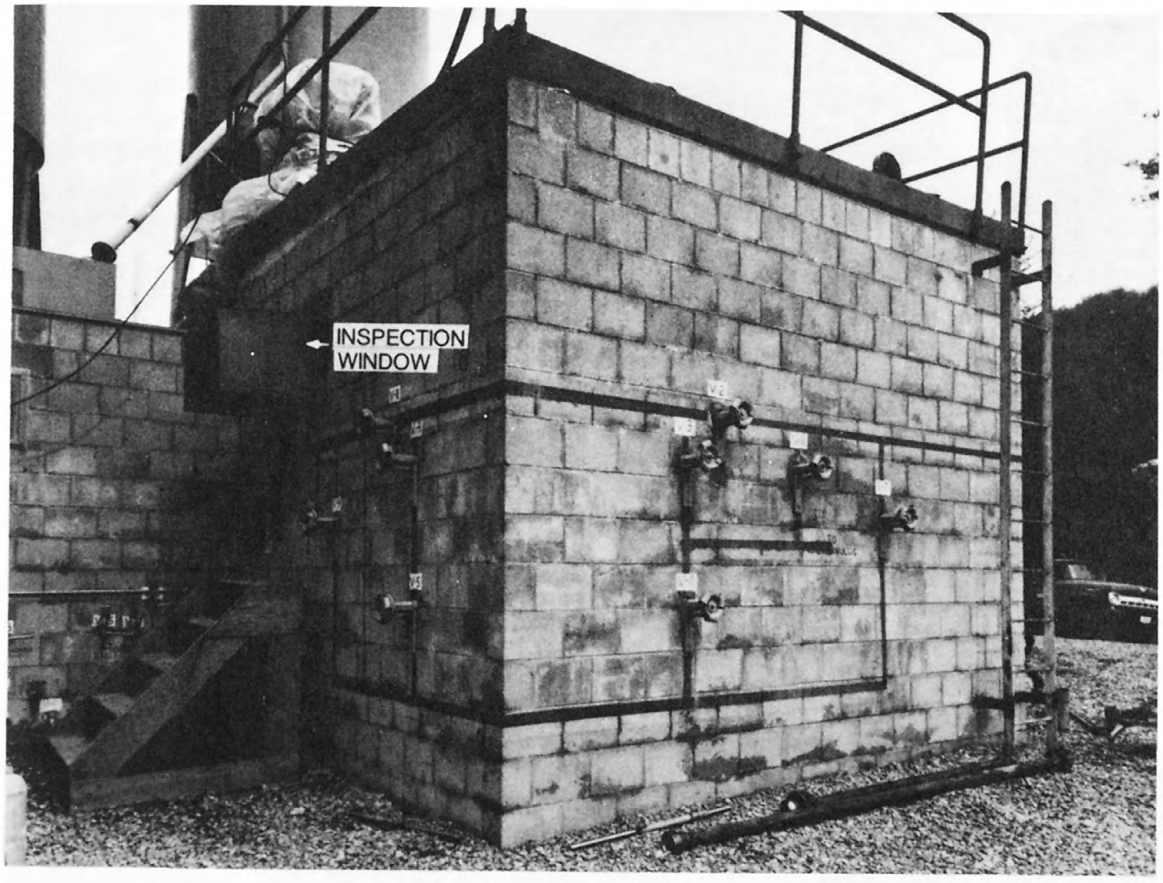

Figure 44.--Cell enclosing well head of waste injection well, Oak Ridge National Laboratory, Tennessee (Courtesy of Oak Ridge National Laboratory)

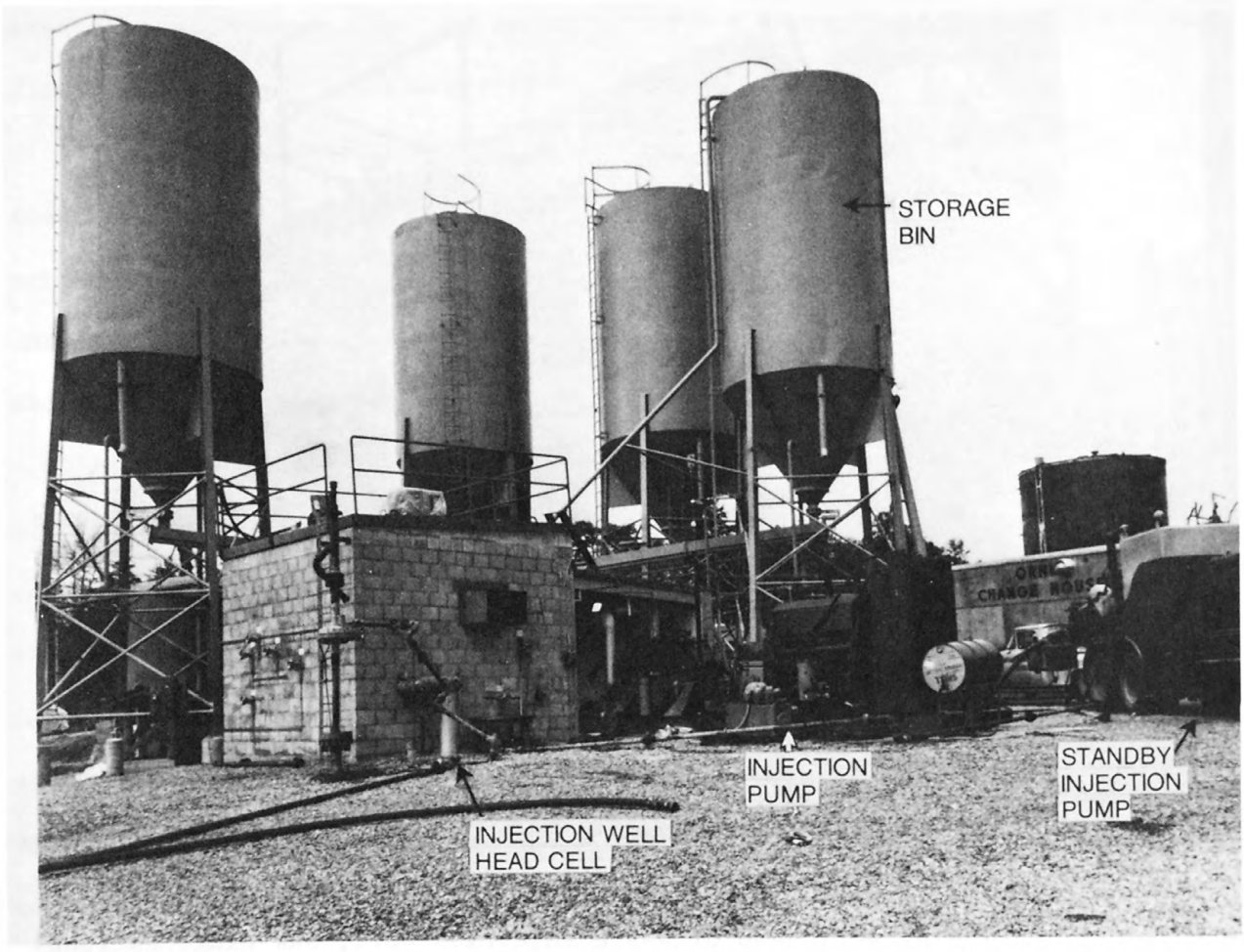

Figure 45.--Photo showing bins, waste injection well-head cell, injection pump and standby injection pump, Oak Ridge National Laboratory, Tennessee (Courtesy of Oak Ridge National Laboratory).

the surface casing and was also pressure cemented for the entire length as shown in figure 46.

Two different types of well heads are used during injections. One is used for slotting and the other for injection. During slotting, a packoff flange is bolted to the 14-cm tubing head (fig. 47). A string of tubing (64 mm in diameter with a swivel is placed at a desired injection depth and is supported by a crane. A stream of slurry consisting of sand and water is pumped down through the tubing under pressure and discharges out of a jet nozzle. The tubing string is slowly rotated by a hydraulic power swivel, therefore, the high abrasive pressure can cut the casing, cement wall and shale around a complete circle. The slurry, after most of its energy has been spent, returns to surface through the annulus. The schematic diagram of the slotting operation is shown in figure 48. The contaminated water used in slotting is stored in a waste pit and can be used for fracture initiation or injected with waste.

During waste injection the packoff flange is replaced by an adapter flange and shut off valve (figs. 49 and 50). The adapter flange supports the 64 mm tubing

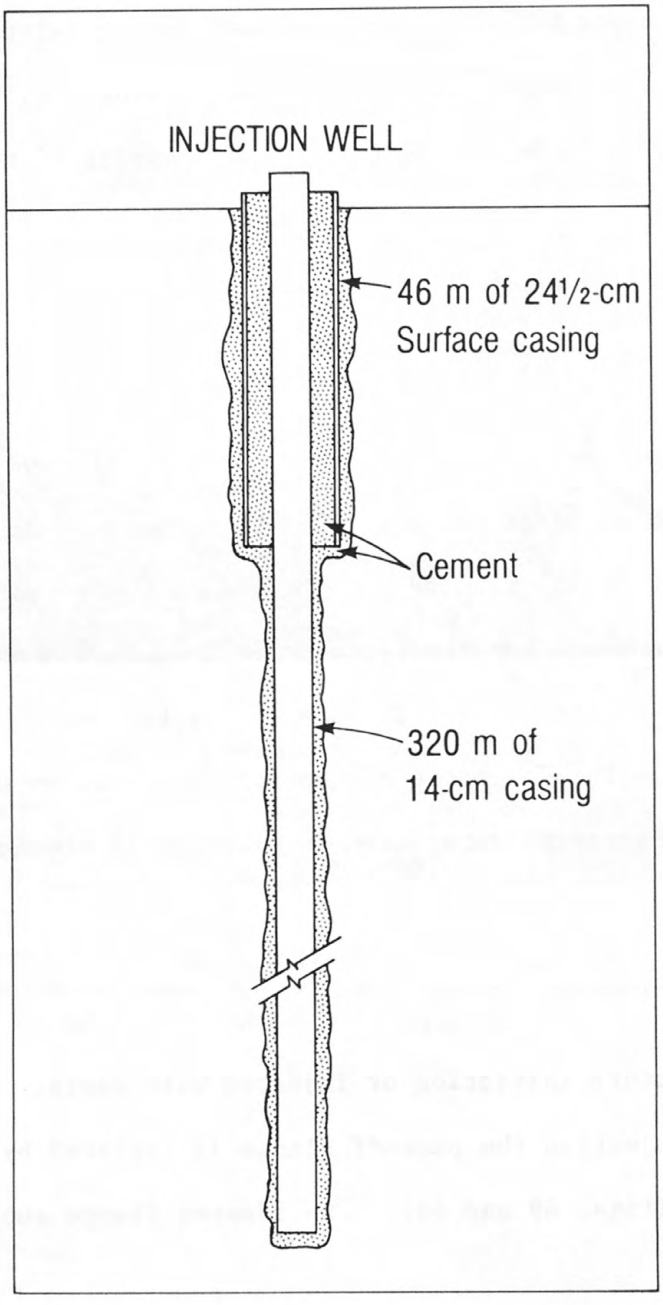

Figure 46.--Schematic diagram showing construction of waste injection well, Oak Ridge National Laboratory, Tennessee (from deLaguna and others, 1971).

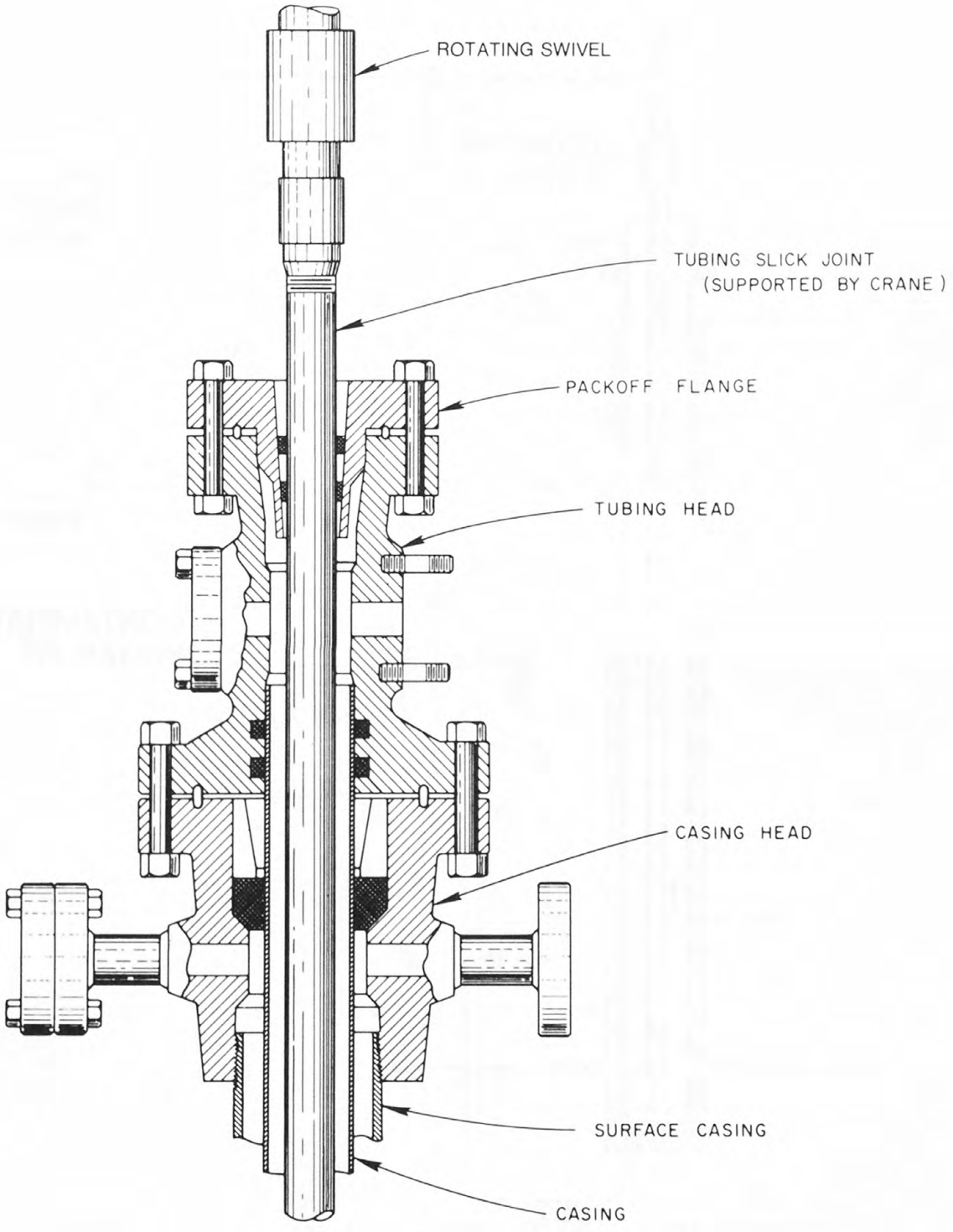

Figure 47.--Well-head arrangement for slotting by hydraulic jet, Oak Ridge National Laboratory, Tennessee (Courtesy of Oak Ridge National Laboratory).

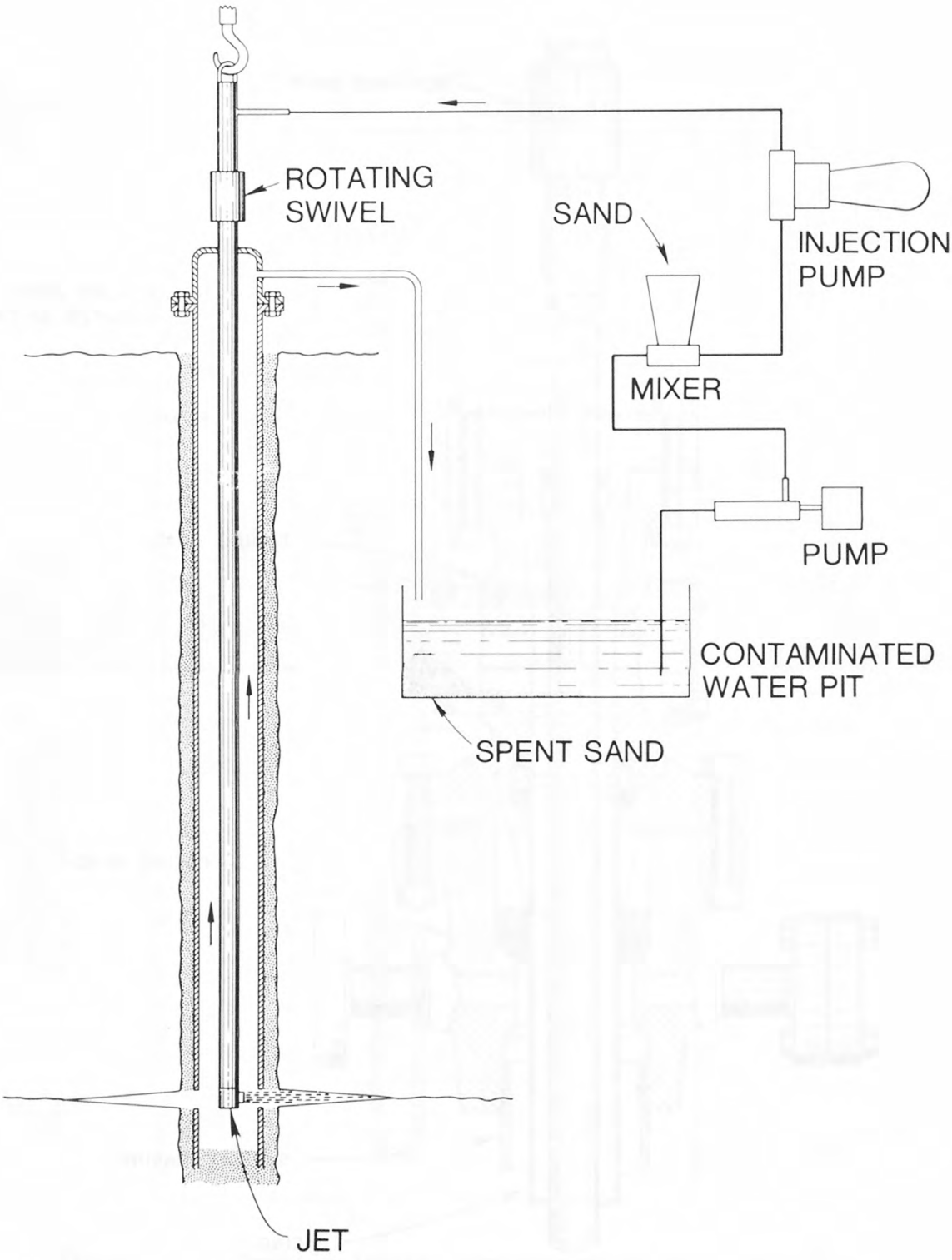

Figure 48.--Schematic diagram showing slotting operation for hydraulic fracturing and waste grout injection, Oak Ridge National Laboratory, Tennessee (Courtesy of Oak Ridge National Laboratory).

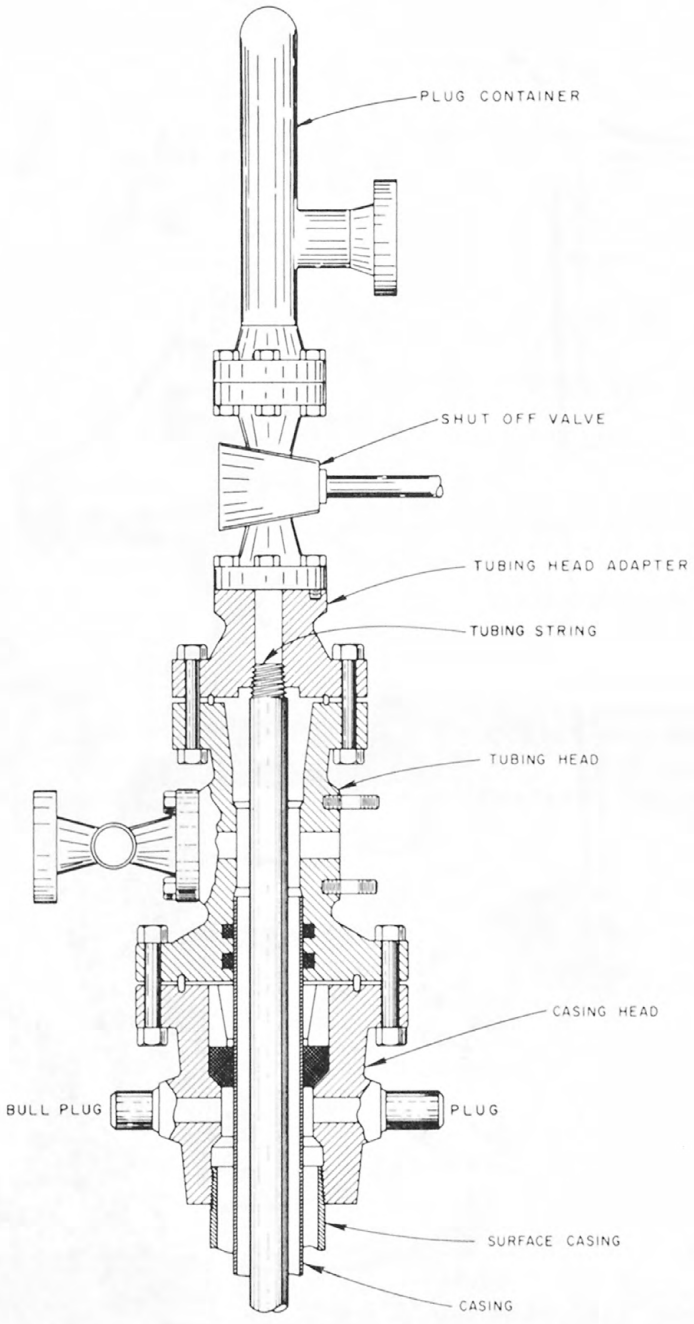

Figure 49.--Well-head arrangement for waste grout injection, Oak Ridge National Laboratory, Tennessee (Courtesy of Oak Ridge National Laboratory).

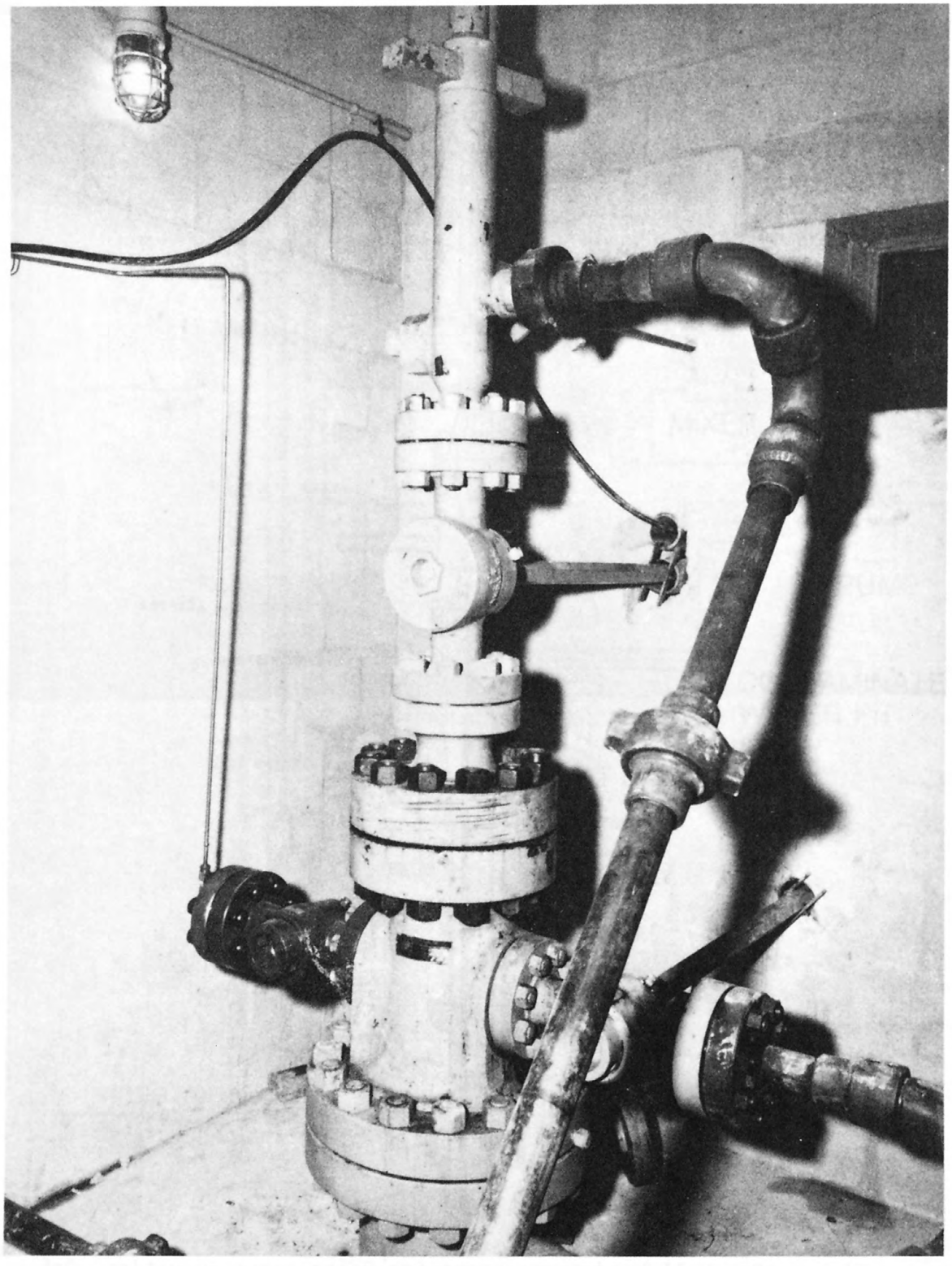

Figure 50.--Photo showing well head of injection well, Oak Ridge National Laboratory, Tennessee (Courtesy of Oak Ridge National Laboratory).

string which is placed at a depth of several meters above the desired injection depth. The annulus between the tubing string and the 14-cm casing is filled with water. Since the tubing string is open to the annulus near the bottom of the well, the pressure in the annulus is equal to injection pressure without consideration of friction loss in the tubing. After a fracture was initiated by water, the grout injection followed. When the last of the waste solution has been injected, a small volume of fresh water is pumped down the well to "overflush" the grout out of the injection well for use in the next injection. The injection well is then shut in under pressure until the grout sets. Several injections can be made through the same slot (table 11), then the old slot is plugged with cement and a new slot is made at a depth of a few meters above the old slot.

A2.6 Injections

By the end of 1978, 25 injections had been made through the present injection well. Seven were experimental injections, one was a water injection and the others were operational grout injections. During injection 6, an experimental injection, trouble with cement flow developed. The injection was made in two stages, which were named 6A and 6B. Four operational injections were also named A and B (table 11) because the injection was interrupted either due to lack of storage capacity at the disposal site, such as ILW-1A and ILW-1B, or due to difficulties of achieving desirable mixing ratio of solids and wastes, such as ILW-2A and ILW-2B, or due to other mechanical troubles. After the fourth operational injection, the injection number was not divided again, even if the injection was interrupted.

Most of the injections have been discussed by ORNL investigators (deLaguna and others, 1968 and 1971; Weeren, 1974 and 1976). The following are injection

examples to show the correlation between the grout size estimated on the basis of the uplift model (section 5.3.2) and that observed in field, and to show operational grout mixing as well as grout sheet determined by gamma-ray logs.

2.6.1 Experimental injections

Two experimental injections were made in September 1960 through the second experimental well. Twenty-four core holes were drilled in determination of the grout sheet. Precise leveling was run after each injection. The injection data are summarized in table 12 and the core hole results and uplift of ground surface are shown in figures 2 and 3. The calculated maximum grout thickness and radius of grout sheet are shown in table 12 and the comparison of grout uplift between calculated and observed values are shown in figures 51 and 52. Generally speaking, the calculated uplift is in good agreement with the observed uplift.

The corehole data indicated that the induced fractures probably were formed in the weakest bedding planes and grout did not flow radially from the injection well. The maximum thickness of grout sheet did not occur near the injection well (figs. 2 and 3). This was probably due to water injection at the end of each injection to clean grout out of the injection well. The thickness of grout sheet as measured in core is less than the calculated fracture separation (table 12). This is not surprising in view of the fact that the induced fractures must have enough separation for slurry to flow during injection, because the calculated fracture separation is the condition that existed during the injection time. After the injection the separation of the induced fractures was reduced due to compaction under overburden pressure. The grout in the core appeared to be nearly as hard as the shale into which the slurry was injected (fig. 1).

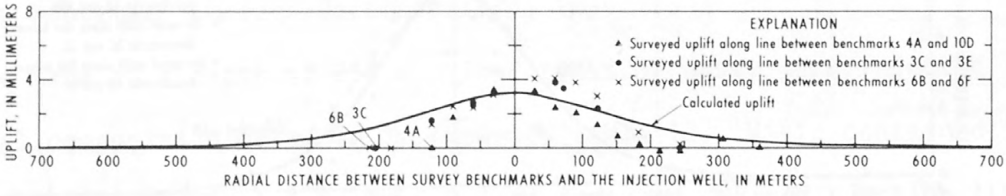

Figure 51.--Calculated and surveyed surface uplift produced by grout injection, September 3, 1960, second experiment site, Oak Ridge National Laboratory, Tennessee (location of benchmarks shown in figures 2 and 3).

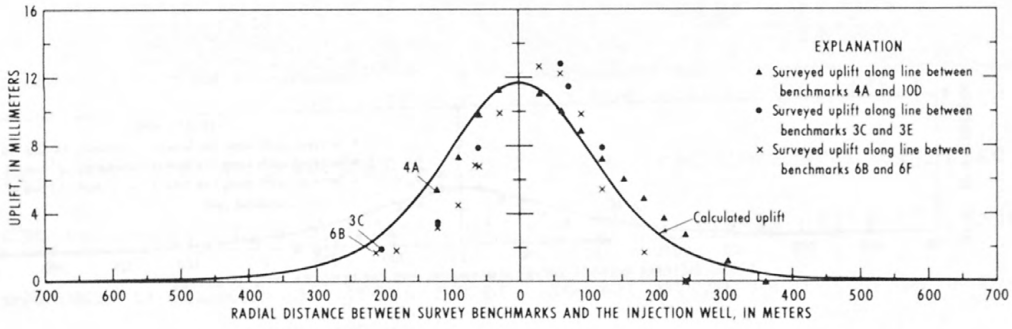

Figure 52.--Calculated and surveyed surface uplift produced by grout injection, September 10, 1960, second experiment site, Oak Ridge National Laboratory, Tennessee (location of benchmarks shown in figures 2 and 3).

The uplift model was further tested by comparison of the calculated uplifts with the observed uplifts during the experimental injections 1 through 7 at the present disposal well, 0.8 km west of the second experimental site. The comparison is shown in figure 53 and apparently is in good agreement. The location of survey benchmarks is shown in figure 54. The uplifts were also surveyed after operational injectiosn ILW-7 and ILW-11, however, the author has no detailed injection data of these injections, therefore, there are no calculated uplifts for comparison.

A2.6.2 Operational injections

At end of 1978, there had been 17 operational injections. A total volume of 5,000 m^3 of radioactive liquid waste contained in 8,100 m^3 of grout had been injected at depths between 244 m to 266 m (table 11). Half of the injections have been discussed by Weeren (1974; 1976), and deLaguna and others (1968). The following discussions were summarized from these reports.

During September through December 1972, injections ILW-8 through ILW-11 were made at a depth of 254 m. Four tanks of waste were injected. The chemical composition of waste is shown in table 13. Waste contained in tank 1 and part of the wastes in tank 2 were injected during injection ILW-8. Only waste in tank 2 was injected during injection ILW-9. Injection ILW-10 included 38 m^3 of waste remaining in tank 2 and the wastes in tank 3 and 4. The remaining wastes in tank

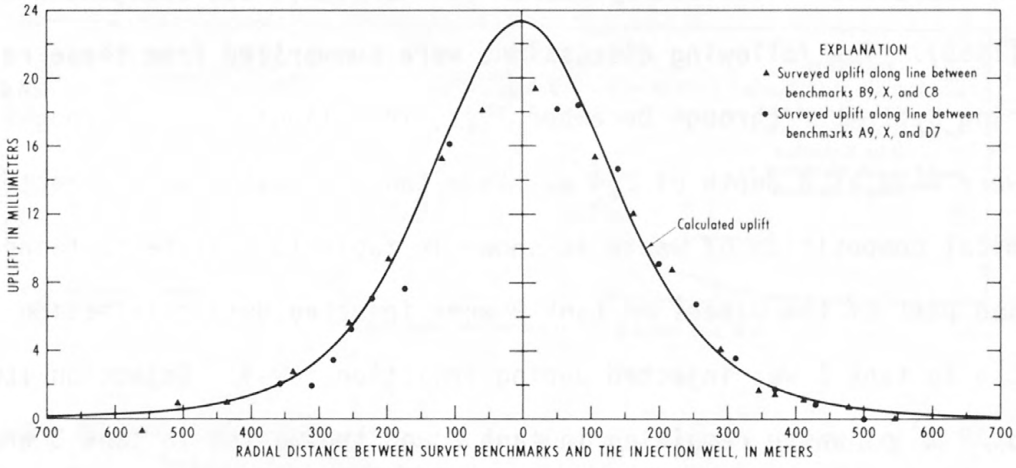

Figure 53.--Calculated and observed surface uplift produced by experimental injections 1 through 7, present fracturing site, Oak Ridge National Laboratory, Tennessee (location of benchmarks shown in figure 54).

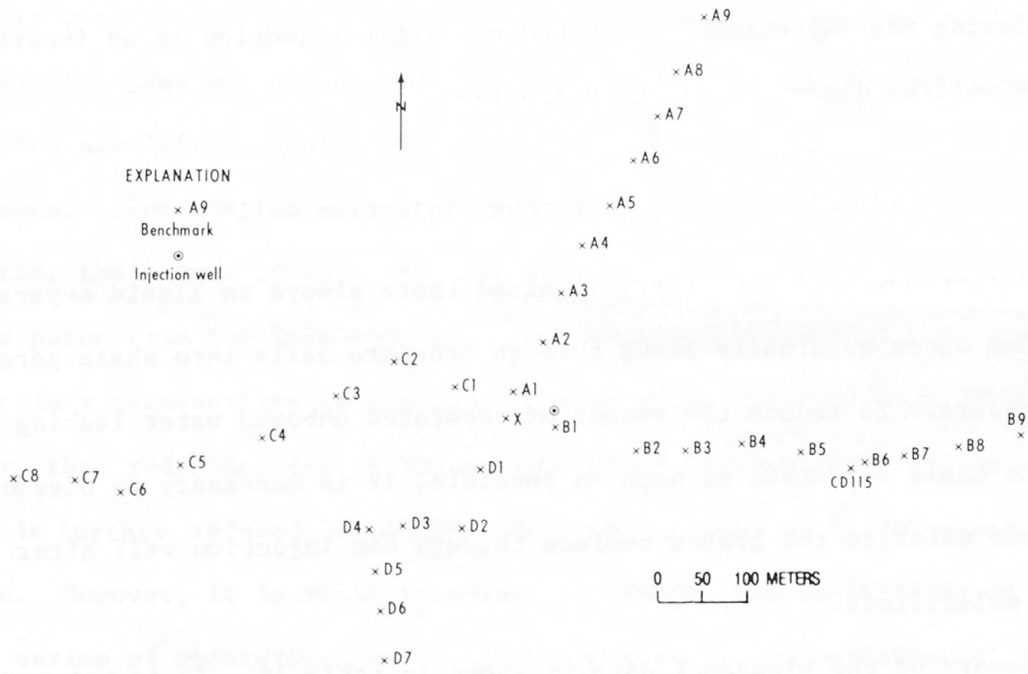

Figure 54.--Map showing location of benchmarks, present fracturing site, Oak Ridge National Laboratory, Tennessee.

3 and 4 were injected during injection ILW-11. The composition of solids used in all four injections was approximately as follows:

Materials	Percent by weight
Portland cement	38.45
Fly ash	38.45
Attapulgite 150	15.38
Grundite	7.69
Retarder	0.03

The average solid and waste mixing ratio is indicated in table 11. The concentrations of radionuclides in the injected waste are shown in table 14. It was learned during the injections that bleedback after injection is an important factor as will be discussed in the following.

A2.6.2.1 Bleedback through injection well

No matter how well the slurry is mixed there always is liquid separation. The unbound water eventually leaks through fracture walls into shale pores under pressure. To reduce the amount of separated unbound water leaking from grout into shale formation as much as possible, it is necessary to bleedback the unbound water to the ground surface through the injection well after the grout has been solidified.

A summary of the bleedback data is shown in table 15. It is not surprising that both well-head pressure and initial rate of bleedback decrease drastically with increase in shut-in time, because the unbound water leaks through fracture walls under pressure during shut-in time despite the low permeability of the shale. The concentrations of radionuclides in the bleedback water are shown in table 16. Although the bleedback is only 4 percent of the total injected volume and

the radionuclides contained in the bleedback are only several tenths of one percent of the total injected radionuclides, the concentration of radionuclides of the bleedback is still high and, therefore, the bleedback was stored for use during next injections. Because of the low permeability of the shale, some of the separated liquid which could not be bled back through the injection well probably would be trapped in induced fractures or in the shale. During the drilling of observation well S-100, when the grout sheet of experimental injection 3 was intersected at a depth of 276 m, water flowed slowly from the grout seam. A sample of the flowing water was analyzed, indicating the following results, Cl^{-1}, 36,500; Na^{+}, 31,100; NO_3^{-}, 28,600; Ca^{2+}, 2,930; OH^{-1}, 2,000; SO_4^{2-}, 1,620; Mg^{2+}, 380; all in parts per million; H^3, 7.3×10^{-7}; Sr^{90}, 6.8×10^{-8}; and Cs^{137}, 3.7×10^{-7}; all in Ci/l (deLaguna and others, 1968). This finding raises the concern that free radionuclides are left in shale, whether as a result of phase separation or for other reasons. From the bleedback data and the water found in the grout seam, it seems that the amount of free radionuclides in shale is low. If the ground-water flow paths from the injection area to a nearby ground-water body are long, and the shale's permeability is low and its adsorption capacity high, then the concern that radionuclides in the unbound water could migrate to the nearby biosphere is further reduced by radioactive decay as well as hydrodynamic dispersion. However, it is still necessary to monitor the possibility of migration through a series of observation wells constructed along the perimeter of the injection area and in formations lying above the injection zone.

A2.6.2.2 Position of grout sheet

The extent and altitude of the injection grout sheet can be determined by coring after solidification of the grout, however, this process is costly and time consuming. If a series of observation wells has been constructed and

if the injection wastes contain gamma-emitting radionuclides, then one alternative would be obtaining gamma-ray logs in the observation wells before and after injection. Intensified gamma-ray peaks above background gamma activity of shale would indicate that the induced fractures have intercepted the wells at the depth indicated. In logs made after 2 or 3 injections it is difficult to associate the observed gamma-ray peaks with the appropriate injections.

Only logs made after each injection are available for injections ILW-8 through ILW-11 (Weeren, 1974). Figure 55 indicates the location of the observation wells in which the gamma-ray logs were run. Figure 55 shows the grout sheets found in the observation wells projected on a line passing through the injection well in the direction along the formation dip. The actual observed grout sheets intercept with observation wells and the locations are shown in table 17. From figures 55, 56, and table 17, it seems that the grout sheets have formed along bedding planes and lie in a vertical interval of 20 m above or below the injection altitude, however, these data might not indicate the true altitude of the grout sheets because there are no data available regarding well deviations. The experience obtained during a later site investigation indicated that the unadjusted altitudes of grout sheets were usually 7 to 8 m higher than those adjusted for well deviation, and that the location of the grout sheets also were shifted several tens of meters away from the surface location of the observation wells (see section A2.8.2.1). Therefore, these unadjusted results may be in error.

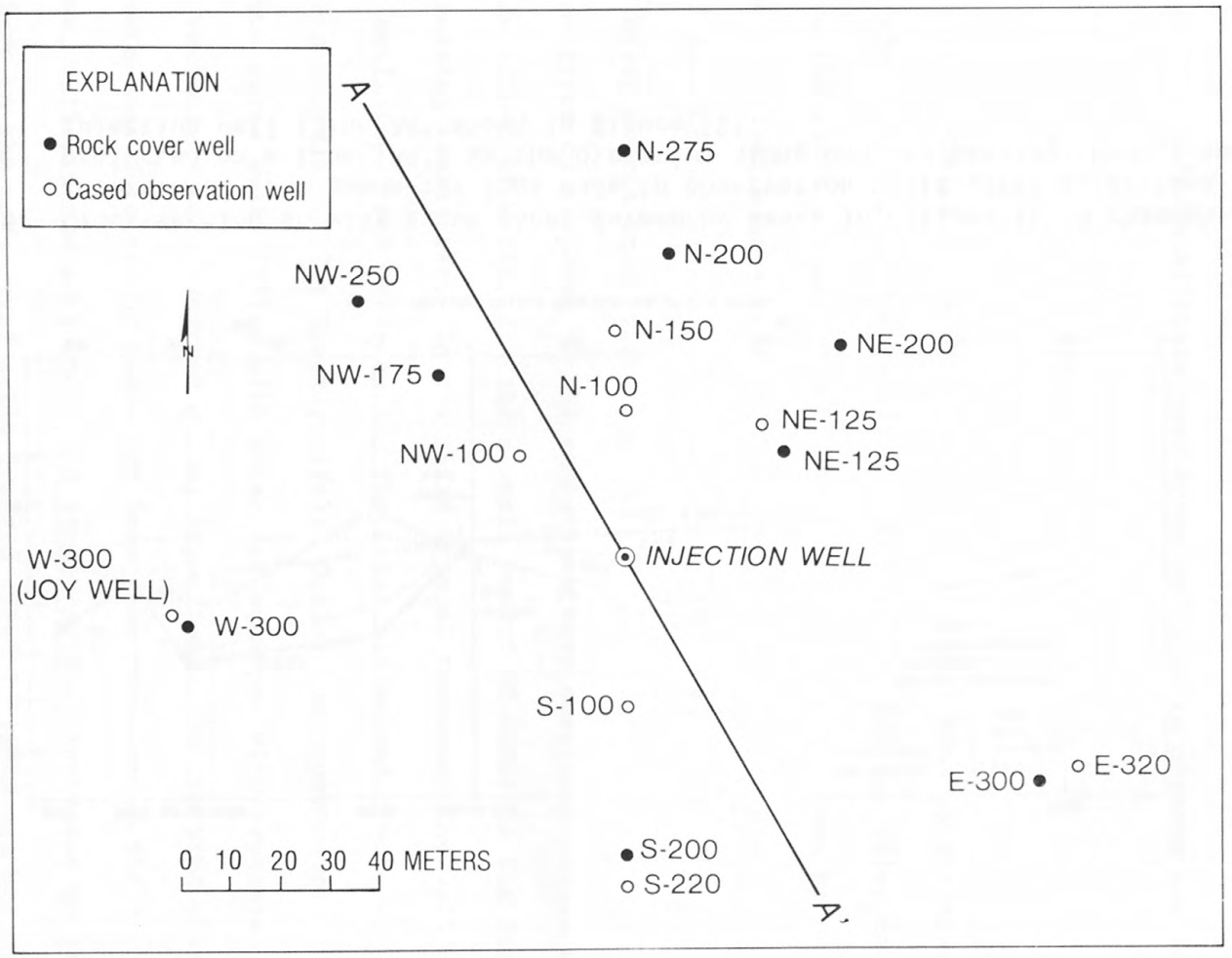

Figure 55.--Map showing location of observation wells, present fracturing site, Oak Ridge National Laboratory, Tennessee (Courtesy of Oak Ridge National Laboratory).

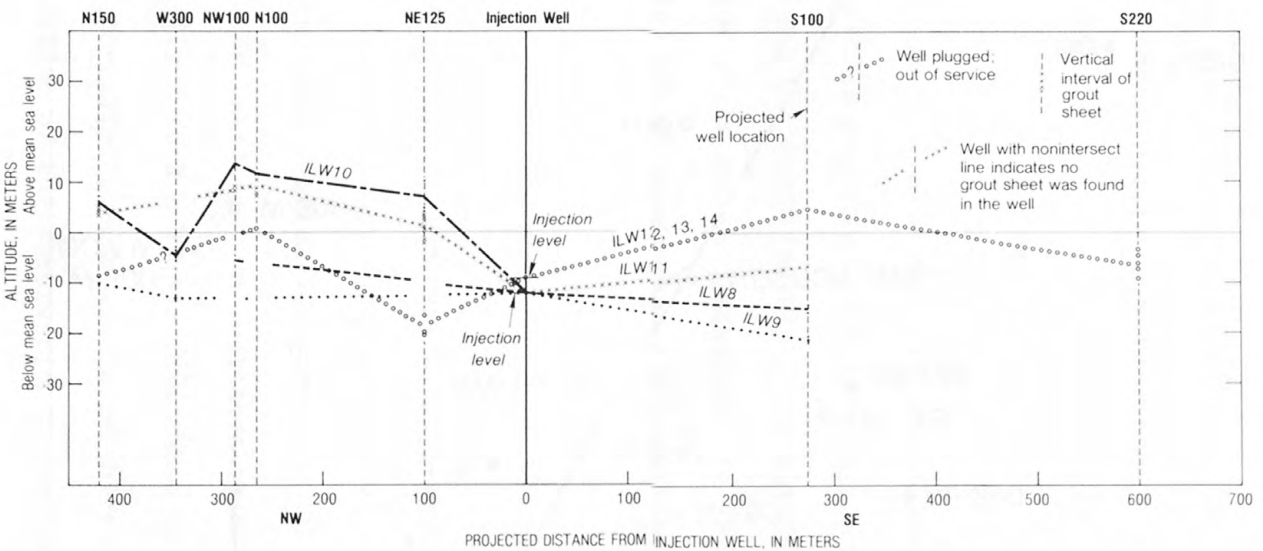

Figure 56.--Cross-section showing grout sheet formed by waste injections ILW-8 through ILW-14, interpreted from gamma-ray logs made in observation wells after injections and projected on a line (AA') in the direction along dip and passing through center of injection well (line AA' shown in figure 55).

A2.7 Monitoring system

In addition to observation wells for gamma-ray logging, ORNL also constructed a series of so-called rock cover monitoring wells. The well location is indicated in figure 55. These wells are cased and pressure cemented to a depth of 152 m, and have 30 m of open hole below the cased and cemented section (fig. 57). The purpose of these rock cover wells is to observe the integrity of the shale formation lying above the waste disposal zone to assure that no vertical fracture should be formed due to injections, so that surface water could not migrate to the waste disposal zone. The integrity test is done by pumping water into rock cover wells at a standard well-head pressure of 0.5 MPa to observe the change of rate of acceptance before and after injections. The tests are repeated at about every fourth injection.

Three types of response of the tests have been observed. Wells may take no measurable volume of water, or take a small amount of water in the first hour then decreasing thereafter. In the third type of response, the well may take the same small amount of water during the first and second hour of the test (deLaguna and others, 1971; Weeren, 1974). During the experimental injections, in the rock cover wells filled with water and equipped with pressure gages, pressure variations were observed during injections. In the area where the grout sheets were detected by gamma-ray logs, the pressure in the rock cover wells rose, while in the area where the gamma-ray logs indicated no grout sheets the pressure in the rock cover wells dropped slightly (deLaguna and others, 1971). This evidence probably can be explained by the shale around the open-hole section of the rock cover wells. In the grout sheet area the shale probably is compressed by

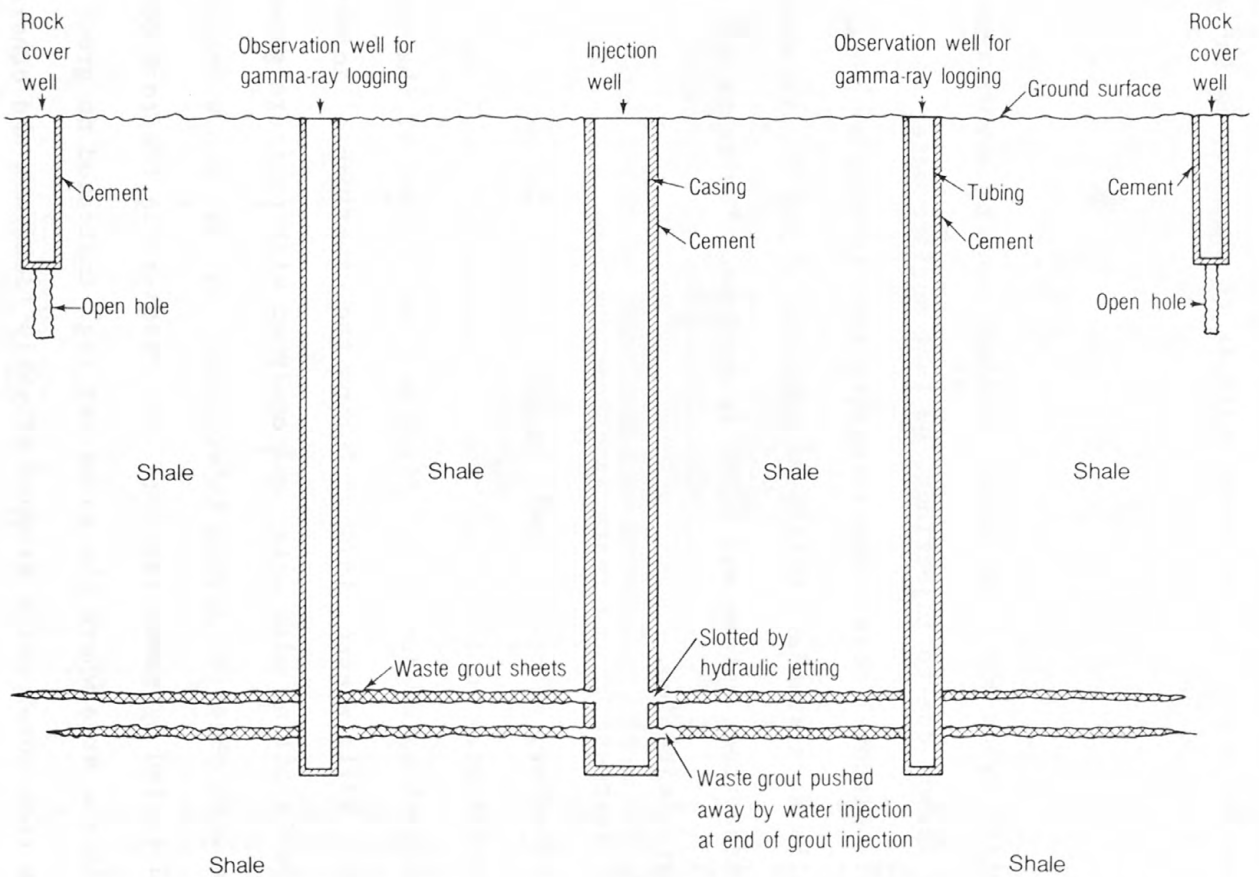

Figure 57.--Schematic diagram showing injection well, observation well and waste grout in shale, Oak Ridge National Laboratory, Tennessee.

thus increasing pressure in the rock cover wells. uplift due to accommodation of the injected grout,/ The uplift does not stop at the edge of the grout sheet and must extend away from the edge without physically shearing the rock. Therefore, the volume of rock beyond the edge of the grout sheet should expand, thus increasing the rock porosity slightly which causes the pressure in the rock cover wells to drop slightly. The observed pressure changes in rock cover wells and the grout sheets indicated by gamma-ray logs for the injections ILW-8 through ILW-11 are shown in table 18.

A2.8. Site investigation

Because the present disposal site is approaching its full injection capacity and the current disposal facility cannot handle the injection of accumulated sludge, a new fracturing site is being proposed which is 245 m south of the present facility (fig. 34). The new site was evaluated jointly by ORNL and USGS in 1974 (Sun, 1976; Weeren and others, 1974). The following is a summation of the evaluation.

A2.8.1 Test drilling

Although the proposed site is only 245 m away from the present disposal site where numerous test holes and injections have been made in past years, one test hole with core was drilled at the proposed site to insure that the subsurface geology and hydrology would not deviate dramatically from that found at the present site. Cores were taken from 212 down to 362 m. In the interval from 212 to 250 m the rock is gray shale interbedded with thin limestone layers. From 250 to 302 m the shale is purple in color, silty, and without limestone layers. From 302 m to the top of the Rome Formation (357 m) the shale is gray or purple in color and increasingly sandy. From 357 to 362 m the rock is hard white sandstone interbedded with shale and is part of the Rome Formation.

Bedding planes are well developed and dip 10^{o} to 20^{o} southeast. The subsurface geology indicated by core is similar to that found at the present site. The purple and gray shale between 250 and 357 m comprises the Pumpkin Valley shale of the Conasauga Group into which radioactive waste is scheduled to be injected.

The test hole was converted into an observation well known as the South-observation well. Gamma-ray logs were made in this well before and after the well was cased and cemented. Three more observation wells, namely, the East-, West-, and North-observation wells, were constructed at a radial distance of 60 m from the injection well, and were also cased and pressure cemented. The injection well was constructed with a 14-cm casing and pressure cemented in the similar conditions as the present injection well. The locations of all wells are shown in figure 58 and table 19. Gamma-ray logs were also made in all wells before they were cased and pressure cemented. Thereafter, gamma-ray logs were made again in some of the wells. These gamma-ray logs were used to determine not only the background level of gamma activities of the injection shale, but also the contacts between rock units.

Laboratory determinations of rock tensile strength had never been made for shales at the New York and Oak Ridge sites. Therefore, the author took advantage of this site evaluation to determine (in the laboratory) tensile strength of the shale scheduled for injection for comparison with tensile strength calculated from test injections.

Well deviation, determination of dip and strike and tensile strength of the injection shale are discussed below.

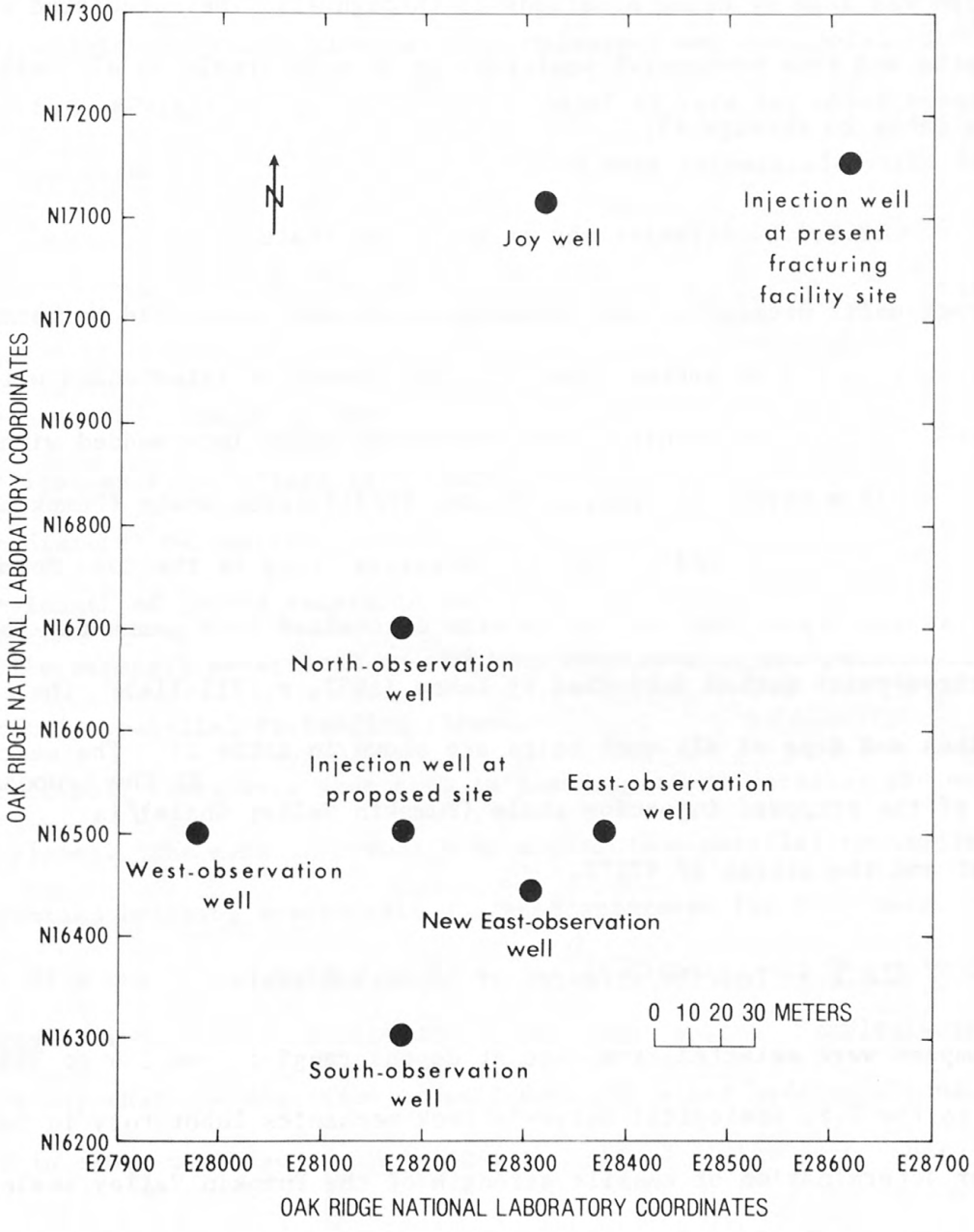

Figure 58.--Map showing location of wells, proposed disposal site, Oak Ridge National Laboratory, Tennessee.

A2.8.1.1 Well deviation

All wells drift from the vertical axis as indicated by deviation logs. All measured depths were corrected for the angle of deviation to obtain true vertical depths and true horizontal locations at particular depths of interest. The correction was made by using equations 38 through 41. The calculated true vertical depths and true horizontal positions at 30 m intervals in all wells are shown in table 20 through 25.

A2.8.1.2 Stratigraphy of injection shale

Three rock units present in the Conasauga Group are identified by gamma-ray logs and core. From top to bottom, they are gray limestone interbedded with calcareous shale, 195 m thick; gray calcareous shale interbedded with less limestone, 34 m thick; and purple or gray argillaceous shale (Pumpkin Valley shale), 100 m thick. Underlying the Conasauga Group is the Rome Formation.

The strike and dip of the rock units were determined from gamma-ray logs and by the three-point method described by Lahee (1952, p. 711-714). The calculated strikes and dips of all rock units are shown in table 26. The calculated average dip of the proposed injection shale (Pumpkin Valley Shale) at the proposed site is 13° southeast and the strike of N71°E.

A2.8.1.3 Tensile strength of injection shale

Rock samples were selected from core at depths ranging from 214 to 360 m and shipped to the U.S. Geological Survey's rock mechanics laboratory in Denver, Colorado, for determination of tensile strength of the Pumpkin Valley shale and the sandstone of the Rome Formation. One hundred and thirty-seven samples were selected and 87 were used in the tensile strength tests. R. A. Farrow of the U.S. Geological Survey supervised the tests.

Three methods were used in the tests, namely, line load, point load, and direct pull. Both the line and point loads were applied by using a device described by Reichmuth (1968). Direct pull tests were made in directions parallel and normal to bedding planes. Samples were cemented by epoxy to flat plates designed for the tests and then stressed to failure. Test loads, in all tests, were applied with a Baldwin Lima Hamilton Universal machine, Model FTG[1/] with a rate of 0.6 MPa/s for direct pull test and of 45 kg/s for other tests.

Tensile strengths determined by line load were calculated by the following equation.

$$T = 6.2 \times 10^{-2} P/dh \qquad (64)$$

where

T = tensile strength in MPa

P = load at rock failure in Kg-force

d = diameter of tested sample in cm

h = length of tested sample in cm

The tensile strength determined by the line load test is the tensile strength in a direction parallel to bedding planes.

Direct pull tests were made both in the directions parallel and normal to bedding planes. The tensile strength in a direction parallel to bedding planes was determined by using a specially designed apparatus for this test. The apparatus consists of a thick wall tubing of 57 mm inside diameter and 56 mm long. The tubing was split axially and fitted with pulling flanges. Samples were oriented in such a way that the direction of pull would be along bedding planes, then cemented in place with epoxy. Masking tape, placed at the joint where the two

---

[1/] The use of brand names in this report is for identification purposes only and does not imply endorsement.

halves of the tubing jointed, prevented epoxy from cementing the tubing. Most of the tests resulted in epoxy bond failure at stresses ranging from 3 to 6 MPa, instead of rock failure. Direct pull tests made along the axis of the core is not necessarily truly orthogonal to bedding planes because of the dip and deviation of the corehole. The samples were pulled in a direction 80° to the bedding planes. Therefore, the tensile strength in the direction normal to bedding planes is probably a few percent less than that determined in the laboratory.

The results of point-load tests were disappointing; only 9 of 29 samples produced results.

In summary, 83 samples of Pumpkin Valley shale and 4 samples of Rome sandstone were tested. The average tensile strength in a direction parallel to bedding planes is 12.4 MPa for Rome sandstone and 6.2 MPa for Pumpkin Valley shale. The tensile strength in a direction normal to bedding planes ranges from 0 to 3.4 MPa for Pumpkin Valley shale. The maximum, minimum, and standard deviation values of all tests are shown in table 27.

It is necessary to note that all rock samples used in the tests were weakened by expansion resulting from removal of confining stresses. The actual in-situ tensile strengths in all directions are probably higher than the values determined in the laboratory.

A2.8.2 Test injections

The test injections were not carried out in an order suggested by the U.S. Geological Survey that a water injection would be made before a grout injection. The ORNL was concerned that a certain amount of water probably would be left in the shale after a water injection and that water could adversely affect the retention of radionuclides during waste injections. The ORNL also

considered that since the proposed site is only 245 m from the present site where a water injection was made in 1967, it would not be necessary to conduct multiple injections as suggested by USGS for site evaluations. The USGS objected to ORNL's view on the basis of the following reasons: (1) the natural joint system can change considerably within a distance of a few hundred meters; (2) all formations are already saturated with water in some degree, so that a small amount of water left by a water injection probably will not seriously affect the system; (3) a water injection not only indicates the degree of permeability of the injection zone, but also can confirm the test results by comparing both water and grout injection results and, (4) local vertical earth stress can be determined from pressure decay of a water injection. Nevertheless, ORNL decided to make only one grout injection.

After the grout injection only two of the four observation wells, the South- and West-observation wells, indicated by the gamma-ray logs that the induced fractures had intercepted the wells. The observed locations of the induced fractures correlated well with the calculated orientations. However, no gamma-ray peaks were noted in the East-observation well, presumably because the well depth was 5 m shallower than the calculated altitude where the induced fractures would be expected to intercept the observation well. The North-observation well is located near the present fracturing site. A gamma-ray log made before the test grout injection indicates that some induced fractures formed by past waste injections at the present site had already intercepted the well. Therefore, unless some new gamma-ray peaks were formed outside of the depth range where the induced fractures formed during past waste injections had intercepted the well, there is no way to distinguish the previously induced fractures from the newly formed fractures. The gamma-ray log made in the North-observation well after the test grout injection nearly repeated the one made before the injection.

Therefore, it cannot be concluded from the gamma-ray log whether or not the injected grout had reached the vicinity of the North-observation well during the test grout injection.

It is not necessary that all four observation wells should intercept the induced fractures, however, it is desirable and indeed necessary to have more than two out of four observation wells yielding a positive sign that the induced fracture had reached the observation wells. Because if only two observation wells intercepted the grout, it may be interpreted that the interception is accidental. Therefore, it was concluded that the test grout injection was not sufficient to make an affirmative conclusion and the USGS suggested two more injections--a water and a new grout injection-- be made after deepening the East-observation well (Sun, 1976). Since then, both ORNL and USGS agreed that a water injection was needed.

Because the test grout injection was made before the water injection, the test grout injection will be discussed first in the following paragraphs.

A2.8.2.1 Test grout injection

A test grout injection was made on June 14, 1974. In April 1974 the author, using information obtained from pressure decay of a water injection made in 1967 at the present fracturing site and the estimated shale tensile strength on the basis of injections made at West Valley, New York (Sun and Mongan, 1974) made calculations to predict well-head breakdown and shut-in pressure for the test injection. On the basis of pressure decay of the water injection in 1967, the estimated vertical earth stress at the proposed site is 1.8 times the value of the calculated overburden pressure. For prediction purposes the injection depth was assumed to be 335 m and the density of shale 2.7 (deLaguna and others, 1968) then the vertical stress was estimated as:

$$(2)\ (2.7)\ (335)\ (9.8 \times 10^{-3})$$

$$= 17.7 \text{ MPa}$$

By experience obtained in West Valley, New York, the tensile strength of shale in the direction normal to bedding planes and the cohesive stress at fracture tip were assumed to be 4 MPa and 2.5 MPa (for f = 0.6) or 1.2 MPa (for f = 0.3), respectively. The estimated well-head breakdown pressure was calculated as:

Well-head breakdown pressure

= bottom-hole breakdown pressure - static head in the casing

= $17.7 + 4 - 9.8 \times 10^{-3} \times 335$

= 18.4 MPa

The well-head shut-in pressure was estimated as the sum of overburden pressure and cohesive stress at fracture tip subtracting the static pressure in the casing and was 16 MPa (16.8 MPa for f = 0.6 and 15.6 MPa for f = 0.3).

These predicted values were given to Oak Ridge Operations Office, DOE (then U.S. Atomic Energy Commission) by the U.S. Geological Survey, April 29, 1974 (letter addressed to J. J. Schreiber by G. D. DeBuchananne).

The shale was fractured at 18.3 MPa well head pressure during slotting on June 12, 1974 (Weeren and others, 1974), virtually confirming the predicted value. The well-head shut-in pressure of the grout injection was 14.5 MPa (table 28) also closely approximating the calculated value. As this was the only prediction made so far, it may have coincided accidentally, and therefore needs further testing.

A2.8.2.1.1 Interpretation of injection data

The injection well was slotted by a hydraulic jet at a depth of 332 m measured along the casing, while the true injection depth after adjustment for well deviation was 324 m. The grout injection was started at 0940 hours EDT

(Eastern Daylight Saving Time) on June 14, 1974, and immediately ran into difficulties. The mixture of the grout could not be controlled and the mixer was jammed with solids. The injection was interrupted at irregular intervals. When the injection pump was off, the instantaneous shut-in pressures were 14 MPa well-head pressure, or 17 MPa bottom-hole pressure. The normal injection was actually started at 1310 hours. The injection was then stopped again for a brief period from 1430 hours to 1440 hours for cleaning the window of the surge tank; hereafter this stop is referred to as a brief pause. A total volume of 370 m^3 of grout tagged with the radioactive tracer Au^{198} (half-life is 2.7 days) was injected into the Pumpkin Valley shale. The injection was completed at 1940 hours.

The grout was injected through a string of tubing which was placed 3 m above the injection level. The annulus between the casing and tubing was filled with water. Injection pressures were monitored in the annulus at the well head of the injection well. The bottom-hole pressure could be calculated by adding static pressure in the well to the observed well-head pressure. The calculated bottom-hole pressure, therefore, excludes the friction losses of the grout in the tubing.

Except for the 40-minute period from 1805 hours to 1845 hours, the injection rate was kept constant at 0.015 m^3/s for the entire injection period. During this 40-minute period, the injection rate dropped suddenly from 0.015 m^3/s to 0.010 m^3/s, thereafter the injection rate increased to 0.015 m^3/s. The observed injection pressures and injection rates are shown in table 28 and figure 59.

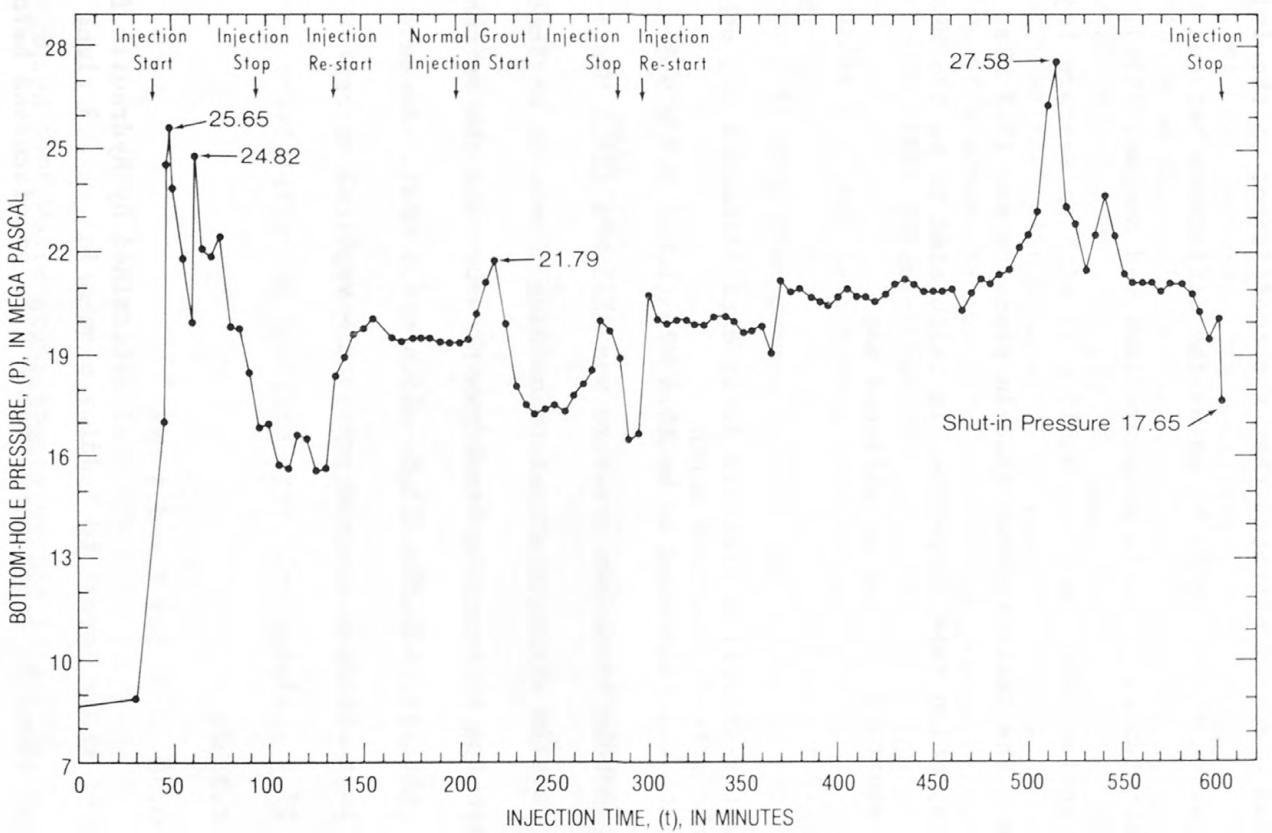

Figure 59.--Pressure versus time, test grout injection at 332 meters, June 14, 1974, proposed disposal site, Oak Ridge National Laboratory, Tennessee.

Outside of the 40-minute period, the variation of injection rates was only 0.0006 m^3/s, so that the statistical random variation of the injection rate cannot be separated from the observation error. In essence, the injection rate is equivalent to a single rate, consequently, the linear regression method cannot be used to find the relation between the injection pressure and injection rate. However, it has been demonstrated that the coefficient of the injection rate in a linear equation can be found by using the difference between the injection pressure and the instantaneous shut-in pressure (Sun and Mongan, 1974).

The average injection rate was 0.015 m^3/s with an average injection pressure of 20.7 MPa. The instantaneous shut-in pressure was 17.7 MPa. The coefficient of the injection rate therefore, is calculated to be 196 MPa (m^3/s). The linear equation is then established as:

$$P = 17.7 + 196\ Q \qquad (65)$$

From the 1967 water-injection pressure decay data (deLaguna and others, 1968) the actual injection depth
the vertical stress at/ was estimated to be 15.4 MPa ($1.8 \times 2.7 \times 9.8 \times 10^{-3} \times 324 = 15.4$ MPa). The bottom-hole breakdown pressure was 21.5 MPa ($18.3 + 9.8 \times 10^{-3} \times 324 = 21.5$ MPa). Tensile strength normal to bedding planes is estimated from the difference between the bottom-hole breakdown pressure and the estimated vertical stress, that is, 6.1 MPa (21.5 - 15.4 = 6.1 MPa). Because,

fT = instantaneous shut-in pressure - vertical stress

= 17.7 - 15.4

= 2.3 MPa

therefore, f = 0.38 for T = 6.1 MPa

as determined by hydraulic fracturing
The tensile strength of shale normal to bedding planes/is 3 times higher than the average value found in laboratory (table 27), as discussed before, this is probably due to stress relaxation when confining stress is removed from the core.

A2.8.2.1.2 Altitude of induced fractures

The altitudes of induced fractures were determined by gamma-ray logs made in observation wells before and after the test grout injection. Repeated logs were made to confirm that the logs were reproducible. The logger amplifier has 7 sensitivity ranges, namely, 0.001, 0.002, 0.005, 0.01, 0.02, 0.05, and 0.1 milliroentgen per hour (mr/hr). The sensitivity of determining gamma-ray activity decreases as the number of the sensitivity range increases. For example, the logger is 100 times more sensitive to gamma energy with a sensitivity range of 0.001 mr/hr than that with a sensitivity range of 0.1 mr/hr. The amplitude of a deflection of a gamma-ray log made with a sensitivity range of 0.001 mr/hr is, therefore, 100 times greater than that indicated on a log made with a sensitivity range of 0.1 mr/hr from the same source. Therefore, it is necessary to keep the sensitivity range in mind when gamma-ray logs are compared.

A2.8.2.1.2.1 Past waste grout sheets intercepted by North-observation well

The location of the North-observation well is about 190 m, S45°W from the present injection well. Four peaks of gamma-ray activity above the background level of shale were noted from the gamma-ray logs made in the North-observation well before the test grout injection. The peaks were at depths of 242, 246, 271, and 324 m, respectively (fig. 60 and table 29). These peaks indicate that the well has intercepted past waste grout sheets during injections made at the present injection well north of the observation well.

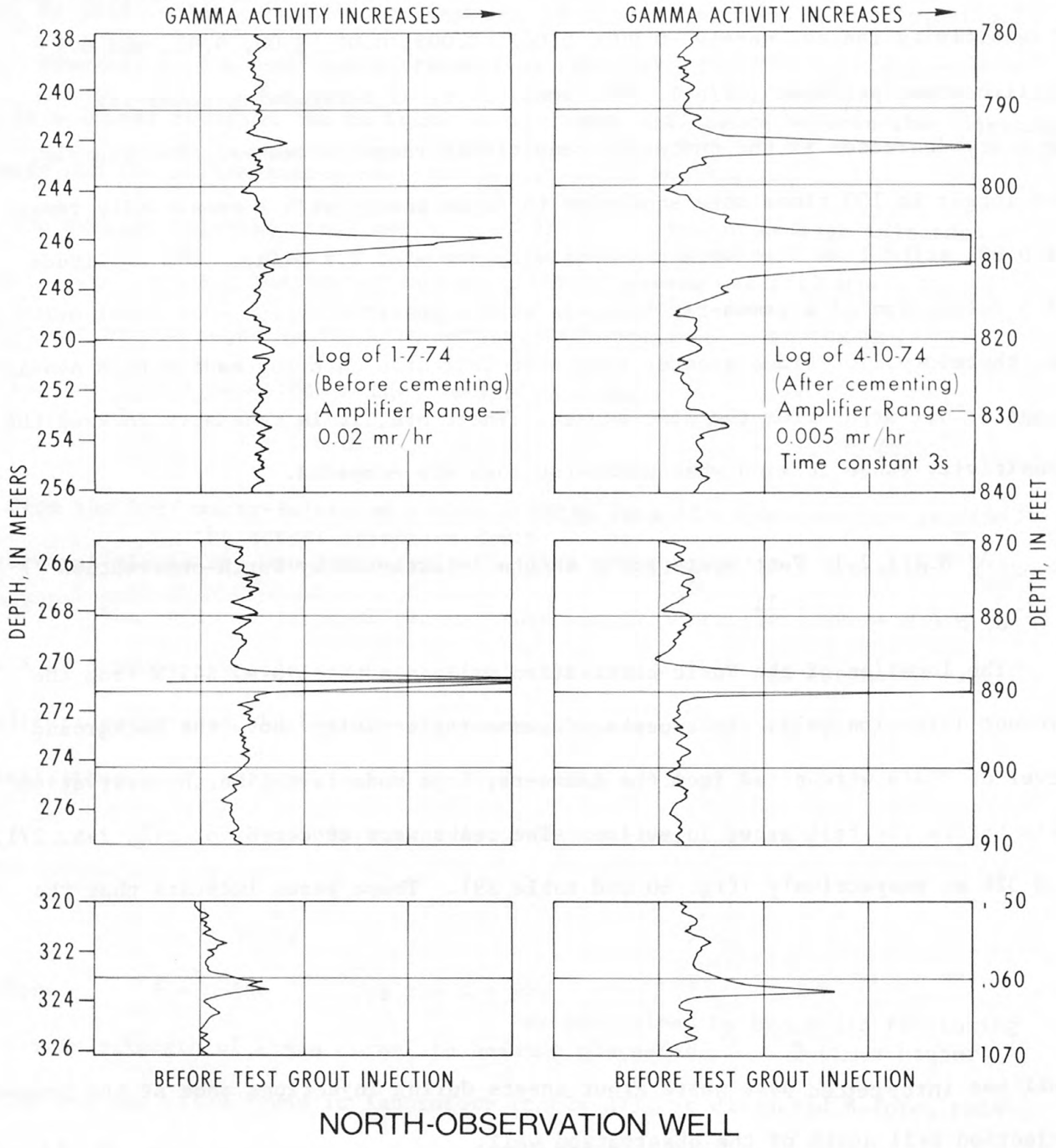

Figure 60.--Gamma-ray activities surveyed in North-observation well along casing axis, before test grout injection, June 14, 1974, proposed disposal site, Oak Ridge National Laboratory, Tennessee.

The strongest gamma-activity among the four peaks was at a depth of 271 m measured along the casing (fig. 60). Adjusted for well deviation the altitude of this peak is at -27 m (table 29) below mean sea level (msl), and if the calculated dip and strike (13° and N71°E, table 26) of the Pumpkin Valley shale found at the proposed site were used, then bedding-plane fractures of this peak would intercept the present injection well at an altitude of -16 m. Most of the wastes were injected at altitudes ranging from -12 to -18 m (table 11). Therefore, it can be concluded that this gamma-ray peak was a result of past waste injections at the present injection well.

The second strongest gamma-activity peak was observed at an altitude of -4 m msl. Using the same dip and strike the projected altitude at which this second peak might intercept the present injection well is at an altitude of 9 m msl. The other two gamma-activity peaks observed at altitudes of -0.5 and -74 m msl, when projected to the present injection well are either 24 m above or 21 m below the past waste injection altitude. Table 11 indicates that all wastes were injected between the altitudes of -12 to -47 m msl, therefore, it may be concluded that some waste grout probably has migrated 20 m above or below the injection level during past injections at a distance at least 200 m from the injection site.

A2.8.2.1.2.2 Grout sheets produced by test grout injection

Comparison of gamma-ray logs made in the North-observation well before and after the test grout injection shows no significant change of gamma activity at any depth. Two of the logs obtained after the test grout injection were made by using sensitivity ranges of 0.002 mr/hr and 0.01 mr/hr, respectively. If the gamma activity shown by the log made at a sensitivity of 0.002 mr/hr is reduced by a factor of 5, then the shape and the relative quantity of the gamma activity

on the log would be similar to that of the log made at a sensitivity of 0.01 mr/hr. This indicates the reproducibility of the logs. If the log made at a sensitivity of 0.002 mr/hr is reduced by a factor of 2.5, the activity recorded on the log would be very close to that recorded on the log made in the North-observation well before the test grout injection at a sensitivity of 0.005 mr/hr. Comparison of the logs indicates that no additional grout sheets have been intercepted by the North-observation well since the test grout injection. The probable altitude at which the North-observation well would intercept the bedding-plane fractures induced by the test grout injection at the proposed disposal site was calculated to be at -67 m msl. A gamma-activity peak produced by past waste injections is at -74 m msl or about 7 m below the calculated altitude at which the induced fractures would be expected to be intercepted. Therefore, it cannot be determined whether the injected grout did not reach the vicinity of the North-observation well, or whether the injected grout did reach the observation well and followed weak planes between past waste grout sheets and shale at -74 m msl; in the latter case, the gamma activity produced by the tracer in the test grout injection could not be differentiated from that produced by past waste injections.

Six gamma-activity peaks were noted on a gamma-ray log made in the West-observation well after the test grout injection at depths ranging from 328 to 332 m measured along the casing (table 30 and fig. 61). Grout sheets were formed within a 5-m zone. From the well deviation records the projected horizontal position of the six gamma activity peaks and the altitudes of the grout sheets were calculated and are shown in table 30. The horizontal distance between the

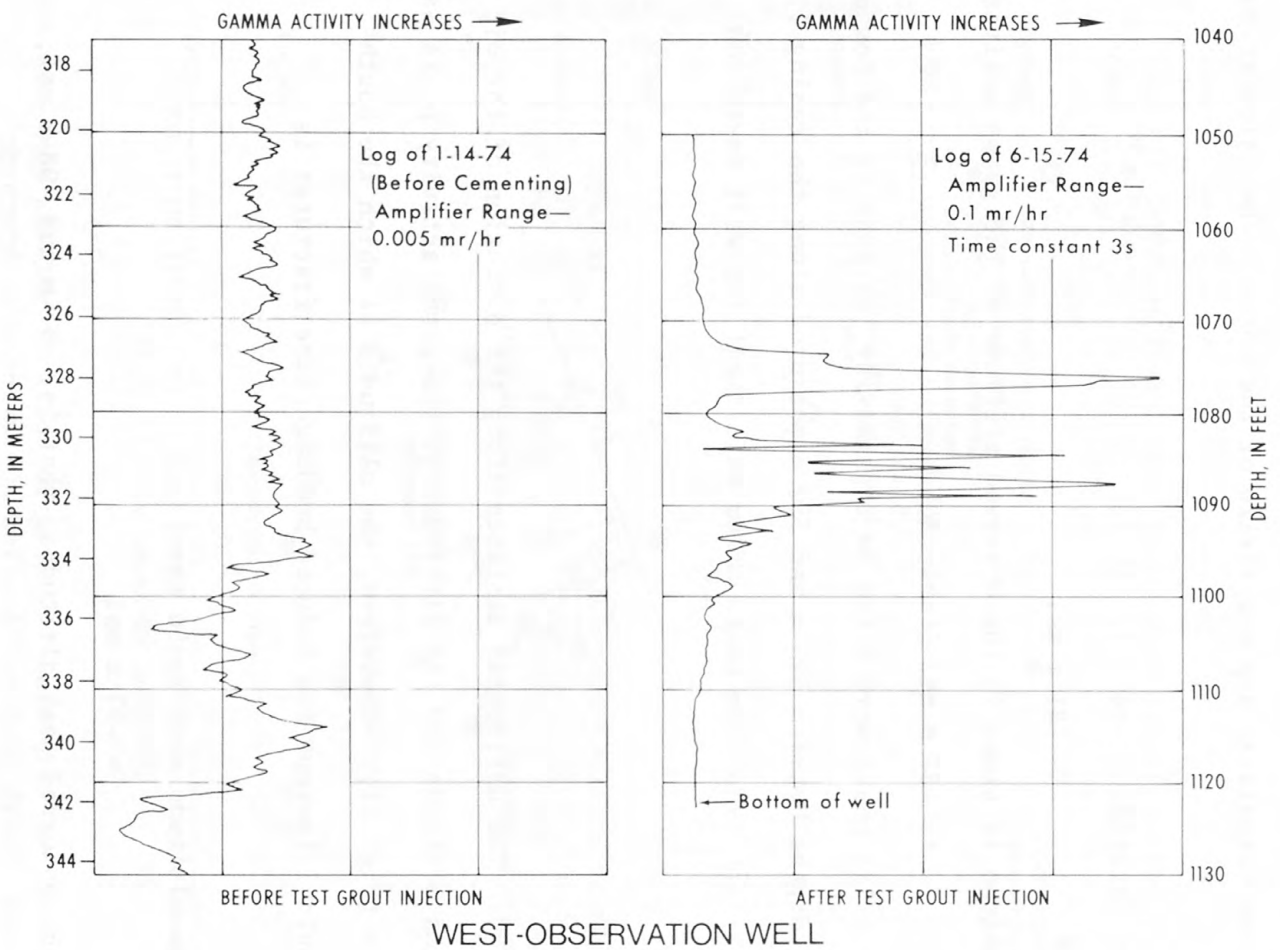

Figure 61.--Gamma-ray activities surveyed in West-observation well along casing axis, before and after test grout injection, June 14, 1974, proposed disposal site, Oak Ridge National Laboratory, Tennessee.

injection depth and the observed gamma-activity peaks along a line perpendicular to the calculated strike of the Pumpkin Valley shale and was estimated to be 12 m (fig. 62). The injection depth was at -84 m msl. If bedding-plane fractures are to be induced in the vicinity of the West-observation well, then the altitude at which they would be intercepted by the West-observation can be estimated by using the calculated dip and strike of the shale. The calculation is:

$$\text{Fracture altitude} = -84 + 12 \tan 13$$
$$= -81 \text{ m msl}$$

This calculated altitude is close to the observed altitude of the gamma activity peaks which are from -82 to -87 m msl (table 30).

Three gamma activity peaks were noted on a gamma-ray log made in the South-observation well at depths between 349 m and 350 m measured along the casing (table 30 and fig. 63). The altitudes of the peaks after adjustment for well deviation are shown in table 30. The horizontal distance along the direction of the dip between the injection altitude and the altitudes of the gamma activity peaks was estimated to be 56 m (fig. 62). Therefore, the altitudes at which the South-observation well would intercept the induced bedding-plane fractures is calculated as:

$$\text{Fracture altitude} = -84 - 56 \tan 13$$
$$= -97 \text{ m msl}$$

which is close to the observed peak altitudes, that is, -97 m and -98 m msl, respectively.

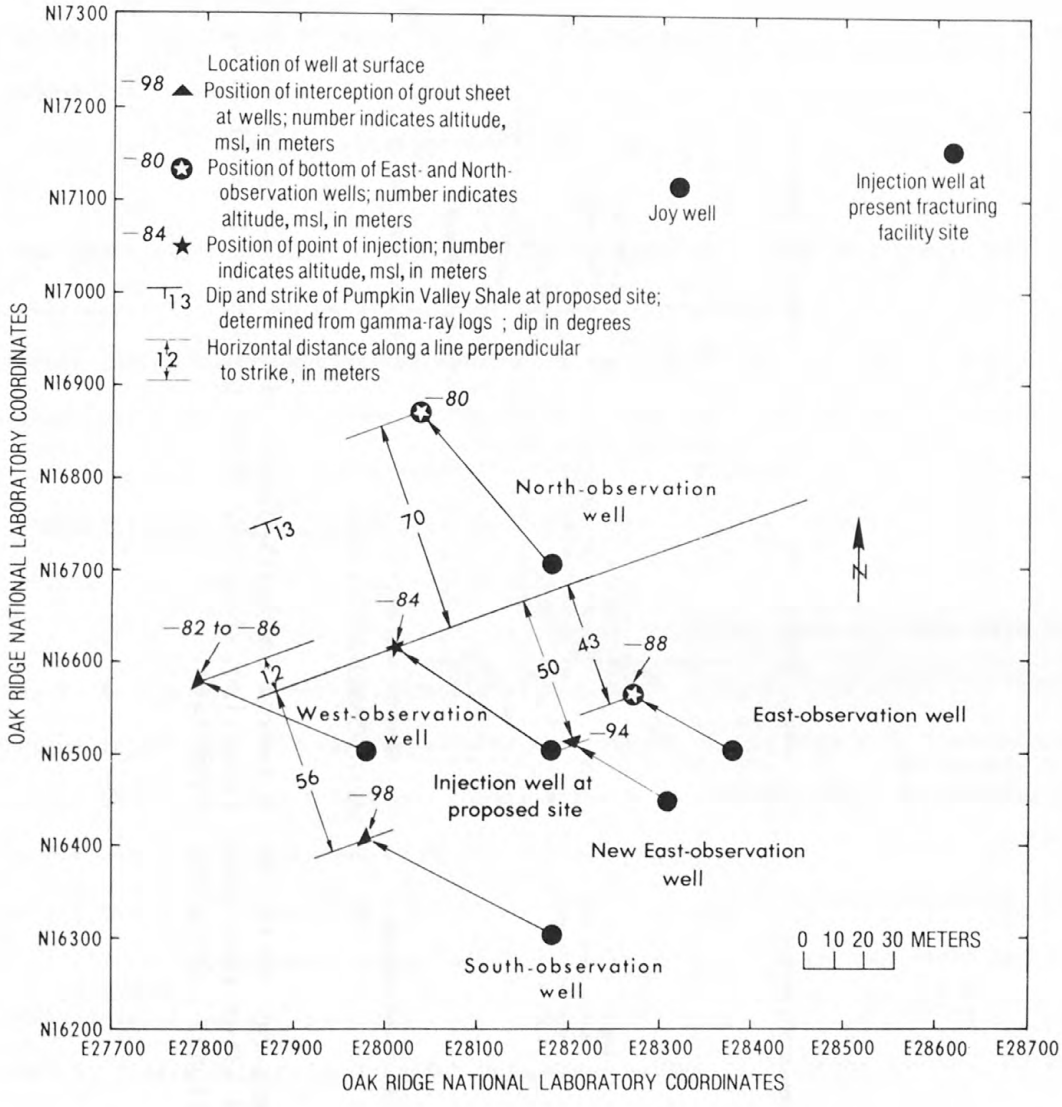

Figure 62.--Map showing location of point of injection and gamma-ray peaks observed in observation wells after test grout injection, June 14, 1974, proposed disposal site, Oak Ridge National Laboratory, Tennessee.

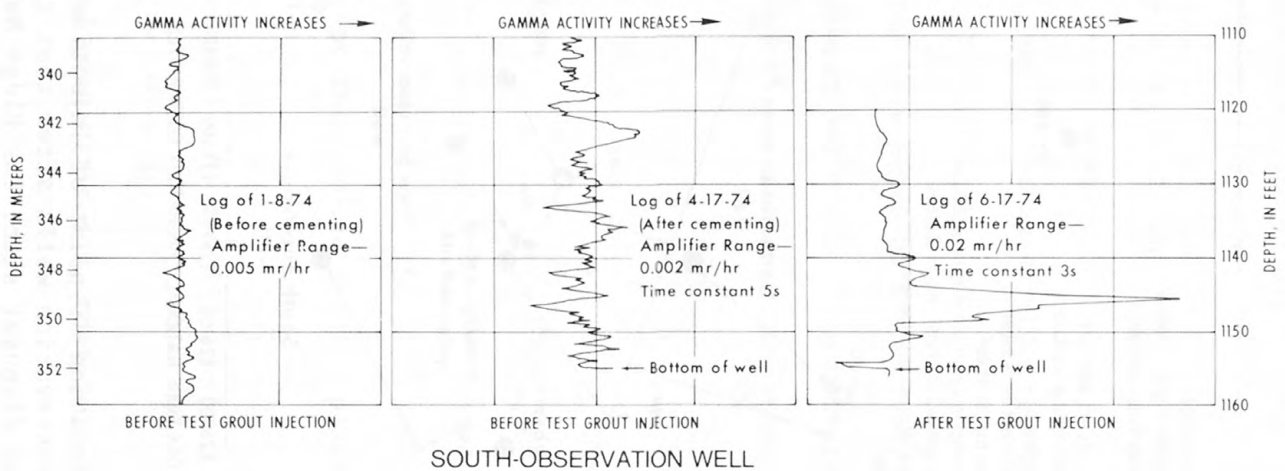

Figure 63.--Gamma-ray activities surveyed in South-observation well along casing axis, before and after test grout injection, June 14, 1974, proposed disposal site, Oak Ridge National Laboratory, Tennessee.

was
No significant change of gamma activity/registered on logs made in the East-observation well before and after the grout injection. The projected horizontal distance along the dip between bottom of the East-observation well and the injection altitude was estimated to be 43 m (fig. 62). The altitude at which the East-observation well would intercept the induced bedding-plane fractures is calculated as:

$$\text{Fracture altitude} = -84 - 43 \tan 13$$

$$= -94 \text{ m msl}$$

The depth corresponding to this altitude measured along the casing adjusted by well deviation was to be 340 m. The total drilling depth was 344 m, however, after casing and cementing the well depth was reduced to 334 m which is 6 m shallower than the calculated altitude where the East-observation well would intercept the induced fractures. The gamma-ray log indicates two possibilities: (1) induced fractures intercept the well beneath the well bottom; or, (2) no grout sheets reached the well.

the
Before / water injection made on October 30, 1975, gamma-ray logs were made again in all four observation wells in September 1975, 87 days after the test grout injection. All logs reproduced the pattern of the logs made immediately distinctly
after the test grout injection. Gamma activity peaks were still observed/at the zones discussed above, but these peaks could not have been due to the tracer, Au^{198}, which has a half life of 2.7 days. After 32 half lives (87 days after the injection) the tracer should have decayed to below the detection limits. As explained by personnel
ORNL/several hundred gallons of contaminated waste pit water containing Cs^{137} and Sr^{90} were injected during the test grout injection (written commun., J. A. Lenhard, Oak Ridge Operations, DOE, November 16, 1976), and thus the gamma peaks observed on logs
/resulted from Cs^{137} not from tracer Au^{198}.

A new East-observation well was drilled by ORNL 30 m/west of the south old East-observation well. A single gamma activity peak was noted on a gamma-ray log made in the new/observation well at a depth of 341 m measured along the East- casing (fig. 64). Adjusted for well deviation the altitude that the observation well intercepts the induced fractures was calculated to be -94 m. The horizontal distance along the dip between the injection altitude and the altitude of gamma-ray peak was estimated to be 65 m (fig. 62). The projected altitude that the new East-observation well could intercept the test injection grout sheet is calculated as:

$$\text{Fracture altitude} = -84 - 50 \tan 13$$

$$= -96 \text{ m msl}$$

which is close to the observed altitude -94 m msl.

Thus, three of four observation wells have intercepted the grout sheets produced by the test grout injection near the calculated altitudes, and, it is concluded that bedding-plane fracutres have been induced by the test grout injection.

A2.8.2.2 Test water injection

A test water injection was made on October 30, 1975, through the same slot as the test grout injection made on June 14, 1974. The scheduled injection volume was 378 m^3 of water tagged with 25 curies of Au^{198} and 25 curies of Au^{199}. The injection rates were scheduled to start at 0.003 m^3/s, increase to 0.006 m^3/s, then 0.013 m^3/s, and finally increase to the full capacity of the injection pump (0.017 m^3/s). The first three steps would last two hours for each step.

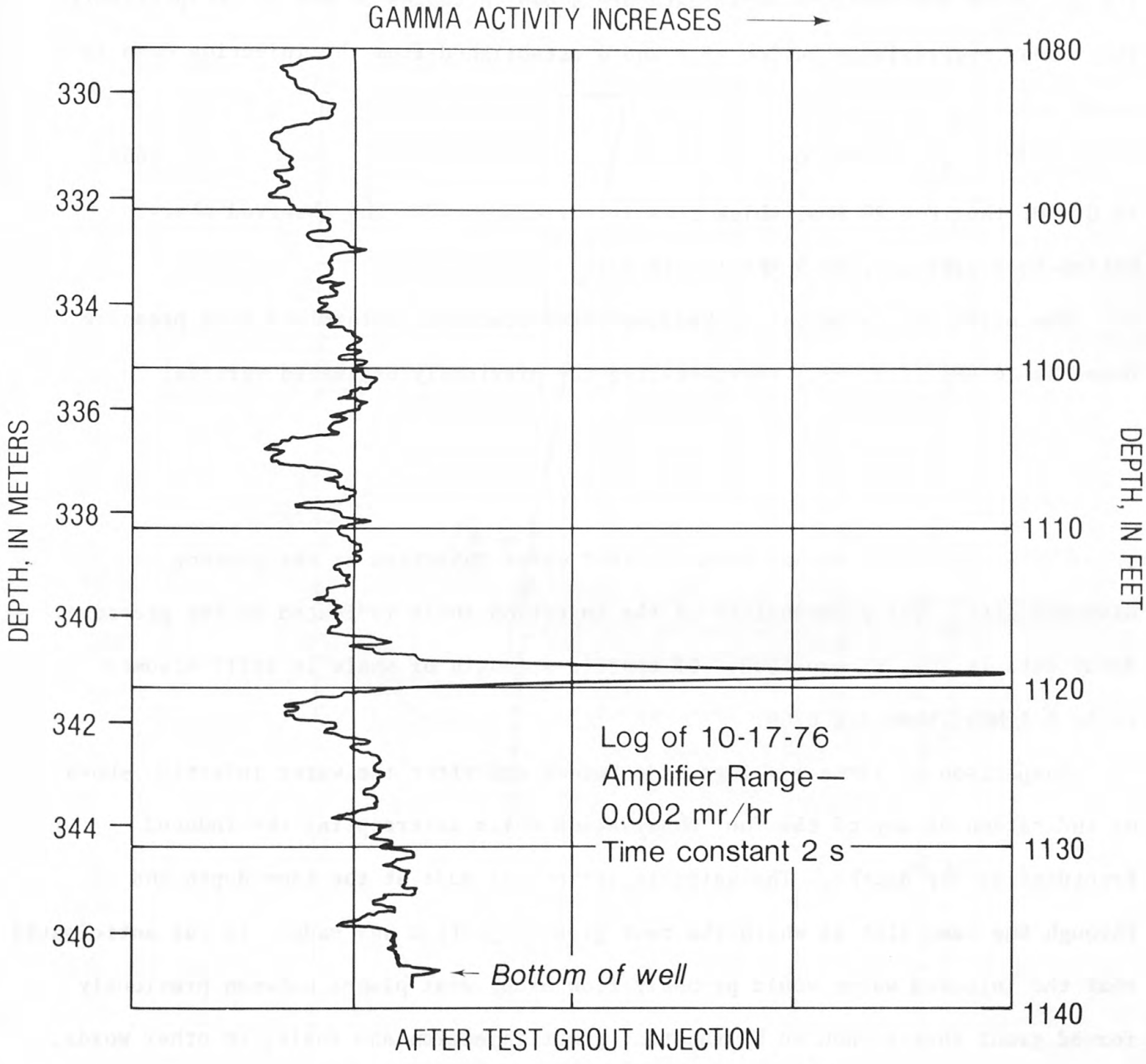

Figure 64.--Gamma-ray activities surveyed in new East-observation well along casing axis, 85 days after test grout injection, June 14, 1974, proposed disposal site, Oak Ridge National Laboratory, Tennessee.

Unfortunately one of the two injection pumps broke down after about one hour of injection at the pump's highest capacity, and the injection was stopped shortly thereafter. The final injection volume was 209 m^3 tagged with half the prepared tracers. Pressure decay was observed for about 18 days after the injection. The injection and pressure decay data are shown in tables 31 and 32, respectively. The linear regression equation of P and Q established from the injection data is given by:

$$P = 20 + 197\ Q \qquad (66)$$

if Q = 0; then P = 20 MPa, which closely correlates with the observed shut-in bottom-hole pressure, 19.9 MPa (table 32).

The earth stress normal to bedding-plane fractures determined from pressure decay is 16 MPA (fig. 65), corroborating the previously estimated vertical stress, 15.4 MPa, determined from the 1967 water injection at the present disposal site. The permeability of the injection shale indicated by the pressure decay data is low, as expected. If tensile strength of shale is still assumed to be 6.1 MPa; then f = 0.66.

Comparison of gamma-ray logs made before and after the water injection shows no indication of any of the four observation wells intercepting the induced fractures at any depths. The water injection was made at the same depth and through the same slot at which the test grout injection was made. It was anticipated that the injected water would probably flow along weak planes between previously formed grout sheets induced by the test grout injection and shale, in other words, that a series of thin fractures would be induced in the grout sheet zone. Because the grout sheets are contaminated by cesium-137 which produces higher gamma energy than those

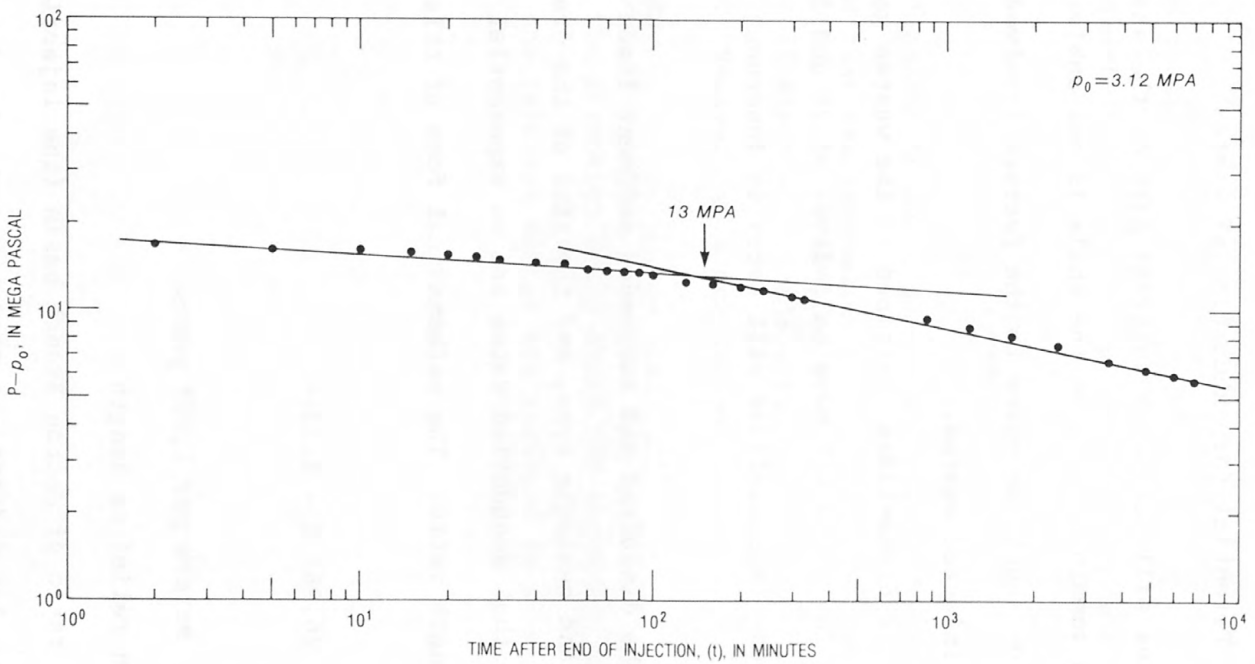

Figure 65.--Pressure decay versus time, test water injection at 332 meters, October 30, 1975, proposed disposal site, Oak Ridge National Laboratory, Tennessee.

produced by the tracers in the injection water, it is not surprising that none of the gamma-ray logs made in the observation wells after the water injection show evidence that fractures induced by the water injection have been intercepted. However, the water injection pressure / data confirms the conclusions reached from data observed during the test grout injection.

A2.9 Potential for exhumation of wastes

The injected wastes will become an integral part of the shale after solidification of grout and so remain as long as the shale is not subject to erosion. Therefore, consideration should be given to the factors involved in eroding and possibly exposing the injected wastes.

Over 99 percent of radionuclides contained in the wastes generated at ORNL are Sr^{90} and Cs^{137} (table 11), which have half-lives of 28 and 30 years, respectively. Within 1,000 years, these radionuclides will decay to innocuous radiation-emission levels.

On the basis of the dissolved and suspended sediment loads of streams, the climate, topographic, and geologic type, and the size of the drainage areas, Schumm (1963) concludes that denudation rates are an exponential function of the drainage relief and length ratio. The mathematical form of this relationship is as follows:

$$\log D = 26.966\ H - 2.2398 \qquad (67)$$

where,

D = denudation in meters per 1,000 years

H = ratio of basin relief to length

The relief-length ratio of Melton Branch basin (the injection site) is taken as 0.031 [(365.8 - 231.6)/4328 = 0.031], then the denudation rate of the basin is estimated to be 0.04 m per 1,000 years. Wastes are to be injected into

Pumpkin Valley shale which is about 213 m below the surface. Using the estimated denudation rate, it would take 5.4×10^6 years to expose the wastes injected in the uppermost part of the Pumpkin Valley shale by erosion. Even if the unlikely erosion rate of 1 m per 1,000 years is assumed, which is the average maximum erosion rate for young mountain ranges of high relief such as the Alps (Schumm, 1963), it would still take 2×10^5 years to expose the grout sheets. This time interval would be sufficient for the radionuclides contained in the wastes to decay to harmless radiation-emission levels, and thus the possibility of their contaminating the biosphere by erosion processes is negligible.

2.10 Summary

On the basis of injection data, gamma-ray logs, and estimation of erosion rate it is concluded that the hydraulic fracturing disposal sites at ORNL are safe for the purpose of disposal of radioactive wastes generated at ORNL by grout injections in shale. However, as a precaution monitoring more/observation wells need to be constructed extending to areas not expected to be reached by waste grout sheets and in the formation lying above the injection zone, thus increasing the confidence that the injected wastes are isolated in a known horizon.

B. NOMENCLATURE

A	linear regression constant; instantaneous shut-in pressure
a'	internal radius of a thick wall cylinder; radius of induced fracture
a	radius of stress-altered fracture region as shown in figure 6
B	constant; maximum fracture separation
b	intermolecular distance; external radius of a thick wall cylinder
C	constant; activity of a particular radionuclide in waste at time t; horizontal distance measured perpendicular to the average strike of shale beds
Co	activity of a particular radionuclide in waste at disposal time
D	inside diameter of a pipe; denudation rate
d	diameter of a tested sample; edge region of a fracture as shown in figure 6
E	Young's modulus
F(Q,L,W)	friction loss in a vertical fracture
F(Q,r,W)	friction loss in a horizontal fracture
fT	average cohesive force at a fracture tip
f	$0 \leq f \leq 1$; Fanning factor
g	acceleration due to gravity
H	ratio of basin relief to length; horizontal displacement of a hole
h	depth of induced fracture; length of a tested sample
K	horizontal stress coefficient (σ_h/σ_v)
Ka	coefficient of "active earth pressure"
Ko	coefficient of "earth pressure at rest"
K'	fluid consistence index (kg-force-sec$^{n'}$/m^2)
k	constant
L	fracture length; length of casing

MD	depth measured along casing axis
n	number of half-lives of a particular radionuclide
n'	fluid flow behavior index (dimensionless)
P	internal pressure in a thick wall cylinder; bottom-hole pressure in injection well; load at rock failure during tensile strength test
P_i	initiation pressure or breakdown pressure to induce a fracture
P_p	propagation pressure to extend a fracture
ΔP	pressure loss due to friction
p_o	pore pressure
Q	injection rate
R_e	Reynold's number
r	radial distance
T	tensile strength of rock
T_a	tensile strengh of rock in the direction parallel to bedding planes
T_n	tensile strength of rock in the direction normal to bedding planes
T_{σ_y}	tensile strength of rock in the direction parallel to stress σ_y
T_{σ_z}	tensile strength of rock in the direction parallel to stress σ_z
$T_{1/2}$	half-life of a particular radionuclide
t	time
U	horizontal movement of ground surface
v	flow velocity
W	fracture opening
$\bar{W}$	surface uplift
x	x-axis; horizontal departure, distance east or west of North-South axis

y	y-axis; horizontal departure, distance north or south of East-West axis
Z	true vertical distance between two adjacent measured points
z	z-axis; vertical depth
α	a'/a; vertical deviation angle; angle with the direction of the least principal stress σ_3
β	angle of joints with respect to well axis; magnetic bearing
γ	weight density of rock
θ	polar angle from x-axis; dip angle
ν	Poisson ratio
ρ	density
σ	normal stress
σ_a	stress in the direction parallel to bedding planes
σ_n	stress in the direction normal to bedding planes
σ_h	horizontal earth stress
σ_v	vertical earth stress
σ_r	radial stress
σ_t	tangential stress
σ_x	stress along x-axis
σ_y	stress along y-axis
σ_z	stress along z-axis; overburden pressure
$\sigma_1, \sigma_2, \sigma_3$	principal stresses, the order of magnitude is represented by subscript numbers, σ_3 being the least stress
τ	shear stress
ϕ	angle of internal friction of clastic sediments
ω	angle of bedding planes with respect to well axis

C. REFERENCES

Anderson, R. E., and Laney, R. L., 1975, The influence of late Cenozoic stratigraphy on distribution of impoundment-related seismicity at Lake Mead, Nevada-Arizona: U.S. Geol. Survey Jour. Research, v. 3, no. 3, p. 337-343.

Badgley, P. C., 1965, Structural and tectonic principles: New York, Harper & Row, 521 p.

Barenblatt, G. I., 1962, The mathematical theory of equilibrium cracks in brittle fracture, in Advances in Applied Mechanics, Dryden, H. L., and Von Karman, T., ed.: New York, Academic Press, p. 55-129.

Bear, Jacob, 1972, Dynamics of fluids in porous media: New York, American Elsevier, 764 p.

Belter, W. G., 1972, Deep disposal systems for radioactive wastes, in Cook, T. D., ed., Underground Waste Management and Environmental Implications: Am. Assoc. Petroleum Geologists, Mem. 18, p. 341-354.

Bieniawski, Z. T., 1967, Mechanism of brittle fracture of rock: Int. Jour. Rock Mech. Min. Sci., v. 4, p. 395-406.

Bredehoeft, J. D., England, A. W., Stewart, D. B., Trask, N. J., and Winograd, I. J., 1978, Geologic disposal of high-level radioactive wastes--Earth Science Perspectives: U.S. Geol. Survey Circular 779, 15 p.

Brooker, E. W., and Ireland, H. O., 1965, Earth pressure at rest related to stress history: Canadian Geotech. Jour., v. 2, no. 1, p. 1-15.

Bugbee, J. M., 1953, Discussion of rock rupture as affected by fluid properties by Scott, P. P., Jr., Bearden, W. G., and Howard, G. E.: AIME, Trans. v. 198, p. 111-124.

Carter, D. S., 1945, Seismic investigation in the Boulder Dam area, 1940-1944, and the influence of reservoir loading on local earthquake activity: Seismol. Soc. America, Bull., v. 35, p. 175-192.

_____, 1970, Reservoir loading and local earthquakes: Geol. Soc. America Eng. Geology Case Histories, no. 8, p. 51-61.

Chenevert, M. E., and Gatlin, Carl, 1965, Mechanical anisotropies of laminated sedimentary rocks: Jour. Petroleum Engineers, v. 5, no. 1, p. 67-77.

Clark, J. B., 1949, A hydraulic process for increasing the productivity of wells: AIME, Trans. 186, p. 1-8.

Cottrell, A. H., 1964, The mechanical properties of matter: New York, John Wiley, 430 p.

Daneshy, A. A., 1967, Initiation and extension of hydraulic fractures in rocks: Jour. Petroleum Engineers, September, p. 310-318.

_____, 1973, A study of inclined hydraulic fractures: Jour. Petroleum Engineers, April, p. 61-69.

Davis, S. N., 1969, Porosity and permeability of natural materials, in Roger, J. M., DeWiest, ed., Flow through porous media: New York, Academic Press, p. 53-89.

Davis, C. V., and Sorensen, K. E., 1969, Handbook of applied hydraulics: New York, McGraw-Hill, p. 2-6.

deLaguna, Wallace, 1972, Hydraulic fracturing test at West Valley, New York: Oak Ridge Nat. Lab., ORNL-4827, 64 p.

deLaguna, Wallace, Tamura, Tsuneo, Weeren, H. O., Struxness, E. G., McClain, W. C., and Sexton, R. C., 1968, Engineering development of hydraulic fracturing as a method for permanent disposal of radioactive wastes: Oak Ridge Nat. Lab., ORNL-4259, 261 p.

deLaguna, Wallace, Weeren, H. O., Binford, F. T., Witkowski, E. J., and Struxness, E. G., 1971, Safety analysis of waste disposal by hydraulic fracturing at Oak Ridge: Oak Ridge Nat. Lab., ORNL-4665, 41 p.

Eardley, A. J., 1951, Structural geology of North America: New York, Harper & Brothers, 623 p.

Evans, D. M., 1966, The Denver area earthquakes and the Rocky Mountain Arsenal disposal well: Mtn. Geologist, v. 3, no. 1, p. 23-26.

Fenner, R., 1938, Investigation on analysis of rock pressure (in German): Gluckauf, v. 74, no. 32, p. 681-695.

Freeze, R. Allan, and Cherry, John A., 1979, Groundwater: New Jersey, Prentice-Hall, 604 p.

Gatlin, Carl, 1960, Petroleum Engineering--drilling and well completions: New Jersey, Prentice-Hall, 341 p.

Gibbs, J. F., Healy, J. H., Raleigh, B. C., and Coakley, John, 1972, Earthquakes in the oil field at Rangely, Colorado: U.S. Geol. Survey open-file report, 27 p.

Goodier, J. N., 1968, Mathematical theory of equilibrium cracks in fractures, Leibowitz, H., ed.: New York, Academic Press, v. 2, p. 1-66.

Haimson, Bezallel, 1968, Hydraulic fracturing in porous and nonporous rock and its potential for determining in-situ stresses: Minneapolis, U. Minnesota, Ph.D. dissertation, 234 p.

Haimson, Bezallel, and Fairhurst, Charles, 1969, Hydraulic fracturing in porous-permeable materials: Jour. Petroleum Technology, July, p. 812-817.

Hantush, M. S., 1964, Hydraulics of wells, in Chow, V. T., ed., Advances in Hydroscience, v. 1: New York, Academic Press, p. 281-432.

Harrison, Eugene, Kieschnick, W. F., Jr., and McGuire, W. J., 1954, The mechanics of fracture induction and extension: AIME, Trans., v. 201, p. 252-263.

Healy, J. H., Jackson, W. H., and Van Schaack, J. R., 1966, Microseismicity studies at the site of the Denver earthquakes in geophysical and geological investigations relating to earthquakes in Denver area, Colorado: U.S. Geol. Survey open-file report, pt. 5, 19 p.

Heck, E. T., 1955, Fractures and joints: Producers Monthly, February, p. 20-23.

_____, 1960, Hydraulic fracturing in light of geologic conditions: Producers Monthly, September, p. 12-13 and p. 16-19.

Hobbs, D. W., 1964, The tensile strength of rocks: Int. Jour. Rock Mech. Mining Sci., v. 1, p. 385-396.

Howard, J. H., 1966, Vertical normal stress in the earth and the weight of overburden: Geol. Soc. America, Bull., v. 77, p. 657-660.

Howard, G. C., and Fast, C. R., 1970, Hydraulic fracturing: AIME, Monograph v. 2, 203 p.

Hubbert, M. K., 1957, Reply to Reynolds, J. J., and Coffer, H. F., Discussion on mechanics of hydraulic fracturing by Hubbert, M. K., and Willis, D. G., 1957, in AIME Trans. v. 210, p. 153-166: AIME, Trans. v. 210, p. 167-168.

_____, 1971, Natural and induced fracture orientation: Am. Assoc. Petroleum Geologists, Mem. 18, p. 235-238.

Hubbert, M. K., and Willis, D. G., 1957, Mechanics of hydraulic fracturing: AIME, Trans. v. 210, p. 153-166.

Hubbert, M. K., and Rubey, W. W., 1959, Role of fluid pressure in mechanics of overthrust faulting, part 1: Geol. Soc. America, Bull. v. 70, no. 2, p. 155-166.

_____, 1960, Role of fluid pressure in mechanics of overthrust faulting--A reply: Geol. Soc. America, Bull. v. 71, no. 5, p. 617-628.

Interagency Review Group on Nuclear Waste Management (U.S.), 1979, Report to the President by the Interagency Review Group on Nuclear Waste Management: U.S. Department of Energy, TID-29442, 149 p.

International Atomic Energy Agency, 1971, Leach testing of immobilized radioactive waste solids, a proposal for a standard method, Hespe, E. D., ed.: Atomic Energy Review, v. 9, no. 1, p. 195-207.

Jaeger, J. C., 1962, Elasticity, fracture and flow with engineering and geological applications: New York, John Wiley, 208 p.

Jaeger, J. C., and Cook, N. G. W., 1969, Fundamentals of rock mechanics: London, Methuen & Co., 513 p.

Kenny, Peter, and Campbell, J. D., 1967, Fracture toughness: Progress in Material Sci., v. 13, 181 p.

Kunz, V. J., 1971, The fundamentals of crack mechanics--a critical review: Technica, v. 17, p. 1535-1557.

Lahee, F. H., 1952, Field Geology: New York, McGraw-Hill, 883 p.

Lamont, Norman, and Jessen, F. W., 1963, The effects of existing fractures in rocks on the extension of hydraulic fracturing: AIME, Trans. v. 228, p. 203-209.

Magara, Kinji, 1978, Compaction and fluid migration--practical petroleum geology: New York, Elsevier Scientific Publishing Co., 319 p.

Major, M. W., and Simon, R. B., 1968, A seismic study of the Denver (Derby) earthquakes: Colorado School Mines Quart. v. 63, no. 1, p. 9-55.

McClain, W. C., and Meyers, H. O., 1970, Seismic history and seismicity of the southeastern region of the United States: Oak Ridge Nat. Lab., ORNL-4582, 46 p.

McGarr, Arthur, and Gay, N. C., 1978, State of stress in the earth's crust: Ann. Review Earth Planetary Science, v. 6, p. 405-436.

McGinnis, L. D., 1963, Earthquakes and crustal movement as related to water load in the Mississippi Valley Region: Illinois State Geol. Survey Circ. 334, 20 p.

McMaster, W. M., 1963, Geologic map of the Oak Ridge Reservation, Tennessee: Oak Ridge Nat. Lab., ORNL-TM-713, 23 p.

_____, 1967, Hydrologic data for the Oak Ridge area, Tennessee: U.S. Geol. Survey, Water Supply Paper 1839-N, 60 p.

McMaster, W. M., and Waller, H. D., 1965, Geology and soils of Whiteoak Creek Basin, Tennessee: Oak Ridge Nat. Lab., ORNL-TM-1108, 37 p.

Melton, L. L., and Saunders, C. D., 1957, Rheological measurements of non-Newtonian fluids: AIME, Trans v. 210, p. 196-201.

Moye, D. G., 1958, Rock mechanics in the investigation and construction of T.1 underground power station, Snowy Mountains, Australia: Geol. Soc. America Eng. Geol. Case Histories, no. 3, p. 13-44.

Moore, J. G., Godbee, H. W., Kibbey, A. H., and Joy, D. S., 1975, Development of cementitious grouts for the incorporation of radioactive waste part 1: leach studies: Oak Ridge Nat. Lab., ORNL-4962, 111 p.

Moore, J. G., 1976, Development of cementitious grouts for the incorporation of radioactive wastes part 2: Continuation of cesium and strontium leach studies: Oak Ridge Nat. Lab., ORNL-5142, 144 p.

Obert, Leonard, and Duvall, W. I., 1967, Rock mechanics and the design of structures in rock: New York, John Wiley, 650 p.

Ostle, Bernard, 1954, Statistics in research; basic concepts and techniques for research workers: Iowa State College Press, 487 p.

Overbey, W. K., Jr., and Rough, R. L., 1968, Surface studies predict orientation of induced formation fractures: Producers Monthly, June, p. 16-19.

Perkins, T. K., 1967, Application of rock mechanics in hydraulic fracturing theories: 7th World Petroleum Congress, Mexico, Proc. v. 3, p. 75-84.

Perkins, T. K., and Krech, W. W., 1968, The energy balance concept of hydraulic fracturing: Jour. Soc. Petroleum Engineers, March, p. 1-12.

Prickett, T. A., and Lonnquist, C. G., 1971, Selected digital computer techniques for ground-water resource evaluation: Illinois State Geol. Survey, Bull no. 55, 62 p.

Raleigh, B. C., 1972, Earthquakes and fluid injection: Am. Assoc. Petroleum Geologist, Mem. 18, p. 273-279.

Reichmuth, D. R., 1968, Point load testing of brittle materials to determine tensile strength and relative brittleness: AIME, 9th Symposium on Rock Mechanics, April 17-19, 1967, Golden, Colorado, p. 134-160.

Rice, J. R., 1965, Plastic yielding at a crack tip: 1st Int. Conference on Fracture, Japan, Proc. v. 1, p. 283-308.

Schleicher, David, 1975, A model for earthquakes near Palisades Reservoir, Southeast Idaho: U.S. Geol. Survey, Jour. Research, v. 3, no. 4, p. 393-400.

Schumm, S. A., 1963, The disparity between present rates of denudation and orogeny: U.S. Geol. Survey, Prof paper 454H, 13 p.

Simonson, E. R., Abou-Sayed, A. S., and Clifton, R. J., 1978, Containment of massive hydraulic fractures: Soc. Petroleum Engineers Jour., February, p. 27-32.

Slagle, K. A., 1962, Rheological design of cementing operations: Jour. Petroleum Technology, March, p. 323-328.

Sun, R. J., 1969, Theoretical size of hydraulically induced horizontal fractures and corresponding surface uplift in an idealized medium: Jour. Geophys. Research, v. 74, no. 25, p. 5995-6011.

_____, 1973, Hydraulic fracturing as a tool for disposal of wastes in shale: Symposium Am. Assoc. Petroleum Geologist Underground Waste Management and artificial recharge, September 26-30, 1973, New Orleans, Louisiana, v. 1, p. 219-270.

Sun, R. J., 1976, Geohydrologic evaluation of a site for disposal of radioactive wastes by grout injection and hydraulic fracturing at Holifield National Laboratory (formerly Oak Ridge National Laboratory), Oak Ridge, Tennessee: U.S. Geol. Survey open-file report 75-671, 77 p.

_____, 1977, Possibility of triggering earthquakes by injection of radioactive wastes in shale at Oak Ridge National Laboratory, Tennessee: U.S. Geol. Survey, Jour. Research, v. 5, no. 2, p. 253-262.

Sun, R. J., and Mongan, C. E., 1974, Hydraulic fracturing in shale at West Valley, New York--A study of bedding-plane fractures induced in shale for waste disposal: U.S. Geol. Survey, open-file report 74-365, 152 p.

Tamura, Tsuneo, 1971, Sorption phenomena significant in radioactive waste disposal, in Cook, T. D., ed., Underground waste management and environmental implications: Am. Assoc. Petroleum Geologists, Mem. 18, p. 318-330.

Timoshenko, Stephen, and Goodier, J. N., 1951, Theory of elasticity: New York, McGraw-Hill, 506 p.

U.S. Bureau of Radiological Health, 1970, Radiological health handbook: U.S. Public Health Service, 458 p.

U.S. Energy Research and Development Administration (presently U.S. Department of Energy), 1977, Management of intermediate level radioactive waste, Oak Ridge National Laboratory, Oak Ridge, Tennessee--Final environmental impact statement: U.S. Energy Research Devel. Adm., ERDA-1553, 3113 p.

U.S. National Oceanic and Atmospheric Administration and U.S. Geological Survey, 1975, United States Earthquakes, 1973: U.S. Dept. Commerce and U.S. Dept. Interior, 112 p.

Voight, Barry, 1966, Interpretation of in situ stress measurement: Internat. Soc. Rock Mechanics, 1st Cong. Proc. Lisbon, v. 3, p. 332-348.

Walton, W. C., 1970, Ground-water resource evaluation: New York, 664 p.

Weeren, H. O., 1974, Shale fracturing injections at Oak Ridge National Laboratory--1972 series: Oak Ridge Nat. Lab., ORNL-TM-4467, 97 p.

_____, 1976, Shale fracturing injections at Oak Ridge National Laboratory--1975 series: Oak Ridge Nat. Lab., ORNL-TM-5545, 69 p.

Weeren, H. O., Brunton, G. D., deLaguna, Wallace, and Moore, J. G., 1974, Hydrofracture site proof study at Oak Ridge National Laboratory: Oak Ridge Nat. Lab., ORNL-TM-4713, 43 p.

Winograd, I. J., 1974, Radioactive waste storage in the arid zone: Am. Geophys. Union, Trans. v. 55, no. 10, p. 884-894.

Youash, Y. Y., 1965, Experimental deformation of layered rocks: Texas, Austin Univ., Ph.D. dissertation, 195 p.

Young, Allen, Low, P. F., and McLatchie, A. S., 1964, Permeability studies of argillaceous rocks: Jour. Geophys. Research, v. 69, no. 20, p. 4237-4245.

Table 1.--Injection pressure of water injection at 442 meters, October 9, 1969, West Valley, New York

Time (min)	Observed well-head pressure in MPa	Calculated bottom-hole pressure in MPa	Rate of injection in $m^3/s \times 10^{-3}$	Accumulated injection volume in m^3	Remarks
2	0.97	5.3	0	0	
20	6.48	10.81	0	0	
22	9.65	13.98	trace	trace	
23	7.65	11.91	trace	trace	
25	7.17	11.50	trace	trace	
26	7.58	11.91	trace	trace	
28	7.58	11.91	1.04		
31	7.58	11.91			
35	7.52	11.91	1.04	0.4	
39	7.72	12.05	1.89		
41	7.65	11.98			
48	7.69	12.02			
49	7.65	11.98			
53	7.58	11.91			
54	8.45	12.78			
55	8.96	13.29	1.89	2.7	
56	9.10	13.42	3.15		
57	9.65	13.98			
58	9.51	13.84			
59	10.00	14.32			
60	9.52	13.84			
62	9.65	13.98			
64	10.00	14.32	3.15	4.6	
68	10.89	15.19	6.31		
69	9.38	13.67			
70	8.55	12.84			
71	8.45	12.74		5.9	
72	8.34	12.64			
73	8.21	12.50			
75	8.17	12.43		7.5	
76	8.14	12.43			
78	8.00	12.29		9.1	
80	7.93	12.22			
82	7.86	12.16			
83	7.83	12.12		11.1	
86	7.79	12.09			
87	7.79	12.09			
89	7.79	12.09			
93	7.86	12.16			
98	7.86	12.16	6.31		
99	8.41	12.61	12.62		
101	8.41	12.61			
103	8.27	12.47		20.2	
108	8.14	12.33		24.0	

TABLE 1 (CONT.)

Time (min)	Observed well-head pressure in MPa	Calculated bottom-hole pressure in MPa	Rate of injection in $m^3/s \times 10^{-3}$	Accumulated injection volume in m^3	Remarks
113	8.07	12.27		27.8	
118	8.07	12.27		31.8	
123	8.03	12.23		35.5	
128	8.07	12.27	12.62	39.4	
133	8.48	12.33	25.23		
138	8.41	12.27	25.23		
143	7.93	12.22	6.31		
148	7.79	12.09		55.6	
150	7.79	12.09		56.3	
153	7.76	12.05		57.5	
158	7.76	12.05		59.9	
163	7.79	12.09		62.0	
164	7.79	12.09		62.2	
168	7.79	12.09	6.31	63.9	
170	8.00	12.20	12.62		
173	8.07	12.27			
181	8.07	12.27		69.9	
183	8.07	12.27		72.2	
185	8.07	12.27		73.9	
188	8.07	12.27		75.8	
193	8.07	12.27		79.6	
198	8.07	12.27		83.5	
203	8.00	12.20		87.3	
206	8.03	12.23			
208	8.03	12.23	12.62	90.6	
211	8.34	12.20	25.23		
213	8.41	12.27		95.5	
218	8.62	12.47		107.0	
223	8.69	12.54		110.0	
228	8.69	12.54			
233	8.65	12.51		125.4	
238	8.62	12.47	25.23		
241	7.79	12.09	6.31		
243	7.76	12.05		139.1	
248	7.76	12.05		140.7	
253	7.76	12.05			
258	7.76	12.05		144.3	
263	7.76	12.05			
268	7.76	12.05	6.31	148.6	
271	8.07	12.27	12.62		
273	8.07	12.27		151.8	
278	8.10	12.30			
283	8.07	12.27		160.1	
288	8.07	12.27			
293	8.10	12.30		167.9	
298	8.10	12.30	12.62	171.7	
303	8.83	12.68	25.23		

TABLE 1 (CONT.)

Time (min)	Observed well-head pressure in MPa	Calculated bottom-hole pressure in MPa	Rate of injection in $m^3/s \times 10^{-3}$	Accumulated injection volume in m^3	Remarks
305	8.96	12.82			
308	8.89	12.75		185.8	
313	8.79	12.64			
318	8.76	12.61		202.4	
323	8.79	12.64			
328	8.79	12.64		219.1	
331	8.76	12.61	25.23	223.7	
					45-minute pause, injection stopped at 331 minutes
332	8.72	12.05	0		
333	7.65	11.98			
334	7.58	11.91			
335	7.55	11.88			
336	7.52	11.85			
337	7.48	11.81			
338	7.46	11.79			
339	7.45	11.78			
340	7.41	11.74			
341	7.38	11.71			
342	7.38	11.71			
343	7.35	11.68			
348	7.27	11.60			
353	7.21	11.53			
358	7.16	11.49			
363	7.10	11.43			
368	7.07	11.40			
373	7.02	11.35			
376	7.00	11.33	0		
					Injection restarted at 379 minutes
379	11.51	15.37	25.23		
380	10.69	14.54		226.2	
381	10.20	14.06		227.8	
383	9.72	13.58		230.8	
388	9.45	13.30		238.6	
393	9.31	13.16		246.4	
398	9.31	13.16		254.4	
403	9.21	13.06		262.6	
406	9.21	13.06			
408	9.17	13.02	25.23	270.6	
411	7.96	12.26	6.31		
413	7.89	12.19		274.7	
418	7.86	12.16			
423	7.86	12.16		278.8	
428	7.86	12.16		280.9	
433	7.86	12.16			
438	7.86	12.16	6.31	284.6	

TABLE 1 (CONT.)

Time (min)	Observed well-head pressure in MPa	Calculated bottom-hole pressure in MPa	Rate of injection in $m^3/s \times 10^{-3}$	Accumulated injection volume in m^3	Remarks
441	8.62	12.82	12.62		
443	8.69	12.89			
448	8.69	12.89			
453	8.69	12.89		295.2	
458	8.69	12.89			
463	8.69	12.89		303.2	
468	8.72	12.92	12.62		
471	10.00	13.85	25.23		
473	9.79	13.64		311.4	
476	9.65	13.51			
478	9.51	13.37		319.2	
483	9.45	13.30			
488	9.38	13.23		334.9	
493	9.38	13.23		343.2	
498	9.38	13.23	25.23	351.3	
501	7.93	12.22	6.31		
503	7.93	12.22			
508	7.93	12.22		358.8	
513	7.86	12.16			
518	7.86	12.16		362.6	
523	7.93	12.22		364.4	
528	7.93	12.22	6.31	366.3	
531	8.83	13.02	12.62		
533	8.83	13.02		368.7	
538	8.79	12.99			
543	8.79	12.99		376.6	
548	8.83	12.99		380.7	
553	8.83	12.99			
558	8.89	12.99	12.62	388.5	
561	10.14	13.99	25.23		
563	10.07	13.92		394.1	
568	9.72	13.58			
573	9.72	13.58		409.5	
578	9.65	13.51		415.7	
583	9.58	13.44		432.7	
586	9.52	13.37	25.23	428.4	
588				432.6	End of injection

Calculated bottom-hole pressure (for injection) = observed well-head pressure + static pressure in casing - frictional loss in injection pipe.

Calculated bottom-hole pressure (for pressure decay) = observed well-head pressure + static pressure in casing.

Table 2.--Pressure decay of water injection at 442 meters, October 9, 1969, West Valley, New York

Time since end of injection (min)	Observed well-head pressure in MPa	Calculated bottom-hole pressure (P) in MPa	$(P-p_o)$ in MPa
0	7.65	11.98	7.89
1	7.58	11.91	7.82
2	7.52	11.85	7.76
3	7.48	11.81	7.72
4	7.46	11.79	7.70
5	7.46	11.79	7.70
10	7.32	11.65	7.56
15	7.25	11.58	7.49
20	7.21	11.53	7.44
25	7.17	11.50	7.41
30	7.15	11.48	7.39
45	7.07	11.40	7.31
60	6.99	11.32	7.23
75	6.94	11.27	7.18
90	6.89	11.22	7.13
105	6.85	11.18	7.09
120	6.82	11.15	7.06
135	6.78	11.11	7.02
165	6.72	11.05	6.96
195	6.67	11.00	6.91
225	6.63	10.96	6.87
255	6.61	10.93	6.84
285	6.59	10.92	6.83
315	6.56	10.89	6.80
345	6.54	10.87	6.78
375	6.49	10.82	6.73
405	6.46	10.79	6.70
435	6.42	10.75	6.66
465	6.39	10.72	6.63
495	6.34	10.67	6.58
525	6.30	10.63	6.54
555	6.27	10.60	6.51
585	6.23	10.56	6.47
615	6.19	10.52	6.43
645	6.16	10.49	6.40
705	6.09	10.42	6.33
735	6.05	10.38	6.29
765	6.01	10.34	6.25
795	5.97	10.30	6.21
825	5.94	10.27	6.18
885	5.87	10.20	6.11
915	5.83	10.16	6.07
945	5.79	10.12	6.03

TABLE 2 (CONT.)

Time since end of injection (min)	Observed well-head pressure in MPa	Calculated bottom-hole pressure (P) in MPa	$(P-p_o)$ in MPa
1,005	5.73	10.06	5.97
1,185	5.56	9.89	5.80
1,305	5.45	9.78	5.69
1,575	5.29	9.62	5.53
2,205	5.03	9.36	5.27
2,415	4.98	9.31	5.22
2,625	4.93	9.26	5.17
2,985	4.83	9.16	5.07
3,705	4.67	9.00	4.91
3,930	4.62	8.95	4.86
4,295	4.53	8.86	4.77
5,065	4.41	8.74	4.65
5,775	4.27	8.60	4.51
6,585	4.15	8.48	4.39
7,185	4.07	8.40	4.31
7,995	3.96	8.29	4.20
8,745	3.88	8.21	4.12
9,465	3.79	8.12	4.03
10,065	3.73	8.06	3.97
10,905	3.66	7.99	3.88
11,265	3.63	7.96	3.87

Static ground water pressure at injection level (p_o) = 4.09 MPa

Table 3.--Injection pressure of water injection at 442 meters, June 26, 1970, West Valley, New York

Time (min)	Observed well-head pressure in MPa	Calculated bottom-hole pressure in MPa	Rate of injection in $m^3/s \times 10^{-3}$	Accumulated injection volume in m^3	Remarks
1	6.21	10.54	very slow		
2	7.86	12.19	"		
3	7.93	12.26	"		
4	8.07	12.40	"	0.4	
8	8.27	12.60	"		
10	8.76	13.09	rate increased		
11	11.38	15.71	"		
13	11.72	16.05	"		To fix leaks
36	11.03	15.36	"		
37	11.72	16.05			
38	13.24	17.58	2.14	2.8	
43	12.13	16.46			Start isotope
50	11.72	16.04		3.7	
55	12.27	16.60		4.5	
62	13.24	17.56		5.5	
73	13.24	17.56		7.1	
88	12.41	16.73		9.4	
98	14.13	18.46	2.14	10.8	
110	15.86		rate increased		
113	19.99	24.24	10.09	14.2	
115	13.10	17.35	10.60	15.4	
118	19.31	23.53	11.92	17.1	
120	19.17	23.37	13.25	18.1	
124	17.24	21.43	13.75	22.2	
132	18.27	22.48	13.25	26.9	
142	17.93	22.03	18.04	32.6	
153	12.41	16.74	0	42.9	
156	7.75	12.09	0	42.9	
168	17.24	21.34	18.04	53.0	
183	16.55	20.65		70.5	
191	13.79	17.89		78.5	
202	14.48	18.58		89.7	
208	15.17	19.27		96.1	
220	14.48	18.58		109.0	
234	14.48	18.58		122.8	
246	15.17	19.27	18.04	135.8	
263	14.48	18.57	18.55	154.2	
276	13.79	17.89	18.04	158.0	
298	14.13	18.24		179.5	
313	13.79	17.89		194.8	
325	13.79	17.89	18.04	208.2	

TABLE 3 (CONT.)

Time (min)	Observed well-head pressure in MPa	Calculated bottom-hole pressure in MPa	Rate of injection in $m^3/s \times 10^{-3}$	Accumulated injection volume in m^3	Remarks
333	13.79	17.89	18.04		
343	13.79	17.89	18.04	226.7	
363	13.79	17.91	17.47	246.8	
378	13.79	17.91		261.9	
393	13.44	17.56		277.4	
411	13.44	17.56	17.47	294.9	
421	12.41	16.60	13.75	303.2	
423	13.10	17.20	18.04	305.1	
438	13.10	17.20		320.6	
458	13.10	17.20		337.6	
468	13.10	17.20	18.04	346.7	
483	13.10	17.20	18.55	363.0	
498	12.41	16.63	12.43	375.9	
515	12.41	16.63	12.43	388.3	
528	12.41	16.64	11.92	397.6	End of isotope injection
543	12.41	16.64	11.67	408.4	
558	12.41	16.64	11.67	416.7	
569	12.41	16.65	11.10	424.9	End of injection

Table 4.--Pressure decay of water injection at 442 meters, June 26, 1970, West Valley, New York

Time since end of injection (min)	Observed well-head pressure in MPa	Calculated bottom-hole pressure in MPa	$(P-p_o)$ in MPa
1	8.96	13.29	9.20
2	7.79	12.12	8.03
3	7.65	11.98	7.89
4	7.58	11.91	7.82
5	7.52	11.85	7.76
6	7.45	11.78	7.69
7	7.45	11.78	7.69
8	7.38	11.71	7.62
9	7.38	11.71	7.62
10	7.34	11.67	7.58
12	7.31	11.64	7.55
13	7.31	11.64	7.55
14	7.27	11.60	7.51
15	7.24	11.57	7.48
18	7.17	11.50	7.41
20	7.17	11.50	7.41
24	7.12	11.45	7.36
29	7.10	11.43	7.34
34	7.03	11.36	7.27
39	7.00	11.33	7.24
44	7.00	11.33	7.24
49	6.95	11.28	7.19
54	6.93	11.26	7.17
64	6.89	11.22	7.13
79	6.86	11.19	7.10
94	6.83	11.16	7.07
109	6.79	11.12	7.03
124	6.76	11.09	7.00
139	6.72	11.05	6.96
169	6.69	11.02	6.93
199	6.62	10.95	6.86
229	6.58	10.91	6.82
259	6.55	10.88	6.79
299	6.48	10.81	6.72
319	6.48	10.81	6.72
349	6.45	10.78	6.69
379	6.41	10.74	6.65
439	6.38	10.71	6.62
469	6.34	10.67	6.58
499	6.31	10.64	6.55
529	6.27	10.60	6.51

TABLE 4 (CONT.)

Time since end of injection (min)	Observed well-head pressure in MPa	Calculated bottom-hole pressure in MPa	$(P-p_o)$ in MPa
559	6.24	10.57	6.48
589	6.21	10.54	6.45
619	6.21	10.54	6.45
649	6.17	10.50	6.41
679	6.17	10.50	6.41
709	6.17	10.50	6.41
739	6.17	10.50	6.41
799	6.14	10.47	6.38
859	6.10	10.43	6.34
987	6.03	10.36	6.27
1,024	6.00	10.33	6.24
1,039	6.00	10.33	6.24
1,219	5.93	10.26	6.17
1,399	5.86	10.19	6.10
1,639	5.72	10.05	5.96
2,269	5.47	9.80	5.71
2,359	5.45	9.78	5.68
2,419	5.43	9.76	5.67
2,479	5.40	9.73	5.64
2,584	5.38	9.71	5.62
2,629	5.38	9.71	5.62
2,689	5.34	9.67	5.58
2,749	5.32	9.65	5.56
2,809	5.31	9.64	5.55
2,839	5.31	9.64	5.55
3,079	5.24	9.57	5.48
3,509	5.09	9.42	5.33
3,769	5.03	9.36	5.27
3,979	4.98	9.31	5.22
4,234	4.92	9.25	5.16
4,489	4.87	9.20	5.11
5,164	4.76	9.09	5.00
5,389	4.74	9.07	4.98
5,899	4.70	9.03	4.94
6,619	4.60	8.93	4.84
6,799	4.60	8.93	4.84
7,339	4.54	8.87	4.78
7,999	4.48	8.81	4.72
8,359	4.45	8.78	4.69
8,839	4.40	8.73	4.64
9,469	4.35	8.68	4.59
10,219	4.30	8.63	4.54
10,969	4.27	8.60	4.51
11,134	4.23	8.56	4.47
11,629	4.19	8.52	4.43

TABLE 4 (CONT.)

Time since end of injection (min)	Observed well-head pressure in MPa	Calculated bottom-hole pressure in MPa	$(P-p_o)$ in MPa
12,439	4.14	8.47	4.38
13,039	4.10	8.43	4.34
13,729	4.03	8.36	4.27
14,269	4.03	8.36	4.27
14,509	4.02	8.35	4.26
15,589	3.99	8.32	4.23
16,819	3.90	8.23	4.23
18,274	3.82	8.15	4.06

Static ground water pressure at injection level (p_o) = 4.09 MPa

Table 5.--Injection pressure of water injection at 152 meters, May 29, 1971, West Valley, New York

Time (min)	Observed well-head pressure in MPa	Calculated bottom-hole pressure in MPa	Rate of injection in $m^3/s \times 10^{-3}$	Accumulated injection volume in m^3	Remarks
0	2.76	4.25	0	0	
3	2.69	4.19	0.69	0.4	
5	2.62	4.12	3.09	0.8	
10	2.52	4.01	1.96	1.4	
15	2.45	3.94		2.0	
20	2.41	3.91	1.96	2.6	
25	2.38	3.88	2.02	3.2	
30	2.38	3.88		3.8	
35	2.38	3.88		4.4	
40	2.38	3.88		5.0	
45	2.38	3.88		5.6	
50	2.38	3.88		6.2	
55	2.38	3.88	2.02	6.8	
60	2.38	3.88	2.08	7.4	
65	2.45	3.94	3.09	8.4	
70	2.45	3.94	3.47	9.4	
75	2.48	3.96	3.85	10.6	
80	2.48	3.96	4.79	12.0	
85	2.48	3.96	5.17	13.6	
90	2.48	3.96	6.18	15.4	
95	2.48	3.96	7.44	17.6	
100	2.48	3.96	7.26	19.8	
105	2.52	3.99	8.71	22.4	
110	2.52	3.99	9.34	25.2	
115	2.52	3.99	10.41	28.4	
121	2.55	4.01	11.23	32.4	
125	2.55	4.01	11.99	35.3	
130	2.59	4.04	13.12	39.2	
135	2.92	4.34	17.54	44.5	
140	2.92	4.24	25.74	52.2	
145	2.92	4.25	26.37	60.1	
150	2.92	4.25	26.50	68.1	
155	2.92	4.25	26.87	76.1	
160	2.92	4.25	27.00	84.2	
165	2.90	4.22	27.63	92.5	
170	2.85	4.17	27.63	100.8	
175	2.83	4.14	27.88	109.2	
185	2.83	4.14	28.32	126.2	
190	2.85	4.16	28.14	134.6	
195	2.85	4.16	28.51	143.2	
200	2.85	4.16	28.51	151.7	
205	2.85	4.16	28.64	160.3	
210	2.85	4.16	28.39	168.8	
215	2.85	4.16	28.89	177.5	
220	2.84	4.15	28.51	186.0	
225	2.84	4.15	28.51	195.0	End of injection

Table 6.--Pressure decay of water injection at 152 meters, May 29, 1971, West Valley, New York

Time since end of injection (min)	Observed well-head pressure in MPa	Calculated bottom-hole pressure (P) in MPa	$(P-p_o)$ in MPa
0	2.30	3.80	2.55
1	2.25	3.74	2.49
2	2.21	3.71	2.46
3	2.19	3.68	2.43
4	2.17	3.66	2.41
5	2.15	3.65	2.40
6	2.14	3.63	2.38
7	2.12	3.62	2.37
8	2.11	3.61	2.36
9	2.10	3.59	2.34
10	2.09	3.58	2.33
15	2.03	3.53	2.28
20	1.98	3.47	2.22
25	1.93	3.42	2.17
30	1.89	3.38	2.13
35	1.84	3.34	2.09
40	1.81	3.31	2.06
45	1.77	3.26	2.01
50	1.73	3.23	1.98
55	1.70	3.20	1.95
60	1.67	3.16	1.91
65	1.63	3.13	1.88
70	1.60	3.09	1.84
75	1.57	3.06	1.81
80	1.54	3.04	1.79
85	1.51	3.01	1.76
90	1.49	2.99	1.74
100	1.45	2.94	1.69
110	1.40	2.90	1.65
120	1.37	2.86	1.61
130	1.33	2.83	1.58
140	1.31	2.80	1.55
155	1.26	2.76	1.51
170	1.23	2.73	1.48
185	1.20	2.70	1.45
200	1.17	2.67	1.42
215	1.15	2.65	1.40
230	1.13	2.63	1.38
245	1.11	2.60	1.35
260	1.09	2.59	1.34
275	1.07	2.56	1.31
290	1.05	2.55	1.30

TABLE 6 (CONT.)

Time since end of injection (min)	Observed well-head pressure in MPa	Calculated bottom-hole pressure (P) in MPa	$(P-p_o)$ in MPa
230	1.03	2.52	1.27
350	1.01	2.50	1.25
380	0.99	2.48	1.23
410	0.97	2.46	1.21
440	0.94	2.44	1.19
470	0.93	2.43	1.18
500	0.91	2.41	1.16
530	0.90	2.39	1.14
560	0.88	2.38	1.13
590	0.88	2.37	1.12
620	0.87	2.36	1.11
650	0.86	2.36	1.11
680	0.85	2.34	1.09
710	0.84	2.34	1.09
740	0.83	2.33	1.08
770	0.83	2.32	1.07
800	0.82	2.31	1.06
830	0.81	2.31	1.06
860	0.80	2.30	1.05
890	0.80	2.30	1.05
920	0.79	2.29	1.04
950	0.79	2.28	1.03
980	0.78	2.28	1.03
1,010	0.77	2.27	1.02
1.040	0.77	2.26	1.01

Static ground water pressure at injection level (p_o) = 1.25 MPa

Table 7.--Injection pressure of grout injection at 152 meters, July 23, 1971, West Valley, New York

Time (min)	Observed well-head pressure in MPa	Calculated bottom-hole pressure in MPa	Rate of injection in $m^3/s \times 10^{-3}$	Accumulated injection volume in m^3	Remarks
0	0.28	1.77	0.32		Water
3	2.07	3.56			
4	2.38	3.87	0.32		
5	2.45	3.94	0.63		
10	2.21	3.70	0.32		
15	2.52	4.01	0.95		
22	2.59	4.08	0.95	0.1	
25	2.55	4.05	1.14	0.3	
30	2.52	4.01	1.14	0.6	Start isotope
45	2.48	3.97	2.93	3.3	
50	2.55	4.04	2.12	3.9	
55	2.55	4.04	2.73	4.7	
60	2.55	4.04	2.78	5.5	
65	2.55	4.04	2.78	6.4	
70	2.55	4.04	2.84	7.2	
75	2.55	4.04	3.41	8.3	
80	2.55	4.04	3.41	8.9	Start cement and bentonite
85	2.17	4.05	2.90	9.8	Grout (average) density= 1.44 g/cm^3
90	2.17	4.05	2.52	10.5	
95	2.38	4.25	2.84	11.4	
100	2.28	4.16	2.46	12.1	
105	2.21	4.07	4.54	13.5	
110	2.21	4.07	3.66	14.6	
115	2.31	4.17	5.36	16.2	
120	2.14	4.00	4.98	17.7	
125	2.21	4.07	6.43	19.6	
130	2.28	4.14	5.80	21.3	
135	2.55	4.41	8.20	23.8	
140	2.55	4.41	8.96	26.5	
145	2.62	4.47	9.08	29.2	
150	2.55	4.41	8.77	31.9	
155	2.41	4.27	9.59	34.7	
160	2.21	4.05	9.78	37.7	
165	2.34	4.19	10.72	40.9	
170	2.28	4.12	11.54	44.3	
175	2.28	4.12	13.69	48.4	
180	2.28	4.12	12.36	52.2	
185	2.38	4.21	14.64	56.5	
190	2.41	4.25	14.89	61.0	
195	2.41	4.25	15.90	65.8	

TABLE 7 (CONT.)

Time (min)	Observed well-head pressure in MPa	Calculated bottom-hole pressure in MPa	Rate of injection in $m^3/s \times 10^{-3}$	Accumulated injection volume in m^3	Remarks
201	2.34	4.18	14.95	71.2	
205	2.34	4.18	17.22	75.3	
210	2.34	4.18	15.90	80.1	
215	2.28	4.11	16.02	84.9	
220	2.14	3.98	15.01	89.4	
225	2.21	4.04	15.65	94.1	
230	2.21	4.04	15.52	98.7	
235	2.14	3.97	15.65	103.4	
245	2.10	3.94	15.96	113.0	
260	2.14	3.97	15.65	127.0	
265	2.14	3.97	15.52	131.7	
275	2.07	3.90	16.60	141.3	End of isotope injection
280	2.07	3.90	15.90	146.0	Water
290	2.07	3.90	15.27	155.2	End of injection

Table 8.--Ground elevation affected by grout injection at 152 meters, July 23, 1971, West Valley, New York

Bench mark	Distance from injection well (m)	Altitude of benchmark (m)		Uplift (mm)
		before injection	after injection	
A1	16.89	423.95586	423.95763	1.77
A2	51.08	416.85725	416.85871	1.46
B1	7.59	423.56822	423.57007	1.86
B2	15.30	423.65289	423.65469	1.80
B3	30.36	422.64138	422.64266	1.28
B4	68.34	419.50151	419.50276	1.25
B5	92.08	424.90601	424.90702	1.01
B6	159.11	428.23041	428.23114	0.73
B7	250.12	434.91805	434.91878	0.73
B8	340.58	449.27322	449.27383	0.61
B9	430.19	468.33834	468.33940	1.07
C1	37.73	424.60810	424.60978	1.68
D1	7.65	423.81577	423.81751	1.74
D2	22.95	423.89557	423.89719	1.62
D3	60.84	423.05368	423.05515	1.46
D4	92.84	423.80447	423.80514	0.67
D5	153.71	422.60438	422.60514	0.76
D6	245.39	423.14275	423.14311	0.37
D7	336.74	424.93817	424.93863	0.46
D8	428.21	427.21890	427.21926	0.37
D9	488.41	428.61936	428.61994	0.58
E1	7.62	423.57760	423.57919	1.59
E2	30.51	423.90603	423.90773	1.71
E3	60.93	423.88317	423.88490	1.74
E4	91.41	423.79273	423.79441	1.68
E5	152.40	424.59713	424.59835	1.22
E6	243.81	425.00410	425.00468	0.58
E8	315.16	426.36396	426.36396	0
E9	399.29	426.36811	426.36799	-0.12
E10	490.73	427.64775	427.64729	-0.46
E11	593.14	425.99863	425.99814	-0.49
E12	688.85	429.60950	429.60914	-0.37
F1	7.59	423.41191	423.41374	1.83
F2	15.24	423.38692	423.38884	1.92
F3	68.55	424.10131	424.10277	1.46
F4	144.72	425.59922	425.60029	1.07
F5	227.62	424.28053	424.28157	1.04

TABLE 8 (CONT.)

Bench mark	Distance from injection well (m)	Altitude of benchmark (m)		Uplift (mm)
		before injection	after injection	
G1	7.68	423.30758	423.30947	1.89
G2	38.04	423.77731	423.77914	1.83
G3	76.23	423.50271	423.50424	1.52
G4	152.46	424.83265	424.83384	1.19
G5	243.84	423.47092	423.47175	0.82
G6	676.66	421.84518	421.84564	0.46
H1	7.65	423.39116	423.39314	1.98
H2	23.07	422.82359	422.82554	1.95
H3	60.81	423.14147	423.14342	1.95
H4	91.17	423.28265	423.28448	1.83
H5	160.57	422.48252	422.48371	1.19
H6	253.99	422.82039	422.82121	0.82
H7	341.86	423.10218	423.10285	0.67
H8	746.76	421.03304	421.03292	-0.12
J1	7.62	423.40996	423.41182	1.86
J2	15.24	423.22903	423.23092	1.89
J3	33.50	420.21697	420.21874	1.77
J4	90.28	423.95431	423.95549	1.19
J5	157.67	423.00427	423.00540	1.13
J6	242.19	424.31345	424.31458	1.13
J7	333.18	427.78747	427.78875	1.28
J8	424.83	429.44055	429.44165	1.10

Table 9.--Instantaneous shut-in pressure, calculated overburden pressure, tensile strength of shale, average cohesive force at fracture tip and value of f, West Valley, New York.

Injection No.	Injection Date	Injection Depth (m)	Injection fluid	Total injection volume m^3	Calculated overburden pressure MPa		Instantaneous shut-in pressure MPa		Calculated tensile strength MPa	Calculated average coehsive force at fracture tip (fT) MPa	Value of f	Remarks
					by specific gravity	by pressure decay data	observed	predicted				
1	10/9 1969	442	Water	433	10.90	10.84	12.05	11.96	3.09	1.06	0.34	Before 45-minute pause
							11.98	11.96	3.92	1.06	0.27	After 45-minute pause
2	6/26 1970	442	Water	425	10.40	10.43	13.29	15.20	3.87	1.78	0.46	
3	8/27 1970	374	Water	343	9.16	9.49	9.87	9.89	4.15	0.73	0.18	
4	5/10 1971	308	Water	374	7.48	7.36	8.06	Regression equation has not been established	3.12	0.58	0.19	
5	5/29 1971	152	Water	195	3.52	3.10	3.80	3.88	0.73	0.36	0.49	
6	7/23 1971	152	Water and Grout	9-water 142-grout	3.52	--	Did not observe	4.00	0.76-0.83	0.48	0.58-0.63	

Average cohesive forces at fracture tip (fT) are calculated on basis of the regression equations of P and Q. The values of (fT) calculated on basis of the observed instantaneous shut-in pressures are essentially the same as those based on the regression equations.

Table 10.--Approximate waste composition produced at Oak Ridge National Laboratory, Tennessee (data from de Laguna and others, 1971; Weeren, 1976; ERDA, 1977)

NaOH	0.05 - 0.7 M (moles/liter)
$Al(NO_3)_3 \cdot 9H_2O$	0.005 - 0.04 M
NH_4NO_3	0.003 - 0.06 M
$NaNO_3$	0.1 - 1.0 M
Na_2SO_4	0.09 - 0.2 M
NaCl	0.04 - 0.2 M
Na_2CO_3	0.01 - 0.2 M
$Al_2(SO_4)_3$	0.005 - 0.2 M
$(NH_4)_2SO_4$	0.01 - 0.2 M
Cs^{137}	0.3 Ci/l
Sr^{90}	0.03 Ci/l
Cm^{244}	0.3 mCi/l
Long lived radionuclides (half life > 30 yrs)	< 10nCi/g

Table 11.--Radioactive waste injected in Pumpkin Valley shale, Oak Ridge National Laboratory, Tennessee, 1964-1978

	Name of injection	Injection date	Injection depth (m)	Injection altitude (m)(msl)	Waste injected (m^3)	Grout volume (m^3)	Solids/liquid (kg/m^3)	Radionuclides (Ci, except Pu^{239} and Cm^{244} in g)								Data source
								Sr^{90}	Cs^{137}	Ru^{106}	Co^{60}	Ce^{144}	Au^{198}	Pu^{239}	Cm^{244}	Remarks	
Test Injection	1	02/13/64	288.0	-46.7	141.2	152.8	75.2									Synthetic waste	delaguna and others, 1968; 1971
	2	02/20-21/64	281.6	-40.3	107.1	143.0	813.0						30			Synthetic waste	
	3	04/08/64	278.0	-36.6	126.8	247.2	1565.5	4.9	74	0.4	0.1						
	4	04/17/64	274.3	-33.0	135.9	217.5	1329.8	0.9	50	1.2	0.1						
	5	05/28/64	271.3	-29.9	558.7	799.7	942.0	608	193	35	4	4099					
	6A	05/19/65	268.2	-26.9	16.7	21.5	454.8	Activity merged in 6B								Stopped due to difficult mixing	
	6B	05/22/65	265.8	-24.4	242.2	351.2	719.0	330	1562	2	1						
	7	08/16/65	265.8	-24.4	263.3	467.1	828.7	492	3358	2	14						
Operational Injection	ILW-1A	12/12/66	265.8	-24.4	141.7	208.2	744.7	41	11500	1	16	20	NA	NA			
	ILW-1B	12/13/66	265.8	-24.4	98.4	152.1	742.4	38	7600	8	3	13					
	ILW-2A	04/20/67	262.7	-21.4	308.1	461.0	718.5	564	31329	99	236						
	ILW-2B	04/24/67	262.7	-21.4	243.5	411.0	773.4	474	26350	83	199		NA	NA			
	ILW-3A	11/28/67	262.7	-21.4	117.3	555.5	659.1	9000	17000	400	200		NA	NA			delaguna and others, 1971
	ILW-3B	11/29/67	262.7	-21.4	196.8												
	Water test	12/13/67	259.7	-18.3		169.2											
	ILW-4A	04/03/68	259.7	-18.3	90.9	494.6	611.2	4300	51900	200				17.8	NA		
	ILW-4B	04/04/68	259.7	-18.3	235.4												
	ILW-5	10/30/68	256.6	-15.3	309.6	435.9	671.1	500	69400	300	100			18.5	NA		
	ILW-6	06/11/69	256.6	-15.3	300.3	478.2	647.1	8900	89000	100	200			3.9	NA		
	ILW-7	09/23/70	256.6	-15.3	314.2	551.4	659.1	2747	44833	236	72			28.6	0.23		
	ILW-8	09/29/72	253.6	-12.3	275.2	411.1	874.8	45	27917	2523				2.13	0.002		Weeren 1974
	ILW-9	10/17/72	253.6	-12.3	258.5	431.5	934.7	231	23359	376				None	0.068		
	ILW-10	11/08/72	253.6	-12.3	320.8	503.3	850.9	1331	18817	593				None	0.346		
	ILW-11	12/05/72	253.6	-12.3	286.8	495.0	862.8	1099	23486	379				None	1.791		
	ILW-12	01/24/75	250.5	- 9.2	97.3	159.3	791.0	1324	12752					None	0.012		Weeren 1976
	ILW-13	04/29/75	250.5	- 9.2	306.6	477.3	755.0	3368	35750					0.49	0.214		
	ILW-14	06/20/75	250.5	- 9.2	314.0	525.0	802.9	2874	30592					None	0.043		
	ILW-15	06/30/75	250.5	- 9.2	344.4	549.0	503.3	138.3	26390					10.75	None		Weeren, written commun., 1979
	ILW-16	11/17/77	247.5	- 6.2	208.9	300.9	862.8	1618	14964					None	None		
	ILW-17	09/01/78	244.4	- 3.1	311.5	520.4	838.9	90	22270					1.19	0.027		
	Total				6672.1	10689.9		40118.1	590446	5338.6	1045.2	4132	30	83.35	2.733		
Total radioactivity								641,342.7 curies									

NA = not analyzed

Table 12.--Physical properties of grout, injection pressure, calculated grout radius and maximum fracture separation, September 1960, Oak Ridge National Laboratory, Tennessee

Injection date	September 3	September 10
Injection depth, m	285	212
Inside diameter of injection casing, mm	104	104
Injection rate, m^3/s	0.009	0.016
Injection volume, m^3	346	503
Well-head breakdown pressure, MPa	15.89	15.20
Well-head injection pressure, MPa	12.75	14.91
Bottom-hole injection pressure, MPa	16.28	17.56
Calculated overburden pressure, MPa	13.58	10.10
Assumed Young's modulus, MPa	18,000	18,000
Assumed Poison ratio	0.1	0.1
Density of fluid, Kg/m^3	1.38×10^3	1.44×10^3
n'	0.109	0.065
K', newton-$sec^{n'}/m^2$	16.04	29.69
Calculated grout radius, m	77	65
Calculated maximum fracture separation, mm	29	62
Observed grout thickness, mm	8	12

Table 13.--Chemical composition of waste disposed of by injections, September-December, 1972, Oak Ridge National Laboratory, Tennessee (from Weeren, 1974)

Constituent	Composition, moles/liter			
	Tank			
	1	2	3	4
Na^{+}	1.66	1.24	0.57	0.59
Al^{3+}	0.007	0.037	0.002	0.0011
NH_4^{+}	0.003	0.03	0.044	0.05
OH^{-}	0.13	0.28	0.15	0.16
NO_3^{-}	0.84	1.03	0.30	0.30
Cl^{-}	0.093	0.217	0.049	0.044
SO_4^{2-}	0.094	0.183	0.111	0.125
CO_3^{2-}	0.193	0.288	0.093	0.10

Table 14.--Major radionuclides contained in wastes disposed of by injections, September-December 1972, Oak Ridge National Laboratory, Tennessee (from Weeren, 1974)

Radionuclides	Specific Activity, Ci/ℓ			
	Injection number			
	ILW-8	ILW-9	ILW-10	ILW-11
Sr^{90}	1.65×10^{-4}	8.93×10^{-4}	4.15×10^{-3}	3.83×10^{-3}
Cs^{137}	1.01×10^{-1}	9.04×10^{-2}	5.87×10^{-2}	8.19×10^{-2}
Ru^{106}	9.17×10^{-3}	1.45×10^{-3}	1.85×10^{-3}	1.32×10^{-3}
Cm^{244}	6.74×10^{-7}	2.18×10^{-5}	8.98×10^{-5}	5.20×10^{-4}
Pu	4.76×10^{-7}	none	none	none

Table 15.--Bleedback from injections, September-December 1972, Oak Ridge National Laboratory, Tennessee (from Weeren, 1974)

Injection No.	Injection date	Well-head valve open date	Days after injection	Well-head pressure at valve opening MPa	Initial flow rate m^3/s	Final flow rate m^3/s	Recovered volume m^3	Remarks
ILW-8	9/29/72	10/9/72	10	1.69	1.16×10^{-5}	6.52×10^{-6}	4.4	
ILW-9	10/17/72	10/27/72	10	2.14	1.26×10^{-4}	7.57×10^{-5}	12.8	Valve closed again
ILW-10	11/08/72	11/20/72	12	1.41	4.99×10^{-4}	4.10×10^{-4}	2.5	
		11/30/72	22	1.03	2.71×10^{-4}	2.33×10^{-4}	2.2	
ILW-11	12/05/72	12/14/72	9	1.69	3.22×10^{-4}	--	2.16	Valve closed again
		12/29/72	24	1.17	1.70×10^{-4}	--	1.6	Valve closed again
		01/19/73	45	0.97	1.01×10^{-4}	--	1.1	Valve closed again
		04/04/73	120	0.57	4.73×10^{-5}	5.99×10^{-7}	43.9	Measured at 04/22/73

Table 16.--Radionuclides in bleedback solution, September-December 1972, Oak Ridge National Laboratory, Tennessee (from Weeren, 1974)

	Specific activity, Ci/ℓ			
	Injection number			
	ILW-8	ILW-9	ILW-10	ILW-11
Gross α	$<4.5\times10^{-9}$	4.0×10^{-8}	Not analyzed	1.5×10^{-8}
Sr^{90}	9.8×10^{-5}	4.8×10^{-5}	1.4×10^{-4}	1.5×10^{-4}
Cs^{137}	--	5.5×10^{-4}	--	6.6×10^{-4}
Ru^{106}	Not analyzed	6.9×10^{-4}	Not analyzed	Not analyzed
Cs^{134}	Not analyzed	8.5×10^{-6}	Not analyzed	Not analyzed
Co^{60}	Not analyzed	6.6×10^{-6}	Not analyzed	Not analyzed
Na	24 mg/mℓ	--	22 mg/mℓ	35.3 mg/mℓ
pH	12.3	12.6	11.4	10.0

Table 17.--Altitude of grout sheet determined from gamma-ray logs made in observation wells, September-December 1972, Oak Ridge National Laboratory, Tennessee (from Weeren, 1974)

Observation well	Altitude (m), msl			
	Injection number			
	ILW-8	ILW-9	ILW-10	ILW-11
Injection altitude	-12	-12	-12	-12
W 300	Not found	-12 to -14	-3 to -6	Not found
NW 100	-5	Not found	+14	+9
N 100	Not found	Not found	+12	+7 to +12
N 150	Not found	-10	+5 to +7	+3 to +5
NE 125	Not found	Not found	+4 to +10	-2 to +4
E 320	Not found	Not found	Not found	Not found
S 100	-14 to -16	-16	Not found	-7
S 220	Not found	Not found	Not found	Not found

Table 18.--Pressure observed in rock cover wells and results of gamma-ray logs, September-December 1972, Oak Ridge National Laboratory, Tennessee (from Weeren, 1974)

Injection number	Result of gamma-ray log		Pressure in rock cover well		
	Positive	Negative	Positive	Negative	Ambiguous (no clear sign of positive or negative)
ILW-8	NW 100 S 100	W 300 N 100 N 150 NE 125 E 320 S 220	NW 175 NW 250 NE 125	N 275 N 200 NE 200	W 300 S 200 E 300
ILW-9	W 300 N 150 S 100	NW 100 N 100 NE 125 E 320 S 220	NE 125 NE 200 S 200	E 300 N 200 N 275 NW 250	W 300 NW 175
ILW-10	W 300 NW 100 N 150 N 100 NE 125	E 320 S 100 S 220	NW 175 N 275 N 200 NE 125 NE 200	W 300 S 200 E 300	NW 250
ILW-11	NW 100 N 150 N 100 NE 125 S 100	W 300 E 320 S 220	NW 175 N 200 NE 125 NE 200	NW 250 W 300 S 200 N 275 E 300	

Table 19.--Coordinates and altitude of wells at proposed disposal site, Oak Ridge National Laboratory, Tennessee

Well	Oak Ridge National Laboratory coordinates		Altitude (m) msl
	N	E	
Injection well at present fracturing site	17,155	28,617	241.3
Injection well at proposed disposal site	16,503	28,179	240.3
Old East-observation well	16,503	28,378	240.2
New East-observation well	16,445	28,307	241.3
South-observation well	16,304	28,179	243.6
West-observation well	16,502	27,978	238.5
North-observation well	16,702	28,172	235.1

Table. 20.--Observed and calculated data from deviation survey made in injection well at proposed disposal site, Oak Ridge National Laboratory, Tennessee

Measured depth (m)	Course length MD (m)	Vertical deviation angle α	Vertical depth (m)		Horizontal displacement H (m)	Magnetic bearing β	y (m)		x (m)		Total (m)			
											Y		X	
			Z	Total			N	S	E	W	N	S	E	W
30.48	30.48	1°45'	30.47	30.47	0.93	N30W	0.81			0.47	0.81			0.47
60.96	30.48	4°	30.41	60.88	2.13	N40W	1.63			1.37	2.44			1.84
91.44	30.48	8°	30.18	91.06	4.24	N55W	2.43			3.47	4.87			5.31
121.92	30.48	9°12'	30.09	121.15	4.87	N73W	1.42			4.66	6.29			9.97
152.40	30.48	12°	29.81	150.96	6.34	N72W	1.96			6.03	8.25			16.00
182.88	30.48	9°48'	30.04	181.00	5.19	S85W		0.45		5.17	7.80			21.17
213.36	30.48	10°36'	29.96	210.96	5.61	N72W	1.73			5.33	9.53			26.50
243.84	30.48	21°30'	28.36	239.32	11.17	N58W	5.92			9.47	15.45			35.97
274.32	30.48	16°	29.30	268.62	8.40	N52W	5.17			6.62	20.62			42.59
304.80	30.48	16°36'	29.21	297.83	8.71	N35W	7.13			4.99	27.75			47.58
343.51	38.71	17°18'	36.96	334.79	11.51	N33W	9.65			6.27	37.40			53.85

Total depth after cementing and casing = 338 m

Table 21.--Observed and calculated data from deviation survey made in old East-observation well at proposed disposal site, Oak Ridge National Laboratory, Tennessee

Measured depth (m)	Course length MD (m)	Vertical deviation angle α	Vertical depth (m)		Horizontal displacement H (m)	Magnetic bearing β	Y (m)		X (m)		Total (m)			
											Y		X	
			Z	Total			N	S	E	W	N	S	E	W
30.48	30.48	0	30.48	30.48	0	--	0		0		0		0	
60.96	30.48	2°30'	30.45	60.93	1.33	N35E	1.09		0.76		1.09		0.76	
91.44	30.48	4°24'	30.39	91.32	2.34	N85E	0.20		2.33		1.29		3.09	
121.92	30.48	5°36'	30.33	121.65	2.97	S55E		1.71	2.44			0.42	5.53	
152.40	30.48	2°30'	30.45	152.10	1.33	S30E		1.15	0.66			1.57	6.19	
182.88	30.48	4°	30.41	182.51	2.13	S80W		0.37		2.09		1.94	4.10	
213.36	30.48	12°	29.81	212.32	6.34	N60W	3.17			5.49	1.23			1.39
243.84	30.48	16°42'	29.19	241.51	8.76	N55W	5.02			7.17	6.25			8.56
274.32	30.48	18°18'	28.94	270.45	9.57	N58W	5.07			8.12	11.32			16.68
304.80	30.48	15°24'	29.39	299.84	8.09	N73W	2.37			7.74	13.69			24.42
345.95	41.15	16°30'	39.46	339.30	11.69	N63W	5.31			10.41	19.00			34.83

Total depth after cementing and casing = 334 m

Table 22.--Observed and calculated data from deviation survey made in new East-observation well at proposed disposal site, Oak Ridge National Laboratory, Tennessee

Measured depth (m)	Course length MD (m)	Vertical deviation angle α	Vertical depth (m)		Horizontal displacement H (m)	Magnetic bearing β	Y (m)		X (m)		Total (m)			
											Y		X	
			Z	Total			N	S	E	W	N	S	E	W
45.72	45.72	1°	45.71	45.71	0.80	N60E	0.40		0.69		0.40		0.69	
76.20	30.48	4°	30.41	76.12	2.13	N60E	1.07		1.84		1.47		2.53	
106.68	30.48	4°	30.41	106.52	2.13	N80E	0.37		2.10		1.84		4.63	
137.16	30.48	3°	30.44	136.96	1.60	N70E	0.55		1.50		2.39		6.13	
167.64	30.48	2°	30.46	167.42	1.06	N48W	0.71			0.79	3.10		5.34	
198.12	30.48	4°30'	30.39	197.81	2.39	S85W		0.21		2.38	2.89		2.96	
228.60	30.48	14°	29.57	227.38	7.37	N80W	1.28			7.26	4.17			4.30
259.08	30.48	16°	29.30	256.68	8.40	N80W	1.46			8.27	5.63			12.57
289.56	30.48	16°30'	29.22	285.91	8.66	N64W	3.79			7.78	9.42			20.35
320.04	30.48	20°	28.64	314.55	10.42	N56W	5.83			8.64	15.25			28.99
350.52	30.48	14°	29.57	344.12	7.37	N28W	6.51			3.46	21.76			32.45

Total depth after cementing and casing = 347 m

Table 23.--Observed and calculated data from deviation survey made in South-observation well at proposed disposal site, Oak Ridge National Laboratory, Tennessee

Measured depth (m)	Course length MD (m)	Vertical deviation angle α	Vertical depth (m)		Horizontal displacement H (m)	Magnetic bearing β	Y (m)		X (m)		Total (m)			
											Y		X	
			Z	Total			N	S	E	W	N	S	E	W
30.48	30.48	3°30'	30.42	30.42	1.86	N88W	0.06			1.86	0.06			1.86
60.96	30.48	5°48'	30.32	60.75	3.08	N60W	1.54			2.67	1.60			4.53
91.44	30.48	4°30'	30.39	91.14	2.39	N65W	1.01			2.17	2.61			6.70
121.92	30.48	8°36'	30.14	121.28	4.56	N65W	1.93			4.13	4.54			10.83
152.40	30.48	11°12'	29.90	151.18	5.92	N58W	3.14			5.02	7.68			15.85
182.88	30.48	12°30'	29.76	180.94	6.60	N58W	3.50			5.60	11.18			21.45
204.22	21.34	13°	20.79	201.73	4.80	N62W	2.25			4.24	13.43			25.69
207.26	3.05	13°36'	2.96	204.69	0.72	N62W	0.34			0.63	13.77			26.32
213.36	6.10	14°24'	5.91	210.60	1.52	N63W	0.69			1.35	14.46			27.67
243.84	30.48	14°36'	29.50	240.10	7.68	N65W	3.25			6.96	17.71			34.63
274.32	30.48	16°	29.30	269.40	8.40	N65W	3.55			7.61	21.26			42.24
304.80	30.48	17°30'	29.07	298.47	9.17	N62W	4.31			8.10	25.57			50.34
335.28	30.48	17°	29.15	327.62	8.91	N62W	4.18			7.87	29.75			58.21
364.24	28.96	15°30'	27.91	355.53	7.74	N62W	3.63			6.83	33.38			65.04

Total depth after cementing and casing = 352 m

Table 24.--Observed and calculated data from deviation survey made in West-observation well at proposed disposal site, Oak Ridge National Laboratory, Tennessee

Measured depth (m)	Course length MD (m)	Vertical deviation angle α	Vertical depth (m)		Horizontal displacement H (m)	Magnetic bearing β	Y (m)		X (m)		Total (m)			
											Y		X	
			Z	Total			N	S	E	W	N	S	E	W
30.48	30.48	1°	30.48	30.48	0.53	N90W	0			0.53	0			0.53
60.96	30.48	3°	30.44	60.91	1.60	S80W		0.28		1.57		0.28		2.10
91.44	30.48	5°	30.36	91.28	2.66	N80W	0.46			2.62	0.18			4.72
121.92	30.48	7°15'	30.48	121.76	3.85	N85W	0.34			3.83	0.52			8.55
152.40	30.48	11°30'	29.87	151.63	6.08	N83W	0.74			6.03	1.26			14.58
182.88	30.48	12°30'	29.76	181.38	6.60	N82W	0.92			6.53	2.18			21.11
213.36	30.48	15°	29.44	210.83	7.89	N72W	2.44			7.50	4.62			28.61
243.84	30.48	18°45'	28.86	239.69	9.80	N58W	5.19			8.31	9.81			36.92
274.32	30.48	19°30'	28.73	268.42	10.17	N58W	5.39			8.63	15.20			45.55
304.80	30.48	15°	29.44	297.86	7.89	N55W	4.52			6.46	19.72			52.01
335.28	30.48	11°30'	29.87	327.73	6.08	N38W	4.79			3.74	24.51			55.75
351.13	15.85	11°30'	15.53	343.26	3.16	N45W	2.23			2.23	26.74			57.98

Total depth after cementing and casing = 342 m

Table 25.--Observed and calculated data from deviation survey made in North-observation well at proposed disposal site, Oak Ridge National Laboratory, Tennessee

Measured depth (m)	Course length MD (m)	Vertical deviation angle α	Vertical depth (m)		Horizontal displacement H (m)	Magnetic bearing β	Y (m)		X (m)		Total (m)			
											Y		X	
			Z	Total			N	S	E	W	N	S	E	W
30.48	30.48	3°30'	30.42	30.42	1.86	S70E		0.64	1.75			0.64	1.75	
60.96	30.48	5°18'	30.35	60.77	2.82	S55E		1.61	2.31			2.25	4.06	
91.44	30.48	2°42'	30.45	91.22	1.44	S85E		0.13	1.43			2.38	5.49	
121.92	30.48	2°36'	30.45	121.67	1.38	N35E	1.13		0.79			1.25	6.28	
152.40	30.48	5°36'	30.33	152.00	2.97	N28W	2.63			1.40	1.38		4.88	
182.88	30.48	15°30'	29.37	181.37	8.15	N35W	6.68			4.67	8.06		0.21	
213.36	30.48	23°	28.06	209.43	11.91	N37W	9.51			7.17	17.56			6.95
243.84	30.48	25°30'	27.51	236.94	13.12	N43W	9.60			8.95	27.16			15.91
274.32	30.48	22°30'	28.16	265.10	11.66	N48W	7.80			8.67	34.96			24.58
304.80	30.48	27°24'	27.06	292.16	14.03	N52W	8.64			11.06	43.60			35.64
341.38	36.58	25°12'	33.10	325.26	15.58	N50W	10.01			11.93	53.61			47.57

Total depth after cementing and casing = 330 m

Table 26.--Observed contact between rock units and calculated dip and strike at proposed disposal site, Oak Ridge National Laboratory, Tennessee

Contact between rock units	Injection well at proposed disposal site							Old East-observation well							Altitude (m) (msl)
	Measured depth (m)	True vertical depth (m)	Horizontal position (m)				Altitude (m) (msl)	Measured depth (m)	True vertical depth (m)	Horizontal position (m)					
			Y		X					Y		X			
			N	S	W	E				N	S	W	E		
Rutledge Limestone --Gray shale (Rutledge Limestone?)	167	165	8.0		18.5		75	176	175		1.9		4.6		65
Gray shale -- Rutledge Limestone	198	196	8.7		23.8		45	205	205	0.2			0		36
Rutledge Limestone --Pumpkin Valley Shale	234	230	13.6		32.9		10	242	240	5.9		8.1			0
Pumpkin Valley Shale -- Rome Sandstone	338	330	34.0		51.6		-89	346	339	19.0		34.8			-99

Remarks: Depth of rock contact was observed from gamma-ray logs and adjusted by well deviation logs.

TABLE 26 (CONT)

Contact between rock units	South-observation well							West-observation well						
	Measured depth (m)	True vertical depth (m)	Horizontal position (m)				Altitude (m) (msl)	Measured depth (m)	True vertical depth (m)	Horizontal position (m)				Altitude (m) (msl)
			Y		X					Y		X		
			N	S	W	E				N	S	W	E	
Rutledge Limestone --Gray shale (Rutledge Limestone?)	177	175	10.5		20.3		78	158	157	1.4		15.8		82
Gray shale -- Rutledge Limestone	209	206	14.0		26.7		37	190	188	2.8		22.9		50
Rutledge Limestone --Pumpkin Valley Shale	251	247	18.5		36.3		-3	227	223	6.9		32.3		15
Pumpkin Valley Shale -- Rome Sandstone	357	348	32.4		63.2		-105	334	326	24.3		55.6		-88
Remarks:														

TABLE 26 (CONT)

Contact between rock units	North-observation well							Calculated	
	Measured depth (m)	True vertical depth (m)	Horizontal position (m)				Altitude (m) (msl)	Dip	Strike
			Y		X				
			N	S	W	E			
Rutledge Limestone --Gray shale (Rutledge Limestone?)	152	151	1.8			4.9	84	10°30'	N51E
Gray shale -- Rutledge Limestone	187	185	9.4		0.8		50	9°24'	N53E
Rutledge Limestone --Pumpkin Valley Shale	218	213	18.9		8.2		22	14°36'	N69°42'E
Pumpkin Valley Shale -- Rome Sandstone	330	318	50.6		44.0		-83	13°0'	N71E
Remarks:									

Table 27.--Tensile strength of rocks at proposed disposal site, Oak Ridge National Laboratory, Tennessee, determined in the U.S. Geological Survey Denver Rock Mechanics Laboratory, Colorado

Rock unit	Testing method	Results (MPa)							Remarks
		Arithmetic mean	Maximum value	Minimum value	Standard deviation	Standard error of mean	98 percent confidence of limit		
							Lower	Upper	
Rome sandstone	line load	12.6	15.2	10.5	2.3	1.2	10.3	14.9	4 samples were tested Tensile strength parallel to bedding planes
Pumpkin Valley shale	line load	7.3	12.5	3.6	2.3	0.4	6.5	8.0	35 samples were tested Tensile strength parallel to bedding planes
Pumpkin Valley shale	direct pull	1.6	3.4	0.3	1.1	0.4	0.9	2.4	8 samples were tested Tensile strength normal to bedding planes
Pumpkin Valley shale	direct pull	11 samples were tested. 7 samples resulted in bond failure at stresses ranging from 3.0 to 6.3 MPa. 4 samples failed at 2.4, 2.9, 3.4, and 4.0 MPa, respectively.							Tensile strength parallel to bedding planes
Pumpkin Valley shale	point load	29 samples were tested, only 9 samples had poor results. Average tensile strength parallel to bedding planes is 1.9 MPa.							
Pumpkin Valley shale	--	6.0	12.5	1.9	3.0	0.4	5.1	6.8	Tensile strength parallel to bedding planes. Average results determined by different methods.

Table 28.--Injection pressure of test grout injection at 332 meters June 14, 1974, proposed disposal site, Oak Ridge National Laboratory, Tennessee

Time (min)	Observed well-head pressure in MPa	Calculated bottom-hole pressure in MPa	Rate of injection in $m^3/s \times 10^{-3}$	Remarks
30	5.72	8.89		
45	13.79	16.96		Start injection
46	17.93	21.10		
47	21.37	24.55		
48	22.48	25.65		
50	20.68	23.86		
55	18.62	21.79		
60	16.72	19.89		
62	21.65	24.82		
65	18.89	22.06		
68	22.48	25.65		
70	18.62	21.79		
75	19.31	22.48		
80	16.55	19.72		
85	16.55	19.72		
90	15.31	18.48		
95	13.65	16.82		Stop injection
100	13.79	16.96		
105	12.55	15.72		Injection was on and off irregularly
110	12.41	15.58		
115	13.44	16.62		
120	13.38	16.55		
125	12.34	15.51		
130	12.41	15.58		
135	15.17	18.34		Start injection, most time with water
140	15.86	19.03		
145	16.41	19.58		
150	16.55	19.72		
155	16.89	20.06		
160	16.55	19.72		
165	16.27	19.44		
170	16.20	19.37		
175	16.27	19.44		
180	16.27	19.44		
185	16.27	19.44		
190	16.13	19.31		
195	16.13	19.31		
200	16.13	19.31		
205	16.20	19.37		
210	16.96	20.13		Normal injection started at hour 1310.
215	17.93	21.10		Before this hour, injection was run
220	18.62	21.79	15.27	irregularly.
225	16.69	19.86		
230	14.89	18.06	16.72	

TABLE 28 (CONT)

Time (min)	Observed well-head pressure in MPa	Calculated bottom-hole pressure in MPa	Rate of injection in $m^3/s \times 10^{-3}$	Remarks
235	14.34	17.51		
240	14.07	17.24	16.40	
245	14.20	17.37		
250	14.48	17.65	16.91	
255	14.13	17.31		
260	14.62	17.79	16.72	
265	14.89	18.06		
270	15.31	18.48	17.22	
275	16.96	20.13		
280	16.55	19.72	15.77	
285	15.72	18.89		
290	13.24	16.41		Stop injection for cleaning surge tank
295	13.44	16.62		window
300	17.58	20.75		Start injection
305	16.82	19.99		
310	16.69	19.86	17.03	
315	16.82	19.99		
320	16.82	19.99	16.72	
325	16.69	19.86		
330	16.69	19.86	16.40	
335	16.96	20.13		
340	16.96	20.13	16.40	
345	16.82	19.99		
350	16.41	19.58	17.03	
355	16.55	19.72		
360	16.69	19.86	16.59	
365	15.86	19.03		
370	18.06	21.24	15.96	
375	17.65	20.82		
380	17.79	20.96	16.40	
385	17.51	20.68		
390	17.37	20.55	16.40	
395	17.24	20.41		
400	17.51	20.68	16.72	
405	17.79	20.96		
410	17.51	20.68	16.40	
415	17.51	20.68		
420	17.37	20.55	16.59	
425	17.58	20.75		
430	17.93	21.10	16.28	
435	18.06	21.24		
440	17.93	21.10	15.46	
445	17.65	20.82		
450	17.65	20.82	16.40	
455	17.65	20.82		
460	17.79	20.96	16.40	

TABLE 28 (CONT)

Time (min)	Observed well-head pressure in MPa	Calculated bottom-hole pressure in MPa	Rate of injection in $m^3/s \times 10^{-3}$	Remarks
465	17.10	20.27		
470	17.65	20.82	16.59	
475	18.06	21.24		
480	17.93	21.10	16.40	
485	18.20	21.37		
490	18.27	21.44	16.59	
495	18.96	22.13		
500	19.31	22.48	15.77	
505	19.99	23.17		
510	23.10	26.27	12.93	
515	24.41	27.58		
520	20.13	23.30	14.51	
525	19.65	22.82		
530	18.27	21.44	15.01	
535	19.31	22.51		
540	20.55	23.72	13.56	
545	19.31	22.48		
550	18.20	21.37	16.40	
555	17.93	21.10		
560	17.93	21.10	16.09	
565	17.93	21.10		
570	17.65	20.82	16.72	
575	17.93	21.10		
580	17.93	21.10	16.40	
585	17.65	20.82		
590	17.10	20.27	16.09	
595	16.20	19.37		
600	16.89	20.06		
	14.48	17.65		Instantaneous shut-in pressure

Table 29.--Waste grout sheets intercepted by North-observation well from past waste injections made at present fracturing site (interpreted from gamma-ray logs made in North-observation well at proposed disposal site before test grout injection, June 14, 1974), Oak Ridge National Laboratory, Tennessee

Depth (m) measured along casing	Vertical depth (m) (measured depth adjustment by deviation survey)	Altitude (m) (msl)	Horizontal position (m)				
			Y		X		
			N	S	W	E	
242.3	235.5	-0.5	26.7		15.5		
246.0	238.9	-3.9	27.7		16.5		Second strongest gamma peak
271.0	262.0	-27.0	34.1		23.6		Strongest gamma peak
323.7	309.3	-74.2	48.8		41.8		

Table 30.--Grout sheets intercepted by observation wells from test grout injection at 332 meters, June 14, 1974, proposed disposal site, Oak Ridge National Laboratory, Tennessee

Well	Depth (m) measured along casing	Vertical depth (m) (measured depth adjusted by deviation survey)	Altitude (m) (msl)	Horizontal position (m)				Remarks
				Y		X		
				N	S	W	E	
New East-observation well	341.1	335.0	-93.8	19.7		31.4		Injection altitude = -83.7 meters (msl)
South-observation well	349.0	340.8	-97.3	31.5		61.4		
	349.6	341.4	-97.8	31.5		61.6		
	349.9	341.7	-98.1	31.1		61.7		
West-observation well	328.0	320.3	-81.8	23.3		54.9		
	330.1	322.4	-83.9	23.7		55.1		
	330.4	322.7	-84.2	23.7		55.2		
	331.0	323.3	-84.8	23.8		55.2		
	331.3	323.6	-85.1	23.9		55.3		
	331.9	324.1	-85.7	24.0		55.4		

Table 31.--Injection pressure of test water injection at 332 meters, October 30, 1975, proposed disposal site, Oak Ridge National Laboratory, Tennessee

Time (min)	Observed well-head pressure in MPa	Calculated bottom-hole pressure in MPa	Rate of injection in $m^3/s \times 10^{-3}$	Remarks
1	13.17	16.34		
3	13.44	16.62		
5	13.72	16.89		
6	12.93	16.10		
7	11.93	15.10		
9	11.10	14.27	0	Shut down for repairing leaks
10	10.69	13.86		
				Pressure gauge was out of order
139	11.76	14.93	0	
140	13.20	16.38		
142	14.62	17.79	1.89	
143	14.82	18.00		
146	15.00	18.17		
147	15.10	18.27		
148	15.24	18.41		
150	15.27	18.44		Start injection of tracers
155	15.51	18.68		
160	15.79	18.96		
165	15.96	19.13		
170	16.10	19.27		
175	16.20	19.37		
180	16.31	19.48		
185	16.48	19.65		
190	16.51	19.68	1.89	
195	16.58	19.75	2.40	
200	16.69	19.86		
205	16.79	19.96		
210	16.86	20.03		
215	16.93	20.10	2.40	
220	17.00	20.17	2.65	
225	17.06	20.24		
230	17.10	20.27	2.65	
235	17.10	20.27	2.84	
240	17.10	20.27		
245	17.10	20.27	2.84	
250	17.00	20.17	2.65	
255	18.13	21.30	5.65	
256	18.44	21.62		
257	18.62	21.79		
258	19.13	22.30		
259	19.31	22.48		
260	19.44	22.61	5.65	
265	19.86	23.03	8.45	

TABLE 31 (CONT)

Time (min)	Observed well-head pressure in MPa	Calculated bottom-hole pressure in MPa	Rate of injection in $m^3/s \times 10^{-3}$	Remarks
270	20.03	23.20		
275	20.24	23.41		
280	20.37	23.55		
285	20.42	23.59		
290	20.42	23.59		
295	20.34	23.51		
298	20.27	23.44		
299	20.24	23.41		
300	20.24	23.41		
301	20.24	23.41	8.45	
302	19.44	22.61	5.43	
303	19.20	22.37		
304	19.00	22.17		
305	18.79	21.96		
306	18.62	21.79		
307	18.48	21.65		
308	18.31	21.48		
309	18.17	21.34		
310	18.03	21.20		
311	17.93	21.10		
312	17.83	21.00		
313	17.72	20.89		
315	17.48	20.65	5.43	
318	18.27	21.44	6.62	
319	18.55	21.72		
320	18.86	22.03		
325	19.41	22.58	6.62	
330	19.62	22.79	7.95	
335	19.79	22.96		
340	19.89	23.06		
345	19.89	23.06		
350	19.87	23.04		
355	19.82	22.99	7.95	
360	19.79	22.96	7.59	
365	19.75	22.93		
370	19.68	22.86	7.59	
372	19.79	22.96	9.90	
373	19.82	22.99		
374	19.86	23.03		
375	19.89	23.06		
376	19.93	23.10		
377	19.99	23.17		
378	20.03	23.20		
379	20.06	23.24		
380	20.11	23.28		
385	20.13	23.30	9.90	

TABLE 31 (CONT)

Time (min)	Observed well-head pressure in MPa	Calculated bottom-hole pressure in MPa	Rate of injection in $m^3/s \times 10^{-3}$	Remarks
390	20.10	23.27	13.25	
395	20.06	23.24		
400	19.96	23.13	13.25	
405	19.86	23.03	12.74	
410	19.75	22.93	12.74	
415	19.65	22.82	13.25	
420	19.59	22.77		
425	19.51	22.68		
430	19.41	22.58		
435	19.20	22.37	13.25	
450	19.06	22.24	16.78	
455	19.03	22.20	16.78	
460	18.96	22.13	16.40	
463	19.13	22.30		
464	19.15	22.32		
465	19.17	22.34		
470	19.21	22.38		
475	19.20	22.37		
480	19.17	22.34		
485	19.03	22.20		
490	18.96	22.13		
495	18.87	22.04		
500	18.80	21.97	16.40	One pump was out of order
503	18.20	21.37	9.21	
504	18.10	21.27		
505	18.13	21.30		
506	18.10	21.27		
510	18.00	21.17		
515	17.87	21.04		
520	17.77	20.95		
525	17.66	20.84		
530	17.58	20.75		Stop injection of tracers
535	17.49	20.66		
540	17.44	20.62		
545	17.37	20.55		
550	17.34	20.51		End of injection

Table 32.--Pressure decay of test water injection at 332 meters, October 30, 1975, proposed disposal site, Oak Ridge National Laboratory, Tennessee.

Time since end of injection (min)	Observed well-head pressure in MPa	Calculated bottom-hole pressure in MPa	$(P-p_o)$ in MPa
2	16.72	19.89	16.77
5	16.44	19.62	16.50
10	15.93	19.10	15.98
15	15.62	18.79	15.67
20	15.31	18.48	15.36
25	15.07	18.24	15.12
30	14.86	18.03	14.91
35	14.65	17.82	14.70
40	14.48	17.65	14.53
45	14.31	17.48	14.36
50	14.17	17.34	14.22
55	14.03	17.20	14.08
60	13.89	17.06	13.94
65	13.79	16.96	13.84
70	13.69	16.86	13.74
80	13.48	16.65	13.53
90	13.27	16.44	13.32
100	13.12	16.29	13.17
110	13.17	16.11	12.99
120	12.81	15.98	12.86
130	12.67	15.84	12.72
140	12.63	15.80	12.68
150	12.45	15.62	12.50
160	12.34	15.51	12.39
170	12.22	15.39	12.27
180	12.12	15.29	12.17
190	12.03	15.20	12.08
200	11.93	15.10	11.98
210	11.86	15.03	11.91
225	11.72	14.89	11.77
240	11.62	14.79	11.67
255	11.51	14.69	11.57
270	11.41	14.58	11.46
285	11.31	14.48	11.36
300	11.20	14.38	11.26
315	11.14	14.31	11.19
330	11.03	14.20	11.08
860	9.29	12.46	9.34
890	9.23	12.40	9.28
920	9.19	12.36	9.24
970	9.11	12.28	9.16
1035	9.01	12.18	9.06
1140	8.81	11.98	8.86
1200	8.70	11.87	8.74

TABLE 32 (CONT)

Time since end of injection (min)	Observed well-head pressure in MPa	Calculated bottom-hole pressure in MPa	$(P-p_o)$ in MPa
1260	8.61	11.78	8.66
1430	8.38	11.55	8.43
1675	8.07	11.24	8.12
1930	7.81	10.98	7.86
2160	7.58	10.76	7.64
2400	7.47	10.65	7.53
2640	7.28	10.45	7.33
2880	7.15	10.32	7.20
3120	7.01	10.18	7.06
3360	6.87	10.05	6.93
3600	6.72	9.89	6.77
3850	6.67	9.85	6.73
4105	6.55	9.72	6.60
4315	6.50	9.67	6.55
4560	6.38	9.55	6.43
4800	6.31	9.48	6.36
5040	6.22	9.39	6.27
5335	6.17	9.34	6.22
5490	6.12	9.29	6.17
5760	6.05	9.22	6.10
6000	6.00	9.17	6.05
6240	5.90	9.07	5.95
6480	5.83	9.01	5.89
6720	5.83	9.01	5.89
6960	5.76	8.94	5.82
7200	5.72	8.89	5.77
7440	5.67	8.84	5.72
7650	5.62	8.79	5.67
7920	5.59	8.76	5.64
8400	5.48	8.65	5.53
8700	5.45	8.62	5.50
9180	5.37	8.54	5.42
9625	5.32	8.49	5.37
10140	5.24	8.41	5.29
10620	5.17	8.34	5.22
11320	5.09	8.26	5.14
11580	5.03	8.20	5.09
12080	5.00	8.17	5.05
12540	4.96	8.14	5.02
13020	4.90	8.07	4.95
13500	4.84	8.01	4.89
14460	4.76	7.93	4.81
15360	4.69	7.86	4.74
15655	4.67	7.84	4.72
16795	4.60	7.77	4.65
17080	4.56	7.74	4.62

TABLE 32 (CONT)

Time since end of injection (min)	Observed well-head pressure in MPa	Calculated bottom-hole pressure in MPa	$(P-p_o)$ in MPa
18225	4.48	7.65	4.53
18555	4.47	7.64	4.52
19680	4.38	7.55	4.43
19972	4.37	7.54	4.42
21100	4.30	7.47	4.35
21420	4.28	7.45	4.33
22600	4.21	7.38	4.26
24030	4.14	7.31	4.19
25448	4.08	7.25	4.13
25692	4.05	7.22	4.10

Static ground water pressure at injection level (p_o) = 3.12 MPa

☆ U.S. GOVERNMENT PRINTING OFFICE: 1980 O— 311-344/82